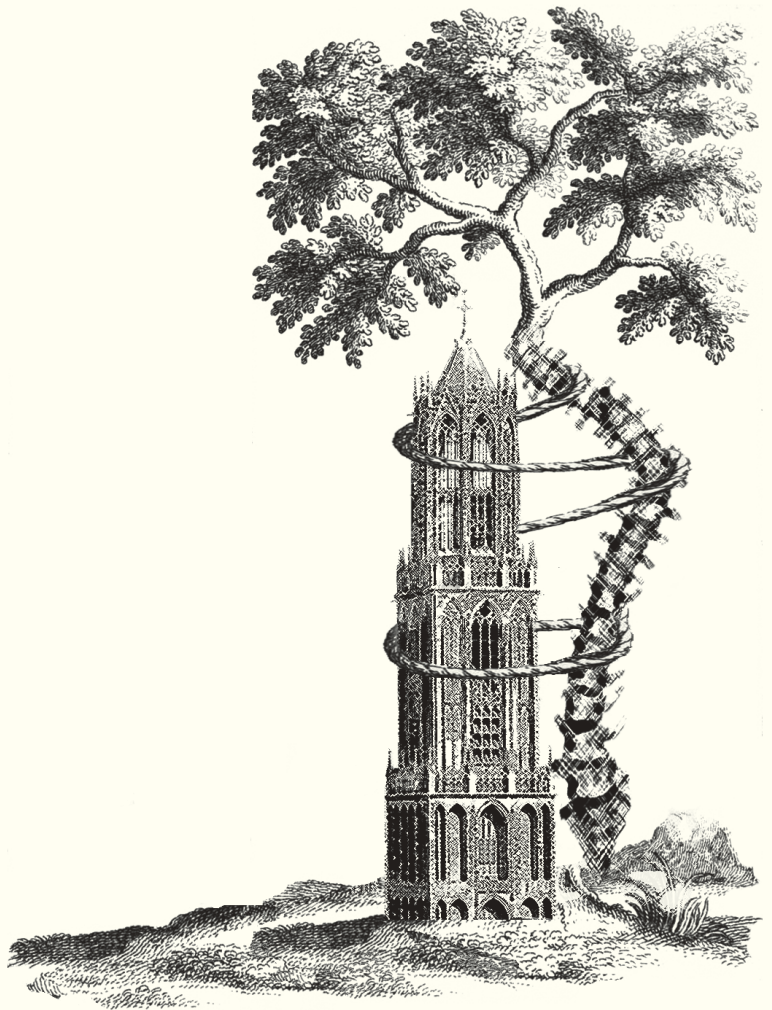# Consequences of the Three-Dimensional Pathoanatomy of Adolescent Idiopathic Scoliosis

ROB C. BRINK

ROB C. BRINK

Consequences of the Three-Dimensional Pathoanatomy of Adolescent Idiopathic Scoliosis

Consequences of the Three-Dimensional Pathoanatomy of
Adolescent Idiopathic Scoliosis

Consequenties van de Driedimensionale Patho-Anatomie van
Adolescente Idiopathische Scoliose
(met een samenvatting in het Nederlands)

Proefschrift

ter verkrijging van de graad van doctor aan de Universiteit Utrecht op gezag van de
rector magnificus, prof.dr. H.R.B.M. Kummeling, ingevolge het besluit van het college
voor promoties in het openbaar te verdedigen op donderdag 28 februari 2019 des
middags te 4.15 uur

door

Rob Cornelis Brink
geboren op 24 juli 1990 te Kampen

THIS THESIS IS BASED UPON THE FOLLOWING PUBLICATIONS AND MANUSCRIPTS

Chapter 2: Schlösser TPC, Brink RC, Castelein RM. The Etiologic Relevance of 3D Patho-anatomy of Adolescent Idiopathic Scoliosis. *Coluna/Columna. 2017;16(4):302-6*

Chapter 3: Brink RC, Vavruch L, Schlösser TPC, Abul-Kasim K, Ohlin A, Tropp H, Castelein RM, Vrtovec T. Three-Dimensional Pelvic Incidence is Much Higher in (Thoraco)Lumbar Scoliosis Than in Controls. *Eur Spine J. 2018 Aug 20*

Chapter 4: Brink RC, Homans JF, Schlösser TPC, van Stralen M, Vincken KL, Shi L, Chu WCW, Viergever MA, Castelein RM, Cheng JCY. CT-Based Study of Vertebral and Intravertebral Rotation in Right Thoracic Adolescent Idiopathic Scoliosis.

Chapter 5: Brink RC, Schlösser TPC, Colo D, Vincken KL, van Stralen M, Hui SCN, Chu WCW, Cheng JCY, Castelein RM. Asymmetry of the Vertebral Body and Pedicles in the True Transverse Plane in Adolescent Idiopathic Scoliosis: A CT-Based Study. *Spine Deformity 5 (2017) 37e45*

Chapter 6: Brink RC, Schlösser TPC, Colo D, Vavruch L, van Stralen M, Vincken KL, Malmqvist M, Kruyt MC, Tropp H, Castelein RM. Anterior Spinal Overgrowth Is the Result of the Scoliotic Mechanism and Is Located in the Disc. *Spine (Phila Pa 1976). 2017 Jun 1;42(11):818-822*

Chapter 7: Brink RC, Schlösser TPC, van Stralen M, Vincken KL, Kruyt MC, Hui SCN, Viergever MA, Chu WCW, Cheng JCY, Castelein RM. Anterior-Posterior Length Discrepancy of the Spinal Column in Adolescent Idiopathic Scoliosis - a 3D CT Study. *Spine J. 2018 May 4. pii: S1529-9430(18)30204-3*

Chapter 8: Brink RC, Schlösser TPC, van Stralen M, Vincken KL, Kruyt MC, Chu WCW, Cheng JCY, Castelein RM. What is the actual 3D Representation of the Rib Vertebra Angle Difference (Mehta's angle)? *Spine (Phila Pa 1976). 2018 Jan 15;43(2):E92-E97*

Chapter 9: Brink RC, Colo D, Schlösser TPC, Vincken KL, van Stralen M, Hui SCN, Shi L, Chu WCW, Cheng JCY, Castelein RM. Upright, Prone, and Supine Spinal Morphology and Alignment in Adolescent Idiopathic Scoliosis. *Scoliosis Spinal Disord. 2017 Feb 22;12:6*

Chapter 10: Tromp IN, Brink RC, Homans JF, Schlösser TPC, van Stralen M, Kruyt MC, Chu WCW, Cheng JCY, Castelein RM. Spinous Processes and Transverse Processes Measurements of the Scoliotic Spine and their Relation to the Cobb angle: a CT Based Study.

Chapter 11: Brink RC, Wijdicks SPJ, Tromp IN, Schlösser TPC, Kruyt MC, Beek FJA, Castelein RM. A Reliability and Validity Study for Different Coronal Angles using Ultrasound Imaging in Adolescent Idiopathic Scoliosis. *Spine J. 2018 Jun;18(6):979-985*

Chapter 12: Vavruch L, Brink RC, Malmqvist M, Schlösser TPC, van Stralen M, Abul-Kasim K, Ohlin A, Castelein RM, Tropp H. Surgical Outcomes of Anterior versus Posterior Fusion in Lenke Type 1 Adolescent Idiopathic Scoliosis. *Spine (Phila Pa 1976) accepted 2019.*

Chapter 13: Brink RC, Homans JF, de Reuver S, van Stralen M, Schlösser TPC, Viergever MA, Chu WCW, Ng BKW, Castelein RM, Cheng JCY. A CT Based Guideline for Pedicle Screw Placement in Adolescent Idiopathic Scoliosis.

TABLE OF CONTENTS

Part III   Therapeutic consequences for adolescent idiopathic scoliosis

Chapter 1

Introduction, Aims and Outline of this Thesis

INTRODUCTION

Scoliosis is a classic orthopedic disorder, a three-dimensional (3D) rotational deformity of the spine and trunk with severe consequences for the patient in terms of self-image, pain and treatment options.[1, 2] There are several known conditions to cause scoliosis, such as congenital spinal abnormalities, neuromuscular disorders and metabolic disorders. However, in most cases, a specific cause is not found, the patients appear otherwise normal, and therefore those cases are called 'idiopathic'. The most common type, adolescent idiopathic scoliosis (AIS), develops in previously healthy children, most often girls, during early puberty and affects 1-4% of the adolescents.[3] Treatment is always a severe burden and consists of rigid and constraining braces that have to be worn a great number of hours during this vulnerable period of life, or extensive surgical procedures that carry severe risks such as neurologic damage. Scoliosis has a huge impact for the individual patient in terms of quality of life, as well as for society in terms of the high costs of treatment.[3, 4]

Despite many years of extensive research into idiopathic scoliosis, the exact etiology of this disorder has still not been resolved, although recent research has elucidated the role of human sagittal alignment on the rotational stability of the spine, as well as certain metabolic and neurogenic factors.[3, 5-9] There are only a few prognostic factors identifying the patients at risk for severe progression.[3, 10] For detection of progressive spinal deformity as well as for clinical decision making, follow-up by frequent full-spine radiographs is standard during the adolescent growth spurt. This results in a high radiation exposure during the critical years of gonadal growth and development which, possibly in combination with some genetic predisposition, results in a five times higher overall cancer rate of predominantly breast and endometrium in later life, as compared to the age-matched population.[11, 12] Because of this lack of understanding of the pathomechanism of the disorder, no adequate, early causal treatment is available to date. Therefore treatment is aimed at the outcome of the disease process and consists of extensive brace treatment or invasive spine surgery. A better knowledge of the evolution of the initially normal spine into the 3D pathoanatomy of AIS is important for understanding its etiopathogenesis, identification of prognostic factors, reduction of radiation exposure as well as for the development of earlier and potentially less invasive treatment options.

Spinopelvic alignment of the human species

Idiopathic scoliosis is exclusively observed in *Homo sapiens*.[13] Although the basic anatomy of the spine is very similar between species, spinopelvic biomechanics, caused by the unique upright position and sagittal morphology of the human spine, have been shown to play an important role.[5, 7] Although there are many bipedal species, only man, due to its unique pelvic anatomy with a pelvic lordosis and its ability to simultaneously

extend both hips and knees, is able to stand fully upright, with the center of gravity of the body straight above the pelvis, in which the pelvis acts as the key regulator of the spinopelvic alignment. All other (bipedal) vertebrates stand with flexed hips and knees and with a straight line between their ischium and ilium, with the center of gravity in front of the pelvis, which imparts essentially different shear loading on the human spine.[14] There is a major difference in sagittal pelvic and spinal morphology between humans and other species. Already in the 1950s, Washburn observed pelvic shape differences between humans and apes as an essential requisite for the bipedal locomotion.[15] The 'pelvic lordosis' – the lordotic angulation between the ischial and iliac bones – and the more horizontal position of the sacral bone within the pelvic ring are the base of the double S-shape of the upright human spine.[15-19]

The importance of the more vertical position of the sacrum in the pelvis for spine pathology was described by During et al. in 1985.[20] In 1992, Duval-Beaupère introduced the "pelvic incidence (PI)", as a spinopelvic parameter for sagittal pelvic morphology.[21] Now, this parameter is globally recognized as the most important parameter and the foundation of an individual's sagittal spinopelvic alignment, characterized by: (1) a certain sagittal pelvic morphology including the pelvic lordosis, (2) dynamic pelvic orientation around the hip axis, (3) subsequent slope of the sacral plate and (4) lordosis of the lower lumbar spine up to the inflection point to kyphosis.[7, 14] As a consequence of man's unique sagittal spinal alignment, biomechanics of the spine differs between man and all other vertebrates, bipedal and quadrupedal alike, with serious consequences for spinal rotational stability. In all quadrupedal as well as bipedal species, the facet joints provide rotational stability because the spines are loaded with an axial compression as well as anterior shear load.[7, 10, 22] This anterior shear only increases rotational stiffness of the segment.[5] In the human spine, however, certain segments are backwardly inclined (Figure 1). In addition to the axial loading, the human upright position induces a posterior shear force in a major part of the thoracic and lumbar spine, which results in rotationally less stable segments.[5, 7, 13] Which segments are posteriorly inclined differs per individual, gender and growth phase and is in general not very well defined.

In 2015 Schlösser et al. described that not only between different species, but also at different stages during ontogenetic growth the natural sagittal spinopelvic alignment changes in boys and girls.[23] In general, the spine starts in utero and early infancy as one big kyphosis, changes into a global double S-shape with a lordosis in the pelvis, the lumbar and in the cervical area around the adult age.[15, 17, 19] This gradual development of the adult sagittal profile is very ill-described and is the subject of our ongoing studies. In girls, the peak of the adolescent growth spurt is earlier than in boys, it occurs at a time when thoracic kyphosis is still less developed and the whole spine is still more posteriorly inclined, whereas the most rapid part of the growth spurt in boys occurs in a period when kyphosis is more developed and the spine shows less posterior inclina-
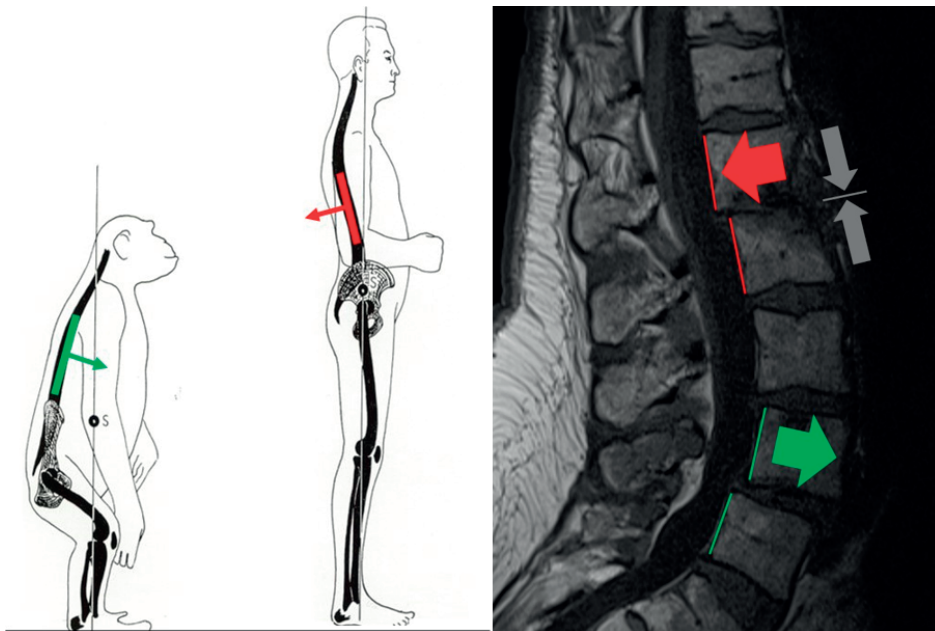
Figure 1. All spines consist of anterior inclined vertebrae (in green). The unique standing position and sagittal spinal morphology of man results in posterior inclined vertebrae as well (in red). Because of the unique position, three forces act on the human spine. These three forces (anterior shear force, posterior shear force and axial force), including the *unique posterior shear,* acting on the human spine can easily be appreciated in this MRI of a spine that demonstrates them all, axial (grey), anterior (green) and posterior (red) force.

tion.[23-25] Spines of girls are thus more affected by posterior shear loads during the peak of the adolescent growth spurt, as compared to boys, implying a less rotationally stable spine during this period. These gender differences are in line with the epidemiological characteristics of the onset and progression of idiopathic scoliosis, which is more prevalent in girls than in boys.[26, 27]

Etiology and 3D pathoanatomy of AIS

Idiopathic scoliosis can be classified according to different criteria: age of onset and the morphology of the curves of the spine. The classification based on the age of onset of the deformity, includes three subtypes; infantile scoliosis (0-3 years old), juvenile scoliosis (4-9 years old) and adolescent scoliosis (10-16 years old), or two subtypes: early onset (0-9 year) and late onset (10-18 year).[28]

Scoliosis morphology
The internationally accepted definition of the American Scoliosis Research Society (SRS) defines scoliosis as a lateral curvature of the spine of at least 10° Cobb angle (the angle between the two most tilted vertebrae) in the coronal plane (Figure 2).[28] However, as

already described by many authors, including 19th century anatomists in cadaveric specimens (Figure 3), idiopathic scoliosis is a complex 3D spine and trunk deformity: lateral deviation and lateral bending in the coronal plane, lordosis of the apical segments and hypertrophy of the facet joints in the sagittal plane, and axial rotation in the transverse plane (Figure 3).[1, 28-30] Since the introduction of radiography, the changes in the coronal plane, however, have been described most extensively in the literature.

Most of the literature on AIS morphology is based on cadaveric specimens or analyses of uni- or biplanar two-dimensional (2D) radiographs. It was observed that the discs were more wedge-shaped than the vertebral bodies in mild scoliotic curves, whereas the wedging of the discs and vertebrae became more or less equal in more severe scoliosis.[31, 32] However, contradictory findings have been reported on the individual contribution of the vertebral bodies as compared to the discs to the coronal deformity, based on 2D radiographs.[31-38]

Since the vertebrae in AIS are rotated and slightly wedged, 2D images of the spine provide insufficient representation of the actual coronal, sagittal and transverse alignment. In addition to the standard PA and lateral radiographic parameters, several authors attempted to increase the added value of standard radiographs,

Figure 2. The Scoliosis Research Society defined scoliosis as a lateral curvature of the spine of at least 10 degrees in the coronal plane as measured using the Cobb angle.[28]

thus rotation measurements, the 'plan d'élection' of Stagnara and the rib vertebra angle difference (RVAD) as a prognostic parameter, were introduced.[11, 31, 39-42]

Despite its radiation burden, computed tomography (CT) is the 'gold standard' for quantitative assessment of the morphology of *in-vivo* osseous structures.[43] Schlösser et al. analyzed the contributions of the vertebral bodies and intervertebral discs in AIS using high-resolution CT scans and described that the intervertebral discs were at least three times more deformed in the true coronal, transverse and sagittal plane.[44] Additionally, the deformations were more pronounced at the apical segments, decreasing towards the neutral region of the scoliotic spine.[44] Grivas et al. described as well that the wedging of the intervertebral disc is larger as compared to the vertebral body.[45]

Anterior overgrowth
It is well known that the anterior part of the spine is longer than the posterior part in idiopathic scoliosis.[2, 46-50] Somerville and Roaf described that during the development of idiopathic scoliosis, the vertebral bodies rotate away from the midline towards the convexity, to a more lateral position than the posterior elements of the spine.[2, 46] The axial rotation towards the convexity of the curve leads to a spinal column that is latero-flexed
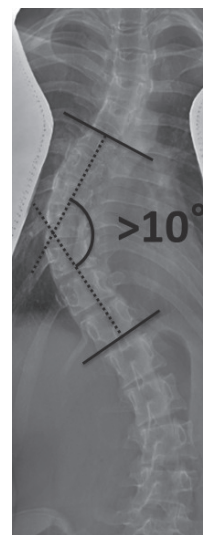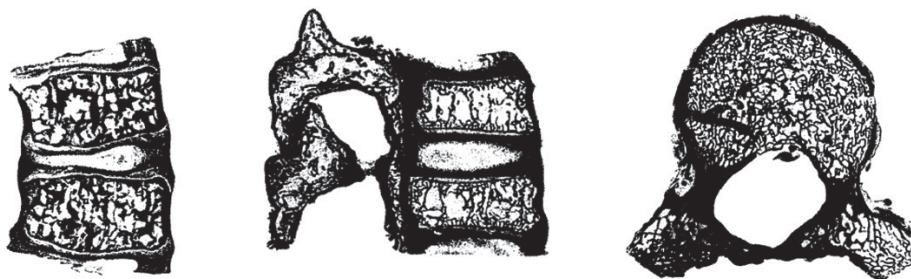
Figure 3. The deformities in the three planes, as described by Nicoladoni: lateral deviation and lateral bending in the coronal plane, lordosis of the apical segments and hypertrophy of the facet joints in the sagittal plane, and axial rotation in the transverse plane. Data compiled from Nicoladoni.[1]

and is longer anteriorly than posteriorly, resulting in a rotated lordosis of the apex. Dickson et al. observed in 70 AIS patients that instead of a normal thoracic kyphosis, 75% of the AIS curves were lordotic, 24% were straight, and only 1% of the included curves were kyphotic.[47, 51] More recently, this so-called relative anterior spinal overgrowth, has been suggested as part of the etiopathogenetic mechanism of AIS, as a potential driver for initiation and progression of the disorder.[52-55] Different explanations have been suggested. It has either been hypothesized to be the result of an active growth disturbance – a lack of synchronicity between two different mechanisms of ossification of different elements of the spinal column, intra-membranous (the laminae) and endo-chondral (the vertebral bodies) that has to rotate and deviate out of the midline in order to keep the head centered over the pelvis and to avoid excess tension on the spinal cord – or a result of a passive response to altered biomechanical loading of the spine.[47, 52-55]

Schlösser et al. described the 3D deformation of different regions of the spine great detail, using high-resolution CT imaging of AIS patients, made for navigation purposes, and a dataset of CT scans of normal children (taken for purposes as trauma, pulmonary disease, etcetera).[44, 50] The 3D development of AIS curves follows a rather uniform pattern with coupling of the different aspects of the deformity in all three planes and all AIS curves, structural as well as nonstructural, primary as well as compensatory, thoracic as well as (thoraco)lumbar, were characterized by greater anterior length measured from Cobb end vertebra to Cobb end vertebra.[50] The junctional segments in-between the curves were more or less straight and in scoliosis the intervertebral discs were at least three times more deformed in the coronal, true transverse and true sagittal plane than the vertebral bodies.[44, 50] Additionally, Schlösser et al. analyzed lateral radiographs of almost 1400 very mild AIS patients (Cobb angle smaller than 20 degrees) to observe the sagittal profile in the thoracic and (thoraco)lumbar AIS patients.[56] At this very early stage, the thoracic kyphosis and posterior inclination of thoracic AIS differs significantly from (thoraco)lumbar AIS as well as from controls; in thoracic scoliosis most thoracic vertebra were more backwardly inclined as compared to (thoraco)lumbar scoliosis and vice

versa.[56] The excess of anterior length is not a global, but rather a regional phenomenon, and these data suggest that the anterior-posterior length discrepancy in AIS is a passive phenomenon, rather than an active growth process.

Imaging of AIS

Upright radiographs are traditionally performed for diagnosis, monitoring of progression and clinical decision making of AIS patients.[3, 11, 57] In addition, supine or prone magnetic resonance imaging (MRI) and CT may be used to obtain more in-depth information about neural axis and bony architecture abnormalities.[3, 58] More recently, standing low-dose biplanar radiography became available and can be utilized for 3D reconstructions.[59] Most methods involve ionizing radiation and the radiation doses are cumulative, resulting in a nine to ten times higher radiation exposure in these patients, leading to an increased life-time risk of cancer in the AIS cohort as compared to the general population.[12, 60] MRI is non-ionizing but does not yet visualize cortical bone very well, is time consuming, expensive and is not performed upright. Therefore, a number of previous authors have attempted to visualize the 3D character of the scoliotic curve without ionizing radiation in the upright position, using imaging modalities such as ultrasound imaging and surface topography.[61-71] Almost three decades ago, Suzuki et al. already described the application of ultrasound to identify the lamina, spinous process (SP) and transverse process (TP) of scoliotic patients.[61] More recently, in several *in-vitro* and *in-vivo* studies the ultrasound spine deformity measurements were compared to the traditional Cobb angle on radiographs in AIS, and validated to measure the severity of the curve without radiation.[62-67, 69, 70]

Therapeutic consequences for AIS

Although 1-4% of the adolescents are affected with scoliosis, treatment is required in 0.3-0.5%.[3] The treatment of AIS varies from simple observation in cases that are non-progressive, to bracing and surgery in curves that do progress. Optimal inclusion criteria for brace therapy include Risser stage 0-2, primary curve angles 25-40°, no prior treatment, and, if female, either premenarchal or less than 1 year postmenarchal.[72] Brace treatment is indicated as well in patients with curves less than 25° that have shown 5° to 10° progression in six months (progression of more than 1° per month), or in patients with pronounced skeletal immaturity (Risser, 0; Tanner, 1 or 2). Braces should generally be worn full-time, with treatment lasting from two to four years, until the end of bone growth.[73] Bracing significantly decreases the progression of high-risk curves to the threshold for surgery (45-50°) in AIS patients; 72% of the patients that wear the brace at least 18 hours per day will not reach the surgery limit of 50°, as compared to 48% in patients that are only observed.[74] Curves larger than 50° degrees are associated with a high-risk of continued worsening throughout adulthood, and thus usually indicate the

need for surgery.[75] The primary goal of corrective scoliosis surgery in adolescents is to halt curve progression to prevent pulmonary dysfunction and pain.[3, 76] Secondary goals of surgical correction and fusion are reduction of the deformity, cosmesis and restoration of 3D spinal alignment.

AIMS AND OUTLINE OF THIS THESIS

After the introduction to the theme in chapter 1, a number of questions are addressed:

Chapter 2. The Etiologic Relevance of the 3D Pathoanatomy of Adolescent Idiopathic Scoliosis

Answers to the most relevant questions that led to this thesis on the etiopathogenesis of idiopathic scoliosis, are reviewed, such as: What is known about the 3D pathoanatomy of AIS in the literature? Why are thoracic curves predominantly right convex in adolescents, but left convex in infantiles? What is the role of relative anterior spinal overgrowth? And the main question:

What is the relevance of the 3D pathoanatomy of AIS?

Chapter 3. Three-Dimensional Pelvic Incidence is Much Higher in (Thoraco)Lumbar Scoliosis Than in Controls

Several other studies described the spinopelvic alignment in normal children during growth and in patients with different pathologies, and suggested a link between the spinopelvic morphology and the onset of spinal deformities.[14, 23, 47, 56, 77-86] The exact difference in pelvic morphology between AIS subjects and non-scoliotic controls has remained unclear, since most of the previous studies obtained 2D referential values using standing lateral radiographs which could lead to a deviation from the true sagittal plane and to a certain degree of distortion of the image.[87, 88] In chapter 3, sagittal pelvic morphology of AIS patients and asymptomatic adolescents are compared, using a previously validated 3D image processing technique, to answer the question:

What are the differences in pelvic alignment between AIS patients and the non-scoliotic controls?

Chapter 4. CT-Based Study of Vertebral and Intravertebral Rotation in Right Thoracic Adolescent Idiopathic Scoliosis

In AIS the apical vertebrae rotate away from the midline in a complex 3D pattern.[2, 46] The rotation of the vertebrae is part of the – to a large extent – unknown pathogenetic mechanism that leads to scoliosis. Insight in the rotation mechanism of the different vertebrae within the curve and whether the rotation is mainly local (located within the

vertebra: intravertebral axial rotation and local mechanical torsion), or a segmental rotation (vertebral axial rotation), is important to help understand possible mechanisms of scoliosis development. A better description of the altered anatomy could give more insights for better treatment of scoliosis. In chapter 4, the different intra- and extravertebral patterns of spinal rotation in the transverse plane in AIS are described, to form an answer to the question:

Where is the longitudinal rotation axis of the AIS vertebrae located, and what are the various extra- and intravertebral rotation patterns?

Chapter 5. Asymmetry of the Vertebral Body and Pedicles in the True Transverse Plane in Adolescent Idiopathic Scoliosis: A CT-Based Study

Transverse plane asymmetry is a well-known part of the 3D deformity in scoliosis and has been described in a number of older as well as more recent anatomical and radiographic imaging studies.[1, 2, 29, 30, 44, 46, 89, 90] The exact transverse plane morphology in AIS is important for our understanding of the true nature of the disorder, as well as for surgical pedicle screw placement. The existence and magnitude of vertebral body as well as pedicle asymmetry in the true transverse plane are described in chapter 5, as an answer to:

How asymmetrical are the pedicles and vertebral bodies in adolescent idiopathic scoliosis?

Chapter 6. Anterior Spinal Overgrowth Is the Result of the Scoliotic Mechanism and Is Located in the Disc

The regional anterior-posterior length discrepancy has been described extensively in *idiopathic* scoliosis, but not in scoliosis *with known origin*.[2, 3, 52-55] If the same 'anterior overgrowth' is found around the apices in the secondary curves of non-idiopathic scoliosis as well, this so-called 'anterior overgrowth' may be a consequence of a more generalized pathoanatomy of scoliosis, rather than its cause.

Does the regional anterior-posterior length discrepancy in idiopathic scoliosis differ from other types of scoliosis?

Chapter 7. Anterior-Posterior Length Discrepancy of the Spinal Column in Adolescent Idiopathic Scoliosis - a 3D CT Study

Relative anterior spinal overgrowth, as observed in the apical regions of the spine, has been suggested as part of the etiopathogenetic mechanism of AIS.[2, 3] The role of the posterior structures of the spine has not yet been studied, so relative anterior lengthening can still be the result of an active disturbance of the growth in height of the laminae, or, alternatively, of passive compression of the interlaminar or interspinous space. This raises the question:

Is the regional anterior-posterior length discrepancy in AIS the result of relative anterior lengthening or relative posterior shortening?

Chapter 8. What is the actual 3D Representation of the Rib Vertebra Angle Difference (Mehta's angle)?

Since we learned from previous studies that the 3D pathoanatomy of the apex of AIS is a regional rotated lordosis, this may have an impact on the representation of the spine and trunk deformity on 2D conventional radiographs. To date, several radiographic parameters to predict the progression of the curve have been described in the literature.[3, 10, 31, 41] In 1972, Mehta introduced the RVAD, which is still widely used as a prognostic factor for progression of early onset idiopathic scoliosis.[41] The curve was shown to be at high-risk for progression if the difference of the angle between the convex and concave apical ribs as compared to the vertebral body exceeds 20°. Because of its prognostic value, the RVAD has been studied widely in early onset, as well as AIS and it has been suggested that the drooping ribs on the convex side could result in decreased stability of the spine.[91-101] After the studies in chapter 2 and 4-7, it was clear that in AIS, there is a 3D deformation of the spine, which also affects the complete trunk. From observations in previous studies, it was hypothesized that the 2D Metha's angle in AIS is just a representation of the complex 3D spinal deformation without significant changes in segmental costovertebral orientation. This resulted in the question:

Are the rib-vertebral junctions asymmetrical in adolescent idiopathic scoliosis, when assessed in 2D and 3D, and do they represent the 3D spinal deformation?

Chapter 9. Upright, Prone, and Supine Spinal Morphology and Alignment in Adolescent Idiopathic Scoliosis

The 3D pathoanatomy of AIS may also have an impact on the representation of the spine when loaded in different directions, thus with the body in different positions. Periodical radiographic follow-up is traditionally performed using posterior-anterior and lateral radiographs.[11, 57] In addition, MRI and CT is frequently used to obtain more in-depth information about neuroaxis and bony architecture abnormalities. Radiographs are mostly made in upright position, whereas the MRI and CT are mostly made in prone or supine position. However, the relationship between the 3D measurements in these different imaging methods and body position remained unclear, so far. In chapter 9, the answer to the following question is described:

Does the 3D morphology of the AIS spine differ between upright, prone and supine position?

Chapter 10. Spinous Processes and Transverse Processes Measurements of the Scoliotic Spine and their Relation to the Cobb angle: a CT Based Study

The coronal Cobb angle, measured on conventional radiographs, is the most widely used parameter for assessment of AIS severity and is based on the endplates of the vertebral bodies.[11] However, Simony et al. described a five times higher overall cancer rate in a Danish AIS population, as compared to age-matched controls, due to radiation exposure.[12] 3D ultrasound imaging of the spine, as a radiation-free alternative method of measuring spinal curvature, has gained growing attention and its feasibility has been demonstrated in several recent studies.[66, 69] However, using ultrasound, the vertebral endplates are not visible and other, more posterior located structures, are used to measure the curve severity. The exact anatomical relation between the posterior elements (SP and TP), which are visible by ultrasound, and the orientation of the vertebral bodies in AIS has been evaluated on high-resolution 3D CT scans, to formulate an answer to the question:

What are the differences in curve severity measurements, based on different anatomical vertebral structures as used in ultrasound of the spine?

Chapter 11. A Reliability and Validity Study for Different Coronal Angles using Ultrasound Imaging in Adolescent Idiopathic Scoliosis

Several *in-vitro* and *in-vivo* studies compared the ultrasound spine deformity measurements to the traditional Cobb angle on radiographs in AIS.[62-67, 69, 70] However, it remained unclear whether the coronal ultrasound angles are stable and consistent (reliability) and which angle is the most appropriate method to measure the severity of the curve (validity), resulting in the question:

Does the curvatures on ultrasound images of AIS patients correspond with the curvatures on radiographs?

Chapter 12. Surgical Outcomes of Anterior versus Posterior Fusion in Lenke Type 1 Adolescent Idiopathic Scoliosis

To halt AIS curve progression, correct the deformity and restore the 3D spinal alignment, two surgical approaches have been described to access the spine in AIS, either an anterior or posterior approach.[102-108] Both approaches enable the surgeon to stop the progression and correct the curve, but both had their own advantages and disadvantages. For clinical decision making, the next question had to be answered:

What are the differences in 2D, 3D and patient reported outcomes between the anterior and posterior fusion of AIS?

Chapter 13. A CT Based Guideline for Pedicle Screw Placement in Adolescent Idiopathic Scoliosis

Pedicle screw fixation at multiple levels has become one of the most powerful techniques in spinal surgery for the 3D correction of AIS.[109-114] There is a lack of study of the

3D spatial orientation of the pedicle axis with reference to the neutral axis of the human body and an external neutral axis. Knowledge of these pedicle orientation and their 3D position with reference to internal and external landmarks, such as the operating table or the laminae, respectively, could serve as important guide for accurate pedicle screw orientation and placement during surgery, raising the question:

What is the intra-operative 3D pedicle orientation for pedicle screw placement in AIS?

Chapter 2

Etiologic Relevance of 3D Pathoanatomy of Adolescent Idiopathic Scoliosis

ABSTRACT.

Despite many years of dedicated research into the etiopathogenesis of adolescent idiopathic scoliosis, there is still not one distinct cause for this puzzling condition. By this overview we try to link knowledge on the complex three-dimensional pathoanatomy of AIS, based on our ongoing research in this field, to etiopathogenetic questions. Evidence from multiple recent cross-sectional imaging studies is provided that supports the hypothesis that AIS has an intrinsic biomechanical basis: an imbalance between the biomechanical loading of the upright human spine due to its unique sagittal configuration on the one hand and the body's compensating mechanisms on the other. What actually implies or induces this imbalance is the remaining enigma in the etiology of AIS, and is the focus of our ongoing research.

INTRODUCTION

Scoliosis is a three-dimensional (3D) deformity of the spine and trunk that primarily affects previously healthy children. It is a classic orthopedic disorder.[1] The most common type of scoliosis is *idiopathic* scoliosis. The term 'idiopathic' (from the Greek: ίδιος=one's own and πάθος=suffering) indicates that the disease is not linked to any physical impairment or previous medical history. Despite many years of dedicated research into the etiopathogenesis of idiopathic scoliosis, there is not one distinct cause for this condition, and a number of intriguing questions remain.[10, 115] The purpose of this study is to provide, based on our ongoing research into the etiopathogenesis of idiopathic scoliosis, answers to some of these questions, namely:

I. *Why is scoliosis a disease of man?*
II. *Why are thoracic curves predominantly right convex in adolescents, but left convex in infantiles?*
III. *What is the role of relative anterior spinal overgrowth (RASO)?*

I.   Why is scoliosis a disease of man?

Idiopathic scoliosis appears to occur exclusively in humans, it has not been observed in any other mammalian.[13] Other spinal deformities have been observed or created in animals, but they either have iatrogenic, post-traumatic, neuromuscular or congenital etiologies. Why is that?

The essential difference between man and all other vertebrates is not any major difference in spinal architecture. This is relatively uniform throughout all species, with broad vertebral endplates and discs to withstand axial loading, and posteriorly located synovial joints and protuberances for muscle and ligament attachment to withstand anteriorly directed shear loads. Nor is it the fact that man is bipedal, there have always been many bipedal species, starting with most dinosaurs. Human posture and locomotion, however, is different from all other vertebrates, quadrupedal and bipedal alike, in two aspects:

1. The uniquely human pelvic lordosis, also known as a lordotic angulation between the ischial and iliac bones,[14, 15, 18, 116] and
2. The ability to simultaneously extend both hips and knees.[117]

Man, unlike any other species, actually has *three* well developed lordosis throughout its spine, at least after infancy, one between the iliac and ischial bone, one in the lumbar area and one in the cervical area. It is generally accepted by anthropologists that human habitual bipedalism, as well as sagittal spino-pelvic alignment can be attributed to the morphological changes of the pelvis in human evolution.[15, 118] In the earliest hominid specimen to date, an *Australopithecus afarensis* that was found in Ethiopia (also known as 'Lucy'), as well as in other hominids, anthropologists observed that angulation of

the ilium relative to the ischium, enabled upright human locomotion.[119] Even in human's closest relatives, the bonobo's and chimpanzees, there is almost no angulation between the ischium and ilium (Figure 1). When a primate tries to stand upright, the trunk simply swings up on the femoral heads to a point that the ischium points almost directly downward. For energy-efficient human bipedal locomotion, however, lordotic angulation of the ilium relative to the ischium, increasing the lever arm of the ischio-crural muscles, was a prerequisite to be able to walk fully upright.[15-17] This resulted in an increase of the ischio-iliac angle and pelvic incidence during human evolution.[14, 15, 18, 116] This, in combination with the ability to fully extend hips and knees at the same time, makes man the only species to consistently carry the body's center of gravity straight above the pelvis, rather than in front (Figure 1). This poses unique biomechanical loads on the human spine that have been shown to lead to a reduction of rotational stiffness of certain exposed segments.[5, 7, 8, 120]
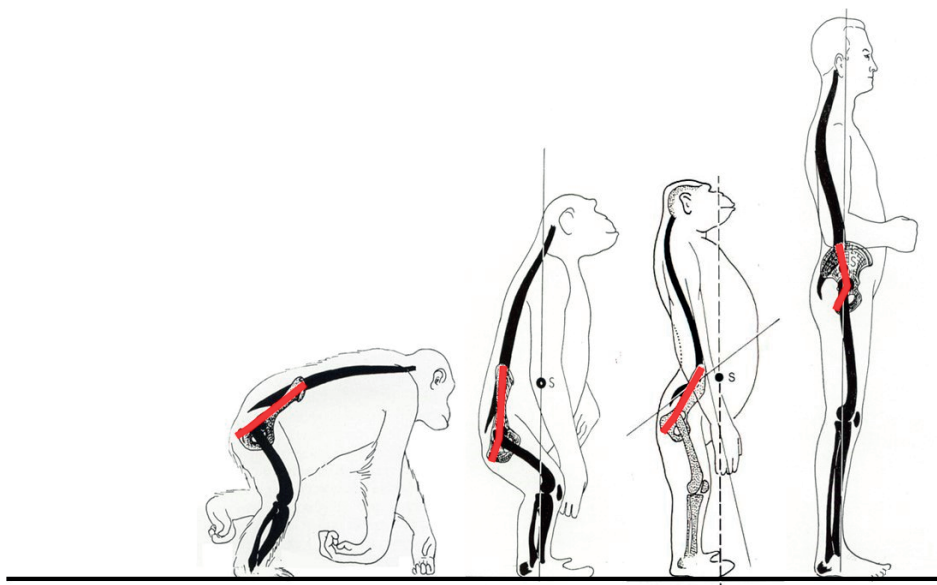
Figure 1. *Hominoidae* (great apes) typically display a 'bent-hip, bent-knee' posture during bipedal locomotion. Due to a backwards-bent pelvic axis (red lines), only humans are able to stand upright.[14, 116]

Previous work by Vercauteren in 1980 and Castelein et al. in 2005 has clarified that a certain area of the human spine in the upright position is posteriorly inclined and affected by posteriorly directed shear loads.[7, 120, 121] From this perspective, Janssen et al. showed that posterior shear loads act on all posteriorly inclined segments of the spine as determined by each individual's sagittal profile (Figure 2).[120, 122] In an experimental setup, Kouwenhoven et al. have shown that an excess of posterior shear loads results in dimin-

ished rotational stiffness of spinal segments.[5] Therefore, the more the spine exhibits areas with posteriorly tilted vertebrae, the more these segments are prone to develop a rotational deformity, in other words scoliosis.[7, 8] Since then, variation in sagittal alignment of the spine is increasingly recognized in relation to the etiopathogenesis of spinal deformities.[123-125]

Pediatric spinal deformities have a well-known age-related preference and gender-related distribution.[126-129] For example, AIS develops most frequently in girls around the adolescent growth spurt. To test the hypothesis that the spine in which a rotational deformity has a chance to develop, is based on differences in sagittal spino-pelvic alignment and makes a child prone to develop a rotational deformity, Schlösser et al. analyzed sagittal spino-pelvic alignment of 156 non-scoliotic children before, at and after the peak of pubertal growth.[130, 131] The results showed that the thoracic kyphosis, pelvic tilt and pelvic incidence increase during growth and that before and at the peak of the growth spurt, a greater number of vertebrae are more posteriorly inclined as compared to after the growth spurt. Moreover, the spines of girls at the peak of the growth spurt showed more posterior inclination and a smaller thoracic kyphosis as compared to boys. This implies that in girls around the peak of the growth spurt the spine is subject to greater posteriorly directed shear loads, and thus shows less resistance to rotation. This can explain why AIS - under still undetermined circumstances during growth - occurs more in girls than in boys. In addition, it can be inferred that thoracic AIS develops in a different sagittal profile as compared to (thoraco)lumbar AIS. From a multicenter database of almost 1400 AIS patients, all lateral radiographs were reviewed of children with an established, but still very small (Cobb angle smaller than 20 degrees) thoracic (Lenke 1 and 2, n=128) and (thoraco) lumbar AIS (Lenke 5, n=64). Systematic analysis of the sagittal

Figure 2. The sagittal spino-pelvic configuration of the double-S shaped human spine in relation to the pelvis determines whether individual verte-brae are subject to either an anteriorly directed, or a posteriorly directed vec-tor (as a vector of the axial loading). In the figure the segments that are affected by posterior shear load-ing, between the apex of the thoracic kyphosis and lumbar lordosis, are shown in red.

profile and exact inclination of each individual vertebra revealed that already at this very early stage, the thoracic kyphosis and posterior inclination of thoracic AIS differs significantly from (thoraco)lumbar AIS as well as from controls.[77, 132, 133] More precise, in thoracic scoliosis most thoracic vertebra were more backwardly inclined as compared to (thoraco)lumbar scoliosis and vice versa. This difference in sagittal profile was shown to already exist at a very early stage of the development of the rotation and the curvature,
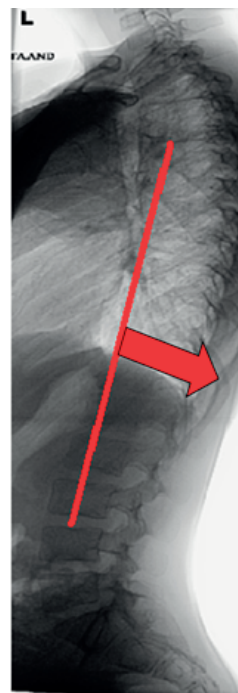
and thus can be postulated to play a role in the pathogenesis of the different curve types.

The pelvis is the key regulator of sagittal spino-pelvic balance. Despite the differences in sagittal spinal alignment between thoracic and lumbar scoliosis, Mac-thiong et al. and Farshad et al. were not able to proof a statistically significant difference in sagittal pelvic anatomy between patients affected by different degrees of thoracic and (thoraco) lumbar scoliosis, using conventional radiographs.[77, 134] Moreover, Schlösser et al. had identical results for the parameter "pelvic incidence" in a population of Lenke type 1 and 5 AIS patients with curves with a Cobb angle less than 20 degrees. Recently, however, Pasha et al. introduced novel pelvic parameters based on 3D reconstructed radiographs and Vrtovec et al. developed a 3D measurement method for "pelvic incidence" on 3D CT scans, demonstrating the improved accuracy of these methods as compared to the traditional measurements on plain lateral radiographs.[82, 135] Using this 3D measurement method, Brink et al. found greater pelvic incidence in a small population of thoraco(lumbar) AIS curves as compared to thoracic curves and controls.[136] Therefore, their findings are consistent with previous theories, suggesting a link between sagittal pelvic anatomy, sagittal spino-pelvic alignment and the development of different curve types in AIS.

II. Why are thoracic curves predominantly right convex in adolescents, but left convex in infantiles?

The most prevalent curve type in AIS is a right convex main thoracic curve with compensatory high-thoracic and (thoraco)lumbar curves to the left.[40] In contrast to adolescent scoliosis, the main thoracic curve in infantile idiopathic scoliosis rotates and deviates far more often to the left, whereas in juvenile idiopathic scoliosis this pattern is more evenly distributed between right and left.[137]

As has been appreciated for a long time, the normal, non-scoliotic spine is also not a symmetrical structure.[138] In 2006, Kouwenhoven et al. demonstrated the presence of an axial rotational pattern in the normal human spine, that is similar to what is seen in the most prevalent curve patterns in idiopathic scoliosis.[139, 140] In 2014, we measured the rotation of each individual thoracic vertebra on CT scans in 146 asymptomatic children (the scans had been taken for reasons other than the spine such as pulmonary disease, poly-trauma, malignancy, not for the purpose of this study). Statistical analysis revealed significant differences in the rotational patterns of the spine between non-scoliotic infantiles, juveniles and adolescents: at the infantile age the spine was rotated to the left at all thoracic levels, at the juvenile age thoracic vertebra were oriented in the midline. In contrast, at the adolescent age the mid- and low thoracic levels (T6-T12) were significantly rotated to the right.[141, 142] Therefore, our analyses of non-scoliotic vertebral columns at different ages shows that transverse plane asymmetry is also a normal fea-

ture of the pediatric spine. Furthermore, the different rotational patterns between the infantiles, juveniles and adolescents in this study match the rotation and convexity of the curve as is normally seen in idiopathic scoliosis. Recently, the hypothesis that the convexity of the curve in idiopathic scoliosis is determined by organ distribution was confirmed in 2017 by Schlösser et al.: they screened a unique population of primary ciliary dyskinesia patients with and without situs inversus totalis for scoliosis, retrieved 16 patients with this unique combination and found a 94% match between organ distribution and scoliosis curve convexity.[143]

In contrast to the normal spine, it has been appreciated for a long time that the scoliotic spine is a completely asymmetrical structure (1). That was based on scoliotic specimens and experimental studies that have shown that asymmetrical growth of the neurocentral junctions of the vertebrae leads to vertebral rotation; in more detail, unilateral lag screw epiphysiodesis of the neurocentral junctions in a growing pig was shown to lead to transverse asymmetry and a rotational deformity, similar to AIS.[2, 144] In man, the growth plate of the pedicles, also known as the neurocentral junctions, however, close before the age of eight, suggesting that any asymmetry should start before that age.[142] In 2017, Brink et al. studied the transverse anatomy of the vertebrae in severe AIS reported the asymmetry of both the vertebral bodies and pedicles, in a population of moderate to severe AIS patients and non-scoliotic controls, in the true transverse plane, using 3D multiplanar reconstruction of high-resolution CT scans for each individual vertebra.[145] They observed that even in non-scoliotic controls a certain degree of vertebral body asymmetry exists, but the asymmetry was slightly more pronounced in AIS; the concave pedicles of the thoracic primary curves were slightly (0.4 mm) thinner and longer (1.8 mm) than for the convex pedicle, especially around the apex. Interestingly, the observed asymmetry was considerably smaller than previously described.[146-148] Additionally, no direct correlation was found between the degree of asymmetry, the magnitude of the Cobb angle or the amount of rotation of the apex in these moderate to severe AIS curves. In summary, because there is almost no asymmetry in the true transverse plane in AIS, it suggests that asymmetrical growth is not the driver for rotation in AIS.

III. What is the role of relative anterior spinal overgrowth (RASO)?

a. Global 3D alignment of adolescent idiopathic scoliosis

The Scoliosis Research Society defines scoliosis as a lateral curvature of the spine of more than 10 degrees in the coronal plane.[28] This formal definition denies the fact that it is actually a complex 3D spinal deformity. Already in the late nineteenth and early twentieth century, using cadaver specimens, anatomists carefully described that adolescent idiopathic scoliosis involves changes in the coronal, transverse as well as the sagittal plane: in the coronal plane it is characterized by lateral deviation and lateral bending, in the transverse plane by axial rotation, asymmetrical growth of the pedicles and asym-

metrical closure of the neurocentral cartilages and in the sagittal plane by lordosis of the apical segments and hypertrophy of the facet joints.[1, 29, 89] A typical feature of the curves in AIS is the coupling between the phenomena in the three different planes. In 1952, Somerville and Roaf described that during the development of AIS the vertebral bodies rotate away from the midline toward the convexity, to a more lateral position than the posterior elements of the spine.[2, 46] By definition, axial rotation towards the convexity of the curve leads to a spinal column that is latero-flexed and is longer anteriorly than posteriorly, in other words, rotated lordosis of the apex. With the advent of radiography, unfortunately scoliosis gradually became regarded as a coronal plane deformity, until a number of authors re-emphasized the importance of the sagittal plane.[2, 46, 47, 51, 149] Because of the rotated apical lordoses in AIS, Stagnara introduced *le plan d'election*, a rotated view to evaluate the true coronal profile of the apical segments of the curvature.[39] Using its equivalent in the sagittal plane, in 1984 Dickson et al. observed in 70 AIS patients that instead of a normal thoracic kyphosis, 75% of the AIS curves were lordotic, 24% were straight and only 1% kyphotic.[47, 51] Ultimately, this has led to the assumption that idiopathic scoliosis may be a problem of generalized anterior overgrowth of the whole spine, or a discrepancy of growth of the spinal cord as compared to growth of the vertebrae.[52, 55, 150-152]

Although the 3D aspect of AIS has been studied for over a century and has been given much attention in recent years in the literature, the true 3D morphology, and especially the sagittal deformation, of the different areas of the scoliotic spine has only recently been described in detail. This overview summarizes the findings of recent 3D studies on a unique dataset of AIS cases that had undergone high-resolution computed tomographic imaging of the spine preoperatively for navigation purposes. The scans were analyzed using special software to generate complete 3D reconstructions and describe the 3D deformation of different regions of the spine in AIS patients in the coronal, transverse and true sagittal plane in great detail (Figure 3). Interestingly, quantitative description of the 3D morphology of AIS revealed that (1) the global 3D development of AIS curves follows a rather uniform pattern with coupling of the different aspects of the deformity in all three planes and that (2) all AIS curves, structural as well as non-structural, primary as well as compensatory, thoracic as well as (thoraco)lumbar, were characterized by greater anterior length (on average 4.1%) measured from Cobb end vertebra to Cobb end vertebra.[50] The junctional segments in-between the curves were more or less straight.

This so called relative anterior spinal anterior overgrowth, or non-synchronous anterior-posterior growth, has been considered as part of the etiologic mechanism of idiopathic scoliosis.[1, 46, 47, 50, 53] However, our recent research has shown that neuromuscular scoliosis demonstrates the same pattern of relative anterior spinal anterior overgrowth as idiopathic scoliosis.[49] This suggests that anterior lengthening of the spine is part of a

more generalized mechanism that is the consequence of the curvature, not its cause.

b.   Segmental 3D morphology of adolescent idiopathic scoliosis

There is an ongoing debate on the development of the excess of anterior spinal length in AIS. In two-dimensional radiographic studies on AIS, contradictory findings have been reported on the individual contribution of the vertebral bodies as compared to the discs to the coronal deformity.[31-38] Because the spinal column in AIS, unlike the normal situation, is longer anteriorly than posteriorly, it has been hypothesized that AIS is the result of active anterior overgrowth of the vertebral bodies, or reduced posterior growth by posterior tethering.[52, 55] Furthermore, disorders of bone metabolism have been suggested to play an etiological role. From our etiological perspective, however, the anterior-posterior length discrepancy in AIS is secondary to axial rotation. Therefore, we addressed the important question in which anatomical structure and in which plane the deformity starts in AIS. We used the same series of high-resolution CT-scans and software as used for the study presented above and investigated at the segmental level whether the 3D deformation of the spine

Figure 3. A posterolateral view that represents a true lateral view of the apical thoracic region of a complete 3D reconstruction of an adolescent idiopathic scoliosis patient demonstrating the that the thoracic curvature is a rotated lordosis.

in AIS is predominantly localized in the vertebral bodies (as a result of active growth) or the discs (as a secondary phenomenon to axial rotation). Segmental parameters were determined for each individual disc (total n=924) and vertebra (total n=1078) between T4 and L5. Interestingly, in contrast to previous studies, in scoliosis the intervertebral discs were at least three times more deformed in the coronal, true transverse and true sagittal plane than the vertebral bodies.[35, 37] Anterior-posterior and coronal wedging was more pronounced at the apices of the curves, whereas mechanical torsion was found in all regions of the spine. Most of the excess anterior length in the scoliotic thoracic spine, both in idiopathic as well as in neuromuscular cases, appeared to be caused by a substantial difference in height of the anterior portion of the disc compared to its posterior aspect, whereas the vertebral bodies showed almost no relative anterior overgrowth
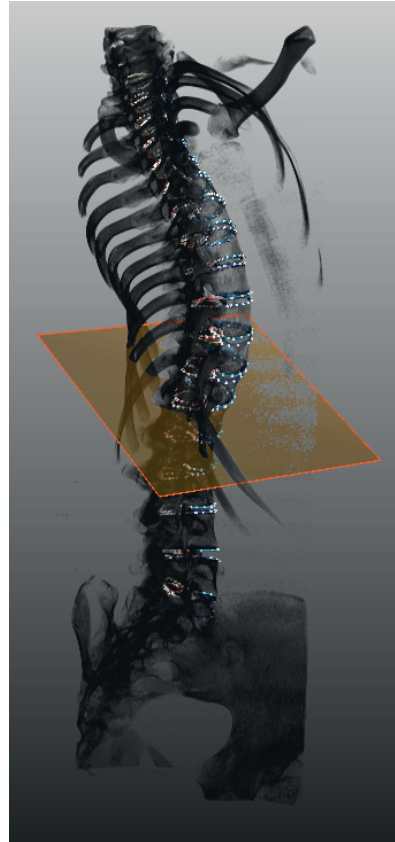
Figure 4. A cranio-caudal view on a 3D reconstruction of the spino-pelvic complex of an adolescent idiopathic scoliosis patients demonstrating the complex rotational pattern of the rotated apical segments.

compared to normal children.[44, 49] Conclusions from this and the previous study are that excess of anterior length is not a global, but rather a regional phenomenon, and that, since the deformity is much more in the disc than in the bone, it seems more of a passive phenomenon than an active growth process. The anterior wedging of the discs could be a mechanical effect caused by unloading of the anterior spine by its position rotated away from the midline in both types of scoliosis.

CONCLUSIONS

In this overview, evidence from multiple cross-sectional imaging studies is provided that supports the hypothesis that rotational stiffness of the human spine in general is less than in all other species due to the existence of destabilizing posteriorly directed shear load that are the result of the unique spino-pelvic alignment of the human spine. Under certain, still ill-defined, circumstances, the delicate balance that normally exists between these rotation-inducing forces, and the body's compensating mechanisms, can be disturbed during the vulnerable period of the growth spurt. We showed that, amongst many other things, also spino-pelvic alignment changes rapidly during puberty, and in a different manner between boys and girls. This may lead to the rotatory decompensation, that we call scoliosis. Our studies also demonstrated that, once the spine decompensates into this rotational deformity, it will follow the pre-existent rotational pattern that also exists in the normal, non-scoliotic spine. This process of rotation away from the midline, in which the posterior structures stay behind, ultimately leads

to the development of a rotated, apical lordosis. This lordosis, or excess anterior length, takes place predominantly in the soft tissues and not in the bone, there is no evidence of an actual disturbance of bony growth. Rather, the discs expand in their anterior aspects and the interlaminar and interspinous soft tissues are compressed posteriorly with the facet joints as a fulcrum, the process resembles passive extension of the normal spine. We can conclude that AIS has an intrinsic biomechanical basis: An imbalance between the biomechanical loading of the upright human spine (i.e. posteriorly directed shear loading) on the one hand and the body's compensating mechanisms on the other.

The question remains: "What underlying mechanisms and structures influence rotational stability of the spine and predisposes the spine of otherwise healthy children to decompensate into a rotational deformity, while the spine of other children stays unaffected?" In one of our studies, it was found that the geometry of the intervertebral disc is most affected in AIS as compared to the vertebral bodies. Moreover, this structure possibly plays a key role in the rotational stability of the pediatric and adult spine. From our perspective, as a first step to answer this question, factors that influence the rotational stability of the intervertebral discs should be elucidated, this is at present the focus of our continuing studies.

Chapter 3

Three-Dimensional Pelvic Incidence is Much Higher in (Thoraco)Lumbar Scoliosis Than in Controls

ABSTRACT

Purpose. The pelvic incidence (PI) is used to describe the sagittal spino-pelvic alignment. In previous studies, radiographs were used, leading to less accuracy in establishing the three-dimensional (3D) spino-pelvic parameters. The purpose of this study is to analyze the differences in the 3D sagittal spino-pelvic alignment in adolescent idiopathic scoliosis (AIS) subjects and non-scoliotic controls.

Methods. Thirty-seven female AIS patients that underwent pre-operative supine low-dose computed tomography imaging of the spine, hips and pelvis as part of their general work-up were included and compared to 44 non-scoliotic age-matched female controls. A previously validated computerized method was used to measure the PI in 3D, as the angle between the line orthogonal to the inclination of the sacral endplate and the line connecting the center of the sacral endplate with the hip axis.

Results. The PI was on average 46.8±12.4° in AIS patients and 41.3±11.4° in controls (p=0.025), with a higher PI in Lenke type 5 curves (50.6±16.2°) as compared to controls (p=0.042), whereas the Lenke type 1 curves (45.9±12.2°) did not differ from controls (p=0.141).

Conclusions. Lenke type 5 curves show a significantly higher PI than controls, whereas the Lenke type 1 curves did not differ from controls. This suggests a role of pelvic morphology and spino-pelvic alignment in the pathogenesis of idiopathic scoliosis. Further longitudinal studies should explore the exact role of the PI in the initiation and progression of different AIS types.

INTRODUCTION

Upright human spinal biomechanics and the sagittal shape of the spine play an important role in the development and progression of spinal deformities such as adolescent idiopathic scoliosis (AIS).[3, 7, 47, 81, 116, 153, 154] In 1985, During et al. described the pelvic sacral angle and later on, Duval-Beaupère et al. used the term pelvic incidence (PI) for a parameter that defines the relationship between the pelvic anatomy and spinal alignment.[20, 21] Several other authors described the spino-pelvic balance in normal children and adolescents during growth and in patients with different pathologies.[14, 23, 56, 77-86] Dickson et al. described that differences in the sagittal plane (reversal of the normal thoracic kyphosis) during growth could initiate a progressive idiopathic scoliosis [47]. Moreover, previous authors suggested a link between the spino-pelvic morphology and spinal deformities in the sagittal plane.[14, 23, 56, 77-86] Most of the previous studies obtained two-dimensional (2D) referential values using standing lateral radiographs that could lead to a deviation from the true sagittal plane and, to a certain degree of distortion of the image. Three-dimensional (3D) images are not affected by the characteristics of radiographic imaging, like the projection plane, and can thus better observe the relationship between the sacrum, pelvis, and hips.[87] Pasha et al. introduced novel pelvic parameters based on 3D reconstructed radiographs, and Vrtovec et al. measured the 3D PI in a non-scoliotic population using computed tomography (CT) scans, demonstrating the improved accuracy of this method as compared to the traditional measurements on plain sagittal X-rays.[82, 87] In previous studies, the exact difference in pelvic morphology between AIS subjects and non-scoliotic controls has remained unclear. Therefore, the purpose of this study was to analyze, using a previously validated accurate 3D technique, the differences in sagittal pelvic morphology between AIS patients and asymptomatic adolescents.

MATERIALS AND METHODS

Study population

This study, the purpose of which is, to analyze the differences in 3D sagittal pelvic morphology between AIS patients and non-scoliotic controls, has been approved by the local research ethics committee. Female patients with thoracic right convex and (thoraco)lumbar left convex AIS requiring surgery between August 2009 and May 2018 were included (demographics in Table 1). All had underwent pre-operative supine low-dose (20-times lower than that of a standard CT scan) CT imaging of the spine at two institutions (Linkoping and Malmö, Sweden).[155, 156] The low-dose CT scan is part of the standard pre-operative protocol in both centers. Patients were included if, in addition to the spine, both femoral heads were visible on the CT scan. Subjects with other spinal

pathologies, a left convex thoracic/right convex (thoraco)lumbar curve and/or previous spinal surgery were excluded. Curve characteristics, including the Cobb angle, thoracic kyphosis (TK: T4-T12) and lumbar lordosis (LL: T12-S1) were determined on the conventional posterior-anterior and lateral radiographs as well as on digitally reconstructed lateral radiographs (DRRs) of the supine CT scans (Table 1). To represent the normal population, a second group was included that consisted of non-scoliotic age-matched female subjects that were selected from a pre-existing database who had undergone CT imaging of the thorax and abdomen for indications other than spinal pathology (for example trauma screening). The non-scoliotic observed cohort was assumed to represent a normal population, since a number of subjects were already excluded from the original cohort due to clinical or radiological evidence of pathology or trauma, evidence for anatomical anomalies, etc.

		AIS patients (n=37)	Controls (n=44)
Age	Range	12 - 21 years	12 - 21 years
	Mean ± SD	15.4 ± 2.4 years	15.4 ± 2.9 years
Females	Number (ratio)	37 (100%)	44 (100%)
Thoracic curve right convexity	Number (ratio)	37 (100%)	/
Thoracic Cobb angle	Range	21 - 84°	/
	Mean ± SD	50.3 ± 14.6°	/
(Thoraco)Lumbar Cobb angle	Range	19 - 78°	/
	Mean ± SD	46.5 ± 13.8°	/
Lenke curve	Type 1	Number (ratio) 21 (57%)	/
	Type 2	Number (ratio) 1 (3%)	/
	Type 3	Number (ratio) 2 (5%)	/
	Type 5	Number (ratio) 9 (24%)	/
	Type 6	Number (ratio) 4 (11%)	/

Table 1. Demographics for all included adolescent idiopathic scoliotic (AIS) patients and controls. Curve characteristics, measured on upright lateral radiographs, are also shown for AIS patients. SD = standard deviation.

Pelvic incidence measurement

The PI is defined as the angle between the line orthogonal to the inclination of the sacral endplate and the line connecting the sacral endplate with the hip axis (Figure 1). On standard lateral radiographs there is always a deviation from the true sagittal plane leading to a certain degree of distortion of the image.[87, 88] The variability of the semi-automatic 3D PI measurement method was 0.8°, whereas the variability of the PI from radiographs was reported to be between 3° and 6°.[87] For the previously validated 3D method, the center of both femoral heads, as well as the center and inclination of the

sacral endplate were used to calculate the PI.[87] First, the femoral heads and the sacral endplate were manually selected to initialize the computerized method by defining the locations of the volumes of interest on the 3D image. Next, the computerized method automatically determined the exact centers of the femoral heads in 3D from the spheres that best fit to the 3D edges of the femoral heads. This created the true sagittal plane of the pelvis. The exact center of the sacral endplate in 3D was then automatically determined by locating the sacral endplate and finding the midpoint of the lines between the anterior and posterior edge and between the left and right edge of the endplate. The previously described computerized model was used to measure the PI in 3D images, based on previously validated image processing techniques, as the angle between the line orthogonal to the inclination of the sacral endplate and the line connecting the center of the sacral endplate with the hip axis (Figure 1).[87] The reliability of the analysis method was previously determined, where a high consistency between manual and computerized pelvic incidence measurements (intraclass correlation coefficient: 0.961) and high interobserver reliability (0.994) were observed.[87]

Statistical analysis

Statistical analyses were performed using SPSS 22.0 for Windows (SPSS Inc., Chicago, IL, USA). Descriptive statistics were computed providing means, ranges and standard deviations. The PI of the patients with AIS and controls, as well as between Lenke type 1 and 5, curves with different apex levels and curves with different lumbar modifiers were compared using the unpaired t-test.[157] Pearson correlation coefficient (r) defined the relationship between the PI, Cobb angle, TK and LL. The statistical significance level was set at 0.05 for all analyses.

RESULTS

Population

CT scans of 43 pre-operative AIS patients contained the whole spine as well as both femoral heads. However, six subjects had to be excluded (five male patients and one patient with a left convex thoracic curve). The final study population consisted of 37 female AIS subjects with an average age of 15.4±2.4 years and 44 non-scoliotic age- and sex matched controls. Demographics and curve characteristics are shown in Table 1. Within the AIS groups, the Lenke type 1 patients were on average 15.4±2.3 years of age and the Lenke type 5 patients 15.8±3.1 years of age (p=0.699).
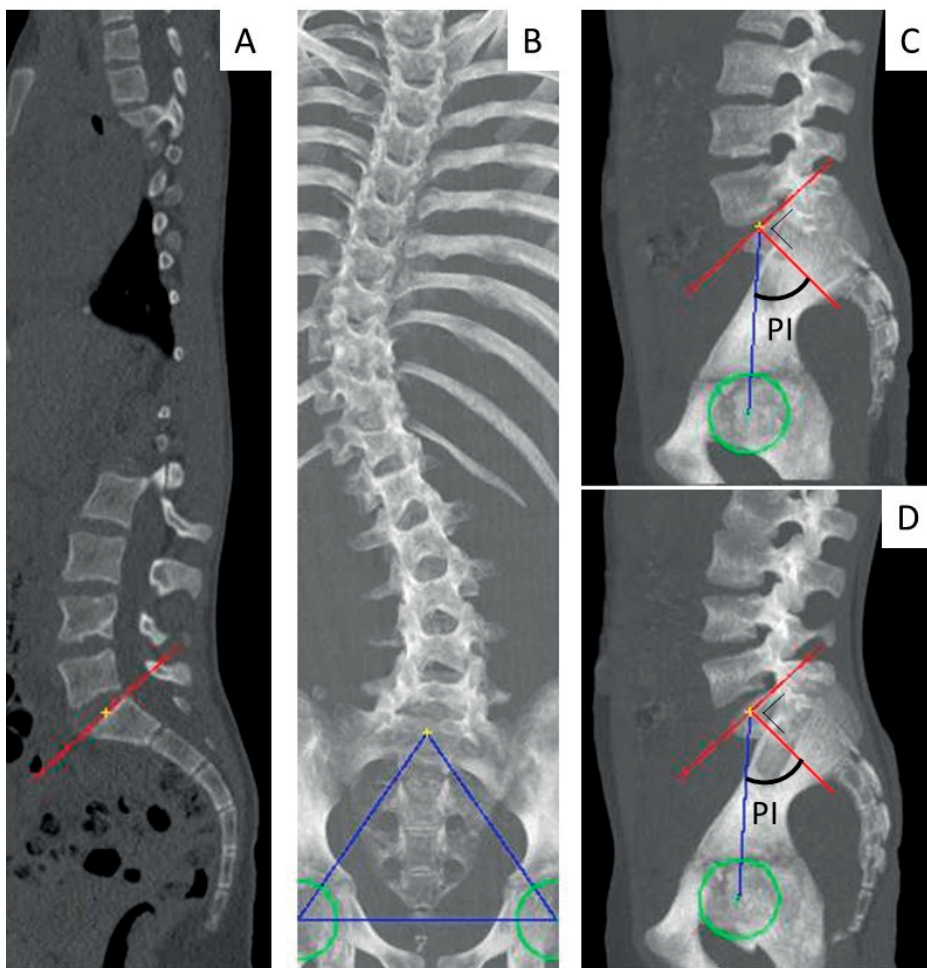
Figure 1. Computerized measurement of the pelvic incidence (PI) on a computed tomography scan. The center and inclination of the sacral endplate (A and B) and the centers of the left and right femoral heads (C and D) were used to calculate the PI. The computerized method automatically determined the exact centers of the femoral heads in three dimensions (3D) from the spheres that best fit to the 3D edges of the femoral heads. The exact center of the sacral endplate in 3D was automatically determined by locating the sacral endplate and finding the midpoint of the lines between the anterior and posterior edge and between the left and right edge of the endplate. The previously validated computerized method was used to measure the PI in 3D images, based on previously validated image-processing techniques, as the angle between the line orthogonal to the inclination of the sacral endplate and the line connecting the center of the sacral endplate with the hip axis [87].

Pelvic incidence

The PI was on average 46.8±12.4° in AIS and 41.3±11.4° in controls (p=0.025; Figure 2). The PI in the Lenke type 5 group was 50.6±16.2° and 45.9±12.2° in the Lenke type 1 group (p=0.384). A statistically significant difference was observed between the Lenke type 5

group and the controls (p=0.042), whereas the Lenke type 1 group and the controls showed no significant difference (p=0.141; Figure 2). No significant correlations were observed between the PI and the thoracic (r=-0.07, p=0.69) and lumbar Cobb angle (r=-0.15, p=0.36). The PI did not differ significantly (p≥0.053) between the curves with different lumbar modifiers; A (n=10), B (n=5) and C (n=6), according to the Lenke classification. No significant PI differences were seen between curves with different levels of the apex (thoracic: p≥0.769, lumbar: p≥0.298).

Sagittal alignment in AIS

Correlation analyses revealed moderate correlations between the LL (DRRs: 47.8±9.7° and radiographs: 58.2±11.1°) and PI (DRRs: r=0.60; p<0.001 and radiographs: r=0.64; p<0.001), however, no significant correlation was observed between the TK (DRRs: 18.9±6.7° and radiographs: 27.5±10.6°) and PI (DRRs: r=0.05; p=0.791 and radiographs: r=0.18; p=0.280). A moderate correlation was found between the TK and LL (DRRs: r=0.51; p=0.001 and radiographs: r=0.58; p<0.001).
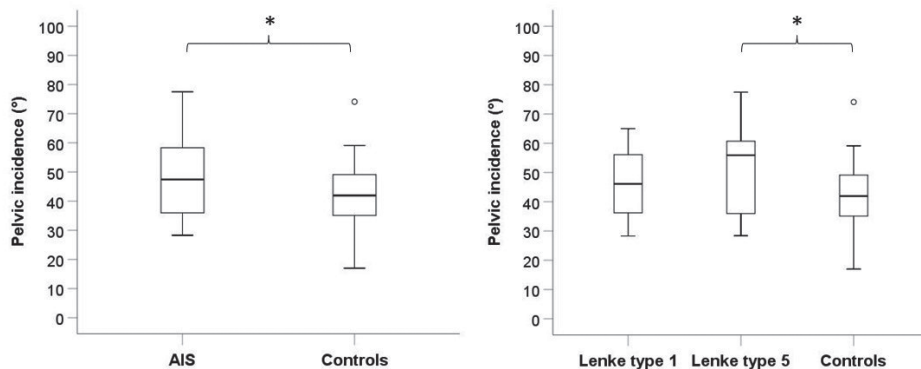
Figure 2. Boxplots of the pelvic incidence for (left) the patients with adolescent idiopathic scoliosis (AIS) and controls, and (right) the typical primary thoracic AIS curves (Lenke type 1), typical primary (thoraco) lumbar AIS curves (Lenke type 5) and controls. *=significant difference.

DISCUSSION

AIS is a disease of the human spine and trunk in which fully upright sagittal spinal biomechanics is known to play an important role.[3, 7, 47, 77, 81, 116, 133, 153, 154] Since its introduction in 1985, the PI has been used to describe pelvic morphology and its relation to the spino-pelvic alignment, as well as the relationship between the spino-pelvic alignment and spinal deformities.[20, 21, 77, 81] However, previous studies used predominantly 2D imaging, that could initiate a certain degree of distortion of the image and influences the

spino-pelvic measurements.[88] Therefore, the true relationship between the 3D pelvic morphology and spinal deformity has remained unclear up to now.[87]

Using the accurate 3D measurement on CT scans, the PI was on average higher in patients with a Lenke type 5 curve as compared to controls, whereas the PI in patients with a Lenke type 1 curve did not differ from controls. In previous studies, the mean PI varied between 41° and 49° for non-scoliotic adolescents and between 42° and 57° for AIS patients, using radiographs.[23, 56, 77, 80-82, 84-87, 158] In these studies, the patients with scoliosis had a moderate to severe thoracic curve (mean Cobb angles varied between 35-60°), however, Schlösser et al. included only mild curves (Cobb angle 20° or lower) and found similar results (PI for thoracic AIS patients: 47°, PI for (thoraco)lumbar AIS patients: 42° and PI for controls: 43°; without significant differences). It has been described that the PI in AIS is higher as compared to the non-scoliotic controls, however, others described no significant differences between AIS patients and non-scoliotic adolescents.[77, 80, 81, 84, 86, 133, 158] Slight PI differences among studies could be explained by the differences in age, since the PI increases with age, but also to the inaccuracy of the 2D method.[14, 159]

The 3D PI of the non-scoliotic population was already described by Vrtovec et al. and Schlösser et al.[14, 87] Pasha et al. introduced novel pelvic parameters, based on 3D reconstructed radiographs of AIS patients and controls.[82] However, the PI of AIS patients was only based on 2D radiographs, whereas the PI of our study was measured using low-dose CT data and a computerized method based on accurate image processing techniques.[87] Mac-Thiong et al. and Farshad et al. found that the scoliotic curve type was not associated with a specific pattern of sagittal pelvic morphology and balance.[77, 80] However, the results of the present study showed a higher PI in Lenke curve type 5 as compared to Lenke curve type 1. By using low-dose CT data and accurate image processing techniques, we were able to quantify the PI on 3D images with high accuracy and reproducibility in AIS patients *versus* controls. Using this 3D CT measurement method, bias due to image acquisition or subject positioning was avoided.

Radiographical measurements may be inaccurate due to the projective nature of radiograph acquisition, because it is usually impossible to obtain the superposition of the two femoral heads.[43, 87, 160] Moreover, the inclination of the sacral end plate in the sagittal plane may be altered by its architecture and inclination in the coronal plane. 3D reconstructed images are not affected by the characteristics of radiographic imaging and generates true sagittal views by aligning the centers of the femoral heads in 3D, resulting in a lower variability as compared to the radiographical measurements.[87] However, if the PI is measured from 3D CT images, it is important to consider that measurements in 2D radiographic images may be overestimated by approximately 5°.[87] CT measurements provide superior imaging precision, however this study does not imply that measurements of PI from plain radiographic images for clinical use should be replaced by CT.

The PI was correlated with the LL, but not with the Cobb angle or the TK. Most studies described a relation between the PI and the (thoraco)lumbar sagittal alignment, but not between the PI and the thoracic alignment.[23, 77, 80, 84, 86, 133, 160] This suggests that the PI influences the (thoraco)lumbar region of the spine, but the thoracic part is independent of the PI. However, the LL correlated with the TK, indicating that the TK is not completely independent of the PI. Additionally, we found a relation between the location of the curve, thoracic or lumbar, and the PI. The PI was higher in primary lumbar curves as compared to controls, whereas the primary thoracic curves did not differ significantly from the controls. This suggests a correlation between the PI and the pathogenesis of the scoliosis, even more because the PI is not influenced by the severity of the curve, suggesting that the PI is not influenced by spinal deformities. However, the exact role of the PI could not be determined in this cross-sectional study. In previous studies it was shown that an excess of posterior shear leads to a decrease in the rotational stiffness of the involved segments, that only posteriorly inclined vertebrae take part in the develop-ment of different scoliotic curve patterns, and that more posteriorly inclined vertebrae are rotationally less stable and could lead to initiation and progression of AIS.[5, 7, 23, 56] The facts that the PI was higher in AIS patients with primary (thoraco)lumbar curves as compared to controls, in contrary of patients with AIS with primary thoracic curves, is consistent with this theory and suggest that the PI is part of the etiopathogenesis of AIS as well as a determining factor for the curve type.

The examinations in this study were made in supine positions. Philippot et al. has shown that positioning (standing, supine or sitting position) does not influence the PI.[161] Because all scans were acquired pre-operatively only moderate to severe AIS curves, no mild AIS curves, were included in this study. Visualizing the femoral heads is not part of the standard low-dose (20-times lower than that of a standard CT for trauma) imag-ing protocol.[155, 156] Therefore, only a small number of scans could be included for the purpose of this study. Minor, not significant, differences were observed between the Lenke type 1 group and the controls and between the Lenke type 1 group and the Lenke type 5 group. Using an alfa error probability of 0.05, a power (1-beta error probability) of 0.80 and the means and standard deviations as described in this study, the power analysis showed a minimum sample size of 101 patients in each group to determine the differences between these groups. However, this study highlighted that the PI was higher in the Lenke type 5 curves, as compared to controls, whereas the Lenke type 1 curves did not differentiate from the normal anatomy.

CONCLUSION

Lenke type 5 curves show a significantly higher PI than controls, whereas the PI in Lenke type 1 curves did not differ from non-scoliotic controls. This suggests a role of pelvic morphology and spino-pelvic alignment in the pathogenesis of idiopathic scoliosis. Further longitudinal studies should explore the exact role of the PI in the initiation and progression of different types of idiopathic scoliosis.

Chapter 4

CT-Based Study of Vertebral and Intravertebral Rotation in Right Thoracic Adolescent Idiopathic Scoliosis

ABSTRACT

Background context. Adolescent idiopathic scoliosis (AIS) is a complex three-dimensional (3D) deformity of the spine and trunk. Although its exact etiology is still unknown, one of its characteristics is that the apical vertebra is the most rotated and translated away from the midline, into the convexity of the thoracic curve. A better understanding and quantification of this rotational mechanism is important to better understand the 3D development of the spinal deformity.

Purpose. To define the longitudinal rotation axis around which individual vertebrae rotate, and to establish the various extra- and intravertebral rotation patterns in thoracic AIS patients.

Study Design/Setting. Cross-sectional.

Patient sample. 70 high-resolution CT scans from an existing database of thoracic AIS patients (Cobb angle: 46-109°), acquired for spinal navigation, were included.

Outcome measures. Vertebral axial rotation, rotation radius, as well as intravertebral axial rotation and local mechanical torsion of the vertebral bodies.

Methods. First, the vertebral axial rotation and rotation radius were determined for each spinal level, using a previously validated image processing technique. Second, the intravertebral axial rotation (between the vertebral body and posterior elements) and local mechanical torsion (between the upper and lower endplate) of the vertebral bodies were calculated.

Results. For all levels, the longitudinal rotation axis, from which the vertebrae rotate away from the midline, was localized far posterior to the spine and became closer to the spine at the apex: apex, $r=11.5\pm5.1$ cm *versus* two levels above ($r=15.8\pm8.5$ cm; $p<0.001$) and two levels beneath ($r=14.2\pm8.2$ cm; $p<0.001$). The vertebral axial rotation, intravertebral axial rotation and local mechanical torsion of the vertebral bodies were largest at the apex ($21.9\pm7.4°$, $8.7\pm13.5°$ and $3.0\pm2.5°$) and decreased towards the neutral, junctional zones ($p<0.001$).

Conclusions. In idiopathic scoliosis, the vertebral bodies rotate away from their original position around an axis that is localized posterior to the spine with a distance to the spine that is maximum at the apical vertebra and gradually decreases away from the apex . The vertebral axial rotation is accompanied by smaller amounts of intravertebral rotation and local mechanical torsion, increasing towards the apical region. The altered morphology and alignment are important for a better understanding of the 3D pathoanatomical development of AIS and could help in better therapeutic planning for bracing and surgical intervention.

INTRODUCTION

Despite many years of dedicated research into its cause, no single etiological mechanism has been established for adolescent idiopathic scoliosis (AIS).[3, 10] One of its characteristics is that the apical vertebrae rotate away from the midline in a complex three-dimensional (3D) pattern.[2, 46] Earlier anatomical studies have looked at the longitudinal rotational axis of the normal spine, which is mostly located within the confines of the vertebral body, but the results were contradicting.[2, 22, 42, 162-172] The rotation of the vertebrae is part of the – to a large extent – unknown pathogenetic mechanism that leads to scoliosis Insight in the rotation mechanism of the different vertebrae within the curve and whether the rotation is mainly local (located within the vertebra: intravertebral axial rotation and local mechanical torsion), or a rotation of the whole segment (vertebral axial rotation), is important to help understand possible mechanisms of scoliosis development and a better description of the altered anatomy, could give more insights in the treatment of scoliosis. Therefore, the objective of this study is to systematically (according to the Scoliosis Research Society 3D Terminology of Spinal Deformity[173]) define all different extra- and intravertebral patterns of spinal rotation in the axial plane in idiopathic scoliosis patients: the vertebral axial rotation and the rotation radius, as well as the intravertebral axial rotation (the rotation between the vertebral body and posterior elements) and the local mechanical torsion (between the upper and lower endplate).

MATERIALS AND METHODS

Study population

This study has been approved by the local research ethics committees. Computed tomography (CT) scans of AIS patients were selected from an existing database, acquired for spinal navigation during posterior scoliosis surgery between 2011 and 2014.[157] All cases that were diagnosed with a primary thoracic (Lenke curve type 1-4) right-convex scoliosis were included.[40] By protocol, the complete pre-operative work-up consisted of standing posterior-anterior and lateral radiographs and supine bending radiographs, magnetic resonance imaging for screening of neural axis abnormalities and CT imaging. CT imaging (slice thickness of 0.625 mm, in-plane resolution of 0.352 mm/pixel, 64 Slice Multi-detector CT scanner, GE Healthcare, Chalfont, St. Giles, United Kingdom) was acquired in prone position. Children with spinal pathology other than AIS, incomplete work-up or previous spinal surgery were excluded. In order to maximize homogeneity of the study population and power of the analyses, only curves with the most prevalent apical levels (between T8 and T10) were included.[174] Demographics and basic curve characteristics were determined by one observer (Table 1).

		AIS (n=70)
Age (years)	Range	10-26
	Mean±sd	16.3±3.0
Girls, n (%)		59 (84%)
Thoracic curve convexity, n (%)	Right convex	70 (100%)
Cobb angle primary thoracic curve (°)	Range	46-109
	Mean±sd	68.8±12.4
Thoracic kyphosis (°)	Range	-5-45
	Mean±sd	26.2±10.3
Lenke type	I	37 (53%)
	II	21 (30%)
	III	9 (13%)
	IV	3 (4%)
Apex level primary thoracic curve	Thoracic 8	18 (26%)
	Thoracic 9	33 (47%)
	Thoracic 10	19 (27%)

Table 1. Demographics are shown for all included AIS patients. sd = standard deviation.

CT measurement method

Two trained observers used a semi-automatic image processing technique and software (ScoliosisAnalysis 4.1, Image Sciences Institute, Utrecht, The Netherlands, developed using MeVisLab, MeVis Medical Solutions AG, Bremen, Germany) to acquire complete spinal reconstructions in a 3D coordinate system. ScoliosisAnalysis 4.1 was described and validated in previous studies (Figure 1).[44, 175] Outcome parameters were defined according to the Scoliosis Research Society 3D Terminology of Spinal Deformity and were acquired using 3D segmentations of high-resolution CT scans.[173] The segmentation consisted of four steps. First, the observer drew a contour around the vertebral endplates and spinal canal which was corrected for coronal and sagittal tilt in order to reconstruct the true axial sections (Figure 1). Second, based on the contour drawn by the observer, the software calculated a center of mass (COM) of the vertebral body and spinal canal in 3D, taking account of angulation and displacement of each individual level in the coronal as well as sagittal plane (Figure 1). Third, a vertebral axis was automatically reconstructed through the COM of the vertebral body and spinal canal in the axial plane. Fourth, the intersection of the vertebral axis and the contours of the vertebral endplate created automatically an anterior and posterior point of the vertebral endplate and the observer segmented the lamina midpoint and the tip of the spinous process as well (Figure 1). The vertebral axis of the sacral endplate, which was considered to have no rotation or translation in thoracic scoliosis, was used as the reference plane for the vertebral axial rotation (Figure 2).[50, 176] Since the longitudinal rotational axis moves farther from the spine in less rotated vertebrae, it is difficult to determine accurately the true neutral
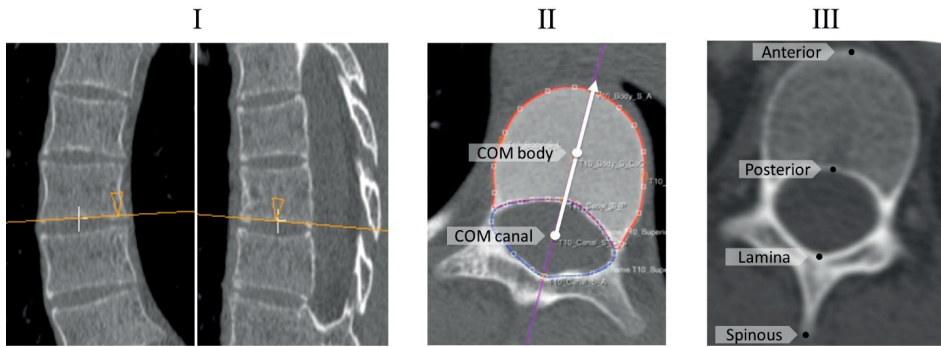
Figure 1. The orientation of the upper and lower endplate of each individual vertebra of the computed tomography scans was determined by using the semi-automatic software, correcting for coronal and sagittal tilt (I), to reconstruct the true axial sections. The observer drew a contour around the vertebral body and spinal canal (II). The software calculated a center of mass (COM) of the vertebral body and spinal canal and reconstructed a vertebral axis through these COMs (II). The intersections between this axis and the contours of the vertebral body, creates the anterior and posterior points (II and III). Next the observer segmented the lamina midpoint and the tip of the spinous process (III).

vertebrae. For practical computing, this parameter was compared between the apical segment, one and two levels above (apex+1, apex +2) and below (apex-1, apex-2) the apex. The rotation radius (r) was defined as the linear distance between the longitudinal rotation axis (the axis from which the vertebral bodies rotates away from the midline) to the center of the spinal canal of that corresponding vertebra (Figure 1 and Figure 2). The vertebral axial rotation was measured as the angle between the vertebral axis (through the center of the vertebral body and spinal canal) and the sacral axis in the axial plane (Figure 2). Next, the intravertebral axial rotation (between the vertebral body and posterior elements) was measured (Figure 2). Last, the local mechanical torsion of the vertebral bodies was defined as the difference in axial rotation of the upper and lower endplate of the same vertebra (Figure 2).

Statistical analysis

Statistical analyses were performed using SPSS 22.0 for Windows (SPSS Inc., Chicago, IL, USA). Descriptive statistics were computed providing means, ranges and standard deviations. Paired samples t tests were used to compare the different rotation and torsion measurements and differences between different levels at, above and under the apex were analyzed with a one-way repeated measured analysis of variances (ANOVA) added with a follow up pairwise comparison between each level. The statistical significance level was set at 0.05 for all analyses.
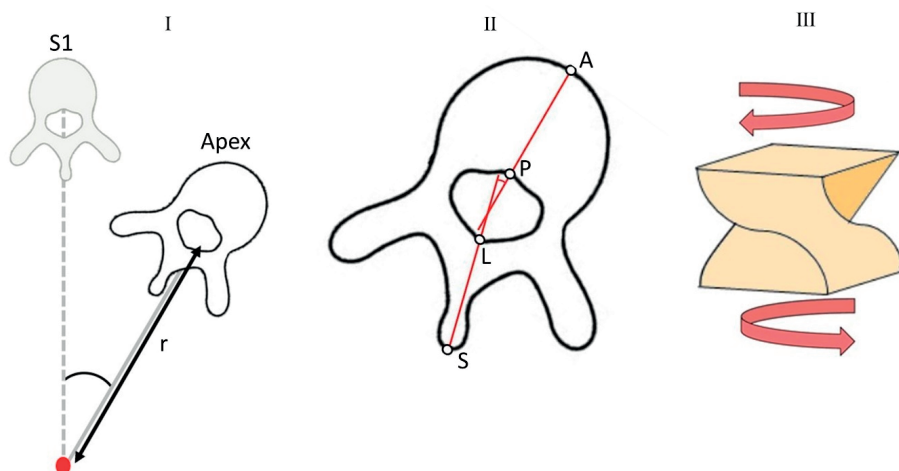
Figure 2. The center of rotation of the vertebra was defined as the intersection between the vertebral axis and the vertical plane through the axis of the sacral endplate. The vertebral axial rotation was defined as the angle between these axes (I). The rotation radius (r) was defined as the distance between the rotation point and the center of mass of the spinal canal (I). A line was reconstructed between the anterior (A) and posterior (P) points of the vertebra, as well as between the lamina (L) and spinous process (S) points (II). The angle between these lines defined the intravertebral axial rotation (II). Last, the local mechanical torsion was defined as the difference in rotation between the upper and lower endplate of the vertebra (III).

RESULTS

The database consisted of 98 CT scans, 28 were excluded (12 had associated congenital or neuromuscular pathologies, 11 had incomplete radiological charts, four had an atypical left convex thoracic curve and one had undergone scoliosis surgery prior to obtaining the CT scan), thus a total of 70 AIS patients were included, with an average age of 16.3±3.0 years (range: 10-26). Coronal Cobb angle of the main thoracic curve varied between 46° and 109°, other demographics are shown in Table 1.[157]

Longitudinal rotation axis and vertebral axial rotation
The longitudinal rotation axis (mean ± standard deviation) of the apex was on average 11.5±5.1 cm posterior to the center of mass of the spinal canal of the apex. The radius length was smallest at the apical levels and increased further away from the apex (apex+2 15.8±8.5 cm, apex+1 12.4±5.8 cm, apex-1 12.2±5.8 cm, apex-2 14.2±8.2 cm; Figure 3). The vertebral axial rotation was largest at the apex (21.9±7.4°) and decreased towards the neutral zone (apex+2 14.2±6.9°, apex+1 19.5±7.1°, apex-1 20.2±7.5°, apex-2 15.3±8.0°; Figure 4).

Figure 3. The rotation radius (r) of the apical vertebra and the two above and below is shown, including standard deviation (error bars). Below, the statistical significance level is shown between the different levels. NS=not significant.

	Apex+2	Apex+1	Apex	Apex+1	Apex+2
Apex+2		-	-	-	-
Apex+1	NS		-	-	-
Apex	p=0.010	NS		-	-
Apex-1	NS	NS	p<0.001		-
Apex-2	NS	p=0.002	p<0.001	p<0.001	
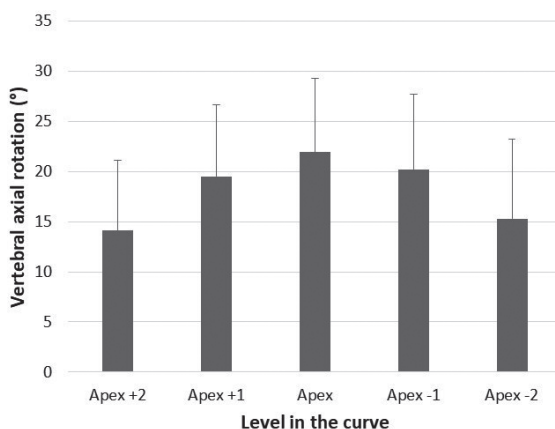
Figure 4. The vertebral axial rotation of the apical vertebra and the two above and below is shown, including standard deviation (error bars). Below, the statistical significance level is shown between the different levels. NS=not significant.

	Apex+2	Apex+1	Apex	Apex+1	Apex+2
Apex+2		-	-	-	-
Apex+1	p<0.001		-	-	-
Apex	p<0.001	p<0.001		-	-
Apex-1	p<0.001	NS	p<0.001		-
Apex-2	NS	p<0.001	p<0.001	p<0.001	
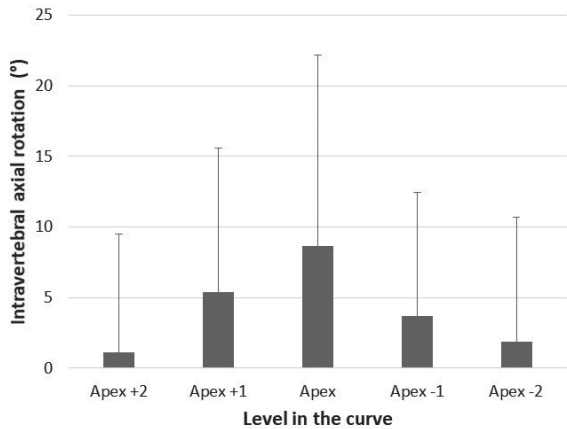
Figure 5. The intravertebral axial rotation of the apical vertebra and the two above and below is shown, including standard deviation (error bars). Below, the statistical significance level is shown between the different levels. NS=not significant.

	Apex+2	Apex+1	Apex	Apex+1	Apex+2
Apex+2		-	-	-	-
Apex+1	NS		-	-	-
Apex	p=0.007	p=0.028		-	-
Apex-1	NS	NS	NS		-
Apex-2	NS	NS	p=0.001	p=0.017	

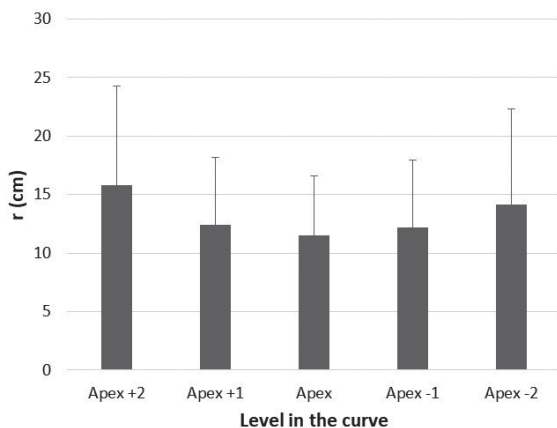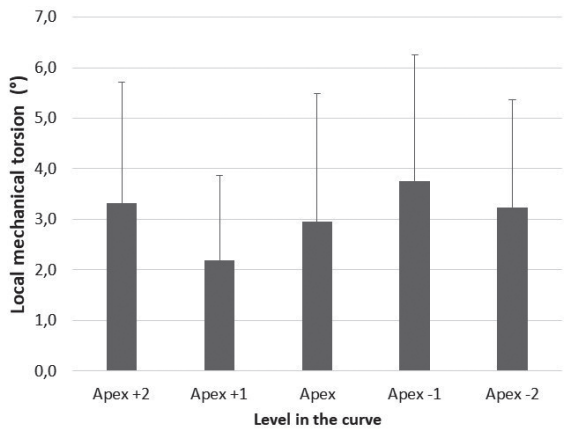**Figure 6.** The local mechanical torsion of the apical vertebra and the two above and below is shown, including standard deviation (error bars). Below, the statistical significance level is shown between the different levels. NS=not significant.

	Apex+2	Apex+1	Apex	Apex+1	Apex+2
Apex+2		-	-	-	-
Apex+1	p=0.022		-	-	-
Apex	NS	NS		-	-
Apex-1	NS	p=0.001	NS		-
Apex-2	NS	p=0.012	NS	NS	

Intravertebral axial rotation and local mechanical torsion

The angle between the vertebral bodies and posterior elements (intravertebral axial rotation) was largest at the apex (8.7±13.5°) and decreased further away from the apex (apex+2: 1.1±8.4°, apex+1: 5.4±10.2°, apex-1: 3.7±8.8°, apex-2: 1.8±8.8°; Figure 5). The local mechanical torsion differed between the different levels of the curve (apex+2 3.3±2.4°, apex+1 2.2±1.7°, apex 3.0±2.5° apex-1 3.8±2.5°, apex-2 3.2±2.1°; Figure 6).

Reliability

The reliability of the vertebral axial rotation and the local mechanical torsion were measured in a previous study; intraclass correlation coefficients for intra- and interobserver reliability were 0.92 (95% confidence interval: 0.82–0.97) and 0.89 (0.74–0.95).[44] Intraclass correlation coefficients for intra- and interobserver reliabilities were 0.95 (95% confidence interval: 0.91–0.97) and 0.96 (0.93–0.98) for r and 0.99 (0.97–1.00) and 0.97 (0.93–0.99) for the intravertebral axial rotation, respectively.

DISCUSSION

The normal spine is only slightly rotated in the axial plane, coronally aligned and shows mild kyphotic and lordotic curvatures in the thoracic and sacral, respectively the cervical and lumbar regions.[44, 175] In idiopathic scoliosis, due to a still unknown cause, each vertebra in the curve rotates away from its normal position. This rotation can be described by the location of the longitudinal rotation axis around which this occurs. Vertebral axial rotation has to a large extent been studied *in vitro,* and in non-scoliotic spines. Within these studies the longitudinal rotation axis was found to be determined by the orientation of the facet joints and to lay mainly within the confines of the vertebra.[22, 42, 165-168] However, the position of the longitudinal rotation axis and the different extra- and intravertebral rotation patterns of the scoliotic spine are still unknown.

   Our study showed the longitudinal rotation axis of the scoliotic apical vertebrae appeared to lie far dorsal from the spine itself; on average 11.5 cm and differed per level in the spine. If there is much vertebral axial rotation, as in the apical vertebral body, the longitudinal rotation axis becomes closer to the vertebra. In the less rotated vertebrae near the end of the curve, the intersection lies farther away. The longitudinal rotation axis of the different levels in the curve formed a parabolic shape in the sagittal plane (Figure 3). Furthermore, the vertebral axial rotation was 21.9±7.4° at the apical vertebrae and the intravertebral axial rotation and local mechanical torsion of the apex were 8.7±13.5° and 3.0±2.5°. The rotation parameters were largest at the apex and decreased towards the neutral zone. The larger rotation at the apex is in line with the increased 3D

wedging and asymmetry of the apex, compared with the neutral zone, as described in previous studies.[44, 50, 145, 172]

In contrast to the previous studies, the longitudinal axis of rotation of this study is based on the vertebral axial rotation, as well as the translation in the coronal plane. White and Panjabi were amongst the first to describe the longitudinal rotational axis. Based on their study, the axis was found to lay within the vertebral body.[22] Most other authors found this axis somewhere within the confines of the vertebra.[165, 167, 168] Others, including Nash and Moe and Molnar et al. in the scoliotic spine, demonstrated the longitudinal rotation axis at the posterior side of the vertebral body, whereas Roaf and Lindahl observed it even more posteriorly, Roaf close to the tip of the spinous processes and Lindahl at the tip of the transverse processes.[2, 42, 165, 170, 177] The major limitation, however, is that all these rotational axes are based on non-scoliotic specimens, cadaveric spines or models. Last decades, other authors described the vertebral rotation of the scoliotic spine using 2D or 3D imaging.[11, 135, 172, 175, 178, 179] Smith et al. hypothesized that if there is a thoracic lordosis, instead of the normal thoracic kyphosis, the longitudinal rotation axis is located posteriorly to the spine, based on two human skeletons with scoliosis and an animal study.[166] Kotwicki et al. observed an average angulation of 15.0° between the vertebral body axis and spinous process axis.[171] Additionally, Kotwicki et al. described the direction of the rotation of the vertebra and spinous process, that is similar to the results of this study.[171] The vertebral body is pushed away from the midline, whereas the spinous process is less pushed away from the midline, probably stabilized by the posterior ligaments, corresponding with the posterior located longitudinal rotation axis (Figure 2). They described that the bone remodeling of the vertebral body and the spinous process deviation act, parallel in time, in opposite direction, as an extension of the theory by Smith et al..[166, 171] Recently, Vavruch et al. described the vertebral rotation and internal deformation.[172] They showed that patients with scoliosis had clear morphologic differences in the midaxial in the apex, decreasing towards the neutral zone.[172]

Despite the detailed description of the vertebral rotation, the longitudinal rotation axis of the scoliotic spine and the different aspects of the rotation mechanism of the vertebrae within the curve, were not described before. The present study confirms that, in scoliosis, unlike in what is described for the normal spine, the longitudinal rotation axis, consistently lies behind the spinal column and its position along the curve shows a parabolic distribution. It is well-known that the thoracic kyphosis of the normal anatomy is deformed in a thoracic lordosis in moderate to severe scoliosis.[47, 49, 50, 52, 53, 180] This mechanism influences partly the posterior position of the rotation axis as well. Additionally, the further aspects of the rotation (vertebral axial rotation, intravertebral axial rotation and local mechanical torsion) were described to clarify the rotation mechanism of scoliosis, to help understand possible mechanisms of scoliosis development and treatments.

This study provides an estimation of the rotational axis of different levels inside the curve and the differences between the axial rotation of the vertebra and the intravertebral torsion. CT scanning is considered the gold standard for studying rotation in the scoliotic spine, but leads to limitations as well.[43] First, CT scans are not made in upright, but in prone position. Previous studies have shown that both Cobb angle and vertebral rotation are influenced by body position.[57, 58, 181-183] The longitudinal rotational axis is likely to vary between different body positions as well. However, data on the longitudinal rotational axis of the vertebrae in the normal spine are usually not obtained upright either, and based on the mentioned comparative studies between different body positions, the observed phenomena in our present study probably only differ quantitatively, not qualitatively from an upright position. Second, for this study, an already existing CT database was used, acquired as part of the general pre-operative workup for navigation guided pedicle screw surgery in one of our institutions, resulting in a cross-sectional study design, including only severe AIS patients. A longitudinal study, including milder curves as well, might provide more insight in the rotation mechanism during the progression of the scoliosis, which hopefully could be done with future validated reliable non-ionising radiation assessment such as ultrasound and others.

CONCLUSION

This study showed the altered morphology and alignment which is important for a better understanding the 3D pathoanatomy, development of AIS and could help in better therapeutic planning both for bracing and surgical intervention. The key observation is that in severe idiopathic scoliosis the apex rotates away from its original position around a longitudinal rotation axis that is localized far posterior to the spine; the distance depends on the level of the vertebra in the spinal curve. The vertebral axial rotation is accompanied by a smaller amount of intravertebral axial rotation and local mechanical torsion, increasing towards the apical region.

Chapter 5

Asymmetry of the Vertebral Body and Pedicles in the True Transverse Plane in Adolescent Idiopathic Scoliosis – A CT based Study

ABSTRACT

Study Design. Cross-sectional.

Objectives. To quantify the asymmetry of the vertebral bodies and pedicles in the true transverse plane in adolescent idiopathic scoliosis (AIS) and to compare this with normal anatomy.

Summary of background data. There is an ongoing debate about the existence and magnitude of the vertebral body and pedicle asymmetry in AIS and whether this is an expression of a primary growth disturbance, or secondary to asymmetrical loading.

Methods. Vertebral body asymmetry, defined as left-right overlap of the vertebral endplates (i.e. 100%: perfect symmetry, 0%: complete asymmetry) was evaluated in the true transverse plane on CT scans of 77 AIS patients and 32 non-scoliotic controls. Additionally, the pedicle width, length and angle and length of the ideal screw trajectory were calculated.

Results. Scoliotic vertebrae were on average more asymmetric than controls (thoracic: AIS 96.0% versus controls 96.4%; P=0.005, lumbar: 95.8% versus 97.2%; P<0.001), more pronounced around the thoracic apex (95.8%) than at the end vertebrae (96.3%; P=0.031). In the thoracic apex; the concave pedicle was thinner (4.5 versus 5.4mm; P<0.001), longer (20.9 versus 17.9mm; P<0.001), the length of the ideal screw trajectory was longer (43.0 versus 37.3mm; P<0.001) and the transverse pedicle angle was greater (12.3 versus 5.7°; P<0.001) than the convex one. The axial rotation showed no clear correlation with the asymmetry.

Conclusions. Even in non-scoliotic controls is a degree of vertebral body and pedicle asymmetry, but scoliotic vertebrae showed slightly more asymmetry, mostly around the thoracic apex. In contrast to the existing literature, there is no major asymmetry in the true transverse plane in AIS and no uniform relation between the axial rotation and vertebral asymmetry could be observed in these moderate to severe patients, suggesting that asymmetrical vertebral growth does not initiate rotation, but rather follows it as a secondary phenomenon.

INTRODUCTION

Transverse plane asymmetry is a well-known part of the three-dimensional (3D) deformity in scoliosis and has been described in a number of older as well as more recent anatomical and radiographic imaging studies.[1, 2, 29, 30, 44, 46, 89, 90] Unfortunately, these data are sometimes inconsistent and conflicting, describing scoliosis of different origin and age at onset of deformity. The exact transverse plane morphology in adolescent idiopathic scoliosis (AIS) is important, because it may further our understanding of the true nature of the disorder and its etiopathogenesis. It is known that all growth cartilage of the pedicles, the neurocentral junctions (NCJ), close before the age of eight, therefore pronounced pedicle asymmetry suggests a disturbance of symmetrical development that has started already before that age.[142] Furthermore, for surgical strategy, the exact morphology of both vertebral body and pedicles is important as a reference for pedicle screw orientation, length and width.[90, 184-189] In addition the existing literature on pedicle asymmetry in AIS, this study aims to existence and magnitude of vertebral body as well as pedicle morphology asymmetry in the true transverse plane in patients with moderate to severe AIS.

MATERIALS AND METHODS

Study population

All AIS patients that had received pre-operative high-resolution computed tomographic (CT) images (64 Slice Multi-detector CT scanner, GE Healthcare, Chalfont, St. Giles, United Kingdom; slice thickness 0.625 millimeters (mm)) – acquired for navigation guided pedicle screw insertion in one of the participating centers – between June 2011 and May 2013, were included. All patients had undergone routine upright posterior-anterior and bending radiography as well as supine magnetic resonance imaging of the full spine for detection of spinal cord abnormalities. Children with other spinal pathology, spinal trauma, previous spinal surgery, neurological symptoms or neural axis abnormalities, syndromes associated with disorders of growth or atypical left convex thoracic curves or right convex (thoraco)lumbar curves were excluded to obtain an as homogeneous population as possible, therefor the right pedicle is always the convex pedicle and the left pedicle the concave pedicle in this study. The control group consisted of thirty-two sex-matched non-scoliotic subjects who had undergone CT imaging of the thorax and abdomen for indications other than spinal pathology.

Computed tomographic measurement method

Vertebral body and pedicle asymmetry were measured for each individual vertebra by two trained observers (R.B. and T.S.), using in-house developed software for semi-automatic analysis (ScoliosisAnalysis, Image Sciences Institute, Utrecht, The Netherlands), based on MeVisLab (MeVis Medical Solutions AG, Bremen, Germany).[175] For intra- and interobserver reliability, two observers (R.B. twice, T.S. once) analyzed a random subset of ten CT scans of AIS patients on separate sittings.

First, the observer selected the upper and lower endplates of the vertebral body, by using the software that was developed for this purpose.[175] Then, the observer used the sagittal and coronal orientation of the endplates to correct for coronal and sagittal tilt to positions each vertebral level in the true transverse plane. Subsequently, for each endplate, its longitudinal axis was calculated automatically after manual segmentation (Figure 1).[175] Axial rotation of each vertebra was calculated, using the 3D orientation of the longitudinal axis of the endplates as relative to the sacrum, since this normally is not rotated in AIS.[175] For measuring the vertebral body asymmetry, the right side of the endplate of the vertebral body was flipped across the longitudinal axis on top of the left side to calculate the overlap between them using the Dice similarity coefficient; i.e. 100% indicates perfect symmetry, 0% complete asymmetry (Figure 2).
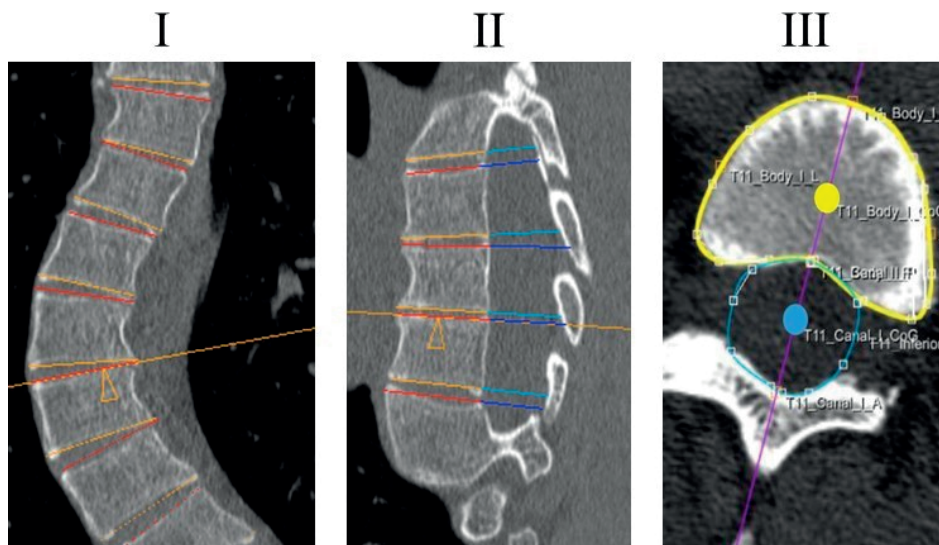
Figure 1. The orientation of the upper and lower endplate of each individual vertebra of the computed tomography scans was determined by using the semi-automatic software, correcting for coronal (I) and sagittal (II) tilt, to reconstruct true transverse sections. The observer drew a contour around the vertebral body (yellow line in III) and spinal canal (blue line in III). The semi-automatic software calculated a center of gravity of the vertebral body (yellow dot in III) and spinal canal (blue dot in III). For each endplate, its longitudinal axis was calculated as the line between those two points (purple line in III).
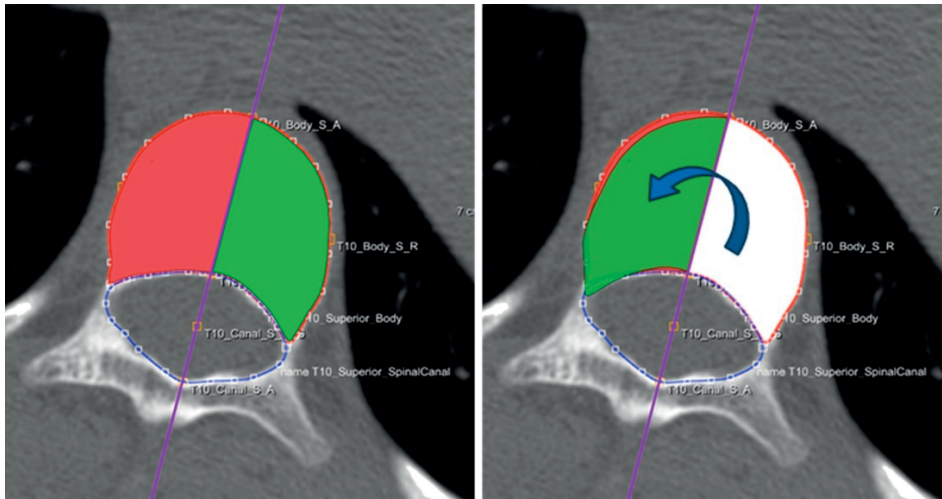
Figure 2. Computed tomographic images showing the true transverse reconstructions of a vertebra. After manual segmentation of the vertebral body and spinal canal the software flipped the right side of the endplate across the longitudinal vertebral axis. The Dice similarity coefficient was used to calculate the percentage of overlap between the left (in *green*) and right (in *red*) side of the vertebral body.

Pedicle asymmetry was also analyzed in the ideal reconstructed transverse sections, parallel to the upper endplate, on which both pedicles were best visible, as previously used by other research groups for pedicle asymmetry analyses.[185, 190] A longitudinal line was placed straight through each pedicle, the pedicle axis, and perpendicular to this axis, a right-left axis was reconstructed. The pedicle width and length, length of the ideal screw trajectory and the pedicle angle were measured by using these axes, specified in Figure 3. Pedicle asymmetry was defined as the difference between the convex and concave pedicle.

For better comparison with previous studies on pedicle asymmetry, pedicles were also classified as proposed by Watanabe *et al.* and Sarwahi e*t al.*[187, 191] This classification describes four pedicle types; type A, a cancellous channel >4 mm; type B, a cancellous channel between 2-4 mm; type C, a cortical channel >2 mm and type D, a cancellous or cortical channel <2 mm.

Statistical analysis

Statistical analyses were performed using SPSS 20.0 for Windows (SPSS Inc., Chicago, IL, USA). Descriptive statistics were computed and chi-square was used to analyze the differences in pedicle classification. Potential outliers were identified. Differences in vertebral body and pedicle parameters between AIS patients and controls were analyzed, using multiple analysis of variances. In addition, paired t-tests were used to analyze the parameters between the concave and convex side, and between the apices and Cobb
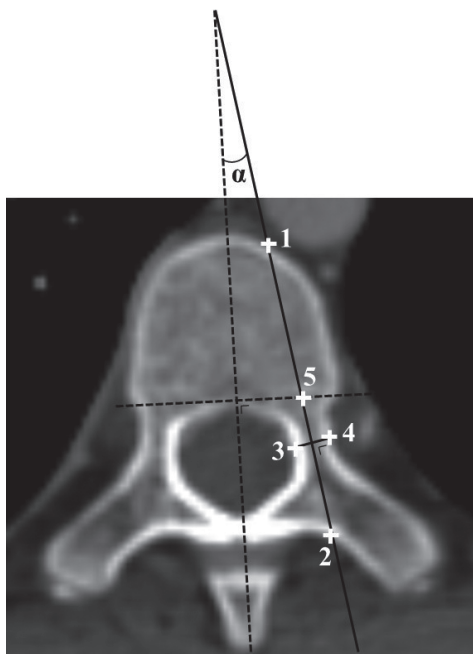
Figure 3. Pedicle width was defined as the narrowest length between the medial outer cortex and lateral outer cortex on the right-left axis (point 3-4); pedicle length as the length between the posterior outer cortex of the lamina and the anterior side of the spinal canal on the longitudinal axis (2-5); length of the ideal pedicle screw trajectory as the length between the posterior outer cortex and the anterior outer cortex of the vertebral body on the longitudinal axis (1-2; mimicking the length of the ideal pedicle screw trajectory in the transverse plane) and the transverse pedicle angle as the angle between the pedicle axis and the vertebral axis (α).

end vertebrae in the AIS group. Pearson's correlation coefficient (*r*) was used to define the relationship between the asymmetry and axial rotation and the intraclass correlation coefficient (ICC) was used to define the intra- and interobserver reliability. The statistical significance level was set at 0.05.

RESULTS

Population

Seventy-seven AIS patients were included, only the vertebrae of the primary structural thoracic (Lenke 1, 2, 3 and 4) and lumbar (Lenke 5 and 6) curves in AIS were included (see Table 1 for exclusion criteria and demographics). To assess potential confounding of the different age of the groups, the effect of age on outcome was analyzed which showed no difference ($P≥0.147$).

Overall asymmetry between AIS and controls

Primary thoracic and lumbar AIS curves had on average, considering the mean of all the vertebrae in the curve, more transverse plane asymmetry than controls in terms of:

- Vertebral body asymmetry (thoracic, 96.0±0.6% in AIS *versus* 96.4±0.5% in controls, $P=0.005$; lumbar, 95.8±1.2% *versus* 97.2±0.4%, $P<0.001$; Figure 4).

Included		AIS (n=77)	Controls (n=32)
Age (years)	Range	11-26	10-18
	Mean±SD	17.1±2.9	15.4±1.8
Girls, n (%)		60 (78%)	25 (78.1%)
Thoracic curve convexity, n (%)	Right convex	77 (100%)	
Lenke curve type			
I		37 (48%)	
II		16 (21%)	
III		7 (9%)	
IV		2 (3%)	
V		6 (8%)	
VI		9 (12%)	
Primary thoracic curves		62 (81%)	
Cobb angle primary thoracic curve (°)	Range	51-105	
	Mean±SD	69±12	
Primary lumbar curves		15 (19%)	
Cobb angle (thoraco)lumbar curve (°)	Range	41-88	
	Mean±SD	41±16	

Excluded	Number (n=11)
Associated congenital of neuromuscular pathologies	6
Atypical left convex thoracic curve	3
Scoliosis surgery prior to CT scan	1
Incomplete radiological chart	1

Table 1. Demographics for all included subjects and exclusion criteria are shown. Curve characteristics (curve type according to the Lenke classification, level of the apex and Cobb angles) were determined on the conventional posterior-anterior and bending radiographs.[11, 131, 157] SD = standard deviation.

- Pedicle width, the AIS concave pedicle being thinner (thoracic, -0.4±0.6 mm left-right difference in AIS *versus* 0.1±0.3 mm left-right difference in controls, $P<0.001$; lumbar, 0.5±0.7 mm *versus* 0.2±0.3 mm, $P=0.036$; Figure 5). All the included curves were right convex, therefore the right pedicle is the convex pedicle and the left pedicle is the concave pedicle.
- Pedicle length in the thoracic spine, the AIS concave pedicle being longer (1.8±1.7 mm left-right difference in AIS *versus* 0.7±0.8 mm in controls; $P<0.001$; lumbar, -0.9±1.2 mm *versus* -0.3±1.2 mm; $P=0.09$; Figure 5).
- Length of the ideal screw trajectory in the thoracic spine, the AIS concave pedicle being longer (4.1±2.3 mm left-right difference in AIS *versus* 1.2±1.0 mm in controls; $P<0.001$). In the lumbar spine the length of the ideal pedicle screw trajectory showed,
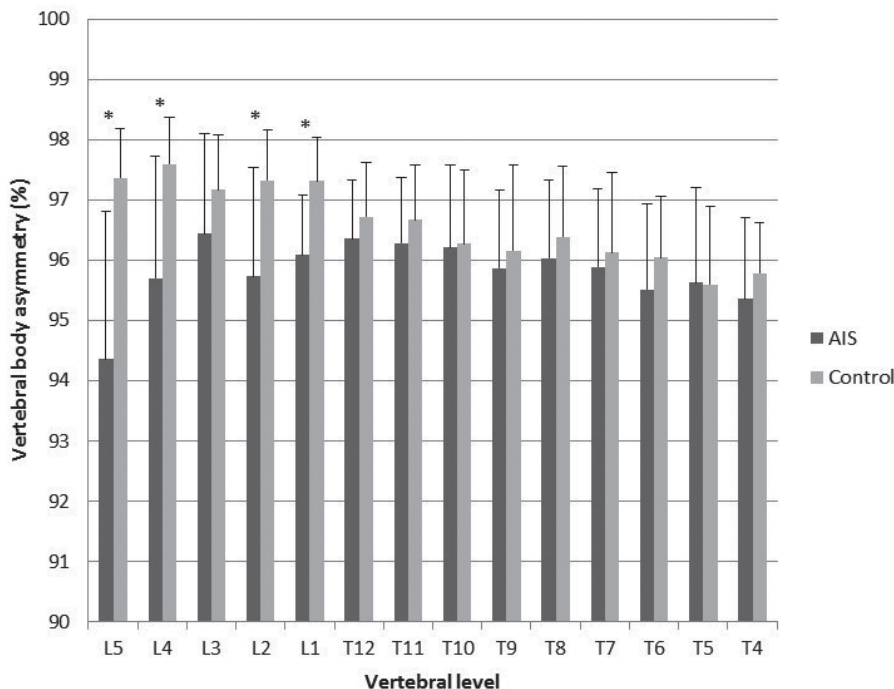
Figure 4. The vertebral asymmetry is shown for each individual vertebral level in the primary thoracic and primary lumbar curve in adolescent idiopathic scoliosis (AIS) and the throacic and lumbar veretbrae in controls. 100% indicates perfect symmetry, 0% complete asymmetry. * = significant difference between AIS and controls.

somewhat surprisingly, more asymmetry in the controls (0.9±1.5 mm) than in AIS patients (-0.2±1.3 mm; *P*=0.015; Figure 5).

- Transverse pedicle angle, the AIS concave pedicle being more angled inward (thoracic, 4.6±3.2° left-right difference in AIS *versus* 1.8±2.1° in controls, *P*<0.001; lumbar, -4.7±4.0° *versus* 2.2±3.3°, *P*<0.001; Figure 5).

Overall asymmetry between concave and convex pedicle in AIS

On average, throughout the thoracic primary curves, the concave pedicle was thinner (concave 5.2±1.0 mm *versus* convex 5.6±0.9 mm; *P*<0.001), longer (concave 20.6±2.0 mm, convex 18.8±1.8 mm; *P*<0.001), the ideal screw trajectory was also longer (concave 41.7±3.6 mm *versus* convex 37.6±3.6 mm; *P*<0.001) and the transverse pedicle angle was greater (concave 10.6±3.6° *versus* convex 6.0±3.0°; *P*<0.001). In the primary lumbar curves the concave pedicle was thinner (concave 6.9±1.1 mm *versus* convex 7.4±1.2 mm; *P*=0.018), but slightly shorter (concave 21.6±1.6 mm *versus* convex 22.5±1.4 mm; *P*=0.009) and the transverse pedicle angle was also greater (concave 18.0±4.7° *versus*
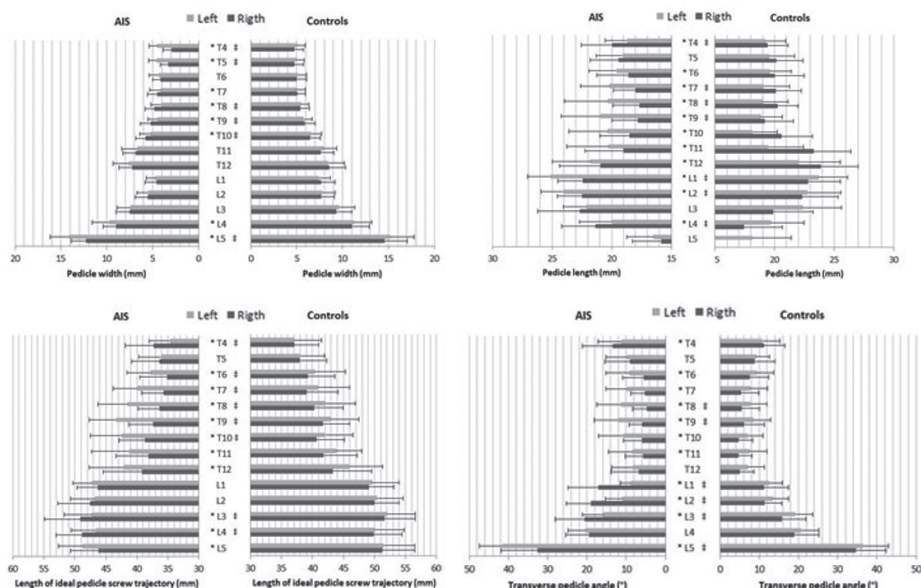
Figure 5. Pedicle asymmetry is shown for each individual pedicle in adolescent idiopathic scoliosis (AIS) patients and controls, representing pedicle width, pedicle length, the length of the ideal pedicle screw trajectory and the transverse pedicle angle. The right pedicle is the convex pedicle in the primary thoracic AIS curves and the concave in the primary lumbar, the left pedicle is the concave in the primary thoracic curves and the convex in primary lumbar curves. Mm = millimeter. * = significant difference between concave and convex pedicle in AIS patients. ‡ = significant difference in asymmetry (difference between right and left pedicle) between AIS patients and controls.

convex 13.3±3.9°; *P*<0.001). There was on average no significant difference between concave (46.5±3.4 mm) and convex (46.3±3.2 mm) regarding length of the ideal screw trajectory in the primary lumbar curves. The pedicles in the controls showed no asymmetry between the left and pedicle for all the parameters (*P*≥0.051)

Pedicle type asymmetry

In the primary thoracic AIS curves, 20.3% of the pedicles were abnormal – type B, C or D – compared to only 7.8% in the corresponding vertebrae in the controls (P<0.001; Table 2). In the primary lumbar curves, 7.7% of the pedicles were abnormal, versus 0.0% in the controls (P<0.001). The concave pedicle in the thoracic AIS curve was more often type B (concave 18% versus convex 12%; P=0.016) or type C (concave 8% versus convex 2%; P<0.001, Table 2) than the convex pedicle. In the lumbar AIS curve there was no difference between the concave and convex pedicle.

Pedicle type	Thoracic				Lumbar			
	Convex n (%)	Concave n (%)	p	Controls n (%)	Convex n (%)	Concave n (%)	p	Controls n (%)
A	353 (86)	304 (74)	<0.001	649 (92)*	74 (95)	70 (90)	0.184	448 (100)*
B	51 (12)	74 (18)	0.016	36 (5)*	2 (3)	4 (5)	0.341	0 (0)*
C	8 (2)	33 (8)	<0.001	19 (3)*	2 (3)	4 (5)	0.341	0 (0)*
D	0 (0)	1 (0)	0.500	0 (0)	0 (0)	0 (0)	-	0 (0)

Table 2. The pedicle classification is shown for the thoracic and lumbar primary curves in adolescent idiopathic scoliosis (AIS) patients and compared to the corresponding vertebrae in the controls. Type A = cancellous channel > 4 mm; type B = cancellous channel between 2-4 mm; type C = cortical channel > 2 mm; type D = cancellous or cortical channel < 2 mm. * = significant difference between AIS and controls.

Vertebral body and pedicle asymmetry in different regions of the spine

The thoracic apical vertebrae of the primary curves showed more asymmetry as compared to the end vertebrae (often also the neutral vertebrae) in left-right overlap (apex, 95.8±1.5% *versus* end vertebra, 96.3±1.0%; P=0.031), the difference between convex and concave pedicle width (0.9±1.1 mm *versus* -0.2±1.1 mm; P<0.001), pedicle length (-3.0±3.8 mm *versus* -0.5±2.7 mm; P<0.001), length of the ideal screw trajectory (-5.7±5.2 mm *versus* -2.0±4.1 mm, P<0.001) and transverse pedicle angle (-6.6±6.8° *versus* -1.7±7.4°; P<0.001; Figure 6). In the lumbar spine, no significant difference in asymmetry was found between the apical and end vertebrae.

Relation with curve severity

No significant, linear correlation could be found between vertebral body or pedicle asymmetry and the Cobb angle or apical vertebral rotation (P>0.05; Table 3).

	Thoracic				Lumbar			
	Apical rotation		Cobb angle		Apical rotation		Cobb angle	
	r	p	r	p	r	p	r	p
Vertebral body asymmetry	0.16	0.21	-0.23	0.07	-0.34	0.21	-0.41	0.14
Pedicle width asymmetry	-0.08	0.56	0.03	0.80	0.54	0.04	0.16	0.57
Pedicle length asymmetry	0.06	0.65	-0.11	0.41	0.44	0.10	0.40	0.14
Ideal pedicle screw trajectory length asymmetry	-0.01	0.92	-0.41	0.75	0.40	0.14	-0.4	0.88
Transverse pedicle angle	-0.94	0.47	-0.13	0.31	0.15	0.59	-0.31	0.26

Table 3. The Pearsons correlation coefficient (*r*) between the asymmetry parameters in the apical vertebra of the primary curves in the transverse plane *versus* axial rotation in the corresponding vertebra and the Cobb angle of the curvature.

Thoracic apex

Vertebral body asymmetry (%) *	95.8±1.5		
	Concave	Convex	P
Pedicle width (mm) *	4.5±1.2	5.4±1.2	<0.001
Pedicle length (mm) *	20.9±3.5	17.9±2.3	<0.001
Pedicle screw trajectory length (mm) *	43.0±5.2	37.3±4.3	<0.001
Transverse pedicle angle (°) *	12.3±6.4	5.7±3.8	<0.001

Cobb end vertebra

	Thoracic			**Lumbar**		
Vertebral body asymmetry (%)	96.3±1.0			95.4±1.2		
	Concave	Convex	P	Concave	Convex	P
Pedicle width (mm)	6.9±1.5	6.7±1.3	0.207	6.2±1.3	6.9±1.6	0.040
Pedicle length (mm)	21.4±3.6	20.9±3.8	0.126	20.0±2.9	22.3±3.7	0.003
Pedicle screw trajectory length (mm)	42.2±6.3	40.2±6.9	<0.001	40.3±5.9	42.3±5.2	0.125
Transverse pedicle angle (°)	9.3±6.1	7.6±6.7	0.070	11.6±8.2	6.1±4.2	0.014

Lumbar apex

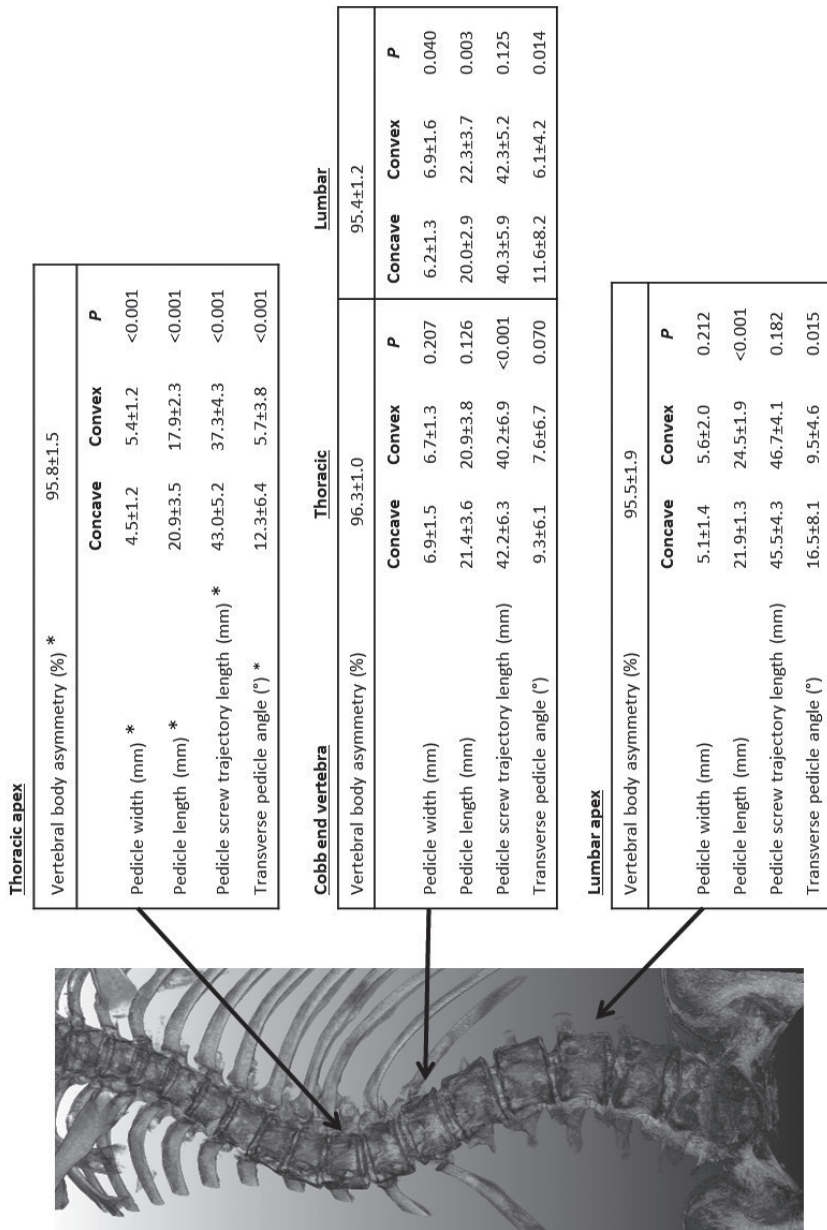| Vertebral body asymmetry (%)	95.5±1.9		
	Concave	Convex	P
Pedicle width (mm)	5.1±1.4	5.6±2.0	0.212
Pedicle length (mm)	21.9±1.3	24.5±1.9	<0.001
Pedicle screw trajectory length (mm)	45.5±4.3	46.7±4.1	0.182
Transverse pedicle angle (°)	16.5±8.1	9.5±4.6	0.015

Figure 6. The vertebral asymmetry and pedicle asymmetry, are shown for the thoracic apex, Cobb end vertebra and lumbar apex of the primary curves in adolescent idiopathic scoliosis (AIS). * = significant difference between the thoracic or lumbar apex *and* the Cobb end vertebra for vertebral asymmetry and pedicle asymmetry (difference between convex and concave).
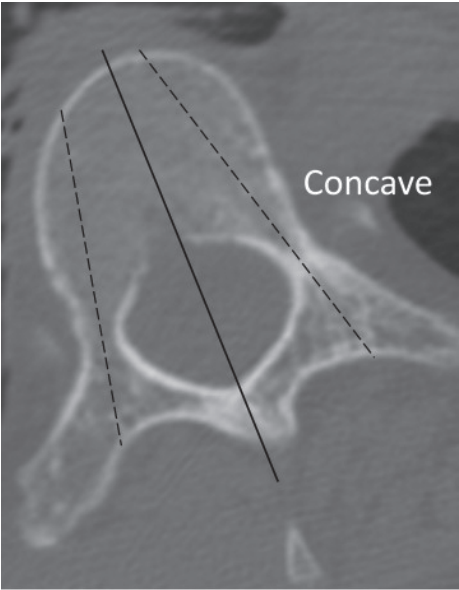
Figure 7. A thoracic apical vertebral body is shown of a severe curve (Cobb angle 69°). The vertebral body axis (black line) and both the pedicle axes (black dashed lines) are illustrated. The bone drift toward the concavity and the increased transverse pedicle angle causes a longer ideal pedicle screw trajectory.

Reliability

In absolute values, the mean intra- and interobserver measurement errors for vertebral body asymmetry measurement were 0.5% and 1.1%, respectively. Since the range of vertebral body asymmetry was relatively small, ICC for intra- and interobserver reliability were relatively low: 0.54 (95% confidence interval: 0.39 – 0.66) and 0.54 (0.39 – 0.66), respectively. ICC for intra- and interobserver reliabilities for pedicle width were 0.98 (0.97 – 0.98) and 0.97 (0.96 – 0.97), for pedicle length 0.83 (0.78 – 0.86) and 0.60 (0.50 – 0.68), for ideal screw trajectory length 0.91 (0.89 – 0.93) and 0.82 (0.77 – 0.85) and for transverse pedicle angle 0.88 (0.85 – 0.90) and 0.70 (0.63 – 0.76), respectively.
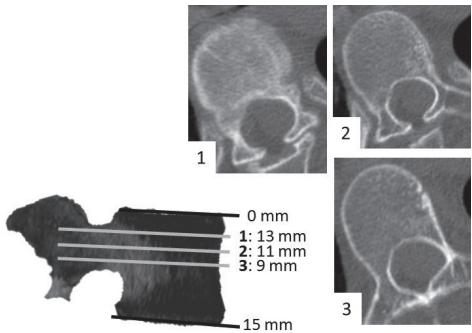

Figure 8. The measurement method and CT scans should be very accurate; slight deviation from the ideal transverse plane of the rotated, translated and tilted vertebrae automatically induces apparent, but not necessarily true asymmetry.

DISCUSSION

Accurate descriptions of the 3D deformity in scoliosis were already given by 19th century anatomists in cadaveric specimen.[1, 29, 30] More recently, with modern imaging techniques, asymmetry in pedicle dimensions between the convex and concave side of the curve were demonstrated in several studies.[90, 147, 184-187] The role of this asymmetry, and whether it represents an active asymmetrical growth pattern, or a passive adaptation due to asymmetrical biomechanical loading as explained by Hueter-Volkmann's and Wolff's law, remains undetermined so far.[188, 189, 192, 193] Experimental studies have shown that asymmetrical growth of the NCJs of the vertebrae can lead to vertebral rotation; unilateral lag screw epiphysiodesis of the NCJ in a growing pig was shown to lead to a rotational, 3D deformity, similar to AIS.[144, 194, 195] If, however, asymmetrical growth of the NCJs (either active or passive) leads to asymmetrical pedicle development in AIS, it implicates that the deformity must already begin to develop before closure of these growth plates, in other words, well before the adolescent growth spurt, when all NCJ's have been reported to be closed.[142, 144, 196] Accurate descriptions of vertebral morphology in scoliosis are therefore important, both theoretically for better understanding its mechanism, as well as practically, for surgical strategy and safe implant placement.

Our study is, to the best of our knowledge, the first to report asymmetry of both the vertebral bodies as well as the pedicles, in a population of moderate to severe adolescent idiopathic scoliosis patients, in the true transverse plane, using 3D multi-planar reconstruction of high-resolution CT scans for each individual vertebra. We used in-house developed software that has been validated in previous studies, to minimize subjectivity in the measurements.[175] In total, the morphology of 1876 pedicles and 1876 vertebral upper and lower endplates has been accurately assessed for this study in AIS and compared to the same levels in controls. We observed that even in non-scoliotic controls a certain degree of vertebral asymmetry exists. The concave pedicles of the thoracic primary curves were on average 0.4 mm thinner, 1.8 mm longer, the ideal screw trajectory was also on average 4.1 mm longer than for the convex pedicle and the transverse pedicle angle was 4.6° greater on the concave side. The asymmetry was found to increase towards the apex, the concave pedicle becoming thinner and longer, up to a difference of 0.9 mm thinner and 3.0 mm longer than the convex pedicle. The lumbar concave pedicles were on average 0.5 mm thinner than convex throughout the curve. Although more asymmetry was found in the more rotated apical segments, no direct correlation was found between the amount of asymmetry, the magnitude of the Cobb angle or the amount of rotation of the apex in these moderate to severe AIS curves. As mentioned in previous studies, the bone drift of the vertebral body toward the concavity and the greater pedicle angle on the concave side, explains the longer ideal pedicle screw trajectory on the concave side (Figure 7).[90]

Our measurements of the pedicle width asymmetry were consistently smaller than the measurements of pedicle width asymmetry that have been reported in previous studies, with a mean differences of 1.0-2.4 mm between the convex and concave pedicle.[90, 146, 147, 197, 198] The average asymmetry of the pedicle lengths that have been reported varied between 0.9 and 2.7 mm, the screw trajectory asymmetry between 1.3 and 5.6 mm and the pedicle angle between 1.3 and 9.0°.[90, 146, 197, 198] Despite CT measurements can be considered the 'gold' standard method for assessment of morphology of *in vivo* bony structures, it completely depends on voxel size in relation to the size of the structure to be measured. On our high-resolution scan (0.625 mm) we observed that even slight deviation from the ideal transverse plane of the rotated, translated and tilted vertebrae automatically induces apparent, but not necessarily true asymmetry (Figure 8). On the other hand, a major disadvantage of high-resolution CT scans are the radiation dose concerns (the average radiation dose received in this study was 10mSv), especially for applicability in longitudinal studies.

Unfortunately, this study was conducted in a cross-sectional design. For further understanding of the true nature of the disorder and its etiopathogenesis, future studies need a longitudinal design, modern low-dose or non-ionizing imaging technologies and should focus on mild scoliosis. Nevertheless, this study is a first attempt, because subjects with several curve magnitudes were included and compared to the normal anatomy. Further studies could include a longitudinal design and mild scoliotic patients.

An important issue is how the vertebral body is determined, it depends on where the dividing line between left and right is drawn in these rather irregular structures. Other studies have used varying, sometimes subjective, methods, often based on manually drawing a line by using manually placed points.[135] Our choice of the axis through the vertebral body may be criticized as well. It relies on a manual segmentation of the bony outline of the vertebra, after which the computer determines the center of mass of both the spinal canal as well as the vertebral body. This creates an objective, very reliable and reproducible line that divides the vertebra in half, allowing the right half of the vertebra to be 'mirrored' to the left half.[135] It also creates some degrees of symmetry, however, because by definition the amount of mass on the left side of this line is identical to the amount of mass on the right side. Although our method will not demonstrate asymmetry in left-right mass distribution, its objectivity and reproducibility, as well as its ability to demonstrate differences in shape between the left and right side of the vertebral body, make it attractive to use.[135]

CONCLUSION

Transverse plane vertebral asymmetry exists to a certain extent in normal vertebral bodies and pedicles, but bony asymmetry is more pronounced in AIS, although less than has been reported. The less asymmetry as described before is relevant for the pedicle screw size and orientation during the surgical treatment. Vertebral bodies were more asymmetrical in primary lumbar AIS than in primary thoracic curves. Pedicles, however, were more asymmetrical in the apical region of the thoracic curve, the concave pedicle being smaller and longer and the transverse pedicle angle greater than on the convex side. Although curves with greater Cobb angles and more rotation show most vertebral asymmetry, there was no linear correlation between the asymmetry and the amount of rotation in these moderate to severe AIS patients. This suggests to us that asymmetrical vertebral growth does not drive rotation, but rather follows it to a variable extent.

Chapter 6

Anterior spinal overgrowth is the result of the scoliotic mechanism and is located in the disc

25

ABSTRACT

Study Design. Cross-sectional.

Objective. To investigate the presence and magnitude of anterior spinal overgrowth in neuromuscular scoliosis and compare this to the same measurements in idiopathic scoliosis and healthy spines.

Summary of Background Data. Anterior spinal overgrowth has been described as a potential driver for the onset and progression of adolescent idiopathic scoliosis (AIS). Whether this anterior overgrowth is specific for AIS or also present in non-idiopathic scoliosis has not been reported.

Methods. Supine CT scans of thirty AIS patients (thoracic Cobb 21-81°), thirty neuromuscular (NM) scoliotic patients (thoracic Cobb 19-101°) and thirty non-scoliotic controls were used. The difference in length in per cents between the anterior and posterior side $(((\Delta A\text{-}P)/P)*100\%$, abbreviated to A-P%) of each vertebral body and intervertebral disc, and between the anterior side of the spine and the spinal canal (A-C%) were determined.

Results. The A-P% of the thoracic curves did not differ between the AIS (+1.2±2.2%) and NM patients (+0.9±4.1%, P=0.663), both did differ, however, from the same measurements in controls (-3.0±1.6%; P<0.001) and correlated linearly with the Cobb angle (AIS r=0.678, NM r=0.687). Additional anterior length was caused by anterior elongation of the discs (AIS: A-P% disc +17.5±12.7% *versus* A-P% body -2.5±2.6%; P<0.001, NM: A-P% disc +19.1±18.0% *versus* A-P% body -3.5±5.1%; P<0.001). The A-C% T1-S1 in AIS and NM patients were similar (+7.9±1.8% and +8.7±4.0%, P=0.273), but differed from the controls (+4.2±3.3%; P<0.001).

Conclusions. So called anterior overgrowth has been postulated as a possible cause for idiopathic scoliosis, but apparently it occurs in scoliosis with a known origin as well. This suggests that it is part of a more generalized scoliotic mechanism, rather than its cause. The fact that the intervertebral discs contribute more to this increased anterior length than the vertebral bodies suggests an adaptation to altered loading, rather than a primary growth disturbance.

INTRODUCTION

Adolescent idiopathic scoliosis (AIS) is a three-dimensional (3D) spinal deformity of still unknown etiology. The spinal canal in scoliotic patients has been shown to be shorter than the anterior vertebral column, this so called anterior overgrowth, or non-synchronous anterior-posterior growth has been considered part of its etiologic mechanism.[47, 52-54] However, no study has looked at the same anterior-posterior measurements in scoliosis with known etiology. If the same phenomenon is found in non-idiopathic scoliosis as well, anterior overgrowth would appear to be part of a more generalized mechanism in the development of different types of scoliosis, rather than the cause of idiopathic scoliosis. To the best of our knowledge, this is the first study to compare anterior overgrowth in idiopathic scoliosis to the same measurements in neuromuscular (NM) scoliosis, and non-scoliotic controls.

MATERIALS AND METHODS

Study population

All patients with a variety of neurological diagnosis, resulting in thoracic scoliosis requiring surgery, were included (demographics and NM diagnosis in Table 1 and Table 2). Patients were included between February 2006 and March 2016, all had received pre-operative supine computed tomographic (CT) imaging of the spine at one institution as part of the standard pre-operative work up. Children with other spinal pathology or previous spinal surgery were excluded. A similar sample size of age-matched AIS patients was included. All patients had undergone routine posterior-anterior radiography as well as the same CT scans as the neuromuscular group. Curve characteristics (Cobb end vertebrae, number of vertebrae including the curve, level of the apex, Cobb angle and thoracic kyphosis) were determined on the conventional posterior-anterior radiographs

Included NM diagnosis	Number (n=30)	Excluded NM patients	Number (n=8)
Cerebral palsy	10	Associated congenital pathologies	6
Psychomotor retardation	10	Scoliosis surgery prior to CT scan	1
Muscular dystrophy	5	Incomplete radiological chart	1
Smith Magnesis syndrome	1		
Angelman syndrome	1		
Charge syndrome	1		
Tetra paresis	1		
Friedreich's ataxia	1		

Table 1. The included neuromuscular (NM) diagnoses and excluded NM patients are shown.

		AIS (n=30)	NM (n=30)	Controls (n=30)
Age (years)	Range	11-19	9-24	11-17
	Mean±SD	15.3±2.4	15.4±4.2	15.2±1.2
Girls, n (%)		25 (83%)	17 (57%)	19 (63%)
Radiograph position, n (%)	Upright	30 (100%)	10 (33%)	30 (100%)
	Sitting	0 (0%)	20 (67%)	0 (0%)
Thoracic curve convexity, n (%)	Right convex	30 (100%)	21 (70%)	
Cobb angle primary thoracic curve (°)	Range	21-81	19-101	
	Mean±SD	55.8±12.9	51.5±21.4	
Thoracic kyphosis	Range	3-53	2-77	
	Mean±SD	24.0±11.0	31.9±19.4	
Number of vertebrae in the curve	Range	6-9	5-12	
	Mean±SD	7.5±0.97	8.4±1.4	

Table 2. Demographics are shown for all included adolescent idiopathic (AIS) and neuromuscular (NM) curves and controls. SD = standard deviation.
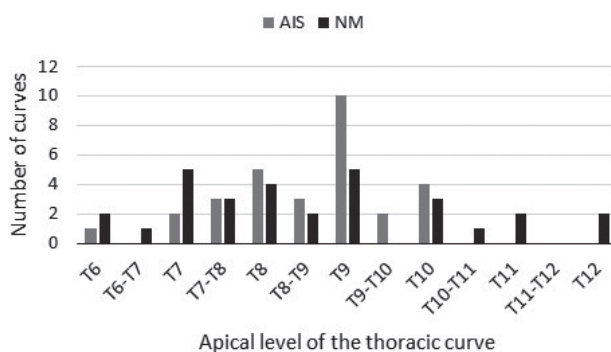
Figure 1. Apical levels of the adolescent idiopathic (AIS) and neuromuscular (NM) thoracic curves. Level of the apex was determined on the conventional posterior-anterior radiographs.

(Table 2 and Figure 1).[11] A third group, to represent the normal population, consisted of non-scoliotic age-matched subjects who had undergone CT imaging of the thorax and abdomen for indications other than spinal pathology (for example trauma screening), and had no spinal pathology.

Computed tomographic measurement method

The anterior and posterior length of the spine and length of the spinal canal were measured, using in-house developed and previously validated image processing technique (Figure 2) and software for semi-automatic analysis (ScoliosisAnalysis 4.1, Image Sciences Institute, Utrecht, The Netherlands), based on MeVisLab (MeVis Medical Solutions AG, Bremen, Germany).[44] Intra- and interobserver reliability for these measurements using

this method was tested in a previous study; intraclass correlation coefficients for intra- and interobserver reliabilities were 0.99 (0.98–1.00) and 0.99 (0.98–1.00), respectively.[44]

First, the observer selected the upper and lower endplates of the vertebral bodies, by using the software that was developed for this purpose (Figure 2). Then, the sagittal and coronal orientation of the endplates was indicated double-oblique to correct for coronal and sagittal tilt. Thus, each vertebral level was reconstructed in the true transverse plane as accurately as possible. Subsequently, for each individual upper and lower endplate, its longitudinal anterior-posterior (A-P) axis was calculated automatically after manual segmentation of the vertebral body and spinal canal. The midpoints of the spinal canal were used to determine the spinal canal length. The intersection of the midsagittal A-P axis and the anterior cortex was used as anterior vertebral point (both of the superior and inferior endplate) and the intersection with the posterior cortex similarly was the posterior point. The anterior height of the vertebral body was the distance between the anterior points of the upper and lower endplate. The same applied to the posterior height and the anterior and posterior height of the intervertebral discs (Figure 2). Anterior-posterior height difference was the sum of the anterior height of the included vertebral bodies and discs minus the sum of the posterior heights. This difference was subsequently converted to a percentage to access relative anterior-posterior length discrepancy ((ΔA-P)/P)*100%, hereinafter abbreviated to A-P%. Positive values of this anterior-posterior height ratio indicate greater anterior length (lordosis). The distances between the midpoints of the spinal canal determined canal length, anterior spine-spinal canal ratio (A-C%) was calculated in the same way as the A-P%. The spinal segment of interest for the A-P% was defined as the Cobb-to-Cobb thoracic curve and A-C% was measured from T1 until the sacral plate.
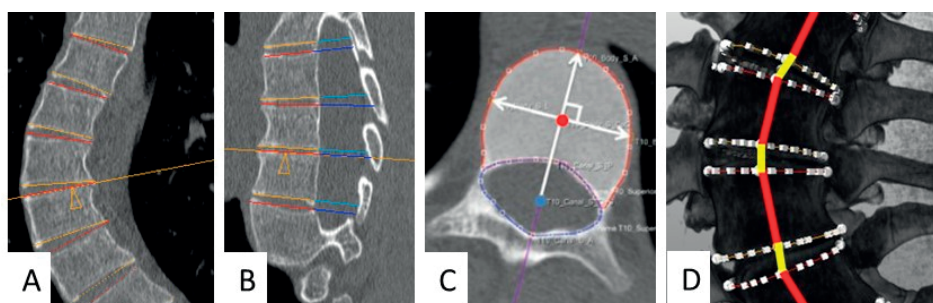
Figure 2. The orientation of the upper and lower endplate of each individual vertebra of the computed tomography scans was determined by using the semi-automatic software, correcting for coronal and sagittal tilt (A and B), to reconstruct the true transverse sections. The observer drew a contour around the vertebral body (red line in C) and spinal canal (blue line in C). The software calculated a center of gravity of the vertebral body (red dot in C) and spinal canal (blue dot in C). The midpoint of the spinal canal was used for the spinal canal length. For each endplate, its longitudinal axis was calculated as the line between those two points (purple line in C). Using this line, anterior as well as posterior heights was computed for all intervertebral discs (yellow line in D) and vertebral bodies (red line in D) in the thoracic curves.

Statistical analysis

Statistical analyses were performed using SPSS 22.0 for Windows (SPSS Inc., Chicago, IL, USA). Descriptive statistics were computed providing means, ranges and standard deviations. Potential outliers were identified. A-P% and A-C% of the AIS and NM patients and controls were compared using unpaired t-tests. Paired t-tests were used to determine the difference in A-P% difference between the intervertebral discs and vertebral bodies within the curves. The Pearson correlation coefficient (r) defined the relationship between A-P% and Cobb angle. Linear regression analysis was used to quantify correlations. The statistical significance level was set at P=0.05 for all analyses. To determine the sample size of this study, the A-P% of the AIS and control group of one of our previous studies was used (AIS +3.8±2.8%, controls -4.1±1.8%).[44] The anterior overgrowth difference between AIS and NM was considered as not relevant if the anterior overgrowth in NM differed 25% or less of the difference between AIS and controls,. Using the standard deviation of the AIS group (2.8%), a power of 0.8 and a P-value of 0.05, the sample size per group must be 26 patients or more to determine the difference of anterior overgrowth between AIS and NM patients.

RESULTS

Population

Of the thirty-eight NM patients, eight subjects were excluded (six had associated congenital boney pathology, one had undergone scoliosis surgery prior to the CT scan and one had incomplete radiological charts). Thirty NM subjects, thirty AIS subjects and thirty non-scoliotic controls were included, with an average age of 15.3±2.4, 15.4±4.2 and 15.2±1.2 years of age (demographics and NM diagnoses are shown in Table 1, Table 2 and Figure 1). To assess potential confounding of the differences in gender distribution between the groups, the effect of gender on outcome was analyzed which showed no difference between the genders (P≥0.103).

Anterior-posterior length difference

The A-P% of the total curve, measured from Cobb to Cobb end vertebra over the vertebral bodies and intervertebral discs of the thoracic curve of the patients with idiopathic scoliosis (+1.2±2.2%) did not differ from the same measurements of the NM patients (+0.9±4.1%, P=0.663), both did differ significantly, however, from measurements over the same levels in controls (-3.0±1.6%; P<0.001). The A-C% T1-S1 of the patients with idiopathic and NM scoliosis (+7.9±1.8% and +8.7±4.0%, P=0.273) differed significantly from the controls (+4.2±3.3%; P<0.001; Figure 3).
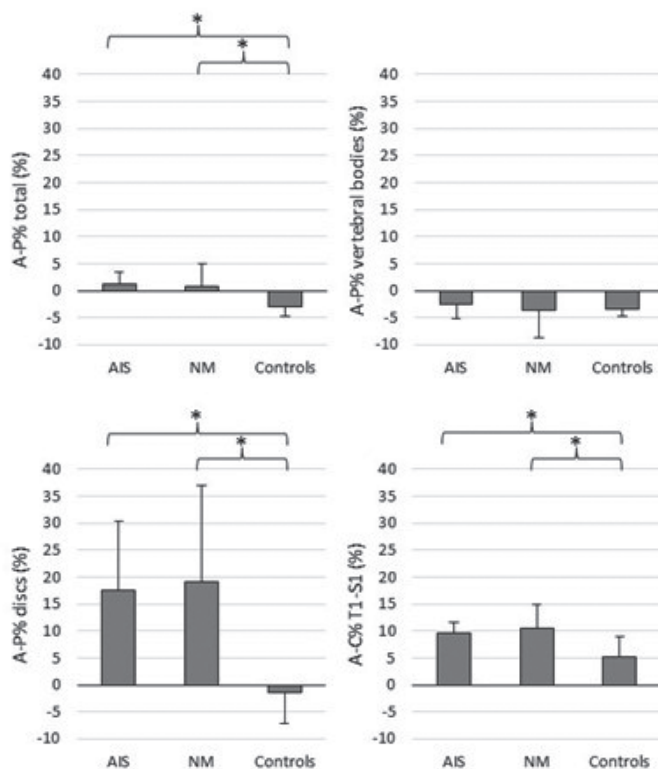
Figure 3. Overall anterior-posterior height ratio (A-P%) of the curve and A-P% of the vertebral bodies and intervertebral discs for the adolescent idiopathic scoliotic (AIS) and neuromuscular (NM) scoliotic thoracic curves and the corresponding levels in controls. In addition, anterior spine-spinal canal ratio (A-C%) is shown between T1 and the sacral plate (T1-S1). A negative percentage indicates a larger posterior length in comparison to anterior length. Error bars indicate SD. * = significant difference.

Relation with curve severity

The A-P% of the idiopathic and NM scoliotic curves correlated linearly with the Cobb angle (AIS r=0.678, NM r=0.687; Figure 4).

Contribution of the intervertebral disc versus vertebral body

The A-P% in the discs of the AIS (+17.5±12.7%) and NM (+19.1±18.0%) curves differed also significantly as compared to the A-P% of the discs in the control group (-1.5±5.6%; $P<0.001$), but the A-P% of the vertebral bodies of the AIS (-2.5±2.6%) and NM (-3.5±5.1%) curves did not differ from the control group (-3.4±1.4%; $P≥0.123$; Figure 3), there was no A-P% difference of the vertebral body and discs between the AIS and NM curves ($P≥0.342$). In the AIS and NM curves, the A-P% of the discs differed significantly from the A-P% in the vertebral bodies ($P<0.001$), but in the control group there was no difference between the A-P% of the vertebral bodies and intervertebral discs ($P=0.096$).
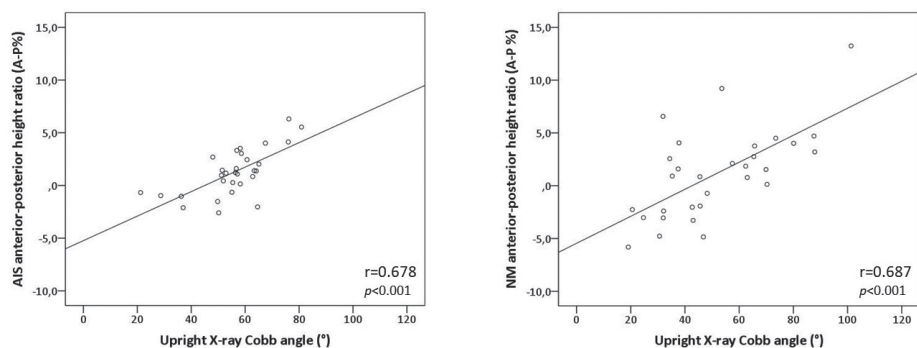
Figure 4. In these scatterplots, the Pearson correlation coefficient (r) between Cobb angle on the upright or sitting radiograph and anterior-posterior height ratio (A-P%) on the 3Dimensional computed tomographic scan is shown for the thoracic adolescent idiopathic scoliotic (AIS) and neuromuscular (NM) scoliotic curves.

DISCUSSION

Idiopathic scoliosis is still an orthopaedic enigma, despite many years of dedicated research into its cause, no single etiopathogenetic mechanism has been established, although unique mechanical loading of the upright human spine appear to play an important role.[3, 10] It is a fact that the anterior part of the spine in AIS is longer than posterior, this has been known for a long time.[2, 46, 47, 50] More recently it has also been described as a potential driver for initiation and progression of the disorder.[47, 52-54] A lack of synchronicity between two different mechanisms of ossification of different elements of the spinal column, intra-membranous (the laminae) and endo-chondral (the vertebral bodies) has been postulated as a primary growth disturbance that leads to a longer anterior column, that has to rotate and deviate out of the midline in order to keep the head centered over the pelvis and to avoid excess tension on the spinal cord.[47, 52, 53, 55] If the same growth disturbance is manifest not only in idiopathic, but also in scoliosis of another, known origin, this suggests that the excess anterior length may be more of a secondary phenomenon that is the consequence of the deformity, rather than its cause. Our study compared anterior overgrowth between scoliosis of a known origin (different types of NM scoliosis), idiopathic scoliosis and non-scoliotic controls. The ratio between the anterior length and the spinal canal length was measured along the whole spine from T1-S1, whereas the anterior-posterior height ratio of the individual vertebral bodies and discs was measured in the thoracic curves from Cobb end vertebra to end vertebra and in the corresponding levels in controls, according to a previously validated method.[44, 51-54] Thoracic curves were chosen because deviations from the normal sagittal profile have been demonstrated mostly in thoracic scoliosis.[44, 54] The control group showed a normal kyphotic anatomy of the thoracic spine; the posterior part was 3.0% longer as compared to the anterior part. In contrast to the normal kyphotic anatomy,

the anterior part of the thoracic scoliotic curves was longer than the posterior part from upper to lower Cobb end vertebra in idiopathic scoliosis (1.2%) as can be expected from previous work.[44, 52, 54] However, the anterior thoracic spine was similarly longer in scoliotic curves caused by different types of neuromuscular disease (0.9%). In both scoliosis groups, the normal thoracic kyphosis was changed into a thoracic lordosis, no difference in the amount of anterior overgrowth could be established between idiopathic scoliosis and scoliosis with a neuromuscular origin. Given the fact that we looked at proportions between anterior and posterior length in our study, it is impossible to differentiate whether the anterior-posterior length difference is a result of increased anterior length or decreased posterior length. Most of the excess anterior length in the scoliotic thoracic spine, both in idiopathic as well as in neuromuscular cases, appeared to be caused by a substantial difference in height of the anterior portion of the disc (AIS +17.5%, NM +19.1%) compared to its posterior aspect, whereas the vertebral bodies showed no different shape from the normal controls. This does not seem to be in accordance with a primary boney growth disturbance, rather it could be a mechanical effect caused by unloading of the anterior spine by its position rotated away from the midline in both types of scoliosis.

CONCLUSION

So called anterior spinal overgrowth is not specific for idiopathic scoliosis, but the same phenomenon is seen in non-idiopathic scoliosis as well. It is caused mainly by a relative increase of anterior height of the disc, the vertebral bodies do not contribute to the additional anterior length in these moderate to severe scoliotic curves. Anterior overgrowth in both idiopathic and non-idiopathic scoliosis increases linearly with increasing Cobb angle in these thoracic curvatures.

Chapter 7

Anterior-Posterior Length Discrepancy of the Spinal Column in Adolescent Idiopathic Scoliosis – a 3D CT Study

ABSTRACT

Background Context. One of the characteristics of reported observations in adolescent idiopathic scoliosis (AIS) is that the thoracic spine is longer anteriorly than posteriorly, more pronounced around the apex than the transitional zones. This reversal of the normal kyphotic anatomy of the thoracic spine is related to questions of etiopathogenesis of AIS. The changes in the anatomy of the anterior column have been described rather in detail, however, the role of the posterior spinal column and the laminae has so far not been elucidated. If the posterior column exhibits a longitudinal growth disturbance, it could act as a tether, leading to a more or less normal anterior column with a deformed and shorter posterior aspect of the spine. So far, it has remained unclear whether this anterior-posterior length discrepancy is the result of relative anterior lengthening or relative posterior shortening, and which tissues (bone, disc, intervertebral soft tissue) are involved.

Purpose. To compare the discrepancy of the anterior-posterior length of the spinal column in the 'true' midsagittal plane of each vertebra in idiopathic scoliosis patients versus controls, using three-dimensional CT scans.

Study Design/Setting. Cross-sectional.

Patient Sample. CT scans of 80 moderate to severe AIS patients (Cobb angle: 46-109°) prior to scoliosis navigation surgery and 30 non-scoliotic age-matched controls.

Outcome Measures. The height of the osseous and non-osseous structures from anterior to posterior in the 'true' midsagittal plane: the anterior side of the vertebral body and disc, the posterior side of the vertebral body and disc, the lamina and interlaminar space and the spinous process and interspinous space, as well as the height ratios between the anterior column and posterior structures of the primary thoracic and lumbar AIS curves and corresponding levels in non-scoliotic controls.

Methods. Semi-automatic software was used to reconstruct and measure the parameters in the true midsagittal plane of each vertebra and intervertebral structure, that are rotated and tilted in a different way.

Results. In AIS, the anterior height of the thoracic curve was $3.6\pm2.8\%$ longer as compared to the posterior height, $2.0\pm6.1\%$ longer than the length along the laminae and $8.7\pm7.1\%$ longer than the length along the spinous processes and this differed significantly from controls ($-2.7\pm2.4\%$, $-7.4\pm5.2\%$ and $+0.7\pm7.8\%$; $p<0.001$). The absolute height of the osseous parts did not differ significantly between AIS and controls in the midsagittal plane. In contrast, the intervertebral structures contributed significantly to the observed length discrepancies. In absolute lengths, the anterior side of the disc of the thoracic curve was higher in AIS (5.4 ± 0.8 mm) than controls (4.8 ± 1.0 mm; $p<0.001$), whereas the interspinous space was smaller in AIS (12.3 ± 1.4 mm *versus* 14.0 ± 1.6 mm; $p<0.001$).

Conclusions. Based on this in vivo analysis, the true three-dimensional anterior-posterior length discrepancy of AIS curves was found to occur through both anterior column lengthening as well as posterior column shortening, with the facet joints functioning as the fulcrum. The vertebrae contribute partly to the anterior-posterior length discrepancy accompanied by more significant and possibly secondary increased anterior intervertebral discs height.

INTRODUCTION

Adolescent idiopathic scoliosis (AIS) is a complex three-dimensional (3D) spinal deformity with still unclear etiology.[3] It has been known for many years that the anterior side of the scoliotic curvatures is longer than posteriorly.[2, 3] This so-called relative anterior spinal overgrowth (RASO) has been suggested as part of the etiopathogenetic mechanism of AIS. Different explanations have been suggested. It has either been hypothesized to be the result of an active growth disturbance between the normally synchronous growth between the laminae and the vertebral bodies, or a result of a passive response to altered biomechanical loading of the spine.[47, 52-54] In a previous study it has been shown that wedging of the vertebral bodies contribute less to the anterior-posterior length discrepancy than the intervertebral discs.[44] Although earlier studies have investigated the sagittal scoliotic profile on lateral radiographs, and measured the morphology in the sagittal plane of the patients, only a few have studied the true anterior-posterior length discrepancy, in the sagittal plane of the individual structures, while taking account of the complex 3D rotational deformation, using 3D imaging.[44, 47, 49, 50, 53, 54, 199-202] The role of the posterior structures of the spine has not yet been studied, relative anterior lengthening can still be the result of an active disturbance of the growth in height of the laminae, or, alternatively, of passive compression of the interlaminar or interspinous space. Therefore, the question whether this anterior-posterior length discrepancy is the result of relative anterior lengthening or relative posterior shortening is the purpose of this study. To quantify the 3D morphometric anterior-posterior length changes in the different osseous and non-osseous spinal structures, we compared spinal morphology between an existing set of high-resolution CT scans of AIS patients with moderate to severe primary main thoracic curves, obtained for intra-operative navigation purposes, and CT scans of non-scoliotic controls. For this analysis we used a previously validated 3D image processing technique, which provides the opportunity to measure morphology in the true midsagittal plane of each different structure by taking translation, rotation and tilt into account.[44]

MATERIALS AND METHODS

Study population
This study was approved by the local research ethics committee. It included a consecutive series of AIS patients that had undergone pre-operative CT scanning for navigation guided posterior pedicle screw instrumentation and magnetic resonance imaging of the spine as well as standard upright and bending X-rays at one academic institution as part of the standard pre-operative work up between 2011 and 2014. Part of this dataset was

previously used for 3D morphometric analysis of vertebral bodies and discs in different regions of the spinal curvatures.[44, 50] Patients with other spinal pathologies, neural axis abnormalities, previous spinal surgery or incomplete radiologic work-up were excluded. Curve characteristics (level of the apex, Cobb angles and curve type according to the Lenke classification) were determined on the conventional standing posterior-anterior and lateral bending radiographs (Table 1).[11, 157] Primary thoracic curves, and corresponding secondary (thoraco)lumbar curves, were included (Lenke curve type 1-4).[157] The control group consisted of 30 age-matched adolescents without spinal pathology who had undergone CT imaging of the thorax and abdomen for indications other than spinal pathology (for example trauma screening or prior to bone marrow transplantation).

Included			AIS patients (n=80)	Controls (n=30)
Age		Range	10-20 years	10-20 years
		Mean±SD	15.7±2.3 years	15.7±1.7 years
Females		n (%)	68 (85%)	23 (77%)
Thoracic curve right convexity		n (%)	80 (100%)	NA
Lumbar curve left convexity		n (%)	80 (100%)	NA
Primary thoracic Cobb angle		Range	46-109°	NA
		Mean±SD	69.5±12.7°	NA
Secondary lumbar Cobb angle		Range	17-76°	NA
		Mean±SD	39.7±12.7°	NA
Lenke curve	Type 1	n (%)	41 (51%)	NA
	Type 2	n (%)	24 (30%)	NA
	Type 3	n (%)	10 (13%)	NA
	Type 4	n (%)	5 (6%)	NA

Table 1. Demographics and curve characteristics are shown for all included adolescent idiopathic scoliotic (AIS) patients and controls. SD = standard deviation.

Computed tomographic measurement method

Two trained observers used previously validated software and a semi-automatic image processing technique for CT scans of the scoliotic spine (ScoliosisAnalysis 4.1, Image Sciences Institute, Utrecht, The Netherlands, developed using MeVisLab, MeVis Medical Solutions AG, Bremen, Germany) to provide complete 3D coordinate systems of the individual structures of the spine.[44] By this method, the exact height of the osseous (anterior and posterior side of the vertebral bodies, the laminae and the spinous processes) and non-osseous structures (anterior and posterior side of the intervertebral discs, interlaminar spaces and interspinous spaces) in the midsagittal plane were measured, while correcting for rotation and tilt in 3D. In contrast to the anatomical midsagittal plane of the patient, this complete 3D analysis method enabled the observer to reconstruct

the midsagittal plane of each structure by taking account of axial rotation and coronal and sagittal tilt, as well as torsion (internal rotation) of each individual structure (Figure 1). Intraclass correlation coefficients for intra- and interobserver reliability for these measurements on high-resolution CT scans were 0.99 (0.98–1.00) and 0.99 (0.98–1.00), respectively.[44]

The mean heights of the structures were calculated from Cobb end to Cobb end vertebra of the primary thoracic and secondary (thoraco)lumbar AIS curve and matched levels in controls. The proportionate length was compared between the scoliotic co-hort and controls and between the osseous and non-osseous structures from anterior to posterior: the anterior side of the vertebral body and disc (A), the posterior side of
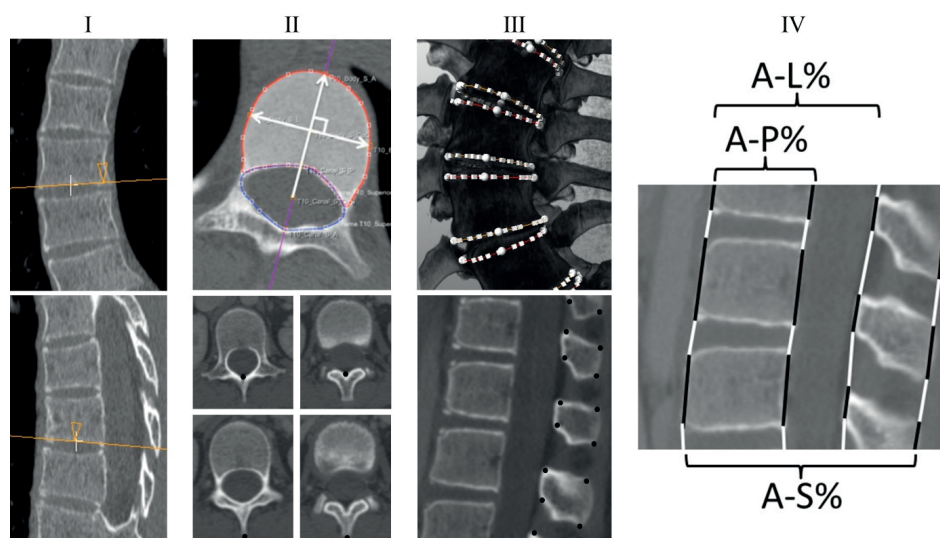

Figure 1. The orientation of the upper and lower endplate of each individual vertebra was determined using the semi-automatic software, correcting for coronal and sagittal tilt (I), to reconstruct the true trans-verse sections. The observer drew a contour around the endplates of the vertebral body and the spinal canal (II upper figure). The software calculated a center of gravity of the vertebral body and spinal canal and reconstructed a longitudinal axis between these points. The intersection of this axis and the contour on the anterior side, defined the anterior point of the endplate and the same applied for the posterior point (II up-per figure). This defined the true anterior and posterior side of each endplate, and thus the true anterior and posterior side of each vertebral body as well as intervertebral disc. The connection between these points is a rotated sagittal plane, but represents the true midsagittal plane of each individual structure. anterior as well as posterior lengths were computed for all vertebral bodies and intervertebral discs (III upper figure). Next, the observer selected the upper endplate and corrected again for the coronal and sagittal tilt. Then, the observer moved down to segment the upper lamina point and moved further down to select the lower lamina point and repeated the procedure for the upper and lower points of the spinous process (II lower figure). By using these points, the lamina and interlaminar height as well as the height of the spinous pro-cess and the interspinous space were calculated (III lower figure). Finally, the anterior-posterior ratio (A-P%, as ((A-P)/P)*100%), the anterior-laminar (A-L%) ratio and the anterior-spinous process ratio (A-S%) were calculated for the osseous parts (black in IV) as well as the non-osseous parts (white in IV).

the vertebral body and disc (P), the lamina and interlaminar space (L) and the spinous process and interspinous space (S). Because the anterior-posterior ratio (A-P%) was calculated as ((A-P)/P)*100%, the anterior-laminar ratio (A-L%) as ((A-L)/L)*100% and the anterior-spinous process ratio (A-S%) as ((A-S)/S)*100%, positive values indicated relative greater anterior lengths (Figure 1).

Statistical analysis

Statistical analyses were performed using SPSS 22.0 for Windows (SPSS Inc., Chicago, IL, USA). Descriptive statistics were computed providing the mean, range and standard deviation. Length ratios of the AIS patients and controls were compared using one-sample t-tests and paired t-tests were used to compared the length ratios within the subjects. A p<0.002 was considered to be statistically significant (Bonferroni's correction for multiple testing).

RESULTS

Population

Forty-six of the 126 AIS patients were excluded (23 had no primary right convex thoracic curve (Lenke curve type 5 or 6), 12 had associated congenital or neuromuscular patholo-gies and 11 had incomplete radiologic work-up). The final study population consisted of 80 AIS subjects and 30 non-scoliotic controls. Demographics and curve characteristics are shown in Table 1.

Anterior-posterior height ratios in the midsagittal plane

The height ratios of the primary curve and corresponding levels in controls showed on average more anterior length in AIS (A-P% = +3.6±2.8%, A-L% = +2.0±6.1% and A-S% = +8.7±7.1%) as compared to controls (A-P% = -2.7±2.4%, A-L% = -7.4±5.2% and A-S% = +0.7±7.8%; AIS *versus* controls p<0.001; Table 2). All the non-osseous structures showed more anterior lengthening in AIS (A-P% = +14.1±11.4%, A-L% = -53.2±10.0% and A-S% = -55.8±8.2%) as compared to controls (A-P% = -3.7±7.6%, A-L% = -61.3±11.6% and A-S% = -65.8±6.4%; AIS *versus* controls p<0.001; Table 2), whereas the osseous structures showed only more anterior lengthening for the A-P% in AIS (+1.3±3.3%) as compared to controls (-2.4±3.0%; p<0.001; Table 2). The height ratios of the secondary (thoraco) lumbar curves showed similar discrepancies as the primary thoracic curves, but to a lesser extent (Table 2). Additionally, the apical vertebral body and intervertebral disc showed most anterior-posterior length discrepancy (A-P% apex +6.0±5.1 versus Cobb end vertebral body and intervertebral disc -2.2±14.2; p<0.001 and A-S% +14.1±17.6 versus -9.3±11.7; p<0.001, A-L% differed not significantly).

		AIS	Controls	*P*
A-P%	Thoracic	+3.6±2.8%	-2.7±2.4%	<0.001
	Lumbar	+13.6±4.7%	+12.1±6.8%	NS
A-P% osseous	Thoracic	+1.3±3.3%	-2.4±3.0%	<0.001
	Lumbar	+3.7±4.6%	+6.2±7.0%	NS
A-P% non-osseous	Thoracic	+14.1±11.4%	-3.7±7.6%	<0.001
	Lumbar	+51.0±17.1%	+32.0±18.7%	<0.001
A-L%	Thoracic	+2.0±6.1%	-7.4±5.2%	<0.001
	Lumbar	+18.9±7.7%	+16.3±11.1%	NS
A-L% osseous	Thoracic	+58.0±22.4%	+50.7±22.8%	NS
	Lumbar	+145.1±39.2%	+128.1±37.4%	NS
A-L% non-osseous	Thoracic	-53.2±10.0%	-61.3±11.6%	<0.001
	Lumbar	-47.8±8.1%	-48.4±9.5%	NS
A-S%	Thoracic	+8.7±7.1%	+0.7±7.8%	<0.001
	Lumbar	+28.9±11.1%	+24.4±17.1%	NS
A-S% osseous	Thoracic	+89.4±26.5%	+101.1±36.1%	NS
	Lumbar	+54.1±21.3%	+64.6±25.8%	NS
A-S% non-osseous	Thoracic	-55.8±8.2%	-65.8±6.4%	<0.001
	Lumbar	-3.6±27.3%	-21.3±24.0%	0.002

Table 2. Anterior-posterior (A-P%), anterior-laminar (A-L%) and anterior-spinous process (A-S%) length ratios, including standard deviations, of the main thoracic and secondary lumbar adolescent idiopathic scoliotic (AIS) curves and matched levels in controls are shown. Additionally, the ratios are shown for the height of the osseous as well as the non-osseous parts. A positive percentage indicates a larger anterior height compared to posterior.

Absolute lengths between AIS and controls

Two significant differences between AIS and controls were observed in the thoracic region: the anterior height of the intervertebral disc was greater in AIS (5.4±0.8 mm) as compared to controls (4.8±1.0 mm; p<0.001), whereas the interspinous height was less in AIS (12.3±1.4 mm) as compared to controls (14.0±1.6 mm; p<0.001; Figure 2).

DISCUSSION

Already more than a century it is well known that idiopathic scoliosis is a complex 3D deformation of the thoracic and lumbar spine, characterized by lateral deviation, rotation and relative lordosis. One of the previously reported and intriguing aspects of idiopathic scoliosis is that the anterior side of the spine is longer than its posterior side.[2, 46-50] However, it remained unclear whether this anterior-posterior length discrepancy is the result of relative anterior lengthening or relative posterior shortening and whether this takes place in the vertebrae or intervertebral structures.
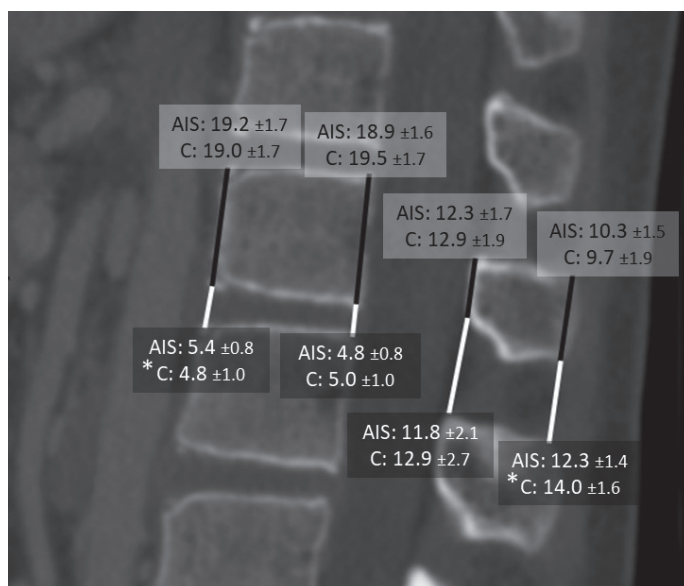
Figure 2. The absolute lengths, in millimeters, of different parts of the thoracic curve of adolescent idio-pathic scoliosis (AIS) patients and corresponding levels in controls (C) are shown; the osseous parts in black and the non-osseous parts in white. * = significant difference between AIS and controls.

Despite our concern for ionizing radiation in a growing population and the prone positioning of the AIS patients, in general, 3D CT reconstructions are considered as the 'gold standard' to assess the morphology of *in vivo* structures.[43] Because of the complex 3D deformation in which each spinal structure is rotated, translated and tilted in a dif-ferent way, conventional parameters, such as thoracic kyphosis and lumbar lordosis as measured on lateral radiographs, may help in understanding global spinal balance, but they are not representative for the true 3D pathoanatomy of the crooked spine. As a result of the spinal deformation in AIS, the true sagittal plane of each vertebral body and intervertebral disc differs along the spine, and even within a single vertebra or disc it may be theoretically impossible to determine the exact anterior and posterior side due to their mechanical torsion.[44] This obstacle has already been described by numerous authors and was tried to overcome by for example Stagnara's *plan d'election* or modern 3D reconstructions of biplanar radiographs.[39, 43, 47, 51, 59] Nevertheless, still many try to describe the sagittal morphology of AIS on conventional lateral radiographs.[39, 47, 49-51, 200]

Previous 2D and 3D studies have shown that the largest part of this discrepancy resides in an anterior opening of the disc, however, the contribution of the posterior elements, i.e. the laminae, interlaminar spaces, spinous processes and interspinous spaces, to this anterior-posterior length discrepancy, has not been studied in detail. Thus, relative anterior spinal overgrowth could be caused either by an active inhibition of the bony growth of the laminae, or by a compression of the soft tissues between the laminae.

For complete description of the true 3D spinal morphology in AIS, as far as the authors know, this study is the first to quantify the absolute and relative anterior-posterior length discrepancy from the anterior aspect of the vertebrae and discs to the posterior aspect of the spinous processes and interspinous spaces, differentiating between bony structures and soft tissues and compare the findings in AIS to controls.

The anterior side of the thoracic vertebral bodies in the thoracic non-scoliotic spine was on average 2.4% shorter than the posterior side, whereas the anterior side of the vertebral bodies in AIS was 1.3% longer than posterior, resulting in a relative anterior lengthening of the vertebrae of 3.7% in AIS as compared to controls. The rest of the bony structures (lamina and spinous processes) showed no significant difference in anterior-posterior ratio between AIS and controls. The differences in height ratios between AIS and controls in the non-osseous structures were 17.8%, 8.1% and 11.7% for the intervertebral discs, interlaminar spaces and interspinous spaces of the thoracic curves and corresponding levels in the non-scoliotic controls. In the secondary, (thoraco)lumbar curves, the same phenomenon was observed in this population: the non-osseous structures contributed most to the relative anterior lengthening and posterior shortening. Next, the absolute lengths were compared to distinguish between relative anterior lengthening and relative posterior shortening. In comparison with the same levels in unaffected adolescents in this study, two differences were observed between the scoliotic and non-scoliotic group; the anterior height of the intervertebral discs of the main thoracic curve was larger, whereas the interspinous height was smaller in AIS as compared to controls.

A variety of concepts are involved in the relative anterior spinal overgrowth and the etiopathogenesis of AIS. Dickson et al. hypothesised that differences in the sagittal plane (reversal of the normal thoracic kyphosis) during growth, could initiate a progressive idiopathic scoliosis, and other authors have proposed a hypothesis of uncoupled endochondral-membranous bone growth in AIS.[47, 52] Porter described that in the scoliotic spine, the length of the spinal canal was consistently shorter than the anterior height of the vertebral bodies and intervertebral discs and postulated a hypothesis on uncoupled neuro-osseous growth.[52-54, 152] In this, asynchronous growth patterns of different spinal structures (active) or tethering of the spinal cord or other posterior soft tissues (passive) could lead to a longer anterior side of the spine.[47, 52, 53, 55] Later on, the asynchronous neuro-osseous growth, as described by Roth and Porter, was extended.[55, 150, 152, 203-206] Chu et al. observed relative anterior overgrowth of the spine, without an increased spinal cord length in moderate to severe AIS patients.[53] They hypothesized that the relative tethering of the spinal cord could lead to a protective relative extension of the spine and thus play a role in the etiopathogenesis of AIS.[53, 205, 206] The relative anterior lengthening could be a result of a slower growth of the posterior structures, like the spinal cord, as compared to the anterior spinal column, during the rapid growth spurt.[152, 204-206]

Schlösser et al. described that the anterior-posterior length discrepancy of AIS curves is mainly caused by an increase of anterior height of the discs, that the vertebral bodies contribute to a much lesser extent and that the junctional zones between the curves are not affected by this so called relative anterior overgrowth, thereby making a generalized growth disturbance less likely.[44, 47, 50, 52-54, 201] Brink et al. showed that anterior overgrowth is not restricted to idiopathic scoliosis, as same phenomenon also occurs in neuromuscular scoliosis and they described that the anterior lengthening was solely observed in the intervertebral discs, whereas the vertebral bodies showed no significant differences in anterior lengthening between either idiopathic or neuromuscular scoliosis, and non-scoliotic controls.[49] It thus appears that the anterior lengthening that is seen in idiopathic scoliosis is a more generalized phenomenon that is part of the scoliotic mechanism.[49]

The current study shows that the anterior-posterior length discrepancy is the result of anterior lengthening as well as posterior shortening, with the facet joints functioning as a fulcrum. This detailed description of the length discrepancy between the anterior and posterior side of the spine is important and relevant, both from the etiopathogenesis as well as a treatment point of view. Anterior to the fulcrum, the vertebral bodies contribute to the anterior lengthening, but the intervertebral discs contributed four times more, in this series of patients with moderate to severe right convex thoracic and left convex (thoraco)lumbar idiopathic scoliosis. The posterior shortening was caused by a compression of the non-osseous structures, not by a growth disturbance of the laminae as compared to the non-scoliotic controls. No active growth processes are known that would cause the anterior part of the disc to grow faster than the posterior part, or the interlaminar and interspinous ligaments to be more constricted, only around the apex of a scoliotic curve, and both in idiopathic scoliosis as well as in neuromuscular curves. The question thus remains: what causes this anterior-posterior length discrepancy? There seem to be two possibilities:

1. The slight but reproducible difference between anterior and posterior height of the vertebral body is part of an active growth disturbance, that leads to secondary adaptations in the disc and interlaminar soft tissue, as a relative posterior tether to the longitudinal growth of the spine, or,

2. All observed differences are secondary phenomena. The suggested mechanism then could start with rotation away from the midline of certain vulnerable spinal segments as an initiating event, thereby unloading the anterior part of the spine and compressing the posterior elements[152, 207, 208]

The major drawback of our 3D CT image analysis method for future studies is obviously the concern for ionizing radiation in a growing population the radiation exposure. For this study, an already existing CT database was used, acquired as part of the general pre-operative workup for navigation guided pedicle screw surgery in one of our insti-

tutions, resulting in a cross-sectional study design. On ethical grounds, it is obviously not possible to obtain longitudinal 3D data based on repeated CT scanning. Another drawback is that the CT scans are not obtained in upright position. The prone position of the CT scans of the AIS patients could affect the configuration of the spine. Therefore, the CT scans of AIS patients were compared to CT scans of non-scoliotic controls, that are neither made in upright position. The CT scans of the AIS patients were made in prone position, whereas the CT scans of the non-scoliotic controls were made in supine position. It may be argued that positioning has affected the general configuration of the spine in our study. If the anterior-posterior length differences were a result of the positioning, this phenomenon would be seen in the apical as well as in the neutral zones. Previous authors, that used the same imaging data as for this study, have shown that the excess anterior length in the scoliotic spine is not a global, but rather a regional phenomenon that is confined to the apical zones.[50] Therefore, the findings of the current study are based on structural differences between AIS patients and non-scoliotic controls, rather than position related differences. Moreover, Brink et al. described that the thoracic kyphosis was larger in prone position as compared to supine position in the same scoliotic patients, i.e. the spine is more extended in supine position than in prone position.[58] Thus, if positioning influenced the measurements, it would only be to minimize rather than exaggerate the observed differences.

CONCLUSIONS

Anterior-posterior length discrepancy of the primary and secondary scoliotic curves is caused by anterior lengthening as well as posterior shortening, with the facet joints as the fulcrum. The vertebral bodies as well as the intervertebral discs contribute to the anterior lengthening, but the intervertebral discs contribute four times more. The posterior shortening appeared to be caused by compression of the inter-laminar space, not by an active growth disturbance of the bony laminae.

Chapter 8

What is the actual 3D Representation of the Rib Vertebra Angle Difference (Mehta's angle)?

ABSTRACT

Study Design. Cross-sectional study.

Background Data. The rib vertebra angle difference (RVAD, also known as Mehta's angle) describes apical rib asymmetry on conventional radiographs and was introduced as a prognostic factor for curve severity in early onset scoliosis, and later applied to other types of scoliosis as well.

Objective. To establish the relevance of the conventional two-dimensional (2D) RVAD and the relationship with the complex three-dimensional (3D) apical morphology in scoliosis.

Methods. An existing idiopathic scoliosis database of high-resolution CT scans used in previous work, acquired for spinal navigation, was used. Eighty-eight patients (Cobb angle 46-109°) were included. Cobb angle and 2D RVAD, as described by Mehta, were measured on the conventional radiographs and coronal digitally reconstructed radiographs (DRR) of the prone CT scans. A previously validated, semi-automatic image processing technique was used to acquire complete 3D spinal reconstructions for measurement of the 3D RVAD in a reconstructed true coronal plane, axial rotation and sagittal morphology.

Results. The 2D RVAD on the X-ray was on average 25.3±11.0° and 25.6±12.8° on the DRR (P=0.990), but in the true 3D coronal view of the apex, hardly any asymmetry remained (3D RVAD: 3.1±12.5°; 2D RVAD on X-ray and DRR *versus* 3D RVAD: P<0.001). 2D apical rib asymmetry in the anatomical coronal plane did not correlate with the same RVAD measurements in the 3D reconstructed coronal plane of the rotated apex (r=0.155; P=0.149). A larger 2D RVAD was found to correlate linearly with increased axial rotation (r=0.542; P<0.001) and apical lordosis (r=0.522; P<0.001).

Conclusions. The 2D RVAD represents a projection-based composite radiographic index reflecting the severity of the complex 3D apical morphology including axial rotation and apical lordosis. It indicates a difference in severity of the apical deformation.

INTRODUCTION

In 1972 Mehta introduced the rib vertebra angle difference (RVAD) as a prognostic factor for progression of early onset scoliosis.[41] The curve was shown to be at high-risk for progression if the angle difference between the convex and concave apical ribs exceeds 20°. Additionally, Mehta classified the position of the apical rib head as phase 1 if there is no overlap of the convex rib head over the apical vertebra, or phase 2, if the convex rib head overlaps the apical vertebra, phase 2 also corresponds to a high risk of progression. Because of its prognostic value, the RVAD has been studied widely in early onset as well as neuromuscular and adolescent idiopathic scoliosis (AIS) and it has been suggested that the drooping ribs on the convex side could result in decreased stability of the spine.[91-101] The RVAD as introduced by Mehta is based on a two-dimensional (2D) coronal projection of a complex three-dimensional (3D) costo-vertebral configuration. Foley et al. measured the RVAD in the true coronal plane of the vertebra, by using 3D reconstructions of two X-rays, and concluded that the RVAD does not indicate asymmetry of the costovertebral junction, but is a reflection of the 3D deformity including the vertebral rotation.[100, 209] However, to measure the exact RVAD in 3D, solely correction for the rotation is not sufficient, but correction in the three planes, including correcting for the sagittal profile, is required. Additionally, the relation between the RVAD and the complex 3D nature of the scoliotic deformity, has not been determined. Our hypothesis was that the 2D RVAD represents a projection-based composite radiographic index reflecting the severity of the complex 3D apical morphology including axial rotation and apical lordosis in the thoracic curve. Therefore, in this study, we investigated the relationship between the conventional 2D RVAD, its 3D version and the true 3D spinal morphology of the scoliotic spine.

MATERIALS AND METHODS

Study population
This study has been approved by the local research ethics committee. Patients with a primary thoracic typical right convex, AIS curve (Lenke curve type 1, 2, 3 and 4[157]) were included from an existing database of computed tomography (CT) scans, partially used in previous studies.[44, 145] These scans had been acquired as part of standard pre-operative work-up between 2011 and 2014 for spinal navigation before posterior scoliosis surgery. All subjects were scanned in the prone position (which resembled the operation posture) with the arms on the side. Patients with other spinal pathology, neural axis abnormalities, previous spinal surgery or incomplete radiologic work-up were excluded. The 2D RVAD, as described by Mehta, was measured on the conventional posterior-anterior standing

radiographs as well as on the coronal digitally reconstructed radiographs (DRR) of the CT scans (mean extinction projection, source to detector distance: 500mm, non-divergent beam), made with MeVisLab, (MeVis Medical Solutions AG, Bremen, Germany; Figure 1).[11, 41] The RVAD was the difference between the concave and convex rib vertebra angle (concave minus convex). Mehta defined the rib vertebra angle as the angle between a line through the rib head and rib neck, and a line perpendicular to the lower endplate of the vertebral body (Figure 1).[41] Additionally, the coronal Cobb angle and Mehta's phase were measured on the plain radiograph. Phase 1 was defined as: the head of the apical rib on the convex side does not overlap the upper corner of the apical vertebra on the radiograph. In phase 2, the rib head overlaps the upper corner of the apical vertebra. Furthermore, the patients were classified in groups based on different 2D RVAD magnitudes as measured on the plain radiograph (group 1: 2D RVAD<20°, group 2: 2D RVAD 20-30° and group 3: 2D RVAD>30°).
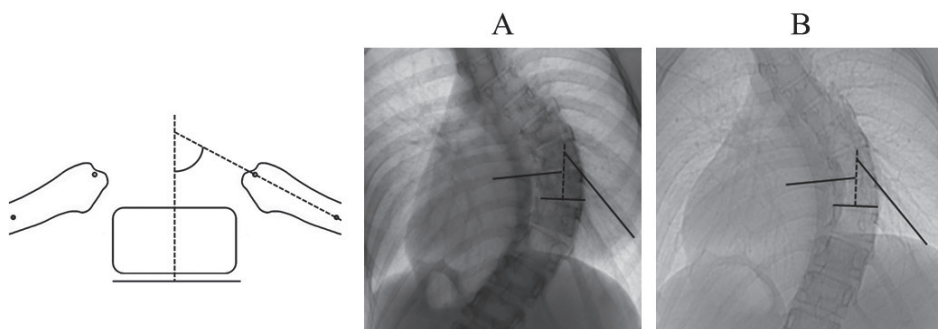

Figure 1. The 2D RVAD, according to Mehta, was measured on the conventional standing posterior-anterior radiograph (A) and digitally reconstructed radiograph (DRR) of the prone CT scan (B).[41] The RVAD was the difference between the convex and concave rib vertebra angle. Mehta defined the rib vertebra angle as the angle between the rib line, a line through the rib head and rib neck, and a line perpendicular to the lower endplate of the vertebral body.[41]

3D measurements

Using a previously validated, semi-automatic image processing technique, complete spinal reconstructions were acquired in a 3D coordinate system based on endplate segmentations (ScoliosisAnalysis 4.1, Center for Image Sciences, UMC Utrecht, The Netherlands), based on MeVisLab, as has been described in previous studies (Figure 2).[44, 175] In short, based on manual endplate and spinal canal segmentations, endplate vectors were automatically calculated in 3D, taking account of coronal and sagittal tilt of each individual level. The longitudinal axis was calculated for each individual vertebra, as a line through the midpoints of the vertebral body and the spinal canal. For this study, a corrected "true" coronal plane view of the apex was reconstructed, perpendicular to the longitudinal vector of the apical vertebra, while taking account for rotation and coronal
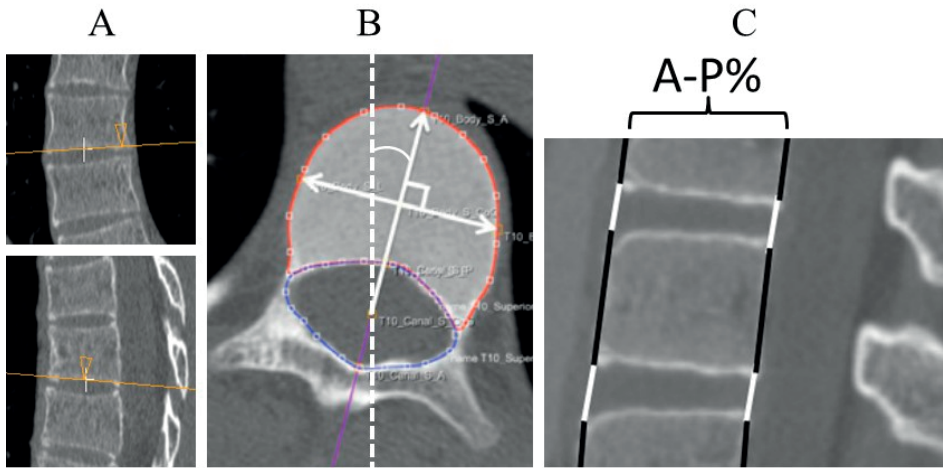
Figure 2. Complete spinal reconstructions were acquired using a previously validated, semi-automatic image processing technique, based on endplate segmentations.[44, 175] First, the observers corrected for the coronal and sagittal tilt, to select the true transverse plane (A). Next, the software reconstructed a vertebral axis through the midpoints of the vertebral body and spinal canal of each endplate, based on manual endplate and spinal canal segmentations (B). As a reference, the midsagittal plane of the sacral plate, which was considered to have no rotation or translation in thoracic scoliosis, was used (B). The mean of the upper and lower endplate vectors of each vertebra was used to quantify the rotation for each individual vertebra in the transverse plane. The intersection of the vertebral body axis of each endplate and the contours of the endplates formed the anterior (A) and posterior (P) points of each endplate (B). The apical lordosis (A-P%) was calculated as ((A-P)/P)*100%, positive values indicated apical lordosis (C).

and sagittal tilt. Next, similar to the conventional RVAD measurement, the angles between the lines connecting the rib head and neck, as well as the line perpendicular to the lower endplate were measured in the 3D coordinate system (Figure 3). In addition, axial rotation of the apical vertebra and apical lordosis of the apical segments (apical vertebra plus one vertebra above and beneath including the intervertebral discs) were measured using the previously validated endplate segmentations and corresponding 3D coordinate system. The apical lordosis was defined as the percentual difference between the anterior (A) and posterior (P) length in the true sagittal plane; ((A-P)/P)*100%, positive values indicated apical lordosis (Figure 2).

Intraclass correlation coefficients for this method (rotation and apical lordosis) for inter- and intra-observer reliability were 0.92 (95% confidence interval: 0.82-0.97) and 0.89 (0.74–0.95). For assessment of intra- and interobserver reliability analysis of the 2D and 3D RVAD measurements, two observers independently analyzed a randomly selected subset of ten subjects.
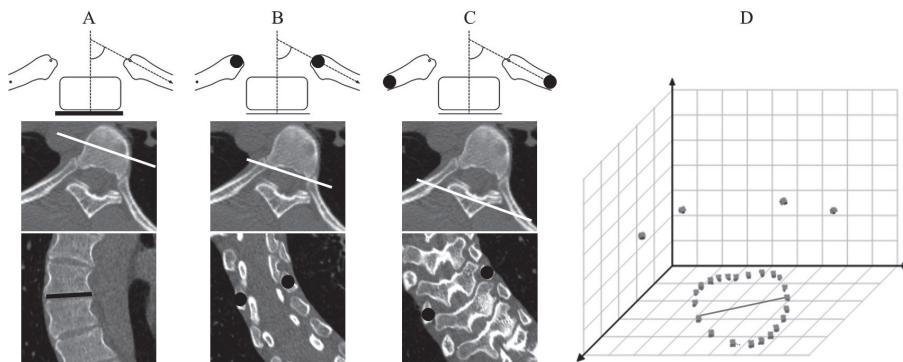
Figure 3. Perpendicular to the vertebral axis of the lower endplate, as used for the rotation (Figure 2), the software reconstructed a right-left axis through the midpoint of the vertebral body. This axis corresponded with the right-left axis of the lower endplate in the true mid-coronal plane, corrected for the rotation of the vertebral body (A). Next, the rib heads of the convex and concave sides (B) as well as the rib necks of both sides (C) were segmented in coronal reconstructions, and the positions in the 3D coordinate system were used to calculate the rib vertebra angle (D).

Statistical analysis

Statistical analyses were performed using SPSS 22.0 for Windows (SPSS Inc., Chicago, IL, USA). Descriptive statistics were computed providing means, ranges and standard deviations. RVAD on the upright radiograph, prone DRR and 3D RVAD on the CT were compared using repeated measures analysis of variance (ANOVA) for dependent t-tests. The relation between 2D and 3D RVAD and the 3D curve morphology parameters was tested using Pearson's correlation coefficient. Moreover, one-way ANOVA was used to compare the vertebral rotation, Cobb angle and apical lordosis between curves with different RVAD phases and values. The intra- and interobserver variability was obtained as intraclass correlation coefficient. The level of statistical significance level was set at 0.05.

RESULTS

Forty-seven of the 135 AIS patients were excluded (twenty-three had no primary right convex thoracic curve (Lenke curve type 5 or 6[157]), twelve had associated congenital or neuromuscular pathologies, eleven had incomplete radiologic work-up and one underwent surgery prior to this study). The final study population consisted of eighty-eight subjects. Demographics and curve characteristics are shown in Table 1. Intraclass correlation coefficients for intra- and interobserver reliabilities were 0.98 (95% confidence interval: 0.92–1.00) and 0.91 (0.64–0.96) for the 2D RVAD on the X-ray, 0.98 (0.94–1.00) and 0.91 (0.56–0.98) for the 2D RVAD on the DRR, and 0.90 (0.59–0.98) and 0.85 (0.38–0.96) for the 3D RVAD, respectively.

		AIS (n=88)
Age in years	range	10-26
	mean±sd	16.3±2.9
Girls	n (%)	75 (85%)
Right convex main thoracic curve	n (%)	88 (100%)
Cobb angle main thoracic curve	range	46-109
	mean±sd	69.2±12.2
Lenke type	I	45 (51%)
	II	26 (30%)
	III	12 (14%)
	IV	5 (6%)

Table 1. Demographics are shown for all included AIS patients and controls. The Cobb angle was measured on the conventional standing posterior-anterior radiograph. sd = standard deviation.

The 2D RVAD was on average 25.3±11.0° on conventional standing radiographs and 25.6±12.8° on the prone DRRs (*P*=0.990; Figure 4). Regarding the same costo-vertebral relationship in a derotated, true 3D coronal view of the apex, hardly any asymmetry remained, the 3D RVAD was 3.1±12.5°; (3D RVAD *versus* 2D RVAD (as measured on plain radiographs as well as DRR): *P*<0.001; Figure 4) and all phase 2 rib heads derotated back into a phase 1 position. Therefore, the 2D RVAD as measured on X-rays as well as DRRs showed no significant correlation with the 3D RVAD (r=0.155; *P*=0.149).

The 2D RVAD, measured on the plain radiograph, correlated significantly with the Cobb angle (r=0.547; *P*<0.001). It also correlated well with axial rotation (r=0.542; *P*<0.001) and apical lordosis (r=0.522; *P*<0.001; Table 2). Furthermore, the mean Cobb angle measured on the plain radiograph was 62.6±8.0°, 67.8±10.4° and 77.0±13.0° in group 1 (2D RVAD<20°), group 2 (2D RVAD 20-30°) and group 3 (2D RVAD>30°; *P*<0.001), the mean vertebral rotation was 17.1±7.1°, 20.6±5.6° and 26.7±7.8° (*P*<0.001) and the mean apical lordosis, defined as the difference between the anterior (A) and posterior (P) length in per cent; ((A-P)/P)*100%), was 3.1±2.9%, 4.6±2.6% and 6.5±3.0% in the three groups (*P*=0.001; Table 3). So, the deformities in the three planes differed significantly between the groups based on different 2D RVAD magnitudes as measured on the plain radiograph, where the least 3D deformation was associated with the lowest RVAD magnitude group. The 2D RVAD on the plain radiograph was larger in the phase 2 curves (27.9±10.3°) as compared to the phase 1 curves (17.1±12.0°; *P*<0.001). Additionally, the Cobb angle, axial vertebral rotation of the apex and apical lordosis were larger in the phase 2 curves as compared to the phase 1 curves (*P*≤0.009), whereas the (minimal) 3D RVAD showed no significant difference between the phase 1 and phase 2 curves as determined on the plain radiograph (*P*=0.129; Table 4).
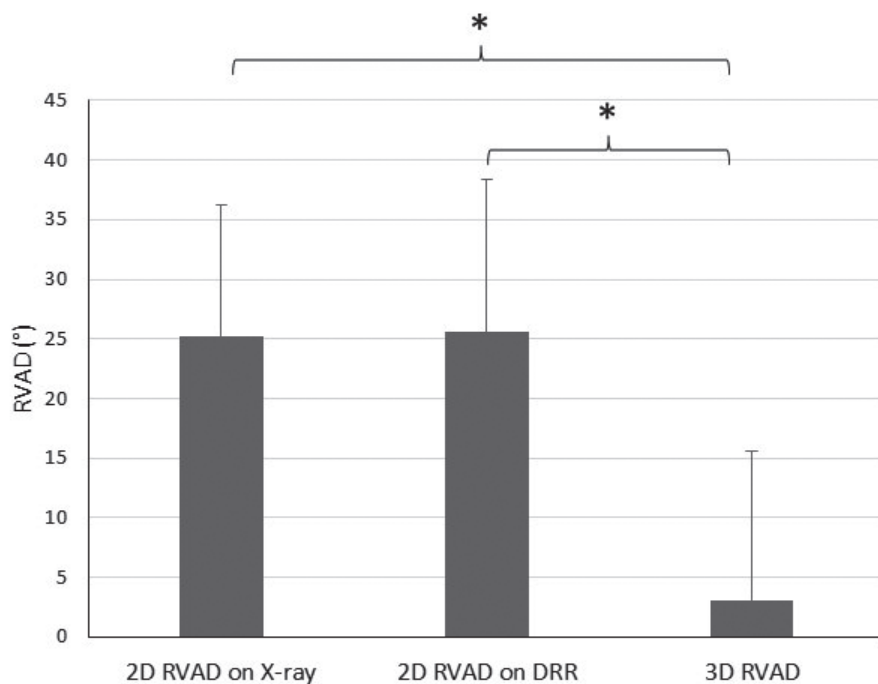
Figure 4. The 2D RVAD measured on the conventional posterior-anterior standing radiographs and on digitally reconstructed coronal radiograph (DRR) of the CT scans in prone position is shown, as well as the 3D RVAD measured on the CT scan. *indicates significant difference.

	Coronal Cobb	Axial rotation	Apical lordosis
2D RVAD	r=0.547, *P*<0.001	r=0.542, *P*<0.001	r=0.522, *P*<0.001
3D RVAD	r=0.171, *P*=0.111	r=0.011, *P*=0.920	r=0.155, *P*=0.149

Table 2. Pearson correlations (r) between RVAD measurements and 3D spinal morphology are shown. The 2D RVAD was measured on the plain radiograph.

	RVAD <20°	RVAD 20-30°	RVAD >30°	p
Thoracic Cobb angle	62.6±8.0°	67.8±10.4°	77.0±13.0°	<0.001
Apical vertebral rotation	17.1±7.1°	20.6±5.6°	26.7±7.8°	<0.001
Apical lordosis	3.1±2.9%	4.6±2.6%	6.5±3.0%	0.001

Table 3. The deformities in the three planes are shown (mean±standard deviation) for the different 2D RVAD magnitudes.

	Phase 1	Phase 2	p
2D RVAD	17.1±12.0°	27.9±10.3°	<0.001
3D RVAD	0.2±7.3°	4.4±13.8°	0.129
Thoracic Cobb angle	61.6±7.9°	72.0±12.4°	<0.001
Apical vertebral rotation	16.5±4.5°	23.4±8.3°	<0.001
Apical lordosis	3.3±3.0%	5.3±3.1%	0.009

Table 4. The RVAD as well as the deformity in the three planes is shown (mean±standard deviation) for the phase 1 and phase 2 curves as measured on the plain radiograph.

DISCUSSION

This study shows that the perceived rib asymmetry around the apex in scoliosis, as defined by the RVAD, is in reality an expression of the severity of the apical 3D deformity. Idiopathic scoliosis is a 3D deformity of the spine and the trunk, including the rib cage, of unknown etiology.[3] Several parameters are traditionally used to describe the relationship of the spine and ribcage, including the RVAD as a predictive measurement for progression, introduced by Mehta in 1972, initially for infantile idiopathic scoliosis.[41, 101] It was later expanded to include other types of scoliosis as well.[41, 93, 97, 98] The RVAD is defined as the angle between the concave and convex ribs at the apex on a standard (coronal) 2D radiograph of the spine.[41] There are several theories about the RVAD; it has for example been hypothesized that the RVAD could be an expression of asymmetric muscle forces acting on the rib cage, originating from the central nervous system.[210, 211] Oda et al. described that the costovertebral joints are important in providing stability to the spine, especially in axial rotation.[92] Injured or deviated costovertebral joints could result in instability of the spine.[92, 95] It was suggested that the 'drooping' of the ribs in the convexity of the curve reflected decreased spinal stability.[92, 93, 95, 97, 98] However, the observed rib asymmetry does not take into account the complex apical 3D morphology, in which rotation and apical lordosis were shown to play an important role.[91, 93, 94, 96-99, 101] Foley et al. were the first to measure the RVAD in the derotated plane by using 3D reconstructions of the spine and concluded that the RVAD in fact does not indicate asymmetry of the costovertebral junction, but is a reflection of the 3D deformity including the vertebral rotation.[100, 209] They computed the 3D RVAD from calibrated biplanar radiographs, using a reconstruction and optimization algorithm and measured the 3D RVAD in a plane corrected for the vertebral rotation.[100, 209] However, this method was not able to accurately determine the relationship between the RVAD and the complex 3D morphology of the scoliotic apex. Using an existing database of high-resolution 3D CT scans, acquired as part of standard pre-operative work-up for spinal navigation before posterior scoliosis surgery , we confirmed that there were no genuine asymmetry

at the costovertebral junction and the RVAD is actually the projected image of the 3D deformity at the apical region in these moderate to severe AIS patients.

The mean 2D RVAD in this study was 25.3° on the X-ray and 25.6° on the DRR, but in the reconstructed true coronal view of the derotated apex, this apparent difference in rib vertebra angles between the concave and convex side almost completely disappeared (3D RVAD: 3.1°). The 2D RVAD, however, demonstrated a significant relation with the deformity in the coronal plane, apical rotation and apical lordosis which suggests it to be a reliable indicator of 3D apical deformation. The results of our study indicate that the 2D RVAD represents in reality the 2D projected image of the 3D morphology of the apical region of the spine, including the severity of the apical lordosis. Our study suggests that, within similar Cobb measurements, a higher RVAD is the result of a more pronounced apical rotation and lordosis and indicates a more severe deformity with worse prognosis. Therefore we believe that the RVAD remains a useful and simple measurement to indicate the severity of the overall 3D apical deformity and the risk of progressive 3D apical deformity, based on a standard 2D radiographic assessment and could be used for clinical radiographic assessment.[39]

In this study, moderate to severe AIS patients, that had all been indicated for surgery, were included. Although the RVAD initially was described for infantile scoliosis, its use was later broadened to include different types of scoliosis as well.[93, 96-98, 101] We therefore expect that the findings of our study concerning 3D apical morphology can be extrapolated to other types of scoliosis as well. Although CT scanning is still considered as the gold standard technique for quantification of 3D in vivo morphology, it obviously is ethically not acceptable to follow children longitudinally with this technique and therefore we were not able to include mild or moderate curves and to follow them during their development.

CONCLUSION

The 2D RVAD, or Mehta's angle, represents a projection-based composite radiographic index reflecting the complex 3D apical morphology including axial rotation and apical lordosis in the thoracic curve in scoliosis. Although the 2D RVAD is a relatively simple measurement, it proves to be effective and reproducible in practice and provides 3D information. Therefore, the RVAD can be used for radiological severity assessment of the scoliotic curve.

Chapter 9

Upright, Prone and Supine Spinal Morphology and Alignment in Adolescent Idiopathic Scoliosis

ABSTRACT

Background. Patients with adolescent idiopathic scoliosis (AIS) are usually investigated by serial imaging studies during the course of treatment, some imaging involves ionizing radiation and the radiation doses are cumulative. Few studies have addressed the correlation of spinal deformity captured by these different imaging modalities, for which patient positioning are different. To the best of our knowledge, this is the first study to compare the coronal, axial and sagittal morphology of the scoliotic spine in three different body positions (upright, prone and supine) and between three different imaging modalities (X-ray, CT and MRI).

Methods. 62 AIS patients scheduled for scoliosis surgery, and having undergone standard pre-operative work-up, were included. This work-up included upright full spine radiographs, supine bending radiographs, supine MRI and prone CT as is a routine in one of our institutions. In all three positions, Cobb angles, thoracic kyphosis (TK), lumbar lordosis (LL) and vertebral rotation were determined. The relationship among three positions (upright X-ray, prone CT and supine MRI) was investigated according to the Bland-Altman test, whereas the correlation was described by the intraclass correlation coefficient (ICC).

Results. Thoracic and lumber Cobb angles correlated significantly between conventional radiographs (68±15° and 44±17°), prone CT (54±15° and 33±15°) and supine MRI (57±14° and 35±16°; ICC≥0.96; P<0.001). The thoracic and lumbar apical vertebral rotation showed a good correlation among three positions (upright, 22±12° and 11±13°; prone, 20±9° and 8±11°; supine, 16±11° and 6±14°; ICC≥0.82; P<0.001). The TK and LL correlated well among three different positions (TK: 26±11°, 22±12° and 17±10°; *P*≤0.004, LL: 49±12°, 45±11° and 44±12°; *P*<0.006; ICC: 0.87 and 0.85).

Conclusions. Although there is a generalized underestimation of morphological parameters of the scoliotic deformity in the supine and prone position as compared to upright position, a significant correlation of these parameters is still evident among different body positions by different imaging modalities. Findings of this study suggest that severity of scoliotic deformity in AIS patients can be largely represented by different imaging modalities despite the difference in body positioning.

BACKGROUND

Adolescent idiopathic scoliosis (AIS) is a complex three-dimensional (3D) deformity of the spine, with a prevalence of 1.5-3% within the general population, that normally develops in the beginning of the growth spurt of previously healthy adolescents.[27, 115] For diagnosis, monitoring of progression and clinical decision making, periodical radiographic follow-up is traditionally performed using posterior-anterior and lateral upright radiographs. The Scoliosis Research Society defines scoliosis as a lateral curvature of the spine of more than ten degrees in the coronal plane on upright radiographs, also emphasizing the importance of radiography.[57] In addition, supine or prone magnetic resonance imaging (MRI) and computed tomography (CT) is frequently used to obtain more in-depth information about neuroaxis and bony architecture abnormalities. Some imaging involves ionizing radiation and the radiation doses are cumulative, resulting in nine to ten times more radiation exposure and a seventeen times higher incidence of cancer in the AIS cohort as compared to the general population.[12, 60] The importance of the 3D character of the scoliotic deformity has long been recognized and the upright X-ray, the gold standard, is not able to accurately represent the true 3D deformity.[1, 44, 89, 212] CT scanning can obtain accurate 3D information of bony structures, but relies on radiation and is not obtained upright.[43] An important step in attempts to visualize this 3D character has been the development of low dose upright imaging modalities that allow for 3D reconstruction such as the EOS apparatus. Alternatively, MRI utilizes no harmful radiation but is considered inferior in visualizing bone and is usually also not obtained upright. This study was designed to compare the morphology of the scoliotic spine on conventional radiographs in the upright position to MRI and CT obtained in a supine and prone position, respectively.

MATERIALS AND METHODS

Study population
A subsequent series of AIS patients of ten or more years of age scheduled for scoliosis surgery in one of our centers between 2011 and 2014 and had complete standard pre-operative work-up, were included in this study. Complete work-up consisted of posterior-anterior and lateral upright radiographs of the spine, supine bending X-rays, T2 weighted MRI (3.0-T MR scanner (Achieva TX; Philips Healthcare, Best, The Netherlands)) of the spinal cord for exclusion of neural axis abnormalities obtained in a supine position, and high-resolution CT (64 Slice Multi-detector CT scanner, GE Healthcare, Chalfont, St. Giles, United Kingdom, slice thickness 0.625 millimeters (mm)), obtained in a prone position. The CT scans were made for navigation purposes according to protocol in one of our institutions, in a position mimicking the position at surgery as closely as

possible. Children with other spinal pathology than AIS, early onset scoliosis, previous spinal surgery, neurological symptoms or neural axis abnormalities, syndromes associated with disorders of growth or atypical left convex thoracic curves or right convex (thoraco)lumbar curves were excluded to obtain an as homogeneous a population as possible. Moreover, cases that had undergone the different imaging methods with an interval of more than six months in between imaging were also excluded. Curve characteristics (curve type according to the Lenke classification, Cobb end vertebrae and apical levels) were determined on the conventional radiographs.[11, 157]

Outcome parameters

The conventional radiographs were analyzed for main thoracic and (thoraco)lumbar Cobb angle, apical rotation (using Perdriolle's method[213]), thoracic kyphosis (TK; superior endplate T4 – inferior endplate T12) and lumbar lordosis (LL; superior endplate L1 – sacral plate), using our Picture Archiving and Communications Systems (PACS) workstation (Carestream solution working station, Carestream Health, Version 11.0, Rochester, New York, USA).

On the MRI and CT images, the main thoracic and (thoraco)lumbar Cobb angle, TK and LL were measured using the same technique as for the conventional radiographs, by using multiplanar reconstruction technique through the midsection of each vertebral body for the MRI and the digital reconstructed radiograph (DRR) for the CT scan (Figure 1). The same levels were used for each patient on the three different imaging methods. Cobb end vertebrae were selected on the radiographs and applied to the other imaging modalities.[214] For measurement of apical rotation on the MRI and CT scans, complete 3D reconstructions were acquired using semi-automatic analysis software (ScoliosisAnalysis 4.1, Imaging Division, Utrecht, The Netherlands) and a previously validated imaging method.[175] The observer selected the upper and lower endplates of the vertebral body. Then, the observer used the sagittal and coronal orientation of the endplates to correct for coronal and sagittal tilt. Thus, each vertebral level was manually positioned in the true transverse plane as accurately as possible. Subsequently, for each endplate, its longitudinal axis was calculated automatically after manual segmentation of the vertebral body and spinal canal. The rotation was defined as the rotation of this axis minus the rotation of the neutral sacral plate (Figure 2).

Intra- and interobserver reliability for measurement of apical rotation using this method was tested in a previous study; intraclass correlation coefficients were 0.92 (95% confidence interval: 0.82-0.97) and 0.89 (0.74 – 0.95) on the 3D scans.[44] In this study, the intra- and interobserver reliability analysis of the rest of the outcome parameters (Cobb angles, TK and LL on all the three modalities and the vertebral rotation on the X-rays) was studied. Two observers independently analysed a randomly selected subset of ten X-rays, CT scans and MRI scans of the subjects.

Figure 1. On the MRI and CT images, the main thoracic and (thoraco)lumbar Cobb angle, thoracic kyphosis and lumbar lordosis were measured using the same technique as for the conventional radiographs on the image where the curve and endplates were best visible by using the multiplanar reconstruction (MPR, figure A) for the MRI and the digitally reconstructed radiograph (Figure B) for the CT scan. Figure C, the conventional X-ray.
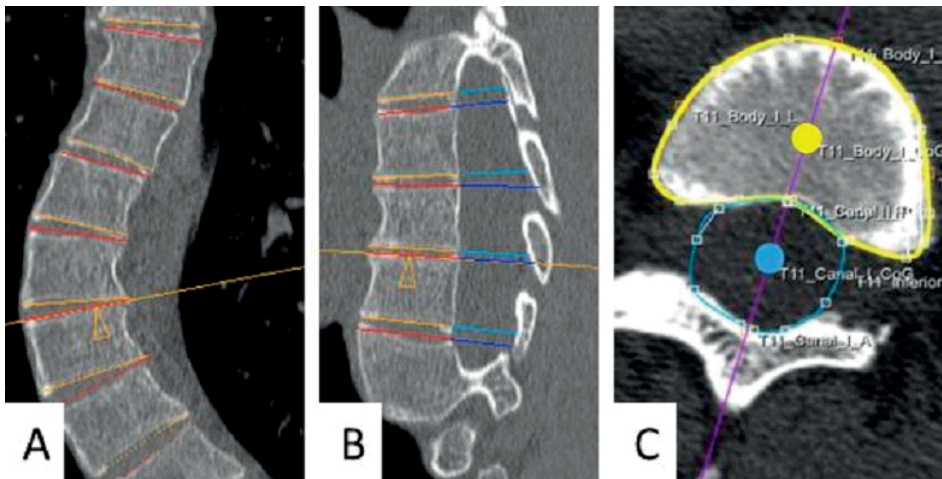
Figure 2. The orientation of the upper and lower endplate of each individual vertebra of the computed tomography scans was determined by using the semi-automatic software, correcting for coronal and sagittal (A and B) tilt, to reconstruct the true transverse sections. The observer drew a contour around the vertebral body (yellow line in C) and spinal canal (blue line in C). The software calculated a center of gravity of the vertebral body (yellow dot in C) and spinal canal (blue dot in C). For each endplate, its longitudinal axis was calculated as the line between those two points (purple line in C). The rotation of this axis minus the rotation of the neutral sacral plate represents the rotation of the endplate.

Statistical analysis

Statistical analyses were performed using SPSS 22.0 for Windows (SPSS Inc., Chicago, IL, USA). Descriptive statistics were computed providing means, ranges and standard deviations. Potential outliers were identified. The agreement between the three positions was tested according to the Bland-Altman plot; first the one-sample t-test showed if there was a significant difference between the measurements, second, if there was no significant difference, the regression analysis showed if there was agreement between the measurements.[215] The two way mixed intraclass correlation coefficient (ICC) was used to evaluate the correlation between the parameters in different body positions. The intra- and interobserver reliability were obtained as intraclass correlation coefficients. The statistical significance level was set at 0.05 for all analyses.

Demographic parameter		n=62
Age at Radiograph (years)	range	10 – 23
	mean±sd	15.6 ± 2.5
Girls, n (%)		56 (90.3%)
Right convexity of main thoracic curve, n (%)	right convex	62 (100%)
Interval CT – Radiograph (days)	range	-7 – 130
	mean±sd	2.98 ± 17.2
Interval Radiograph – MRI (days)	range	-46 – 181
	mean±sd	81.3 ± 51.4
Interval CT – MRI (days)	range	-26 – 181
	mean±sd	84.2 ± 47.1
Lenke curve type		
I		26
II		12
III		6
IV		4
V		5
VI		9
Exclusion criteria		**n**
Scan interval > 6 months		38
No MRI available		14
No CT scan available		10
Incomplete radiologic work-up		1
Associated congenital or neuromuscular pathologies		12
left convex main thoracic curve		4
Prior spinal surgery		1

Table 1. Demographics are shown for all included AIS patients and controls. Besides, the excluded patients are shown. sd = standard deviation.

RESULTS

Population

A total of 142 subjects underwent surgery for AIS during the study period. Eighty sub-jects had to be excluded for several reasons, as shown in Table 1. Ultimately, sixty-two AIS patients with full documentation were left for the purpose of this study. On average the subjects were 15.6±2.5 years of age, fifty-six (90%) were girls and most of the curves were classified as type Lenke 1 of these moderate to severe AIS patients (thoracic Cobb angle 37-110°, lumbar Cobb angle 18-82°; Table 1).

Coronal parameters

In the coronal plane, the main thoracic Cobb angle was on average 68±15°, 54±15° and 57±14° respectively on the upright radiographs, prone CT and supine MRI and differed significantly between all the three positions (*P*<0.001; Table 2). The average (thoraco) lumbar Cobb angle on the conventional upright radiograph was 44±17° as compared to the prone CT (33±15°) and supine MRI (35±16°) (*P*≤0.018, between the three positions). Although the upright angles were larger, the Cobb angles correlated very well between the three positions (ICC: thoracic 0.97 and lumbar 0.96; Table 3; Figure 3). Significant linear correlations were found, indicating that with increasing Cobb angle, differences between the body positions increased simultaneously. The conversion equations that resulted from the correlation analyses of the different parameters between the upright X-ray, prone CT scan and supine MRI could be used for conversion purposes (Table 5).

Thoracic	Upright	Prone	Supine	P-value		
				X vs. CT	X vs. MRI	CT vs. MRI
Cobb (°)	68.2 ± 15.4	53.9 ± 14.8	56.7 ± 13.5	<0.001	<0.001	<0.001
Kyphosis (°)	25.8 ± 11.4	22.4 ± 11.6	17.3 ± 9.8	0.004	<0.001	<0.001
Rotation (°)	21.6 ± 11.7	19.9 ± 8.9	16.3 ± 10.8	0.161 (0.007)	0.001	0.002

Lumbar	Upright	Prone	Supine	P-value		
				X vs. CT	X vs. MRI	CT vs. MRI
Cobb (°)	44.3 ± 16.8	33.1 ± 15.0	35.2 ± 15.9	<0.001	<0.001	0.018
Lordosis (°)	48.8 ± 12.0	45.4 ± 10.8	43.7 ± 12.4	0.006	<0.001	0.341 (0.620)*
Rotation (°)	10.7 ± 12.8	7.5 ± 11.4	6.2 ± 13.7	0.428 (<0.001)	0.663 (0.129)*	0.679 (0.006)

Table 2. Differences (mean ± standard deviation) between upright (X), prone (CT) and supine (MRI) posi-tion for Cobb angle, thoracic kyphosis, lumbar lordosis and apical vertebral rotation in the thoracic as well as lumbar curves. According to the Bland-Altman plot the *P*-value showed if there is agreement by using the t-test. If this test showed no significant different (*P*>0.05), a regression analysis was performed to see is there is agreement, written in brackets. *=agreement according to the Bland-Altman plot.

	ICC (95% CI)	p-value
Thoracic Cobb angle	0.967 (0.950 – 0.979)	<0.001
Lumbar Cobb angle	0.964 (0.945 – 0.977)	<0.001
Thoracic kyphosis	0.873 (0.806 – 0.919)	<0.001
Lumbar lordosis	0.854 (0.777 – 0.907)	<0.001
Thoracic apical rotation	0.815 (0.718 – 0.882)	<0.001
Lumbar apical rotation	0.900 (0.848 – 0.937)	<0.001

Table 3. Two-way mixed intraclass correlation coefficient (ICC) and 95% confidence interval (CI) between upright, prone and supine positions.
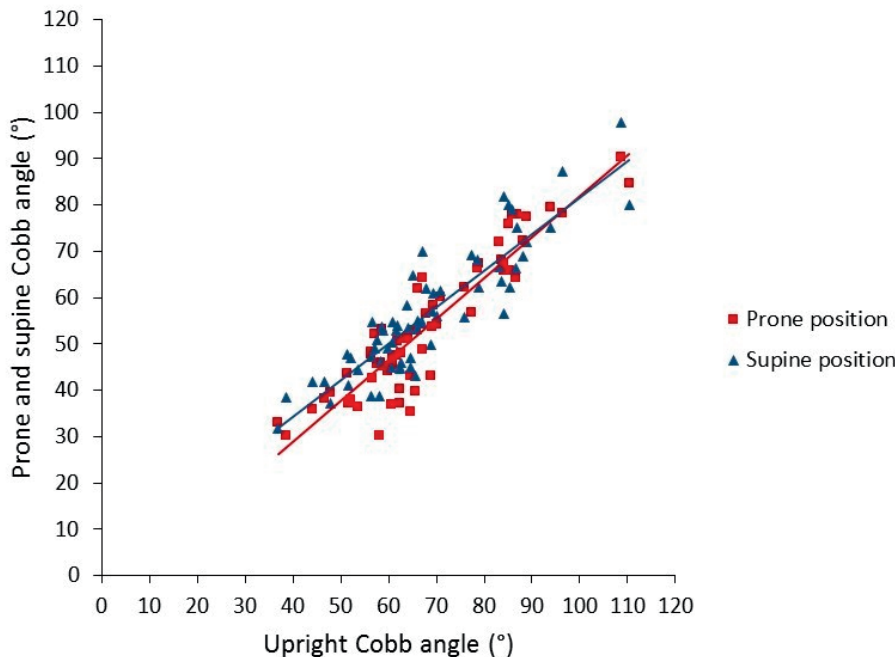
Figure 3. In these scatterplots, the relation between thoracic Cobb angle in upright, prone (red trend line) and supine (blue trend line) position is shown. Although the upright Cobb angle was significantly larger, significant linear correlations were found (ICC: 0.967; $P<0.001$), indicating that with increasing Cobb angle, differences between the body positions increased simultaneously.

Axial rotation

Parallel to the coronal Cobb angles, in both the thoracic curve as well as the (thoraco-)lumbar curve, the mean apical vertebral rotation was larger in the upright position (Table 2). Significant correlations, however, were observed between the apical rotation as measured using the Perdriolle method on upright radiographs and the rotation on the prone CT and supine MRI (ICC: thoracic 0.82 and lumbar 0.90; Table 3 and 5).

	X-ray		CT scan		MRI scan	
	Intra	Inter	Intra	Inter	Intra	Inter
Thoracic Cobb	0.993 (0.971–0.998)	0.972 (0.888–0.993)	0.997 (0.988–0.999)	0.995 (0.980–0.999)	0.995 (0.982–0.999)	0.974 (0.896–0.994)
Lumbar Cobb	0.999 (0.996–1.00)	0.995 (0.980–0.999)	0.999 (0.996–1.00)	0.995 (0.981–0.999)	0.997 (0.990–0.999)	0.986 (0.945–0.997)
Thoracic kyphosis	0.989 (0.954–0.997)	0.922 (0.610–0.984)	0.931 (0.722–0.983)	0.864 (0.454–0.966)	0.992 (0.967–0.998)	0.940 (0.759–0.985)
Lumbar lordosis	0.986 (0.944–0.997)	0.989 (0.956 –0.997)	0.995 (0.980–0.999)	0.973 (0.890–0.993)	0.995 (0.981–0.999)	0.971 (0.884–0.993)
Thoracic rotation	0.979 (0.915–0.995)	0.977 (0.906–0.994)	*	*	0.939 (0.756–0.985)	0.744 (0.409–0.964)
Lumbar rotation	0.975 (0.899–0.994)	0.996 (0.985–0.999)	*	*	0.906 (0.620–0.977)	0.885 (0.539–0.972)

Table 4. Intra- and interobserver reliabilities analysis and 95% confidence interval. *=Intra- and interobserver reliability for the rotation on 3D scans, this method were tested previously (ICC: 0.92 and 0.89).[44]

		Cobb angle		
		Upright X-ray	Prone CT scan	Supine MRI
Cobb angle	Upright X-ray	-	Th:CT(°)=-6.2+0.88*X-ray(°) L: CT(°)=-2.7+0.81*X-ray(°)	Th: MRI(°)=2.9+0.79*X-ray(°) L: MRI(°)=-2.1+0.85*X-ray(°)
	Prone CT	Th: X-ray(°)=16.6+0.96*CT(°) L: X-ray(°)=11.1+1.00*CT(°)	-	Th: MRI(°)=11.0+0.85*CT(°) L: MRI(°)=4.9+0.92*CT(°)
	Supine MRI	Th: X-ray(°)=10.8+1.01*MRI(°) L: X-ray(°)=9.5+0.98*MRI(°)	Th: CT(°)=-2.8+1.00*MRI(°) L: CT(°)=2.6+0.86*MRI(°)	-

Table 5. For translational purposes, the conversion equations that resulted from the linear correlation analyses of the different parameters between the upright X-ray, prone CT scan and supine MRI are provided for the thoracic (Th) and lumbar (L) Cobb angles.

Sagittal parameters

Also in the sagittal plane, the TK in the upright position (26±11°) was significantly larger as compared to prone (22±12°) and supine (17±10°; $P{\leq}0.004$). The upright LL (49±12°) was significantly higher as compared to prone LL (45±11°) and supine LL (44±12°; $P{\leq}0.006$). According to the Bland-Altman method there was agreement between the LL in supine and prone position. The TK as well as the LL correlated well between all the positions (ICC: 0.87 and 0.85; Table 3 and 5).

Reliability

The ICCs for intra- and interobserver reliabilities of the Cobb angles, TK, LL and vertebral rotation on the three modalities were all excellent (>0.93 and inter>0.74, respectively; Table 4).

DISCUSSION

X-rays for scoliosis are, by convention, obtained in an upright position, allowing gravity to have its influence on the morphology of the spine. The drawbacks of this X-ray imaging in analyzing the deformity as well as planning treatment are becoming increasingly clear: the deformity has a complex 3D nature that is hardly appreciated on plain films, and radiation exposure, even with modern day equipment, is becoming a serious concern. Although the use of ultrasound for diagnosis and follow-up of spinal deformities has been explored and seems promising, this technique gives little detail of the anatomy and needs further evaluation.[61, 64, 66] Additional imaging studies are frequently obtained in scoliosis; CT scanning is still considered the gold standard for providing accurate and detailed information on bony anatomy (for instance in cases where congenital malformations are suspected), and can give accurate 3D reconstructions of complex deformities.[43] However, CT carries even more radiation exposure and is performed non-weight bearing.[43] MRI is safe, provides accurate information on the spinal cord and other soft tissues, but is also (usually) performed in a non-weight bearing manner, and is known to show less detail of bony structures. Therefore, it is important to define where these techniques overlap, in order to reduce costs and radiation exposure. Previous studies have already described the differences in morphology of the spine in AIS between different imaging methods and between different body positions.[181-183, 216-219] This study is, however, to the best of our knowledge, the first to look into the relationship between the three different positions in all three planes of the body to visualize the scoliotic spine.

In this study, we observed that there is underestimation of the deformation of the spine in the supine and prone position as compared to the upright position, overall more pronounced in the thoracic curves as compared to the (thoraco)lumbar curves. The lying positions underestimated the thoracic and (thoraco)lumbar Cobb angles for 12-14° and 9-11° respectively, the TK and LL for 3-9° and 3-5° and the thoracic and lumbar apical vertebral rotation for 2-5° and 3-5°. Therefore, the parameters on supine and prone scans could not directly be compared to the upright radiographs. However, good and excellent linear correlations were observed for the morphological parameters in the coronal (ICC≥0.964), sagittal (ICC≥0.854) and axial plane (ICC≥0.815) between X-ray, CT and MRI. This implies that reliable conversion of the parameters between the different positions, is possible. A limitation of this study is the population that only includes relatively severe curves. From our results, the reliability of conversion of parameters between different positions for patients with mild AIS curves, cannot be derived. Shi *et al.* described the correlation of the coronal Cobb angle between upright and supine positions in mild, moderate and severe AIS patients and concluded that the correlation coefficients were more reliable in the severe group, probably due to the reduced curve flexibility in the severe group.[183, 220] As we demonstrated before, evaluation of the true

sagittal plane in scoliosis on plain X-rays is notoriously unreliable, and differs greatly from the true sagittal plane as may be analyzed more accurately on both CT and MRI.[221]

CONCLUSION

There is a good to excellent correlation of the morphology of the scoliotic spine in all three planes between standard upright X-ray, MRI, and CT scan in these moderate to severe AIS patients. Apparently, at least part of the information obtained by these different modalities, overlaps. Findings of this study suggest that severity of scoliotic deformity in AIS patients can be largely represented by different imaging modalities despite the differences in body position. Future longitudinal studies to demonstrate the practical implications of these findings are planned.

Chapter 10

Spinous Processes and Transverse Processes Measurements of the Scoliotic Spine and their Relation to the Cobb angle: a CT Based Study.

ABSTRACT

Purpose. Ultrasound imaging of the scoliotic spine is a valid method to assess curve severity. However, it is currently unknown whether the spinous processes (SP), transverse processes (TP) or center of lamina (COL) should be used as landmarks to assess curve severity. Purpose of this study was to assess the reliability and validity, on CT, between these angles and the conventional coronal Cobb angle.

Methods. CT scans of 105 adolescent idiopathic scoliosis patients were included. Coronal Cobb, SP, TP and COL angles were measured for all curves. The reliability and validity was tested.

Results. The mean Cobb, SP, TP and COL angles were, 54°, 37°, 49° and 51° in the thoracic curves and 34°, 26°, 31° and 34° in the (thoraco)lumbar curves. Intraclass correlation coefficient values for intra-rater measurements of the SP, TP and COL angles were 0.93, 0.97 and 0.95 and 0.70, 0.90 and 0.88 for inter-rater measurements. The correlation between the Cobb and the SP, TP and COL angle in thoracic and (thoraco)lumbar curves was 0.79 and 0.66, 0.87 and 0.84 and 0.80 and 0.70 respectively.

Conclusions. The SP, TP and COL represent structures located more posteriorly than the vertebral bodies, and consequently these angles show systematic differences to the Cobb angles. However, the purpose of this study was to test the reliability and validity and all these measurements are reliable and valid. Based on our CT analysis, the TP and COL angles show the best validity as compared to the Cobb angle, and may be favored for ultrasound use.

INTRODUCTION

The coronal Cobb angle, as measured on upright posterior-anterior radiographs, is still the 'gold standard' to assess curve severity and the progression of adolescent idiopathic scoliosis (AIS).[3, 11] AIS patients undergo repeated radiographs to document progression of the deformity or treatment effectiveness and this covers a relatively long period during their adolescence, at the time that gonadal and breast tissue mature. Simony et al. described a five times higher overall cancer rate in a Danish AIS population, as compared to age-matched controls.[12] Three-dimensional (3D) ultrasound imaging of the spine as a radiation-free alternative method of measuring spinal curvature, has gained growing attention and its feasibility has been demonstrated in several recent studies.[62, 64, 66, 67, 69, 222-227] These studies showed that the spinous processes (SP), transverse processes (TP) and center of lamina (COL) can be used as anatomical landmarks to assess spinal curve severity. It is important to note that ultrasound only visualizes the posterior elements of the spine, not the vertebral endplates, and thus gives a different projection of the 3D deformity than the Cobb angle. Because of this the exact relationship between these posterior landmarks and the conventional coronal Cobb angle has not yet been established and we do not know which posterior landmark is the best choice for ultrasound imaging of the spine. Computed tomography (CT) gives the most accurate assessment of the 3D bony anatomy of the spinal deformity and can therefore provide accurate reconstructions in any given plane.[43] The aim of this study was to investigate the relationship between the different anatomical landmarks (SP, TP, COL and vertebral endplates) using CT imaging, and to test the reliability and validity of the SP, TP and COL as landmarks for curve severity measurements.

MATERIALS AND METHODS

Population

The local ethical review board approved this study and all patients enrolled in this study provided written informed consent. From an existing database of a consecutive series of AIS patients with pre-operative high-resolution CT images (64 Slice Multi-detector CT scanner; GE Healthcare, Chalfont, St. Giles, United Kingdom; slice thickness 0.625 mm) scheduled for scoliosis surgery in one academic center between 2010 and 2016, a total of 105 AIS patients were included. CT scans were obtained as part of the preoperative workup for navigation purposes.[228] Exclusion criteria were non-idiopathic scoliosis, other spinal pathology, previous spinal surgery, neurological symptoms or neural axis abnormalities on pre-operative MRI, or atypical left convex thoracic curves or right convex (thoraco)lumbar curves.

CT measurements

Using a previously validated method for semi-automatic analysis (ScoliosisAnalysis 1.3 Imaging Division, Utrecht, The Netherlands), complete 3D spinal reconstruction were acquired. The Cobb angle was measured manually between the two most tilted cranial and caudal vertebral endplates in the curve on a reconstructed coronal projection.[11] Thereafter, the exact location of the tip of both the postero-caudal SP and supero-lateral TP as well as the deepest point of the COL were manually identified in the 3D reconstruction and extracted into a Cartesian 3D coordinate system (Figure 1). The SP angle was defined as the angle between the most tilted line connecting two consecutive SPs at the cranial and caudal end of the curves (Figure 2). The TP angle was defined as the angle between the most tilted line connecting the left and right tip of the TP at the cranial curve and the most tilted line connecting the left and right side of one TP at the caudal curve (Figure 2) and the COL angle was defined as the angle between the most tilted line connecting the left and right center of lamina at the cranial curve and the most tilted line connecting the left and right lamina at the caudal curve (Figure 2).
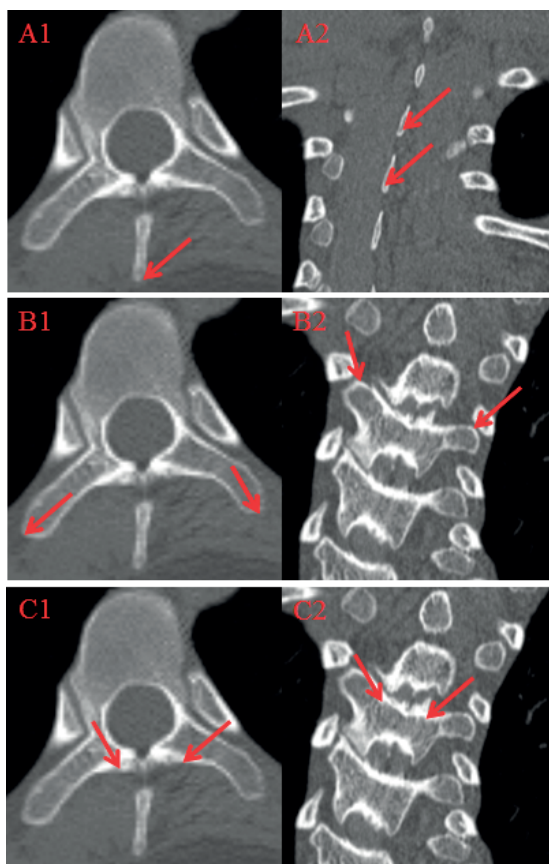

Figure 1. CT image with (1) transversal and (2) sagittal view of a vertebra with marked in red the location of the (A) spinous process tip (SP), (B) transverse process tip (TP) and (C) center of lamina point.
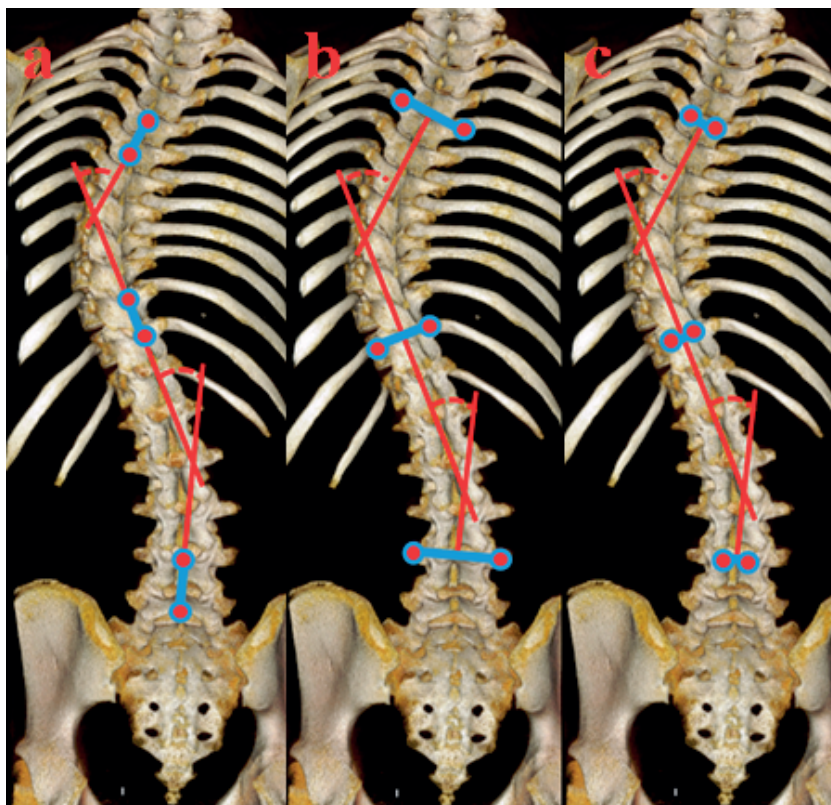
Figure 2. Schematic posterior view of the whole spine with the thoracic and (thoraco)lumbar (a) SP angles, (b) TP angles and (c) COL angles.

Statistical Analysis

Statistical analyses were performed using SPSS Statistics 25 for Windows (SPSS Inc., Chicago, IL, USA). For descriptive statistics mean, standard deviation and ranges were provided. Normality of data was assessed using graphical methods (Q-Q plots and histograms). The Mean absolute error (MAE) was used to describe the difference between the Cobb angle and the anatomical landmark angles. The intra- and inter-rater reliability was calculated as (two-way random effects model and absolute agreement) intraclass correlation coefficient (ICC). The correlation between the Cobb angle and the anatomical landmarks angles were determined using Pearson's correlation (r). The agreement of the anatomical landmark angle measurements and the Cobb angle was tested by using the Bland-Altman method. The Bland-Altman plot was used to describe the agreement between the ultrasound and Cobb angle and possible outliers. The mean absolute deviation (MAD) between the SP, TP and COL angles and the Cobb angle were compared. Paired t-tests were used to measure the differences. The significance level was set at 0.05 for all analyses.

RESULTS

The mean age of the 105 included AIS patients was 16.3±2.7 (range 10.0-26.4) years (Table 1). The mean (±standard deviation) of the Cobb angle, SP angle, TP angle and COL angle of the thoracic curves were: 54°±14°, 37°±11°, 49°±13° and 51°±13°. For the (thoraco)lumbar curves the angles were 34°±14°, 26°±9°, 31°±12° and 34°±14°, respectively (Table 2). The MAE between the Cobb angle and the anatomical landmark angles were; 14° (Cobb-SP), 7° (Cobb-TP) and 7° (Cobb-COL).

		(n=105)
Age in years	Mean±SD	16.3±2.7
	Range	10.0-26.4
Female	n (%)	89 (84)

Table 1. Demographics.

	Mean±SD (°)
Thoracic curves	
Cobb angle	54±14
SP angle	37±11
TP angle	49±13
COL angle	51±13
(Thoraco)lumbar curves	
Cobb angle	34±14
SP angle	26±9
TP angle	31±12
COL angle	34±14

Table 2. Cobb, spinous processes (SP), transverse processes (TP) and center of lamina (COL) angle characteristics measured on CT.

Reliability

Intra-rater reliability analyses showed very reliable values for all anatomical landmark angles (SP angle ICC=0.93, TP angle ICC=0.97 and COL angle ICC=0.95). The inter-rater reliability was moderately reliable, for the SP angle (ICC=0.70) and very reliable for the TP angle (ICC=0.90) and the COL angle (ICC=0.88) (Table 3).

	Intrarater reliability	Interrater reliability
Spinous processes angle	0.93	0.70
Transverse processes angle	0.97	0.90
Center of lamina angle	0.95	0.88

Table 3. Reliability of the anatomical landmarks angles with the Cobb angle on CT measured with intraclass correlation coefficient.

Validity

The correlation of the SP angle with the Cobb angle was moderate to good ((thoraco)lumbar r=0.66), and very good to excellent (thoracic r=0.79). The TP angle had a very good to excellent correlation with the Cobb angle in both curves (thoracic r=0.87 and (thoraco)lumbar r=0.84). The correlation of the COL angle with the Cobb angle was moderate to good ((thoraco)lumbar r=0.70), and very good to excellent (thoracic r=0.80) (Figure 3). The Bland-Altman plot showed a difference between the anatomical landmark angles and the Cobb angle measurements (Figure 4). The MAD between the Cobb angle and the anatomical landmark angles differed significantly. MAD Cobb-SP angle: 5°±9°, MAD Cobb-TP angle 1°±6°, and MAD Cobb-COL angle 1°±8°; (p<0.05).
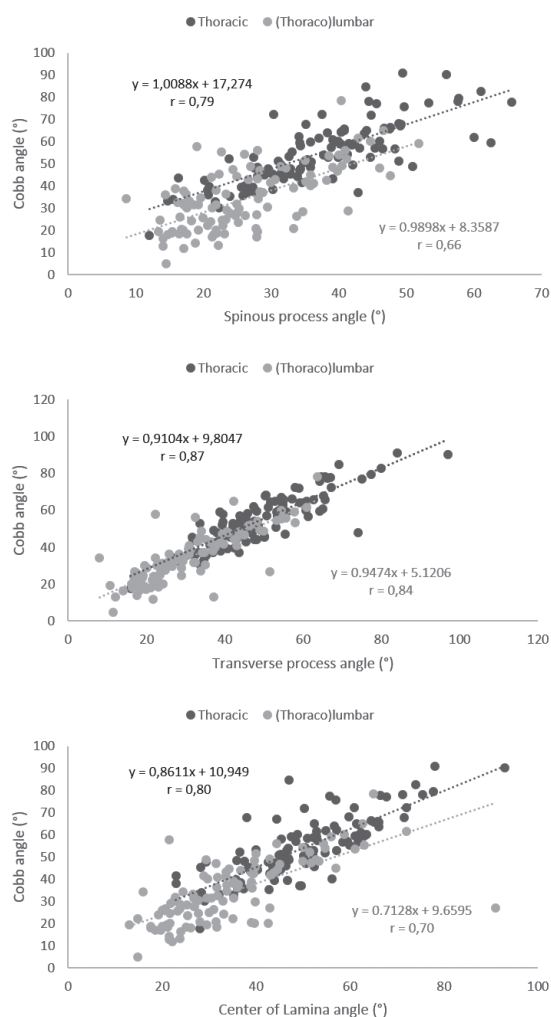

Figure 3. Pearson's correlations (r) and the equations between the Cobb angle on the y-axis and the anatomical landmark angles on the x-axis. The spinous process angle, transverse process angle and center of lamina angle are shown for the thoracic (black) and (thoraco)lumbar (gray) curves.
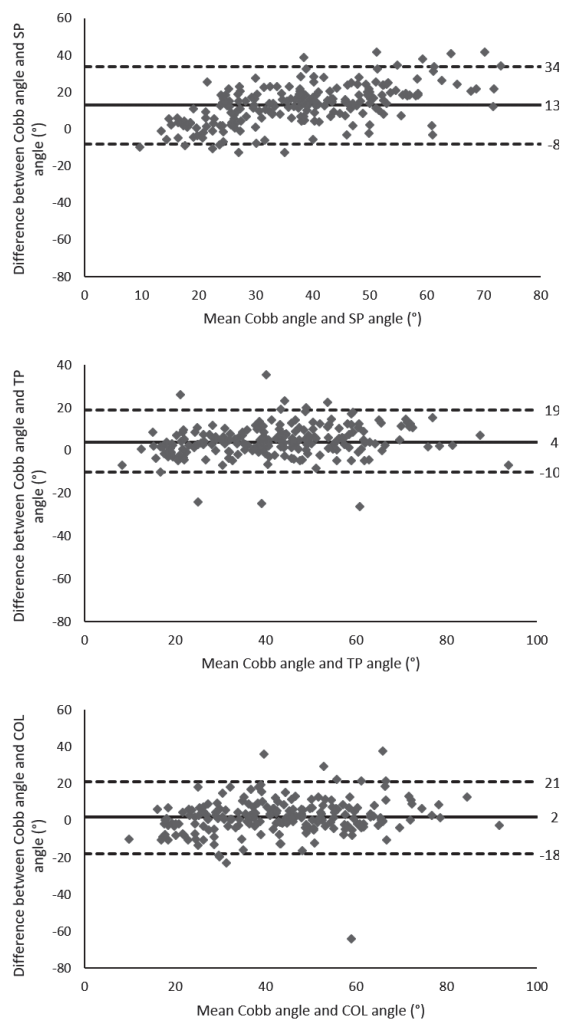
Figure 4. Bland-Altman plots that show the agreement between the Cobb angles and the anatomical landmark angles.

DISCUSSION

The Cobb angle, as measured on posterior-anterior standing full-spine radiographs, is used to assess the AIS curve severity and to monitor the progression of the curve.[3, 11] The limitations of this method include radiation exposure and expression of a 3D deformity in a two-dimensional plane. 3D ultrasound imaging of the spine has gained growing attention as a promising radiation-free alternative method to evaluate the morphology of the spinal curvature.[62, 64, 66, 67, 69, 222-227] Ultrasound, however, can only visualize the spine in a plane more posterior than the vertebral endplates and therefore gives a different projection of the 3D deformity. To date, different anatomical landmarks have been

described as an ultrasound alternative for the Cobb angle, such as the SP, TP and the COL.[62, 64, 66, 67, 69, 222-227] The exact relation between the posterior structures accessible by ultrasound (SP, TP, COL) and the vertebral endplates, as normally used on radiographs, remain unclear. CT is able to provide important and exact information about the relations between the different anterior and posterior anatomical landmarks for assessment of curve severity.

The anatomical landmarks showed different angles than the coronal Cobb method. The difference in curve severity measurements between the SP, TP, COL and the Cobb angle can be explained by the different spinal structures used for the angle measurements. While the TP and COL method are similar to the Cobb method, as the endplates of the vertebral body are along the same line as the TP and COL lines used, the SP line is along a different direction from the Cobb method. Herzenberg et al. also describes that visualized from posterior the spinous process appear to form a curve that is less angulated than the Cobb measured from the vertebral body.[229] It is important to note that with the use of ultrasound approximating the absolute Cobb angle should not be the (ultimate) goal of measuring the scoliotic curve. More importantly, an ultrasound angle measurement method should give a reliable measure of curve progression and severity to be useful for curve assessment.

In this CT based study, moderate to excellent correlations were found between the angles measured using the posterior anatomical landmarks versus the conventional Cobb angle from endplate to endplate (thoracic r≥0.79 and (thoraco)lumbar r≥0.66). In a clinical study Brink et al. showed excellent linear correlations between SP and TP ultrasound angles and the radiographic Cobb angle (thoracic R^2≥0.987 and (thoraco)lumbar R^2≥0.970).[224] Because of the use of high-resolution CT scans there are practical differences between our findings and those of Brink et al. In this study the exact tip of the SP and TP was used for the angle measurements, while, with the ultrasound method, it is not completely clear whether the exact tip of the SP and TP, or part of the bases of the processes, are used for the measurements. This accuracy might have led to different correlations in comparison to the validation study for ultrasound based Cobb angle measurements. Wang et al. showed a high correlation between the COL angle on ultrasound and the coronal Cobb angle on MRI (r>0.9).[67] An explanation for the differences between our finding and those of Wang et al, could be the fact that only 16 patients were included and the average Cobb angle was 21.7°±15.9°, while our study included far more patients, curves were bigger and a distinction was made between thoracic and (thoraco)lumbar curves.

A possible limitation of this study and statistical analysis is the presence of outliers. However as these outliers were correct curve measurements, including them in our analysis showed that the measurements of the anatomical landmark angles are reliable and valid for the whole range of included curves. Angles, based on the SP, TP and COL

measured on CT, although located more posteriorly, are representative for the more anteriorly located end plates and therefore reliable to measure curve severity. When comparing the reliability of the anatomical landmark angles to the Cobb angle the TP angle has the highest intra- and inter-rater correlations.

CONCLUSION

As expected, the posterior-element-based SP, TP and COL angles represent different values in comparison to the endplate-based Cobb angle. Since these anatomical landmarks are located more posteriorly and project differently in the coronal plane than the vertebral bodies, on average, they systematically underestimate the curve angle as compared to the conventional Cobb angle. The SP, TP and COL are valid and reliable anatomical landmarks for coronal curve assessment. Our data suggests that the TP and COL angle are most appropriate for assessment of curve severity on 3D ultrasound.

Chapter 11

A Reliability and Validity Study for Different Coronal Angles using Ultrasound Imaging in Adolescent Idiopathic Scoliosis

ABSTRACT

Background context. Radiation exposure remains a big concern in adolescent idiopathic scoliosis (AIS). Ultrasound imaging of the spine could significantly reduce or possibly even eliminate this radiation hazard. The spinous processes (SP) and transverse processes (TP), were used to measure the coronal deformity. Both landmarks provided reliable information on the severity of the curve as related to the traditional Cobb angle. However, it remained unclear which coronal ultrasound angle is the most appropriate method to measure the curve severity.

Purpose. To test the reliability and validity of several ultrasound angle measurements in the coronal plane as compared to the radiographic coronal Cobb angle in AIS patients.

Study Design/setting. Cross-sectional study.

Patient sample. Thirty-three AIS patients, both males and females (Cobb angle range: 3-90°, primary and secondary curves), who underwent posterior-anterior radiography of the spine.

Outcome Measures. The reliability (intraclass correlation coefficients (ICC) for the intra- and interobserver variability) and validity (linear regression analysis and Bland-Altman method, including the mean absolute difference (MAD)) of different ultrasound measurements.

Methods. The patients were scanned using a dedicated ultrasound machine (Scolioscan, Telefield Medical Imaging Ltd, Hong Kong). The reliability and validity were tested for three coronal ultrasound angles: an automatic and manual SP angle and a manual TP angle as compared to the radiographic coronal main thoracic or (thoraco)lumbar Cobb angles.

Results. The ICC showed very reliable measurements of all ultrasound methods (ICC ≥0.84). The ultrasound angles were 15-37% smaller as compared to the Cobb angles, however, excellent linear correlations were seen between all ultrasound angles and the Cobb angle (thoracic: $R^2 ≥0.987$ and (thoraco)lumbar $R^2 ≥0.970$) and the Bland-Altman plot showed a good agreement between all ultrasound angles and the Cobb angle. The MADs of the ultrasound angles, corrected using the linear regression equation, and the Cobb angles showed no significant difference between the different ultrasound angles (MAD: automatic SP angle 4.9±3.2°, manual SP angle 4.5±3.1° and manual TP angle 4.7±3.6°; p≥0.388).

Conclusions. Coronal ultrasound angles are based on different landmarks than the traditional Cobb angle measurement and cannot represent the same angle values. In this study, we found excellent correlations between the ultrasound and Cobb measurements, without differences in reliability and validity between the ultrasound angles based on the spinous processes and transverse processes. Therefore, the severity of the deformity in AIS patients can be assessed by ultrasound imaging, avoiding hazardous ionizing radiation and enabling more individualized patient care. It also opens possibilities for screening.

INTRODUCTION

Posterior-anterior and lateral upright radiographs are traditionally performed for diagnosis, monitoring of progression and clinical decision making of patients with adolescent idiopathic scoliosis (AIS).[3, 11, 57] In addition, supine or prone magnetic resonance imaging (MRI) and computed tomography (CT) may be used to obtain more in-depth information about neural axis and bony architecture abnormalities.[3, 58] More recently, standing low-dose biplanar radiography became available and can be utilized for three-dimensional (3D) reconstructions.[59] Most methods involve ionizing radiation and the radiation doses are cumulative, resulting in a nine to ten times higher radiation exposure in these patients, leading to an increased life-time risk of cancer in the AIS cohort as compared to the general population.[12, 60] MRI is non-ionizing but does not visualize cortical bone very well, is time consuming, expensive and is not performed upright. Therefore, a number of attempts to visualize the 3D character of the scoliotic curve without ionizing radiation in the upright position have been undertaken, such as ultrasound imaging and surface topography.[61-71] Almost three decades ago, Suzuki et al. already described the application of ultrasound to identify the lamina, spinous process (SP) and transverse process (TP) of scoliotic patients.[61] More recently, several *in-vitro* and *in-vivo* studies compared the ultrasound spine deformity measurements to the traditional Cobb angle on radiographs in AIS.[62-67, 69, 70] In these studies, several structures were reported as accurate landmarks to assess the coronal spinal angle, in which the SP and TP were most used. However, none of them compared the different measurement methods and therefore, it remained unclear which coronal ultrasound angle is the most stable and consistent (reliability) and which angle is the most appropriate method to measure the severity of the curve (validity). Once the most appropriate coronal ultrasound angle has been established, this could be used for radiation-free clinical screening and follow-up of AIS patients. Therefore, the objective of this study was to investigate the reliability and validity of different ultrasound measurement techniques for coronal curve severity.

MATERIALS AND METHODS

The local Medical Research Ethics Committee has granted approval for this study. AIS patients under the age of eighteen, planned for radiography, were recruited consecutively in an academic spine center in The Netherlands. Exclusion criteria were other spinal pathology than idiopathic scoliosis, previous spinal surgery, neurological symptoms or patients unable to stand and syndromes associated with disorders of growth. Informed consent was obtained from all patients and their parents. The patients received conventional standing plain radiographs on the same day as the ultrasound imaging.

Ultrasound measurements

The Scolioscan system (Model SCN801, Telefield Medical Imaging Ltd, Hong Kong), tested previously, was used to obtain the ultrasound images.[69, 223, 230, 231] Imaging of the spine was achieved through freehand scanning using the linear ultrasound probe (center frequency of 7.5 MHz, width of 7.5 cm), combined with a sensor to detect the position and orientation of the probe. During scanning, the patients are in upright position, with the arms on the side. The moving probe is simultaneously shown in real-time on a separate screen, to indicate the location of the ultrasound probe in relation to the upper (level T1) and lower (level S1) boundaries. During scanning, the patient can breathe normally. After scanning, the collected image data together with the recorded position and orientation information of the probe are used for 3D image reconstructions. The final two-dimensional (2D) coronal result is based on the 3D reconstruction.[223] Three different methods to measure the coronal angles of the main thoracic and (thoraco) lumbar curves were applied; 1) the automatic SP angle: using a line provided by the software of the machine through the bone shadows of the SPs, 2) the manual SP angle, based on the same bone shadows of the SPs, and 3) the manual TP angle: using the bone shadows of the TPs (Figure 1). The automatic SP angle was based on the extraction of bony features from volume projection imaging, as described by Zhou et al.[232] For manual coronal ultrasound angles the observer manually identified the SPs and TPs on the 2D ultrasound images. The manual SP angle was defined as the angle between the most tilted SP line (between two SPs) of the upper region of the curve and the most tilted SP line (also between two SPs) of the lower region. The manual TP angle was defined as the angle between the most tilted TP line (line between the right and left TP) of the upper region of the curve and the most tilted TP line (also between the right and left TP) of the lower region. The radiographic coronal Cobb angle and the three coronal ultrasound angles were calculated for the main thoracic as well as the (thoraco)lumbar curves. For intra- and interobserver reliability analysis of the ultrasound angles, two observers (R.B. twice, S.W. once) independently scanned and analyzed ten subjects in two stages (Figure 2). First, the observers (R.B. twice, S.W. once) measured the ultrasound angles independently on the same ultrasound scans of a random subset of patients, to analyze the intra- and interobserver reliability without influence of differences in scanning procedure. Second, the observers scanned the patients independently (R.B. twice, S.W. once) and measured the angles on these scans, to analyze the intra- and interobserver reliability, including the differences in scanning procedure (Figure 2).

Statistical analysis

Statistical analyses were performed using SPSS 22.0 for Windows (SPSS Inc., Chicago, IL, USA). Descriptive statistics were computed providing means, standard deviations and ranges. To test the reliability, intra- and interobserver variabilities were obtained
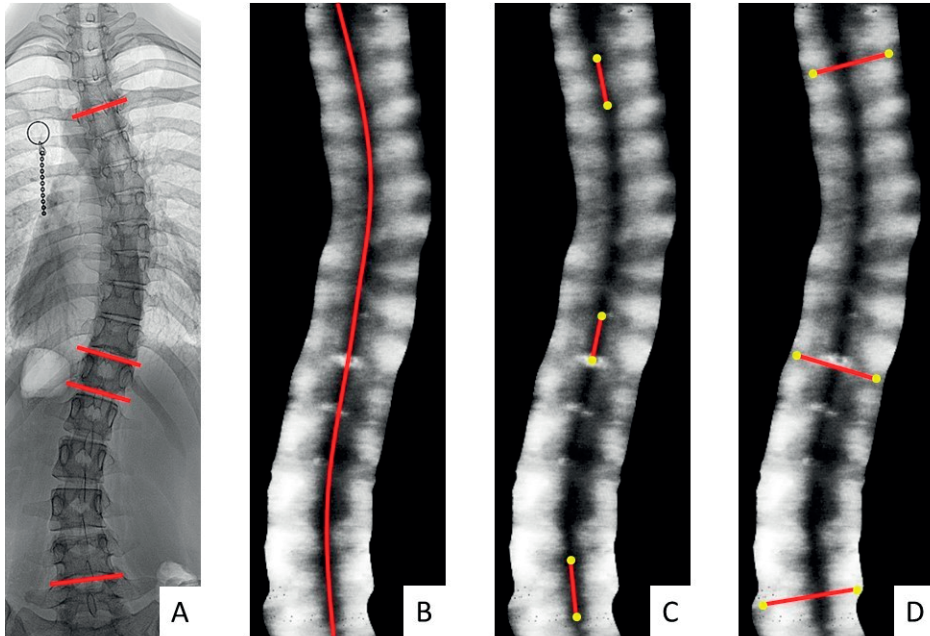
Figure 1. The coronal Cobb angle, measured on radiographs (A), was compared to three coronal ultrasound angles based on the spinous processes (SP) and transverse processes (TP), as marked in yellow: the automatic SP angle (B), the manual SP angle (C) and the manual TP angle (D). The most tilted SP line (between two SPs) at the upper thoracic region and the most tilted SP line (also between two SPs) at the lower thoracic region were used to calculate the thoracic SP angle and the same applied for the (thoraco) lumbar SP angle. TP lines were manually drawn between the right and left TPs of each vertebra. The angle was calculated between the two most tilted TP lines.

as (two-way random and absolute agreement) intraclass correlation coefficients (ICC). The criteria for evaluating ICC values were: very reliable (0.80–1.0), moderately reliable (0.60–0.79), and questionably reliable (≤0.60). To assess the validity, linear regression analyses were used, with correlation coefficient 0.25 to 0.50 indicating poor correlation, 0.50 to 0.75 indicating moderate to good correlation, and 0.75 to 1.00 indicating very good to excellent correlation. The next step to test the validity, was to test the agreement of the ultrasound measurements, adjusted with the linear regression equations with intersections (origin), and the radiographic Cobb angle, by using the Bland-Altman method. The Bland-Altman plot was used to describe the agreement between the ultrasound and Cobb angle and possible outliers. To measure the differences in agreement for the three different ultrasound measurements, the mean absolute differences (MAD) between the Cobb angle and the adjusted ultrasound angles were calculated. The MADs of the different ultrasound measurements were compared using the paired t-tests. The significance level was set at 0.05 for all analyses.
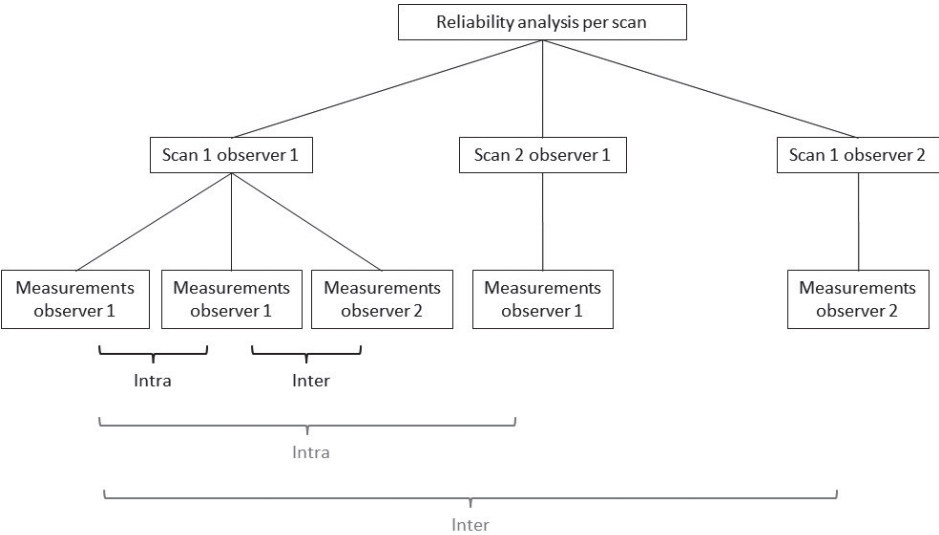
Figure 2. Schematic diagram showing the measurement design for evaluating the intra- and interobserver variability. Two observers made in total three scan of each patient; observer 1 scanned twice and observer 2 scanned once. First, the intra- and interobserver variability (in black) was measured on the same scan. Second, the intra- and interobserver variability (in grey) was measured on different scans.

RESULTS

Of the thirty-eight AIS patients, five subjects were excluded (ultrasound images of three subjects had darkened areas as result of a smaller distance between the scapulae than the width of the probe and two received only posterior-anterior bending radiographs). Thirty-three AIS subjects were thus included, with an average of 13.8±2.3 (range 10-17) years of age (demographics are shown in Table 1). The main thoracic and (thoraco)lumbar coronal Cobb angles, as measured on the radiographs, were on average 38.5±20.4° (range 6-90°) and 28.9±11.3° (range 3-52°). On average, the ultrasound scan took sixty-five seconds per examination. Two patients collapsed after the scanning procedure. The manual angle measurement took on average twenty-five seconds per spine and the automatic angle measurement was generated within twenty seconds. The main thoracic and (thoraco)lumbar coronal ultrasound angles were on average 24.4±13.3° and 21.2±8.5° (automatic SP angle), 26.2±13.3° and 22.4±9.2° (manual SP angle) and 29.8±13.9° and 24.5±9.2° (manual TP angle).

Reliability

The ICCs for intra- and interobserver reliabilities, using the same scans, were 0.97 (95% confidence interval: 0.93–0.99) and 0.95 (0.89–0.98) for the manual SP angle and 0.96 (0.90–0.98) and 0.93 (0.83–0.97) for the manual TP angle (Table 2). The ICCs for the

		AIS (n=33)
Age in years	mean±sd	13.8±2.3
	range	10-17
Girls	n (%)	30 (90%)
Cobb angle main thoracic curve	mean±sd (°)	38.5±20.4
	range (°)	6-90
Cobb angle (thoraco)lumbar curve	mean±sd (°)	28.9±11.3
	range (°)	3-52

Table 1. Demographics are shown for all included adolescent idiopathic scoliosis (AIS) patients. sd = standard deviation.

automatic SP angle, using the same scans, was 1.00, since the automatic method will show the same angle. The ICC for intra- and interobserver reliabilities for the different scan sessions, were 0.97 (0.93–0.99) and 0.94 (0.85–0.97) for the automatic SP angle, 0.96 (0.90–0.98) and 0.86 (0.68–0.94) for the manual SP angle and 0.94 (0.85–0.98) and 0.84 (0.64–0.94) for the manual TP angle, respectively (Table 2).

	Same scan, different measurement moments		Different scans and different measurement moments	
	Intra (ICC)	Inter (ICC)	Intra (ICC)	Inter (ICC)
Automatic SP angle	1.00	1.00	0.97 (0.93–0.99)	0.94 (0.85–0.97)
Manual SP angle	0.97 (0.93 – 0.99)	0.95 (0.89–0.98)	0.96 (0.90 – 0.98)	0.86 (0.68 – 0.94)
Manual TP angle	0.96 (0.90–0.98)	0.93 (0.83–0.97)	0.94 (0.85 – 0.98)	0.84 (0.64 – 0.94)

Table 2. Intraclass correlation coefficients (ICC), including standard deviation, for intra- and interobserver variabilities of the three different coronal ultrasound angles, based on the spinous processes (SP) and transverse processes (TP) are shown. The first analyses were based on the same scan, the first scan of observer 1. Observer 1 measured the angles on the same scan twice and observer 2 measured the angles once on the same scan. The second analyses were based on different scans and scan sessions. Observer 1 made two ultrasound scans of the same patient and calculated the angles on the two different scans. The ICC was calculated between these angles. Observer 2 made one scan of that patient and measured the angles on that scan. The ICC was calculated between these angles and the angles measured by observer 1 on the first scan of observer 1.

Validity

All three coronal ultrasound angles showed excellent linear correlations with the Cobb angles (Figure 3). The lowest R^2 of 0.970 was found for the manual SP angle of the lumbar curve and the highest R^2 of 0.992 was found for the manual thoracic TP angle (Figure 3). Correspondingly, the Bland-Altman plot demonstrated a good agreement between the ultrasound angles corrected with the calculated equations and the Cobb angles (Figure 4). To compare the measurements in terms of validity, the MAD was measured between

these calculated ultrasound angles and the Cobb angle. No significant difference be-
tween the different ultrasound measurement methods was found (MAD: automatic SP
angle 4.9±3.2°, manual SP angle 4.5±3.1° and manual TP angle 4.7±3.6°; p≥0.388).
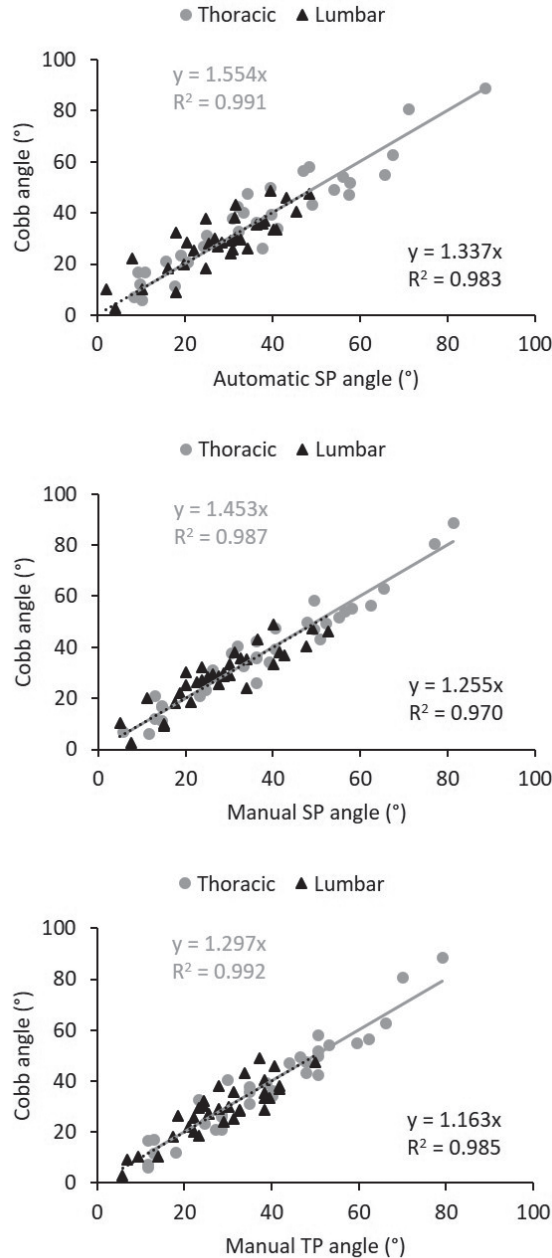
Figure 3. Correlations (R^2) and equations between the Cobb angles (y) obtained using radiographs and the three coronal ultrasound angles (x) based on the spinous processes (SP) and transverse processes (TP): the automatic SP angle, the manual SP angle and the manual TP angle, are shown for the thoracic (grey) and (thoraco)lumbar (black) curves.
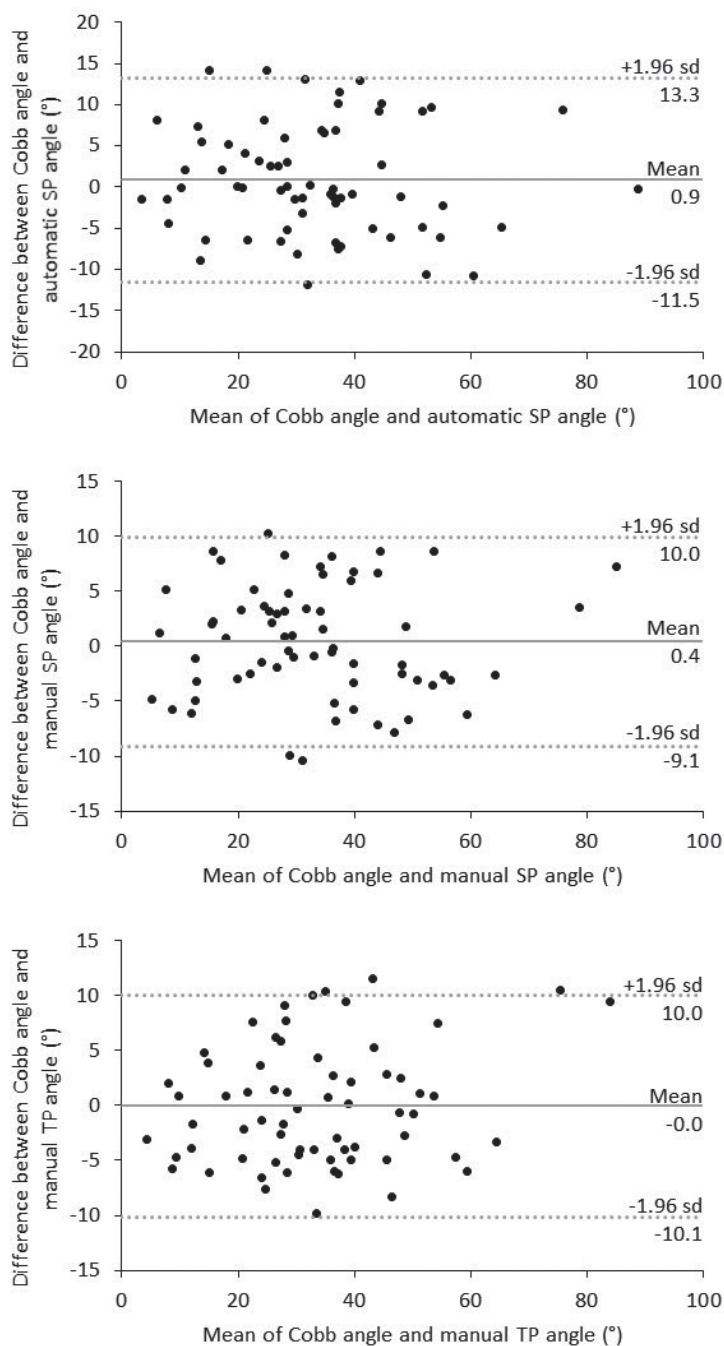
Figure 4. Bland-Altman plots that show the differences between the Cobb angles and the coronal ultrasound angles corrected with the linear regression equations. The automatic spinous process (SP) angle, the manual SP angle and the manual transverse process (TP) angle. sd = standard deviation.

DISCUSSION

Traditionally and by convention, the scoliotic spine is imaged upright, using ionizing radiation, resulting in more radiation exposure and a higher incidence of cancer in this population.[12, 60] To reduce or eliminate the potential radiation hazard, alternative imaging methods have been sought. Low-dose biplanar radiography holds great promise but still uses (some) ionizing radiation, is based on an interpretation of the true shape of the spine provided by the software, is expensive and therefore not available in all centers. Ultrasound imaging is widely used for medical imaging, including for musculoskeletal purposes and is one of the most promising methods with the advantages of the upright position, nonionizing radiation, low cost, portability and dynamic scanning procedure. Previous authors used several landmarks to assess the coronal ultrasound angle.[61-67, 69, 70] However, none of them compared the reliability and validity of different coronal spinal ultrasound angle measurements.

The thoracic and (thoraco)lumbar coronal ultrasound angles were 23-37% and 15-27% lower as compared to the radiologic Cobb angles. This was expected, since the ultrasound measurements are based on structures located more posteriorly than the vertebral body, on which the Cobb angle is based and this leads to a different projection of the complex 3D deformity.[11, 229, 233] We want to stress that the purpose of measuring a scoliosis should not be to approximate the Cobb angle, since this angle also is a simplification of the complex 3D deformity. Other methods will show different values, which are not necessarily less useful. What matters is that the utilized method gives a reliable impression of the severity of the deformation.

Excellent linear correlations were found between the ultrasound angles and Cobb angles (thoracic: $R^2 \geq 0.987$ and (thoraco)lumbar $R^2 \geq 0.970$) in the range of 3-90° degrees (primary and secondary) curves that we measured. The MAD of the ultrasound measurements was below 5°, without significant difference between the different ultrasound measurements. The ICC showed very reliable measurements and corresponded with the ICC of the traditional Cobb angle (range ICC 0.83–0.99), as described in a review by Langensiepen et al.[234] Moderate to strong linear correlations (reflecting validity) were reported earlier between the ultrasound angle, measured using different 3D ultrasound imaging systems, and the Cobb angle ($r > 0.81$ and $R^2 > 0.72$).[62, 66, 67, 69, 70] The ICC (reflecting reliability) varied between 0.70 and 0.86.[62, 66, 67, 69, 70]

The present study showed that the automatic SP angle as well as both manual methods based on the SPs and TPs are reliable and valid to measure the severity of the coronal curve. The TP angle showed the least difference with the Cobb angle, but the automatic SP angle showed slightly better ICCs as compared to the manual methods and is easier to use. For the Dutch population, the relationship between the ultrasound angles and the Cobb angles can be expressed by the equations as given in this study

(Figure 2). Zheng et al. described that the relationship between the ultrasound angle (x) and the Cobb angle (y) could be expressed by the equations y = 1.20x and y = 1.15x for the thoracic and lumbar curves, using forty-nine patients.[69] Their equation deviated slightly from ours, which may be explained by the fact that in the present study the Cobb angle range was wider (3-90°), whereas Zheng et al. included patients with a Cobb angle of 50° or lower.[69] The thus obtained radiation-free imaging enables the spine to be evaluated more frequently, which may prevent sudden deterioration of the curve and lead to a more individualized treatment.[62, 222, 235] Furthermore, ultrasound may be a very useful tool for screening purposes. School screening for scoliosis is still a subject of controversy, but recently, Ohrt-Nissen et al. described that in a health care systems without school screening, patients with AIS referred for scoliosis have larger curve sizes.[236]

Besides ultrasound imaging, surface topography has been used as a radiation-free alternative to plain radiographs with moderate to good validity and reliability.[68, 71, 237-239] However, asymmetry of the torso is influenced by the spine shape, as well as the ribcage, trunk rotation, muscle volume, body fat and posture. Therefore, ultrasound can be expected to be more accurate. In this study, of the five excluded patients, three were excluded because the ultrasound probe was wider than the distance between the scapulae. This is a technical shortcoming, a smaller probe, or the possibility to move the probe obliquely can possibly solve this. This study showed that idiopathic scoliosis patients with an age above ten years are suitable for ultrasound imaging of the spine. The minimum required age for ultrasound imaging of the spine, probably under ten years of age, had to be investigated in further studies with a younger study population. The possibilities of ultrasound to provide information on the sagittal and transverse plane, to obtain bending films for surgical planning, to detect abnormalities (e.g. syringomyelia, Chiari malformation and spina bifida), to measure the morphology in postoperative patients and the ability to measure progression of the scoliotic curves are subjects of our ongoing studies.

CONCLUSIONS

Coronal ultrasound angles are based on different landmarks than the traditional Cobb angle measurement and cannot represent the same angle values. In this study, we found excellent correlations between the ultrasound and Cobb measurements, without differences in reliability and validity between the ultrasound angles based on the spinous processes and transverse processes. Therefore, the severity of the deformity in AIS patients can be assessed by ultrasound imaging, avoiding hazardous ionizing radiation and enabling more individualized patient care. It also opens possibilities for screening.

Chapter 12

Surgical Outcomes of Anterior versus Posterior Fusion in Lenke Type 1 Adolescent Idiopathic Scoliosis

ABSTRACT

Study Design. Retrospective cohort study

Objective. To describe surgical results in two and three dimensions and patient-reported outcomes of scoliosis treatment for Lenke type 1 idiopathic curves with an anterior or posterior approach.

Summary of Background data. Different surgical techniques have been described to prevent curve progression and to restore spinal alignment in idiopathic scoliosis. The spine can be accessed via an anterior or a posterior approach. However, the surgical outcomes, especially in three dimensions, for different surgical approaches remain unclear.

Methods. Cohorts of Lenke curve type 1 idiopathic scoliosis patients, after anterior or posterior spinal fusion were recruited, to measure curve characteristics on conventional radiographs, before and after surgery and after two years follow-up, whereas the vertebral axial rotation, true mid-sagittal anterior-posterior height ratio of individual structures and spinal height differences were measured on 3D reconstructions of the pre- and postoperative supine low-dose CT scans. Additionally, the intraoperative parameters were described and the patients completed the SRS-22 and EQ-5D-3L questionnaire post-operatively.

Results. Fifty-three patients with Lenke curve type 1 idiopathic scoliosis (26 in the anterior cohort and 27 in the posterior cohort) were analysed. Fewer vertebrae were instrumented in the anterior cohort compared with the posterior cohort ($p<0.001$), with less surgery time and lower intraoperative blood loss ($p<0.001$). The Cobb angle correction of the primary thoracic curve directly after surgery was 57±12% in the anterior cohort and 73±12% in the posterior cohort ($p<0.001$) and 55±13% and 66±12% ($p=0.001$) at 2 years follow-up. Postoperative 3D alignment restoration and questionnaires showed no significant differences between the cohorts.

Conclusions. This study suggests that Lenke type 1 curves can be effectively managed surgically with either an anterior or posterior approach. Each approach, however, has specific advantages and challenges, as described in this study, which must be considered before treating each patient.

INTRODUCTION

The primary goal of corrective scoliosis surgery in adolescents is to halt curve progression to prevent pulmonary dysfunction and pain.[3, 76] Secondary goals of surgical correction and fusion are reduction of the deformity, cosmesis and restoration of three-dimensional (3D) spinal alignment. Two surgical techniques have been described to access the spine, either an anterior or posterior approach, by open or minimal invasive techniques.[102-108] The open anterior approach, with or without division of the diaphragm, includes discectomy and rib head resection; both increase the flexibility of the spine, and the growth potential of vertebral bodies is eliminated, which may be advantageous in the younger age cohort to avoid the crankshaft phenomenon.[240] The anterior approach is also advantageous to correct thoracic hypokyphosis in adolescent idiopathic scoliosis (AIS).[241-243] Historically, rod implant failure and pseudarthrosis were common. However, with modern implants, implant failure is rare.[11] One disadvantage with the open anterior technique in the thoracic spine is that a reduction of lung function will occur, but in general, the number of levels operated on is significantly less by the anterior approach compared with posterior techniques.[14, 15, 244] The posterior approach is used in most cases, especially after the introduction of pedicle screw fixation.[245-248] This method achieves a reliable and solid correction, with a low complication rate, but there are concerns regarding the degree of hypokyphosis correction and the number of fused segments.[241-243, 247-250] There is also evidence that the risk of infection may be increased by posterior surgery.[251, 252] Theoretically, to restore physiological thoracic kyphosis, thoracic hypokyphosis in AIS can be treated by either anterior shortening or posterior lengthening of the spine. However, it remains unclear what 3D surgical outcomes are obtained using different surgical approaches. Further knowledge may contribute to a knowledge-based choice of surgical method for the individual patient with scoliosis.[253, 254] The aim of this study is to describe the 3D correction after surgery, as well as the patient-reported outcomes over time after anterior or posterior spinal fusion in AIS.

MATERIALS AND METHODS

Study Population
Consecutive male and female patients with AIS requiring surgery in two Swedish institutions between 2011 and 2015 were included in this study (demographics are shown in Table 1). Patients with spinal pathologies other than AIS and/or previous spinal surgery were excluded. Whole-spine magnetic resonance imaging to detect spinal cord anomalies is part of the standard preoperative protocol in both centers. All patients had undergone preoperative and postoperative supine low-dose computed tomography (CT) im-

		Anterior (n=38)	Posterior (n=39)	p
Age (years)	Range	11–26	13–22	0.710
	Mean±SD	16.1±3.5	16.4±2.4	
Females	Number (ratio)	32 (84%)	32 (82%)	0.800
Thoracic curve right convexity	Number (ratio)	35 (92%)	38 (97%)	0.323
Lenke curve				
Type 1	Number (ratio)	26 (68%)	27 (69%)	
Type 2	Number (ratio)	1 (3%)	0 (0%)	
Type 3	Number (ratio)	0 (0%)	6 (15%)	
Type 4	Number (ratio)	1 (3%)	1 (3%)	
Type 5	Number (ratio)	10 (26%)	5 (13%)	
Type 6	Number (ratio)	0 (0%)	0 (0%)	

Table 1. Demographics of all patients with adolescent idiopathic scoliosis. Curve characteristics, measured on upright radiographs, are also shown. SD = standard deviation.

aging (20 times lower dose than that of a standard CT scan) of the spine, also part of the standard protocol at both institutions.[155, 156] In addition, each patient underwent plain standing posterior-anterior (PA) and lateral radiography preoperatively, postoperatively and after 2 years. Preoperative bending radiographs were used to assess curve flexibility for scoliosis classification. The open anterior approach has been preferred in Linköping for Lenke 1 and 5 curves, using the Aaro Anterior Spine System (Tresona AB, Malmö, Sweden). In Malmö, the posterior approach is preferred for all Lenke types, using the Expedium 6.35 mm titanium alloy Spine System (DePuy Synthes Companies, West Chester, PA, USA). All patients were asked to complete the SRS-22 and EQ-5D-3L questionnaires at least 2 years postoperatively. The EQ-5D-3L includes the following five dimensions: mobility, self-care, usual activities, pain/discomfort and anxiety/depression, and each dimension has three levels ranging from no problems (score 1) to extreme problems (score 3).[255] The results are translated using an index that ranges from 1 (maximum life quality) to −0.594 (a value of 0 equals dead). In addition, the questionnaire contains a health state scale, from 0 (worst imaginable health state) to 100 (best imaginable health state). The EQ5D 3L and health scale was used with permission from EuroQol. The SRS-22 is based on five domains: function, pain, self-image, mental health and overall satisfaction.[256] The scores vary between 5 (best score) and 1 (worst score).

Radiological and CT Measurements

2D curve characteristics, including the thoracic and lumbar coronal Cobb angle, thoracic kyphosis (TK, T4-T12), lumbar lordosis (LL, T12-S1) and sagittal Cobb angle between the upper and lower instrumented segment, were determined on the conventional PA and lateral radiographs. Two trained observers used a semi-automatic image processing technique and software (ScoliosisAnalysis 5.2, Image Sciences Institute, Utrecht, The

Netherlands, developed using MeVisLab, MeVis Medical Solutions AG, Bremen, Germany) to acquire complete spinal reconstructions in a 3D coordinate system, as described and validated in previous studies (Fig. 1).[44, 175] Based on manual endplate and spinal canal segmentations, 3D coordinates of individual structures were automatically calculated, taking account of the angulation and displacement of each individual level in the three planes. The 3D parameters were measured on the pre- and postoperative low-dose CT scans and included vertebral axial rotation, anterior-posterior height ratio (A-P%) and the difference in height of the instrumented part before and after surgery (Fig. 1). The rotation was measured between the apical vertebra and a reference line, defined as the line between the center of the spinal canal and the center of the sternum at level T5, as described previously by Kouwenhoven et al.[175] The reference point in the sternum is based on a dataset from a previous study that showed the least rotation at level T5 in the thoracic scoliotic spine.[58] A-P% was measured as the ratio between the anterior and posterior height of all vertebrae and intervertebral discs between the upper and lower Cobb end vertebra. The increase in height was measured between the upper and lower instrumented vertebrae after surgery, compared with the same measurements preoperatively.
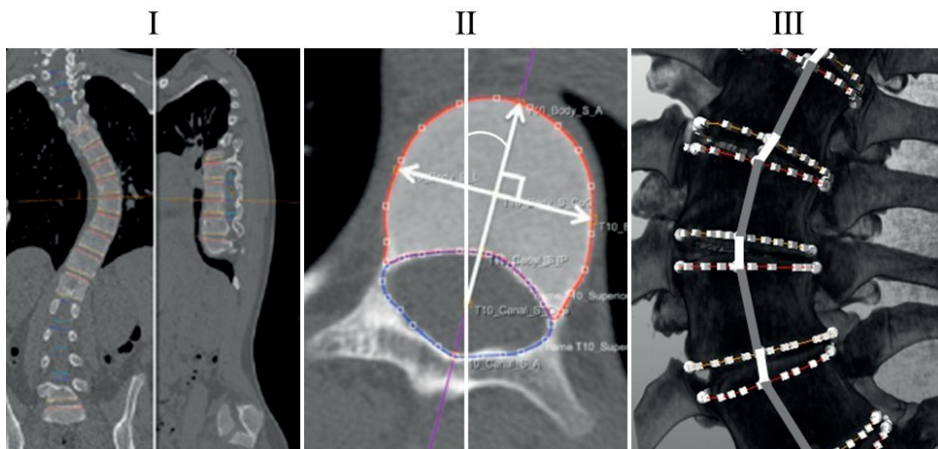
Figure 1. The orientation of the upper and lower endplate of each individual vertebra of the computed tomography scans was determined using semi-automatic software, correcting for coronal and sagittal tilt (I), to reconstruct the true transverse sections. The observer drew a contour around the vertebral body and spinal canal (II). The software calculated the center of gravity of the vertebral body and spinal canal. For each endplate, its longitudinal axis was calculated as the line between those two points (purple line in C), as used for the rotation measurements (II). Using the contours and the longitudinal axis, the anterior and posterior of each vertebral endplate was reconstructed to calculate the exact anterior and posterior height of the vertebral bodies and intervertebral discs (III). Positive values of this A-P height ratio indicate greater anterior length (lordosis).

Statistical Analysis

Statistical analyses were performed using SPSS 23.0 for Windows (SPSS Inc., Chicago, IL, USA). Descriptive statistics for continuous data were computed providing means, ranges and standard deviations; the medians and ranges were calculated for ordinal data. Chi-squared analysis was used for categorical outcomes, analysis of variance was used to compare normally distributed continuous data between the cohorts, the Mann-Whitney U test for ordinal and/or non-normally distributed data, and paired t tests to compare the preoperative, postoperative and follow-up measurements. The level of significance was adjusted to 0.01 based on the Bonferroni method to control for multiple statistical tests. The sample size is based on the data from Newton et al..[254] The preoperative Cobb angle of the thoracic curve was 46±6° in the anterior group and the postoperative Cobb angle was 20° (based on the curve correction of 57%). A postoperative difference of 5° was considered as clinical relevant between the two groups. Using the standard deviation of the preoperative Cobb angle (6°), a power of 0.8 and a P-value of 0.05, the sample size (2-sample, 2-sided equality) per group must be 14 patients or more per group.

RESULTS

Population

Of the 80 consecutive patients, three had to be excluded because of incomplete radiological charts (demographics are shown in Table 1). To avoid heterogeneity, only patients with Lenke curve type 1 were analysed (26 in the anterior approach cohort and 27 in the posterior approach cohort). Twenty patients in the anterior cohort and 17 patients in the posterior cohort completed the SRS-22 and EQ-5D-3L questionnaires on average 43 and 50 months, respectively, after surgery.

Intra- and Postoperative Parameters

Fewer vertebrae were instrumented in the anterior cohort compared with the posterior cohort, resulting in a smaller number of implanted screws (p<0.001; Table 2). Surgery time was shorter and intraoperative blood loss (postoperative blood loss not included) was smaller in the anterior cohort than in the posterior cohort, whereas the number of days in hospital was lower in the posterior cohort (parameters are shown in Table 2).

Curve Reduction: Anterior Approach

In the anterior cohort, the mean thoracic Cobb angle was 56±9° before surgery, 24±7° after surgery (p<0.001) and 25±7° at 2 years follow-up (preoperative versus 2 years follow-up, p<0.001). The lumbar Cobb angle was 32±12° before surgery, 17±11° after surgery (p<0.001) and 16±10° after 2 years follow-up (p<0.001; Table 3 and Fig. 2).

Thoracic kyphosis, lumbar lordosis and sagittal Cobb angle of the instrumented levels are shown in Table 3. In 3D, vertebral rotation reduced from 20.1±9.4° before surgery to 11.5±9.1° after surgery (p<0.001) and thoracic lordosis from Cobb end to Cobb end vertebrae, as observed before surgery, was changed to thoracic kyphosis after surgery (Table 3).

		Anterior (n=26)	Posterior (n=27)	p
Number of instrumented vertebrae	Range	6–8	10–13	<0.001
	Median	7.00 [7.00–7.25]	11.00 [10.00–12.00]	
Number of screws	Range	12–16	17–26	<0.001
	Median	14.00 [14.00–14.50]	21.00 [20.00–24.00]	
Screw density	Range	2.0–2.0	1.7–2.0	0.001
	Median	2.00 [2.00–2.00]	2.00 [1.91–2.00]	
Surgery time (min)	Range	170–248	160–340	<0.001
	Mean±SD	200±21	255±48	
Intraoperative blood loss (ml)	Range	50–900	500–3600	<0.001
	Mean±SD	278±184	1615±901	
Days in hospital	Range	7–14	6–11	0.001
	Mean±SD	9±1.4	8±1.3	
Days in the intensive care unit	Range	1–1	1–2	0.331
	Mean±SD	1±0.0	1±0.2	
Early infection	Number (ratio)	0 (0%)	1 (3.6%)	0.519
Late infection	Number (ratio)	0 (0%)	1 (3.6%)	0.519
Pneumonia	Number (ratio)	1 (3.8%)	0 (0%)	0.481
Construct loosening	Number (ratio)	4 (15.4%)	3 (10.7%)	0.457
Other	Number (ratio)	2 (7.7%)	3 (10.7%)	0.536
Patients with complications	Number (ratio)	6 (23.1%)	7 (25.0%)	0.561
Reoperation	Number (ratio)	1 (3.8%)	3 (10.7%)	0.334
EQ-5D 3L	Mean±SD	0.77±0.26	0.83±0.11	0.452
EQ-5D 3L health state	Mean±SD	82±16	76±11	0.196
SRS-22 function	Mean±SD	4.6±0.5	4.5±0.6	0.501
SRS-22 pain	Mean±SD	4.2±0.7	4.1±0.7	0.562
SRS-22 self-image	Mean±SD	4.3 ±0.7	3.8±0.6	0.053
SRS-22 mental health	Mean±SD	3.9±0.7	3.6±0.8	0.231
SRS-22 satisfaction	Mean±SD	4.5±0.7	4.3±0.7	0.357
SRS-22 total	Mean±SD	4.3±0.6	4.0±0.5	0.181

Table 2. Intra- and postoperative parameters for all patients with Lenke type 1 scoliosis. SD, standard deviation. Median [25th–75th percentile]. EQ-5D-3L score ranges from 1 (maximum life quality) to −0.594 (a value of 0 is equivalent to death) and the health state scale goes from 0 (worst imaginable health state) to 100 (best imaginable health state). The SRS-22 score varies from 5 (best score) to 1 (worst score). Statistical significance level was set at 0.01.

	Pre	Post	p (Pre-Post)	FU	p (Post-FU)
X-rays					
Cobb angle thoracic curve	56±9°	24±7°	<0.001	25±7°	0.144
Cobb angle lumbar curve	32±12°	17±11°	<0.001	16±10°	0.565
Thoracic kyphosis (T4-T12)	25±9°	32±10°	<0.001	33±9°	0.700
Lumbar lordosis (L1-S1)	55±10°	56±10°	0.460	58±9°	0.005
Sagittal angle UIV-LIV	16±11°	24±10°	<0.001	25±10°	0.211
CT scans					
Rotation apex	20.1±9.4°	11.5±9.1°	<0.001	-	-
Rotation Cobb-Cobb end	1.9±8.9°	1.5±7.0°	0.677	-	-
A-P% Cobb-Cobb end	0.7±2.9%	−1.6±2.4%	<0.001	-	-
Height displacement UIV-LIV	-	5.7±8.4 mm	-	-	-
Height displacement UIV-LIV/IV	-	0.8±1.1 mm	-	-	-

Table 3. Curve characteristics of the patients with Lenke type 1 scoliosis, who were operated on using the anterior approach, as measured on plain radiographs and CT scans before surgery (pre), after surgery (post) and at 2 years follow-up (FU). UIV, upper instrumented vertebra; LIV, lower instrumented vertebra; IV, number of instrumented vertebrae. A-P%, anterior-posterior height ratio. Statistical significance level was set at 0.01.
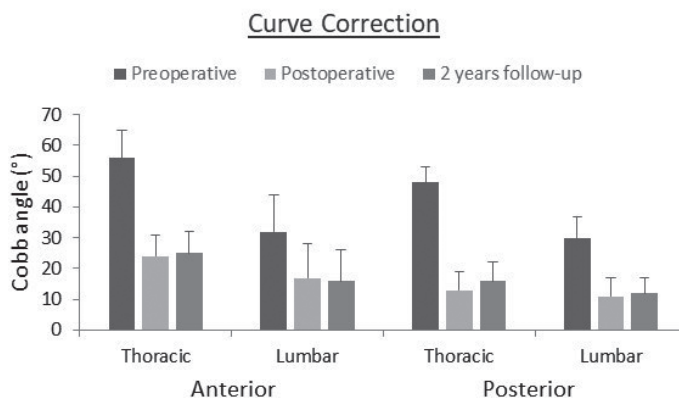

Figure 2. The thoracic and lumbar Cobb angles for Lenke type 1 curves treated with an anterior or posterior approach. Error bars indicate SD.

Curve Reduction: Posterior Approach

In the posterior cohort, the mean thoracic Cobb angle was 48±5° before surgery, 13±6° after surgery (p<0.001) and 16±6° at 2 years follow-up (p<0.001). The lumbar Cobb angle was 30±7° before surgery, 11±6° after surgery (p<0.001) and 12±5° after 2 years follow-up (p<0.001; Table 4 and Fig. 2). Thoracic kyphosis, lumbar lordosis and sagittal Cobb angle of the instrumented levels are shown in Table 4. In 3D, the vertebral rotation reduced from 22.8±6.2° before surgery to 16.3±7.8° after surgery (p<0.001) and thoracic kyphosis increased after surgery (Table 4).

	Pre	Post	p (Pre-Post)	FU	p (Post-FU)
X-rays					
Cobb angle thoracic curve	48±5°	13±6°	<0.001	16±6°	0.004
Cobb angle lumbar curve	30±7°	11±6°	<0.001	12±5°	0.577
Thoracic kyphosis (T4-T12)	28±13°	30±11°	0.222	33±10°	0.153
Lumbar lordosis (L1-S1)	56±8°	48±10°	<0.001	52±13°	0.048
Sagittal angle UIV-LIV	26±15°	26±11°	0.823	29±13°	0.010
CT scans					
Rotation apex	22.8±6.2°	16.3±7.8°	<0.001	–	–
Rotation Cobb-Cobb end	4.4±7.7°	1.9±9.0°	0.190	–	–
A-P% Cobb-Cobb end	−0.7±2.8%	−2.7±1.8%	<0.001	–	–
Height displacement UIV-LIV	–	14.2±8.6 mm	–	–	–
Height displacement UIV-LIV/IV	–	1.3±0.8 mm	–	–	–

Table 4. Curve characteristics of the patients with Lenke type 1 scoliosis, who were operated on using the posterior approach, as measured on plain radiographs and CT scans before surgery (pre), after surgery (post) and at 2 years follow-up (FU). UIV, upper instrumented vertebra; LIV, lower instrumented vertebra; IV, number of instrumented vertebrae; A-P%, anterior-posterior height ratio. Statistical significance level was set at 0.01.

Differences Between Anterior and Posterior Approaches

Before surgery, the main thoracic Cobb angle was on average larger in the anterior cohort (56±9°) than in the posterior cohort (48±5°; p<0.001), whereas the secondary lumbar curve, thoracic kyphosis and lumbar lordosis did not differ significantly between the cohorts. The thoracic Cobb angle correction was 57±12% in the anterior cohort and 73±12% in the posterior cohort (p<0.001) directly after surgery, and 55±13% and 66±12% (p=0.001), respectively, after 2 years follow-up. The lumbar Cobb angle corrections and differences in the sagittal angles are shown in Table 5. The rotation and A-P% correction after surgery and the height displacement did not differ significantly between the cohorts (Table 5). The SRS-22 and EQ-5D-3L questionnaires showed no significant differences between the anterior and posterior cohorts after surgery (Table 2). Self-image was the domain showing the largest difference between the cohorts, however, without a statistically significant difference.

DISCUSSION

Different surgical techniques have been described to prevent curve progression and restore the 3D spinal alignment of patients with idiopathic scoliosis. The spine can be accessed via an anterior or a posterior approach. However, the surgical outcomes for different surgical approaches remain unclear.

		Pre-Post	p	Pre-FU	p
X-rays					
Cobb correction thoracic curve	Ant	57±12%	<0.001	55±13%	0.001
	Post	73±12%		66±12%	
Cobb correction lumbar curve	Ant	50±25%	0.075	52±21%	0.166
	Post	61±19%		60±19%	
Thoracic kyphosis difference	Ant	8±9°	0.030	8±8°	0.263
	Post	2±9°		5±11°	
Lumbar lordosis difference	Ant	1±7°	<0.001	4±5°	0.011
	Post	−8±9°		−4±14°	
Sagittal angle UIV-LIV difference	Ant	7±9°	0.012	8±9°	0.082
	Post	0±11°		3±12°	
CT scans					
Rotation difference apex-T5	Ant	8.5±6.0°	0.161	-	-
	Post	6.5±4.4°		-	
A-P% difference Cobb-Cobb end	Ant	2.3±2.8%	0.668	-	-
	Post	2.0±1.8%		-	
Height displacement UIV-LIV	Ant	5.7±8.5 mm	0.107	-	-
	Post	9.3±6.8mm		-	
Height displacement UIV-LIV/IV	Ant	0.8±1.1 mm	0.969	-	-
	Post	0.8±0.6 mm		-	

Table 5. Differences in curve characteristics between the anterior (ant) and posterior (post) approach for patients with Lenke type 1 scoliosis, between pre- and postoperative (pre-post) and between preoperative and 2 years follow-up (Pre-FU). UIV, upper instrumented vertebra; LIV, lower instrumented vertebra, IV, number of instrumented vertebrae; A-P%, anterior-posterior height ratio. Positive kyphosis and lordosis values indicate a kyphogenic effect (increase in thoracic kyphosis and decrease in lumbar lordosis). Statistical significance level was set at 0.01.

In this study, the outcomes after spinal fusion in patients with Lenke curve type 1 were described using anterior (n=26) and posterior (n=27) approaches. Both resulted in a 3D reduction of the curve. Using the anterior approach, fewer vertebrae were instrumented in a shorter surgery time and with less blood loss compared with the posterior approach, but using the posterior approach, better coronal curve correction was achieved based on radiographs. The preoperative main thoracic Cobb angle was larger in the anterior cohort. This could lead to less correction due to stiffer curves. In both cohorts, the (un-instrumented) secondary lumbar curves were also reduced, without any statistically significant difference between the cohorts, indicating that correction of the primary curve is sufficient to reduce the lumbar secondary curves as well in Lenke 1 deformities. Coronal correction remained unchanged during the follow-up time in the anterior cohort, whereas a small deterioration was seen in the posterior cohort, from 13±6° to 16±6° (p=0.004). The patients scored well on the SRS-22 and EQ-5D-3L ques-

tionnaires, without significant differences between the anterior and posterior cohorts postoperatively.

Newton et al.[254] included 149 patients with Lenke curve type 1 to compare thoracoscopic and open anterior spinal fusion and posterior spinal fusion. They reported that the posterior approach involved on average three to four more fusion levels than the anterior approach with more blood loss, but the surgical time was greater in the anterior cohorts. The different approaches showed similar improvements in the thoracic Cobb angle, coronal balance, the lumbar Cobb angle, questionnaire scores and trunk rotation measures, after two years follow-up, with similar major complication rates.[254] Potter et al.[249] observed better main thoracic and spontaneous lumbar fractional curve correction using posterior fusion than anterior fusion, as well as better rotation correction. Lonner et al.[257] demonstrated a significant shorter surgical time using the posterior approach and a lower rate of implant failure, probably due to the use of two rods.

It has been reported that thoracic kyphosis is not restored very well using the posterior approach, and that anterior spinal fusion and instrumentation is probably the best method to restore thoracic kyphosis.[242, 250, 254] In our study, the anterior approach resulted in an increase in kyphosis of 8±9°, whereas this increase was only 2±9° in the posterior cohort, without significant difference, based on radiographs. Because the scoliotic vertebrae are rotated, 2D images of the spine provide insufficient representation of the actual sagittal alignment. Therefore, low-dose CT scans were used to study the sagittal alignment in the true sagittal plane, but no significant differences were seen between the approaches regarding sagittal plane restoration.

In previous studies, the A-P% was described in patients with adolescent idiopathic scoliosis and controls.[49, 50] The A-P% of the thoracic region was between −3.0% and −3.6% in controls, meaning that the anterior side of the spine was shorter than the posterior side, corresponding to physiological thoracic kyphosis.[49, 50] In this study, A-P% changed from 0.7±2.9% preoperatively to −1.6±2.4% after surgery in the anterior cohort and from −0.7±2.8% to −2.7±1.8% in the posterior cohort. A significant restoration, a kyphogenic effect, was observed after surgery. However, the sagittal alignment was not restored to the normal alignment of the controls, as described in the previous study.[49, 50] After surgery, the instrumented segments of the spine were longer, compared with the same spine segments before surgery, in both cohorts. In the posterior cohort, more segments were fused. No significant difference was seen between the two approaches regarding increased height per fused level.

One concern regarding the anterior approach is the negative effect on pulmonary function. In previous studies, a decrease in all pulmonary function values has been described after surgery using the anterior approach compared with the posterior approach.[254, 258, 259] Nohara et al.[244] observed no significant differences in pulmonary function after 10 years follow-up. Pulmonary evaluation was not part of the standard care

and therefore not included in this study, which is a limitation. Some aspects that could be the result of decreased pulmonary function, such as discomfort, function, health state and overall satisfaction, are included in the questionnaires and may be used as a proxy for pulmonary function. The questionnaires showed no significant differences between the groups. Nota et al.[251, 252] and Fang et al.[251, 252] showed that the risk of infection may be increased by posterior surgery, which was not confirmed by this study. Due to the drain, the number of days in hospital was higher in the anterior group. Additionally, only postoperative questionnaires were available, since the preoperative questionnaires were not part of the standard care.

This study focused on 2D radiographic outcomes, 3D CT outcomes and clinical parameters reflected in patient-reported outcome measures. The radiographs were available before surgery, after surgery and after 2 years follow-up, whereas the low-dose CT scans were only available before and after surgery as part of the standard care in these centers. Longer CT follow-up for the 3D outcomes is not ethically justified due to the radiation exposure. The number of fused segments was significantly higher using the posterior approach than the anterior approach. The lower Cobb end vertebra corresponds with the lowest instrumented vertebra in the anterior cohort, whereas the lowest instrumented vertebra in the posterior cohort was much lower in the spine. For this reason, the analysis of some outcomes was restricted to the primary thoracic curve from Cobb end to Cobb end vertebrae. Despite the limitations, this comprehensive comparison of the anterior and posterior approaches for the treatment of thoracic idiopathic scoliosis highlights the advantages and disadvantages of each approach, while confirming that both remain acceptable options for this patient population. This study reports comprehensive outcomes of the surgical treatment of thoracic idiopathic scoliosis with which current and future treatments may be compared.

CONCLUSIONS

This study describes the surgical and patient-reported outcomes of anterior and posterior surgical approaches and suggests that Lenke type 1 curves can be effectively managed with either an anterior or posterior approach. Each option, however, has specific advantages and challenges that the surgeon must acknowledge when treating each patient. The choice of surgical approach depends on these various factors, as well as the experience of the surgeon.

Chapter 13

A CT Based Guideline for Pedicle Screw Placement in Adolescent Idiopathic Scoliosis

ABSTRACT.

Purpose. To determine the 3D position of the pedicle axis in operative adolescent idio-pathic scoliosis (AIS) patients relative to the operating table and the lamina, as orientation for pedicle screw placement for spine surgeons and residents at the beginning of their careers.

Methods. The convex and concave pedicles of the apex and two adjacent vertebrae cranial and caudal to the apex of 86 right-sided primary thoracic AIS curves, were evaluated using semi-automatic 3D software on high-resolution CT scans, in the same prone position as during the surgical treatment. Pedicle vectors were obtained and calculated as transverse and sagittal angles, as relative to the neutral axis (corresponding with an axis perpendicular to the operating table) and as relative to an axis perpendicular to the lamina.

Results. At the apex, the mean convex and concave transverse pedicle angles were 14.3º (95% confidence interval (95%CI): 12.0 – 16.6) and 30.4º (95%CI: 28.1 – 32.8) to the right. The angles decreased towards the adjacent levels cranial and caudal to the apex (p<0.001) and linearly increased with a higher Cobb angle (r≥0.472; p<0.001). The mean transverse pedicle-lamina angles, sagittal pedicle angles and the sagittal pedicle-lamina angles differed along the curve as well (p<0.001).

Conclusions. Pedicle angulation differs between convex and concave and depends on the position of the vertebra relative to the apex, as well as the curve severity. The transverse and sagittal pedicle angles, as relative to the operating table and laminae, in this study could serve as guideline for pedicle screw placement in AIS.

INTRODUCTION

Adolescent idiopathic scoliosis (AIS) is characterized by three-dimensional (3D) deformities in the vertebral column and trunk [3]. The abnormal vertebral body and pedicle morphology in AIS has been observed in cadaveric specimens for centuries and more recently from radiographic imaging studies [1, 2, 29, 44, 90, 145, 146, 184, 185, 191, 196]. Pedicle screw fixation at multiple levels has become one of the most widely used powerful techniques in spinal surgery for the 3D correction of AIS [109-114]. The complication rate due to pedicle screw misplacement in patients who underwent posterior instrumentation, varies between 0 and 1%, however, the rate of screw misplacement in the thoracic region varies between 5.7 and 50% [114, 247, 260-265]. Complications related to the pedicle screw placement such as nerve root or spinal cord compression, pseudarthrosis, and major vessel injury are particularly in the more severe rigid curves. Studies aiming at more pathoanatomical 3D characterization of the pedicle length, pedicle angle, pedicle diameter and ideal pedicle screw trajectories as well as the ideal pedicle screw entry points has been conducted [90, 145, 146, 148, 184, 185, 190, 196-198, 266-269]. However, the pedicle angles in these previous studies are mostly described as the angle between the convex and concave pedicle, or as the angle between the pedicle and the vertebral axis. There is a lack of study of the 3D spatial orientation of the pedicle axis with reference to the neutral axis of the human body and external neutral axis, like the clinically relevant prone position on the operating table. In 1987, Zindrick et al. described the pedicle angles as relative to the neutral human body axis, but only for the non-scoliotic population [270]. Knowledge of these pedicle angles and their 3D position with reference to the operating table as well as the lamina throughout the scoliotic curve could serve as important guide for accurate pedicle screw orientation and placement during surgery. The objective of this study is to determine the 3D position of the pedicle axis in operative AIS patients relative to the operating table and the lamina, using semi-automatic 3D data generated from a large series of computed tomography (CT) scans of the whole spine of AIS patients taken in the prone position for pre-operative navigation planning .

MATERIALS AND METHODS

Study population

The transverse and sagittal pedicle angles, as relative to the operating table and laminae, in this study could serve as a gross guideline for pedicle screw placement in AIS. This study has been approved by the local research ethics committees. CT scans of AIS patients were selected from an existing database [157]. All AIS patients that had received pre-operative CT images (64 Slice Multi-detector CT scanner, GE Healthcare, Chalfont,

St. Giles, United Kingdom; slice thickness 0.625 millimeters (mm)) between June 2011 and March 2015, with primary thoracic curves (Lenke curve type 1-4) were included. The CT scans were acquired for navigation guided pedicle screw insertion in one of the participating centers and made in prone position, mimicking the intraoperative position for posterior surgery and multi-level pedicle screw fixation. All patients had undergone routine upright posterior-anterior and bending radiography as well as supine magnetic resonance imaging of the full spine for detection of spinal cord abnormalities. Children with other spinal pathology, spinal trauma, previous spinal surgery, neurological symptoms, neural axis abnormalities, syndromes associated with disorders of growth or atypical left convex thoracic curves were excluded to obtain an as homogeneous population as possible. Therefore the right pedicle is always the convex pedicle in this study and the left pedicle always the concave pedicle.

CT measurement method

The pedicle angles were measured for each individual pedicle by two trained observers, using in-house developed software for semi-automatic analysis (ScoliosisAnalysis 5.1, Image Sciences Institute, Utrecht, The Netherlands), based on MeVisLab (MeVis Medical Solutions AG, Bremen, Germany). Four angles were measured of the convex and concave pedicles; the transverse and sagittal pedicle angle as relative to the neutral axis, corresponding with an axis perpendicular to the operating table, and the transverse and sagittal angle between the pedicle axis and the lamina (Fig. 1-3). This process consisted of six steps. First, the observer selected the pedicles of the apex and the pedicles of the adjacent two vertebrae cranial and caudal to the apex on the CT scan, using software developed for this purpose. Second, the observer manually selected the approximate location of the longitudinal line through each pedicle. This axis was not used as pedicle axis, but served to initialize the computerized method by defining the location of the pedicle in the 3D image. Third, the software automatically generated a 3D reproduction of that pedicle, dilated an imaginary cylinder inside the pedicle until it reaches the outer cortex of the pedicle and calculated the vector of the axis through the imaginary cylinder, obtained in a 3D coordinate system (Fig. 1). Fourth, the transverse pedicle angle was measured, as the angle between the transverse pedicle axis and the anterior-posterior axis of the sacral plate, which is considered as neutral in the scoliotic spine, and is perpendicular to the operating table (Fig. 2). Fifth, the sagittal pedicle angle was measured, as the angle between the sagittal pedicle axis and a line perpendicular to the scanning table, corresponding with the operating table, since the prone CT scanning position corresponds with the prone intraoperative position (Fig. 3). Last, as an intravertebral reference, the pedicle-lamina angles were calculated. In the transverse plane, the angle between the pedicle axis and a line perpendicular to the lamina axis was measured. The lamina axis was defined as the line connecting the most ventral part of the posterior
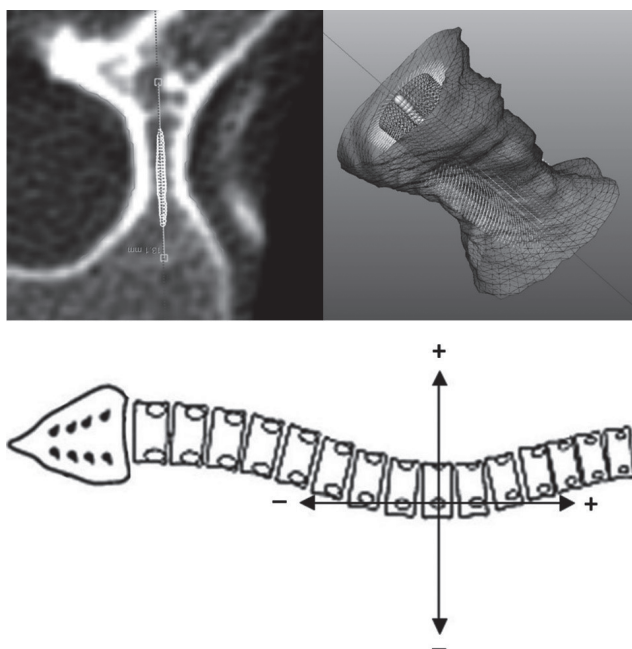
Figure 1. The pedicle angles were measured using the in-house developed software for the purpose if this study. The observer selected manually the approximate location of the longitudinal axis through each pedicle. This axis was not used as pedicle axis, but served to initialize the computerized method by defining the location of the pedicle in the 3D image (upper left). Next, the software generated automatically a 3D reproduction of the pedicle, blew up an imaginary cylinder inside the pedicle until it hits the outer cortex of the pedicle and calculated the vector of the axis straight through the imaginary cylinder, obtained in an 3D coordinate system (upper right). Positive transverse angles indicate angulation to the concave (left) side of the patient, negative values indicate angulation to the convex (right) side (lower). Positive sagittal angles indicate angulation to the cranial side, negative values indicate angulation to the caudal side.

laminar cortex of each lamina at the junction to the transverse processes. In the sagittal plane it was defined as the angle between the pedicle axis and a line perpendicular to the lamina of the corresponding level and one level to cranial (Fig. 2 and 3). Positive transverse angles indicate angulation to the concave (left) side of the patient, negative values indicate angulation to the convex (right) side. Positive sagittal angles indicate angulation to the cranial side, negative values indicate angulation to the caudal side. For intra- and inter-observer reliability, the observers analyzed a random subset of 10 CT scans on separate sittings (observer 1 twice and observer 2 once).

Statistical analysis

The statistical analyses in this study were done in SPSS 23.0 for Windows (SPSS Inc., Chicago, IL, USA). Pedicle angle differences between different levels at the apex and the adjacent cranial and caudal levels, as well as the differences between convex and con-
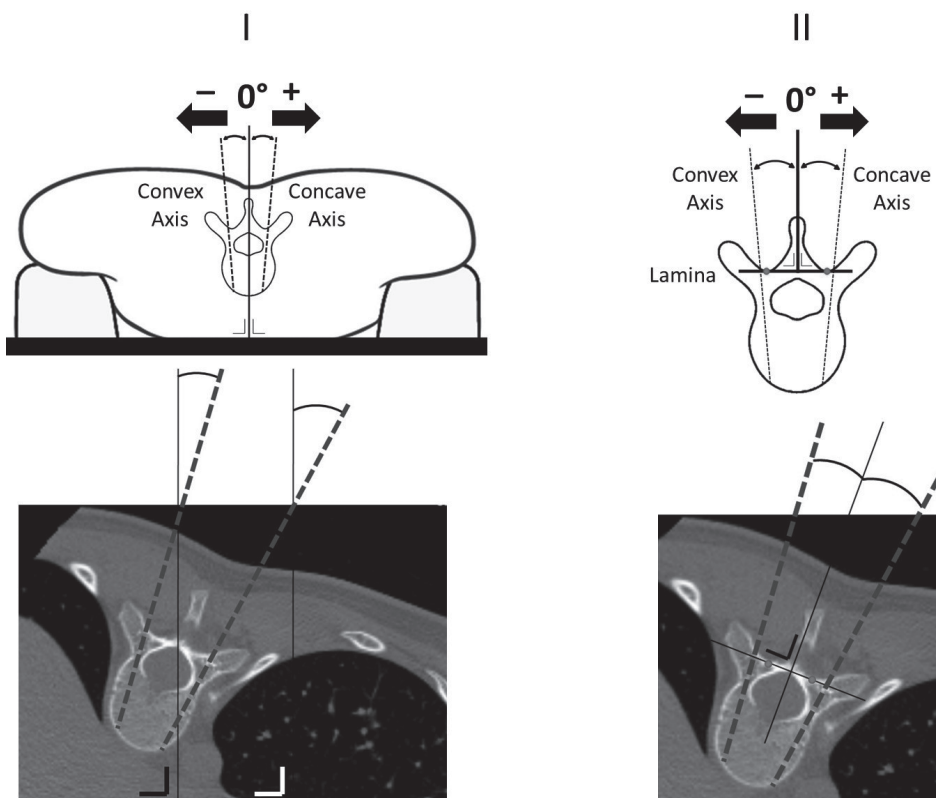
Figure 2. Two transverse angles are measured; the transverse pedicle angle and the transverse pedicle-lamina angle. The transverse pedicle angle was measured, as the angle between the transverse pedicle axis and the anterior-posterior axis of the sacral plate, which is considered as neutral in the scoliotic spine, and is perpendicular to the operating table (I). The pedicle-lamina angles were calculated in the transverse plane as the angle between the pedicle axis and a line perpendicular to the lamina axis (II). Positive transverse angles indicate angulation to the concave (left) side of the patient, negative values indicate angulation to the convex (right) side.

cave, were analyzed with a one-way repeated measured analysis of variances (ANOVA) added with a follow up pairwise comparison and post-hoc Bonferroni correction between each level. ANOVA, including as post-hoc Bonferroni correction, was used as well for analyzing the pedicle angle differences between different Cobb angle subgroups and different curves, based on the level of the apex and length of the curve. Pearson correlation coefficient (r) defined the relationship between the different pedicle angels and the Cobb angle. Finally, intra- and interobserver variabilities were obtained as intraclass correlation coefficients. The statistical significance level was set at 0.05.
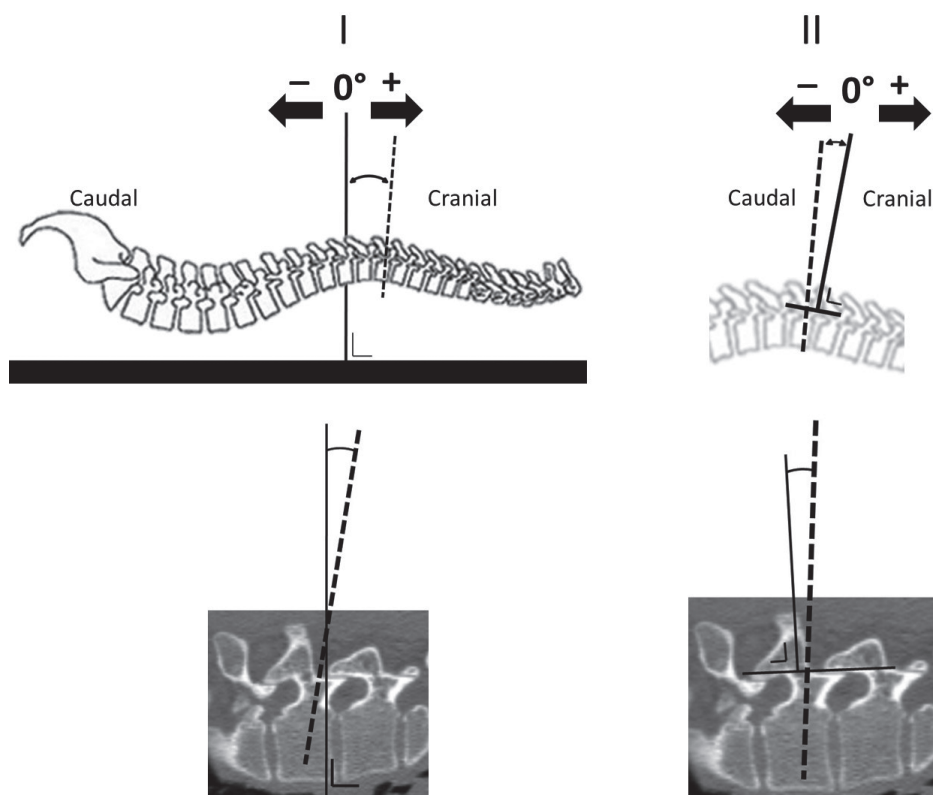
Figure 3. Two sagittal angles are measured; the sagittal pedicle angle and the sagittal pedicle-lamina angle. The sagittal pedicle angles were measured, as the angle between the sagittal pedicle axis and the line perpendicular to the scanning table, corresponding with the operating table, since the prone CT scanning position corresponds with the prone intraoperative position (I). The sagittal pedicle-lamina angles were calculated in the sagittal plane as the angle between the pedicle axis and a line perpendicular to the lamina axis between the lamina of that level and one level beneath (II). Positive sagittal angles indicate angulation to the cranial side, negative values indicate angulation to the caudal side.

RESULTS

Study population

The database consisted of CT scans of 86 AIS patients with primary right thoracic (Lenke type 1-4) curves (Table 1). The level of apex varied between T7 and T11 and the length of the curves varied between five and 10 vertebrae.

Transverse pedicle angle relative to the neutral operating table

At the apex, the mean angle between the transverse pedicle axis and the neutral axis was 14.3º (95% confidence interval (95%CI): 12.0 – 16.6) on the convex side and 30.4º

		AIS patients (n=86)
Age	Range	10-26 years
	Mean±SD	16.2±2.9 years
Females	n (%)	73 (85%)
Thoracic curve right convexity	n (%)	86 (100%)
Primary thoracic Cobb angle	Range	46-109°
	Mean±SD	69.4±12.3°
Cobb angle group	<60°	n (%)	15 (17%)
	60-70	n (%)	39 (46%)
	70-80	n (%)	15 (17%)
	>80°	n (%)	17 (20)
Lenke curve	Type 1	n (%)	43 (50%)
	Type 2	n (%)	26 (30%)
	Type 3	n (%)	12 (14%)
	Type 4	n (%)	5 (6%)
Level of the apex	Thoracic 7	n (%)	7 (8%)
	Thoracic 8	n (%)	23 (27%)
	Thoracic 9	n (%)	34 (40%)
	Thoracic 10	n (%)	21 (24%)
	Thoracic 11	n (%)	1 (1%)

Table 1. Demographics and curve characteristics are shown for all included adolescent idiopathic scoliotic (AIS) patients. SD = standard deviation.

(95%CI: 28.1 – 32.8) on the concave side and was significantly larger as compared to the two levels cranial and caudal to the apex (p<0.001; Table 2). The Cobb angle had a positive correlation with the pedicle angle at the apex (convex pedicle: r=0.472; p<0.001 and concave pedicle: r=0.508; p<0.001). The rest of the levels showed a weak or non-significant correlation with the Cobb angle (the angles based on different curve severity groups are shown in Fig. 4). The level of apex varied between T7 and T11 and the curve length between five and 10 vertebrae. However, the apical transverse pedicle axis differed not between the curves with different apical levels (p≥0.120), or between curves with different lengths (p≥0.897).

Sagittal pedicle angle relative to the neutral operating table

At the apex, the mean angle between the sagittal pedicle axis and the neutral plane was -6.7° (95%CI: -8.3 – -5.0) on the convex side and -6.2° (95%CI: -8.1 – -4.4) on the concave side and was significantly larger as compared to the two levels cranial and caudal to the apex (p≤0.027), except for the convex pedicle one level cranial to the apex (p=0.492) and the concave pedicle two levels cranial to the apex (p=0.312; Table 3). Weak or non-

	Transverse pedicle angle (°)			Transverse pedicle-lamina angle (°)		
	Convex	Concave	p	Convex	Concave	p
+2	1.3 (-0.6 – 3.2)	18.2 (16.3 – 20.1)	<0.001	-8.4 (-10.2 – -6.6)	8.5 (6.9 – 10.1)	<0.001
+1	8.0 (6.1 – 10.0)	25.2 (23.2 – 27.2)	<0.001	-7.7 (-9.1 – -6.3)	9.5 (8.0 – 11.0)	<0.001
Apex	14.3 (12.0 – 16.6)	30.4 (28.1 – 32.8)	<0.001	-3.9 (-5.0 – -2.8)	12.2 10.8 – 13.6)	<0.001
-1	10.0 (7.9 – 12.1)	24.5 (22.3 – 26.7)	<0.001	-5.4 (-6.6 – -4.1)	9.1 (7.6 – 10.7)	<0.001
-2	4.5 (2.2 – 6.7)	16.6 (14.4 – 18.8)	<0.001	-5.1 (-6.7 – -3.6)	7.0 (5.5 – 8.6)	<0.001

Table 2. Mean transverse pedicle angles, as relative to the neutral anterior-posterior axis, as well as the pedicle-lamina angles, including 95% confidence intervals, of the convex and concave pedicles in the primary thoracic curves are shown for the apex and the two adjacent cranial (+1 and +2) and caudal (-2 and -1) levels. Positive transverse angles indicate angulation to the concave (left) side of the patient, negative values indicate angulation to the convex (right) side. The p-values were calculated for the differences between the convex and concave pedicle.
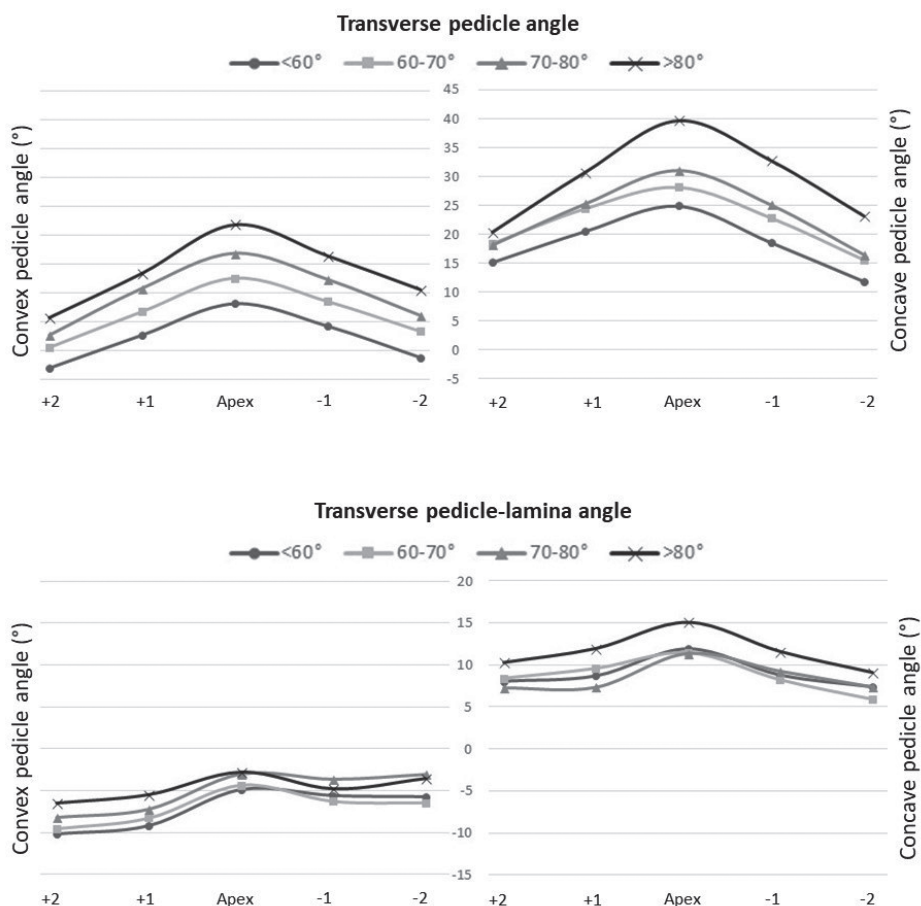

Figure 4. The mean convex and concave transverse pedicle angles and transverse pedicle-lamina angles of the apex and the two cranial (+1 and +2) and caudal (-1 and -2) levels are shown for different curve severities (Cobb angle <60°, Cobb angle 60-70°, Cobb angle 70-80° and Cobb angle >80°).

significant correlations were observed between the sagittal pedicle angle and the Cobb angle (the angles based on different curve severity groups are shown in Fig. 5). The level of the apex and the length of the curves influenced not significantly the sagittal pedicle axis (p≥0.220).
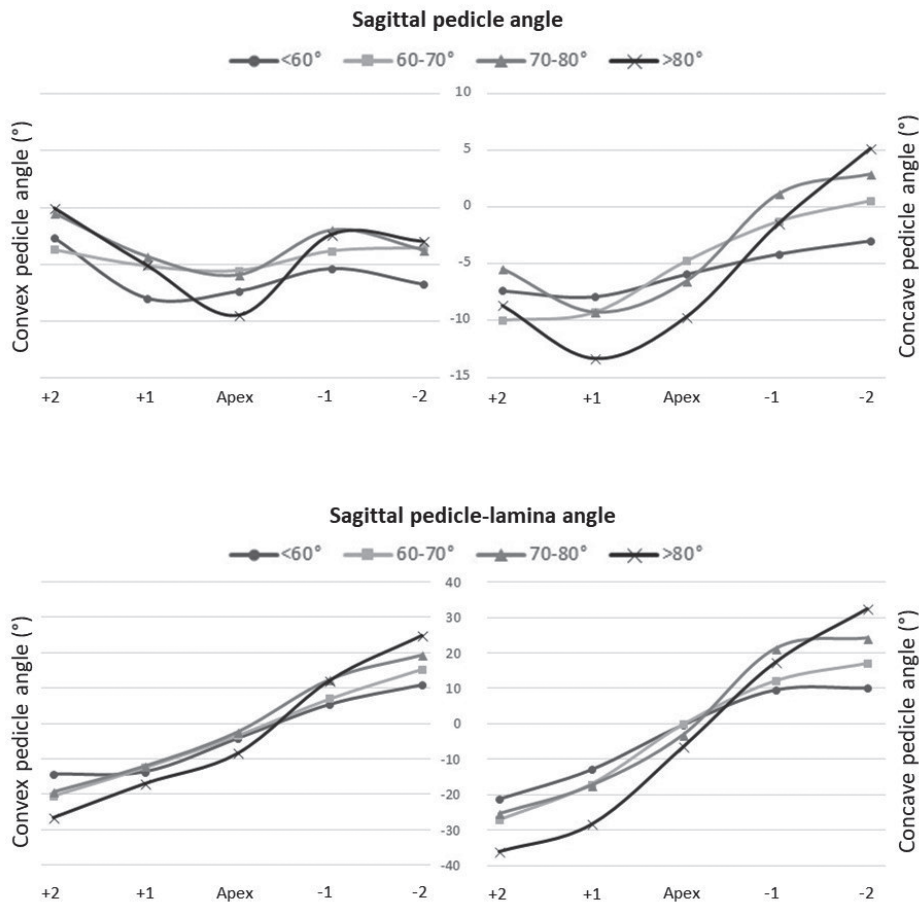

Figure 5. The mean convex and concave sagittal pedicle angles and transverse pedicle-lamina angles of the apex and the two cranial (+1 and +2) and caudal (-1 and -2) levels are shown for different curve severities (Cobb angle <60°, Cobb angle 60-70°, Cobb angle 70-80° and Cobb angle >80°).

Pedicle-lamina angles

The transverse pedicle-lamina angle, was on average larger at the apex as compared to one and two levels cranial and caudal to the apex (p<0.001), except the convex pedicle one and two levels caudal to the apex (p=0.089 and p=0.200; Table 2). The sagittal pedicle-lamina angle was on average larger at the apex, as compared to the adjacent cranial and caudal vertebrae (p<0.001; Table 3). Only weak or non-significant correlations were

	Sagittal pedicle angle (°)			Sagittal pedicle-lamina angle (°)		
	Convex	Concave	p	Convex	Concave	p
+2	-2.2 (-3.9 – -0.6)	-8.4 (-10.2 – -6.7)	<0.001	-20.3 (-22.4 – -18.2)	-27.6 (-30.0 – -25.1)	<0.001
+1	-5.5 (-7.1 – -3.9)	-9.8 (-11.6 – -8.1)	<0.001	-13.4 (-15.4 – -11.4)	-18.6 (-21.1 – -16.2)	<0.001
Apex	-6.7 (-8.3 – -5.0)	-6.2 (-8.1 – -4.4)	0.437	-4.3 (-6.5 – -2.1)	-1.9 (-4.8 – 0.90)	0.007
-1	-3.5 -5.3 – -1.7)	-1.4 (-3.0 – 0.3)	<0.001	8.6 (6.3 – 11.1)	14.2 (11.9 – 16.6)	<0.001
-2	-4.0 (-5.9 – -2.2)	1.3 (-0.5 – 3.0)	<0.001	17.1 (14.8 – 19.4)	20.1 (17.5 – 22.8)	0.01

Table 3. Mean sagittal pedicle angles, as relative to the neutral anterior-posterior axis, as well as the pedicle-lamina angles, including 95% confidence interval, of the convex and concave pedicles in the primary thoracic curves are shown for the apex and the two adjacent cranial (+1 and +2) and caudal (-2 and -1) levels. Positive sagittal angles indicate angulation to the cranial side, negative values indicate angulation to the caudal site. The p-values were calculated for the differences between convex and concave pedicle.

observed between the transverse pedicle-lamina angle and the Cobb angle (the angles based on different curve severity groups are shown in Fig. 4 and 5). The level of the apex and the length of the curves influenced not the sagittal pedicle axis (p≥0.181).

Reliability

Intraclass correlation coefficients for intra- and interobserver reliabilities were 0.93 (95% confidence interval: 0.90–0.95) and 0.94 (0.91–0.96) for the pedicle axes as relative to the operating table, and 0.97 (0.95–0.98) and 0.95 (0.93–0.97) for the pedicle axes as relative to the lamina.

DISCUSSION

Several studies already provided accurate descriptions of pedicle morphology in AIS as the angle between the convex and concave pedicle or as the angle between the pedicle and the vertebral body axis [90, 145, 146, 148, 184, 185, 190, 196, 197, 266]. However, pedicle orientation throughout the curve in AIS, as compared to the neutral axis or operating table, like Zindrick et al. did for the non-scoliotic spine in 1987, remained undetermined so far in AIS [270]. Accurate description of pedicle orientation and morphology is important for pedicle screw placement during the surgical treatment of AIS. Therefore, the 3D orientation of pedicles in moderate to severe primary thoracic AIS curves, as compared to the neutral axis (perpendicular to the operating table), as well as the lamina, using high resolution CT scans was reported in this study.

The mean apical transverse pedicle angle was 14.3º (95%CI: 12.0 – 16.6) on the convex side and 30.4º (95%CI: 28.1 – 32.8) on the concave side and decreased towards the junction zone. This angulation increased in curves with a higher Cobb angle. The sagittal pedicle angle as well as the angles between the pedicle and the lamina differed along the curve as well. However, the level of the apex and the length of the curve did not influence the pedicle angles of the apex. Although this study is the first in describing the pedicle angle as compared to the neutral body axis or operating table, the angle differences between the convex and concave pedicle (12-17°) were in general similar to the findings as described in previous studies [145, 148, 271]. Takeshita et al. already measured the direction of the thoracic and lumbar pedicles, as the angle between the pedicle axis and a line connecting both sides of the middle of the superior facet base, using CT imaging, independent of the location of the apex of the curve [146]. Since the direction of the pedicles is related to the rotation of the vertebra, and therefore related to the position of the vertebrae within the curve, the current study measured the pedicle direction of the apex and the two levels cranial and caudal to the apex. By using in-house developed software for semi-automatic analysis to construct 3D pedicle images and calculate the vector, the measurements are accurate and less vulnerable to observer subjectivity, compared with the use of 2D transverse images and measuring pedicle angles by hand in AIS. Previous studies have shown that the alignment of the scoliosis is influenced by the position of the patient [57, 58, 181-183]. In this study, the CT scans were made in the same prone position as the position during surgery.

Previous studies described the pedicle morphology as the angulation between the convex and concave pedicles or as the angulation between the pedicle and the vertebral body axis [145, 148, 271]. In current study, the pedicle angulation was measured as relative to the sacral axis, in the transverse plane. Since the sacrum is considered as neutral in the scoliotic spine and the position of the patient during scanning and surgery are in the same prone positions, the sacral axis is perpendicular to the operating table. Therefore, the data of current study could be used as guideline for the pedicle screw placement. Additionally, the pedicle-lamina angle, as derived from this study as well, could be used for *in vivo* pedicle screw positioning during surgery as well. Since the pedicle angle differed within the curve, the pedicle angles were shown for different groups of patients, based on the Cobb angle. For this study, an already existing CT database was used, acquired as part of the general pre-operative workup for navigation guided surgery in one of our institutions, resulting in a cross-sectional study design. No additional imaging was made for the purpose of this study. If the pedicle is too narrow for the pedicle screw, or the pedicle or lamina are too much deformed, the surgeon could decide to select an extra-pedicle trajectory between the rib head and the pedicle, parallel to the end plate of the vertebra in the sagittal plane and directed towards the midline in the transverse plane, to maximize the length as well as bone purchase. The ideal entry points, including

the entry point shift due to the extra-pedicle trajectory, are part of our further ongoing study.

CONCLUSION

Values for guidance of pedicle screw placement in AIS are provided for beginning spine surgeons and/or residents. Pedicle angulation differs between concave and convex, the position as relative to the apex, as well as between curves with different severities. The transverse and sagittal pedicle angles, as relative to the operating table and laminae, in different curve severities in this study could serve as a gross guideline for pedicle screw placement in AIS.

Chapter 14

Summary and General Discussion

SUMMARY

Although the Scoliosis Research Society defines scoliosis as a lateral curvature of the spine of at least than 10 degrees in the coronal plane, adolescent idiopathic scoliosis (AIS) involves complex changes in three planes: in the coronal plane, it is characterized by lateral deviation and lateral bending, in the transverse plane by axial rotation, and in the sagittal plane by lordosis, mainly of the apical segments.[1, 29, 89] Knowledge of the deformities in the three planes is important to understand the etiopathogenesis, as well as for imaging and treatment of AIS. In this section, the results of the studies that were performed for this thesis are summarized by addressing the questions that were formulated in the introduction of this thesis (chapter 1).

Etiology and 3D pathoanatomy of AIS

The human posture and locomotion differs from other vertebrates, since the man has three well developed lordoses along the spine: one between the iliac and ischial bones, one in the lumbar region, and one in the cervical region (Figure 1).[15, 118] The lordotic angulation of the ilium relative to the ischium, in combination with the ability to fully extend the hips and knees at the same time, makes man the only species to consistently carry the body's center of gravity straight above the pelvis, rather than in front.[14, 15, 116, 117]

The unique biomechanical load on the human spine leads to a reduction of rotational stiffness of the exposed segments and the more the spine exhibits areas with posteriorly
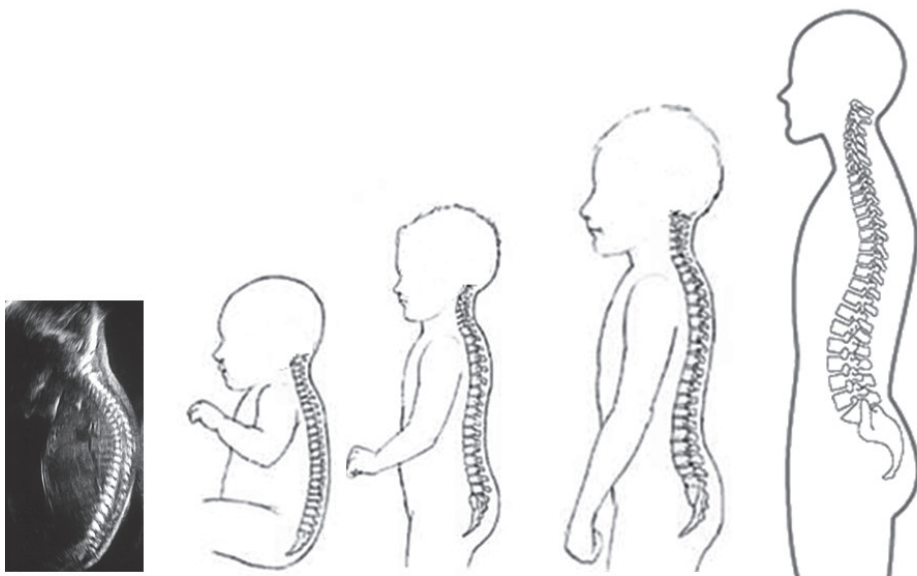

Figure 1. Spinal development from fetal to adult, resulting in the final double S-shaped spine.

tilted vertebrae, the more these segments are prone to develop a rotational deformity and finally scoliosis.[5, 7, 8, 120] In this thesis a number of questions relevant for idiopathic scoliosis are addressed, in a number of chapters.

Chapter 2. The Etiologic Relevance of the 3D Pathoanatomy of Adolescent Idiopathic Scoliosis

What is the relevance of the 3D pathoanatomy of AIS?

AIS develops most frequently in girls around the time of the adolescent growth spurt.[3] Schlösser et al. showed that the thoracic kyphosis, pelvic tilt, and pelvic incidence increase during growth, and that before and during the peak of the growth spurt, a greater number of vertebrae are posteriorly inclined as compared to the period after the growth spurt.[14, 23, 130, 131] At the peak of the growth spurt, the spines of girls showed more posterior inclination as compared to the spines of boys. This suggests that in girls around the peak of the growth spurt, the spine is subject to greater posteriorly directed shear loads, and thus shows less resistance to rotation, that may explain why AIS occurs more often in girls than in boys. Additionally, in thoracic scoliosis, most thoracic vertebrae were more backwardly inclined as compared to (thoraco)lumbar scoliosis, and vice versa, already at a very early stage of development of the rotation and the curvature, and thus can be postulated to play a role in the pathogenesis of the different curve types (Figure 2).
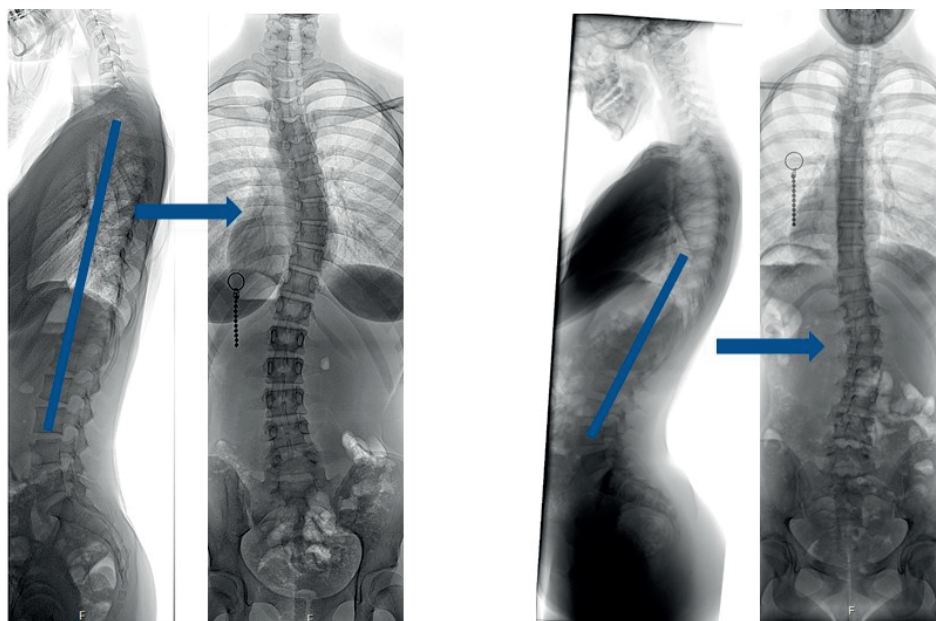

Figure 2. In mild thoracic scoliosis, most thoracic vertebrae were backwardly inclined as compared to (thoraco) lumbar scoliosis and vice versa.

A right convex main thoracic curve with compensatory high-thoracic and (thoraco) lumbar curves to the left is the most prevalent AIS curve type, in contrast to the early-onset scoliosis.[40, 137] The non-scoliotic spine showed some rotation as well, with an axial rotational pattern that is similar to what is seen in the most prevalent curve patterns in idiopathic scoliosis: at the infantile age the spine was rotated to the left at all thoracic levels, at the juvenile age, the thoracic vertebrae were oriented in the midline and at the adolescent age, most thoracic levels were rotated to the right.[139-142]

Differences in the sagittal plane were described between AIS patients and non-scoliotic controls and has led to the assumption that idiopathic scoliosis may be a problem of active anterior overgrowth of the osseous structures, as well as a growth discrepancy of the spinal cord as compared to the vertebrae.[47, 52-54] Schlösser et al. described a global 3D development of AIS curves, following a uniform pattern in all three planes in all AIS curves, structural as well as nonstructural, primary as well as compensatory, thoracic as well as (thoraco)lumbar, characterized by more deformation in the intervertebral discs, rather than the vertebral bodies at the apex, whereas the junctional segments between the curves were more or less straight.[44, 50] These facts are in contradiction with the theory that the anterior overgrowth is a result of excessive active bone growth.

Chapter 3. Three-Dimensional Pelvic Incidence is Much Higher in (Thoraco)Lumbar Scoliosis Than in Controls

What are the differences in pelvic alignment between AIS patients and the non-scoliotic controls?

As key regulator of the spine, the pelvis is of extreme importance in the normal as well as in the deviated spinal alignment. The spinopelvic alignment varies between individuals and ages, as well as between different pathologies.[7, 47, 77] The angulation of the ilium relative to the ischium (pelvic lordosis) is crucial for upright human locomotion. Even bonobo's, human's closest relative, consistently walks with both hip and knee flexed and a center of gravity in front of the pelvis, with almost no angulation between the ischium and ilium.[116] Schlösser et al. described the evolutionary aspects of the spinopelvic morphology by comparing the morphology between the human and different species within the Hominoidae family.[116] They showed an increase of the ischio-iliac angle and PI, related with increasing bipedal gait proficiency during human evolution (Figure 3).

Despite the differences in sagittal spinal alignment between mild thoracic and mild lumbar scoliosis, previous authors were not able to demonstrate a statistically significant difference in sagittal pelvic morphology between patients affected by different degrees of thoracic and (thoraco)lumbar idiopathic scoliosis, using conventional 2D radiographs or biplanar radiography.[77, 133] In 2012, Vrtovec et al. measured the 3D PI in a non-scoliotic population using CT scans, demonstrating the improved accuracy of this 3D method as compared to the traditional measurements on plain lateral radiographs.[82, 87] Using
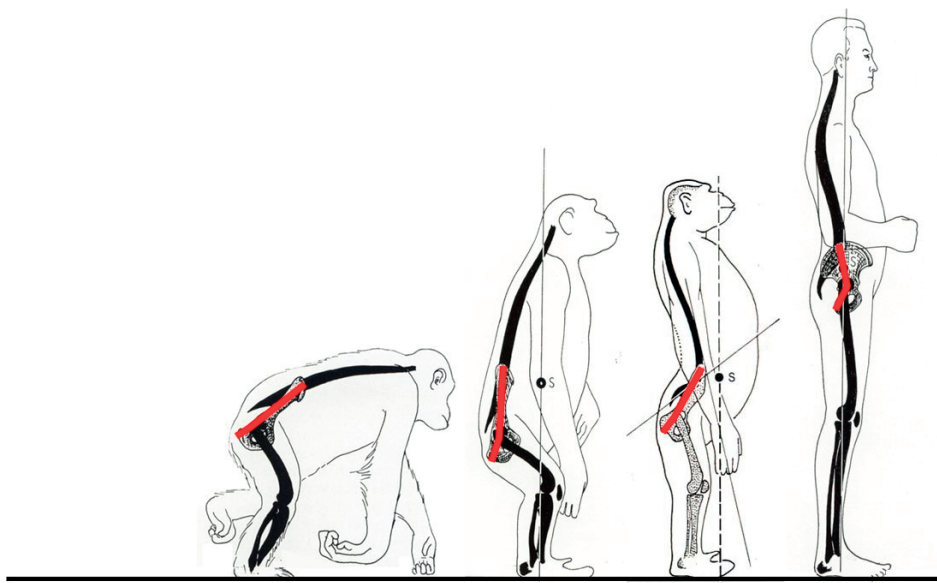
Figure 3. An increase of the ischio-iliac angle and PI measurements is seen, related with increasing bipedal gait proficiency during human evolution.[116]

this 3D measurement method, as described in chapter 3, the PI turned out to be higher in AIS patients with a Lenke type 5 curve (lumbar scoliosis) as compared to controls, whereas the PI in patients with a Lenke type 1 curve (thoracic scoliosis) did not differ from controls. Although this has not been demonstrated before, these observations are consistent with previous theories, suggesting a link between sagittal spinopelvic alignment and the development of different curve types in idiopathic scoliosis.

Chapter 4. CT-Based Study of Vertebral and Intravertebral Rotation in Right Thoracic Adolescent Idiopathic Scoliosis

Where is the longitudinal rotation axis of the AIS vertebrae located, and what are the various extra- and intravertebral rotation patterns?

Additionally to the lateral deviation and lateral bending in the coronal plane, the vertebrae of the scoliotic curves are axially rotated, mainly in the apical regions of the curvatures.[2, 46] If there is a thoracic lordosis, instead of the normal thoracic kyphosis, the longitudinal rotation axis is located posteriorly to the spine, as also suggested by Smith et al..[166] White and Panjabi were amongst the first to describe the longitudinal rotational axis, and this axis was found to lay within the vertebral body.[22] Later on, several authors demonstrated that the longitudinal rotation axis was located at the posterior side of the vertebral body or vertebral arch, based on non-scoliotic specimens, cadaveric spines or

models.[2, 42, 165, 170, 177] However, the contributions of the extra- and intravertebral rotation patterns, remained unclear.

The longitudinal rotation axis of the apical vertebrae in AIS appeared to lie far (11.5 cm) dorsal from the spine itself. The rotation radius, described as the distance between the spine and the longitudinal rotation axis, differed per level within the spine: if there is much vertebral axial rotation, as in the apical vertebral body, the longitudinal rotation axis becomes closer to the vertebra. In the less rotated vertebrae near the end of the curve, the intersection lies farther away and forms a parabolic shape along the curve in the sagittal plane. Additionally, the vertebral axial rotation at the apex (on average 21.9±7.4°), was larger as compared to the intravertebral axial deformation between the anterior and posterior vertebral structures (8.7±13.5°) and local mechanical torsion between the upper and lower part of a single vertebra (3.0±2.5°). Furthermore, this decreased towards the end of the curves. The vertebral body in AIS is rotated and translated away from the midline, whereas the spinous process is less deviated from the midline, probably stabilized by the posterior ligaments, corresponding with the posteriorly located longitudinal rotation axis. Kotwicki et al. described this phenomenon as secondary, due to bone remodeling of the vertebral body and deviation of the spinous process in opposite direction, as an extension of the theory by Smith et al..[166, 171, 172]

Chapter 5. Asymmetry of the Vertebral Body and Pedicles in the True Transverse Plane in Adolescent Idiopathic Scoliosis: A CT-Based Study

How asymmetrical are the pedicles and vertebral bodies in adolescent idiopathic scoliosis?
The rotation in the transverse plane, as well as the asymmetry of the vertebrae in the transverse plane has been described in a number of older as well as more recent anatomical and radiographic imaging studies.[1, 2, 29, 30, 44, 46, 89, 90, 184-187] The role of this asymmetry, and whether it represents an active asymmetrical growth pattern, or a passive adaptation due to asymmetrical biomechanical loading as explained by Hueter-Volkmann's and Wolff's law, is sometimes inconsistent and conflicting so far.[188, 189, 192, 193] Experimental studies have shown that asymmetrical growth of the neurocentral junctions of the vertebrae can lead to vertebral rotation; unilateral lag screw epiphysiodesis of the neurocentral junctions in a growing pig was shown to lead to a rotational, 3D deformity, similar to AIS.[144, 194, 195] It is known that all growth cartilage of the pedicles, the neurocentral junctions, close before the age of eight, therefore pronounced pedicle asymmetry suggests a disturbance of symmetrical development that has started already before that age.[142] If, however, asymmetrical growth of the neurocentral junctions (either active or passive) leads to asymmetrical pedicle development in AIS, it implicates that the deformity must already begin to develop before closure of these growth plates, in other words, well before the adolescent growth spurt, when all neurocentral junctions have been reported to be closed, or it is the result of secondary bone remodeling.[142, 144, 196]

The exact transverse plane morphology in AIS is important, both theoretically for better understanding its mechanism, as practically, for surgical strategy and safe implant placement. The vertebral body as well as pedicle morphology asymmetry in AIS in the true transverse plane has been described in chapter 5, using 3D multiplanar reconstruction of high-resolution CT scans for each individual vertebra and in-house developed software. In the 1876 pedicles and 1876 vertebral upper and lower endplates that have been observed for this study in AIS and non-scoliotic controls, a certain degree of vertebral asymmetry exists in AIS and the non-scoliotic controls. However, the asymmetry was slightly more pronounced in AIS. The concave pedicles of the thoracic primary curves were on average 0.4 mm thinner, 1.8 mm longer, the ideal screw trajectory was also on average 4.1 mm longer than for the convex pedicle and the transverse pedicle angle was 4.6° greater on the concave side. The asymmetry was found to increase towards the apex, the concave pedicle becoming thinner and longer, up to a difference of 0.9 mm thinner and 3.0 mm longer than the convex pedicle. However, no direct correlation was found between the amount of asymmetry, the magnitude of the Cobb angle or the amount of rotation of the apex. As mentioned in previous studies, the bone drift of the vertebral body toward the concavity and the greater pedicle angle on the concave side, explains the longer ideal pedicle screw trajectory on the concave side.[90] The observations, as described in chapter 5, in combinations with the facts that the neurocentral junctions are closed before the adolescent age, most asymmetry was seen in the apical region, whereas the neutral zones corresponds with non-scoliotic controls, suggest that asymmetrical vertebral growth does not drive rotation, but rather follows it to a variable extent as bone remodeling.

Chapter 6. Anterior Spinal Overgrowth Is the Result of the Scoliotic Mechanism and Is Located in the Disc

Does the regional anterior-posterior length discrepancy in idiopathic scoliosis differ from other types of scoliosis?

The link between the asymmetry, as well as the rotation in the transverse plane and the sagittal alignment has been described extensively in previous studies.[2, 3, 22, 46] In 1952, Somerville described scoliosis as a rotational lordosis, instead of the normal straight thoracic kyphosis, as seen in non-scoliotic children.[46] Schlösser et al. described that only posteriorly inclined vertebrae take part of the scoliotic curve and that the sagittal alignment of thoracic scoliosis differs from lumbar scoliosis already at an early stage of the condition.[56] In other words; the posterior inclination, corresponds with the rotation of the segments, that is in accordance with earlier reported findings related to the rotational instability of the human spine and its role in the pathogenesis of scoliosis.[5-7] There is an ongoing debate on the development of this thoracic lordosis, or called the relative anterior spinal overgrowth.

In 2D radiographic studies on AIS, contradictory findings have been reported on the individual contribution of the vertebral bodies, as compared to the discs, to the coronal deformity.[52-55] Schlösser et al. described that this anterior overgrowth is not a generalized phenomenon, but is observed in the primary as well as the compensatory curves, whereas the junctional zones do not exhibit this growth discrepancy and the discs contribute far more to the anterior overgrowth, as compared to the vertebral bodies.[44, 50] Dickson et al. hypothesised that differences in the sagittal plane (reversal of the normal thoracic kyphosis) during growth, could initiate a progressive idiopathic scoliosis, and other authors have proposed a hypothesis of uncoupled endochondral-membranous bone growth in AIS.[47, 52] Porter described that in the scoliotic spine, the length of the spinal canal was consistently shorter than the anterior height of the vertebral bodies and intervertebral discs and postulated a hypothesis on uncoupled neuro-osseous growth.[52-54, 152] In this, asynchronous growth patterns of different spinal structures (active) or tethering of the spinal cord or other posterior soft tissues (passive) could lead to a longer anterior side of the spine.[47, 52, 53, 55] However, in no previous study, the same anterior-posterior measurements were described in scoliosis with known etiology.

The data in chapter 6 showed that anterior overgrowth is not restricted to idiopathic scoliosis, as the same phenomenon also occurs in neuromuscular scoliosis and the anterior lengthening was solely observed in the intervertebral discs, whereas the vertebral bodies showed no significant differences in anterior lengthening between either idiopathic or neuromuscular scoliosis, and non-scoliotic controls. Furthermore, the anterior overgrowth increases linearly with increasing Cobb angle in these thoracic curvatures. It thus appears that the anterior lengthening that is seen in idiopathic scoliosis is a more generalized phenomenon that is part of the scoliotic mechanism, rather than the cause of idiopathic scoliosis.

Chapter 7. Anterior-Posterior Length Discrepancy of the Spinal Column in Adolescent Idiopathic Scoliosis - a 3D CT Study

Is the regional anterior-posterior length discrepancy in AIS the result of relative anterior lengthening or relative posterior shortening?

Although the anterior overgrowth was described in the vertebral bodies and intervertebral discs, the posterior elements were not included in previous studies, that is important to distinguish between relative anterior overgrowth or relative posterior shortening.

In chapter 7 the contribution of the posterior elements, i.e. the laminae, interlaminar spaces, spinous processes and interspinous spaces, to this anterior-posterior length discrepancy, was described using CT scans of AIS patients and non-scoliotic controls. The anterior side of the thoracic vertebral bodies in the thoracic non-scoliotic spine was on average 2.4% shorter than the posterior side, whereas the anterior side of the vertebral bodies in AIS was 1.3% longer than posterior, resulting in a relative anterior lengthening

of the vertebrae of 3.7% in AIS as compared to controls. The rest of the bony structures (lamina and spinous processes) showed no significant difference in anterior-posterior ratio between AIS and controls. The differences in height ratios between AIS and controls in the non-osseous structures were 17.8%, 8.1% and 11.7% for the intervertebral discs, interlaminar spaces and interspinous spaces of the thoracic curves and corresponding levels in the non-scoliotic controls. In the secondary, (thoraco)lumbar curves, the same phenomenon was observed in this population: the non-osseous structures contributed most to the relative anterior lengthening and posterior shortening. To distinguish between relative anterior lengthening and relative posterior shortening, the absolute lengths were compared between AIS and controls. In comparison with the same levels in unaffected adolescents in this study, two differences were observed between the scoliotic and non-scoliotic group; the anterior height of the intervertebral discs of the main thoracic curve was larger, whereas the interspinous height was smaller in AIS as compared to controls (Figure 4). These results showed that the anterior-posterior length discrepancy is the result of anterior lengthening as well as posterior shortening, with the facet joints functioning as a fulcrum and is important and relevant, both from the etiopathogenesis as well as a treatment point of view.
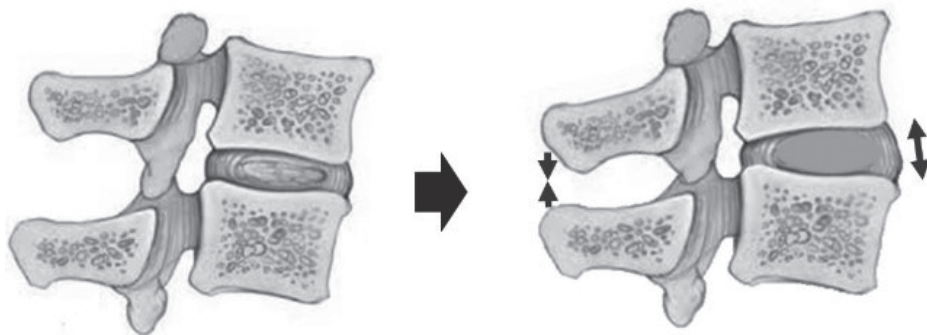

Figure 4. The anterior-posterior length discrepancy of the primary and secondary scoliotic curves is caused by anterior lengthening as well as posterior shortening, of – mostly – the non-osseous structures, with the facet joints as the fulcrum.

Imaging of AIS

Chapter 8. What is the actual 3D Representation of the Rib Vertebra Angle Difference (Mehta's angle)?

Are the rib-vertebral junctions asymmetrical in adolescent idiopathic scoliosis, when assessed in 2D and 3D, and do they represent the 3D spinal deformation?

To visualize the anterior-posterior length discrepancy, lateral radiographs are insufficient, since the scoliosis curves are rotated. Therefore, Stagnara introduced le plan d'election, a rotated view to evaluate the true coronal profile of the apical segments of

the curvature, indicating that the standard PA and lateral radiographs show a deviated image of the deformed spine.[39] In chapter 8, the hypothesis was tested, whether the RVAD, the differences in rib vertebra angle between the convex and concave side, is based on true asymmetry, or based on a 2D simplification of the 3D deformity, due to the 2D radiographs.[41] There are several theories about the RVAD; it has for example been hypothesized that the RVAD could be an expression of asymmetric muscle forces acting on the rib cage, originating from the central nervous system.[210, 211] It was suggested that the 'drooping' of the ribs in the convexity of the curve reflected decreased spinal stability.[92, 93, 95, 97, 98] However, the observed rib asymmetry, based on radiographs, does not take into account the complex apical 3D morphology, in which rotation and apical lordosis were shown to play an important role.[91, 93, 94, 96-99, 101]

The mean 2D RVAD in chapter 8 was 25.3° on the x-ray and 25.6° on the digitally re-constructed radiograph of the CT scan, but in the 3D reconstructed true coronal view of the derotated apex, this apparent difference in rib vertebra angles between the concave and convex side almost completely disappeared (3D RVAD: 3.1°), indicating that the 2D RVAD represents in reality the 2D projected image of the 3D morphology of the apical region of the spine, including the severity of the apical lordosis (Figure 5). However, the 2D RVAD demonstrated a significant relation with the deformity in the coronal plane, apical rotation and apical lordosis which suggests it to be a reliable indicator of 3D apical
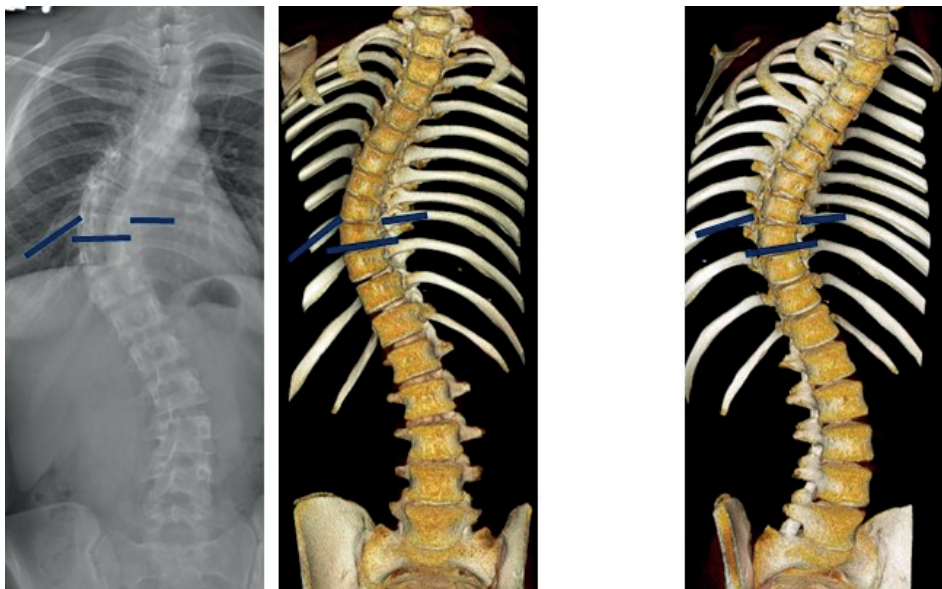

Figure 5. An asymmetry was seen between the concave and convex angle of the rib and the vertebra in 2D. However, on the 3D reconstructed true coronal view of the derotated apex, this apparent difference almost completely disappeared.

deformation and therefore, the 2D RVAD remains a useful measurement to indicate the severity of the overall 3D apical deformity based on a standard 2D radiographic assessment.[39] Within similar Cobb angle measurements, more pronounced apical rotation and lordosis indicate a more severe deformity with worse prognosis.

Chapter 9. Upright, Prone, and Supine Spinal Morphology and Alignment in Adolescent Idiopathic Scoliosis

Does the 3D morphology of the AIS spine differ between upright, prone and supine position? In addition to the PA and lateral upright radiographs, supine or prone MRI and CT is frequently used. Additional to the radiation exposure, another drawback of the radiography is that the 3D deformity is hardly appreciated on plain films. CT scanning is still considered the gold standard for providing accurate and detailed information on bony anatomy and can give accurate 3D reconstructions of complex deformities, but carries even more radiation exposure and is performed non-weight bearing, and MRI is safe, provides accurate information on the spinal cord and other soft tissues, but is also (usually) performed in a non-weight bearing manner, and is known to show less detail of bony structures.[43] It is important to define where these techniques overlap, in order to reduce costs and radiation exposure.

An underestimation of the deformation was observed in supine and prone position as compared to the upright position: the thoracic and (thoraco)lumbar Cobb angles 12-14° and 9-11° respectively, the thoracic kyphosis and lumbar lordosis 3-9° and 3-5° and the thoracic and lumbar apical vertebral rotation 2-5° and 3-5°. Additionally, good and excellent linear correlations were observed for the morphological parameters in the coronal (ICC≥0.964), sagittal (ICC≥0.854) and transverse (ICC≥0.815) plane between the imaging modalities. Therefore, the information obtained by these different modalities, overlaps partly. Findings of this study suggest that severity of scoliotic deformity in AIS patients can be largely represented by different imaging modalities despite the differences in body position.

Chapter 10. Spinous Processes and Transverse Processes Measurements of the Scoliotic Spine and their Relation to the Cobb angle: a CT Based Study

What are the differences in curve severity measurements, based on different anatomical vertebral structures as used in ultrasound of the spine?

A number of authors attempts to visualize the 3D character of the scoliotic curve without ionizing radiation in the upright position, using ultrasound imaging and surface topography, as well as standing low-dose biplanar radiography became available and can be utilized for 3D reconstructions.[59, 61-71] Ultrasound visualizes the spine in a plane more posterior than the vertebral endplates and, therefore, different anatomical landmarks have been described as an alternative for the Cobb angle, such as the spinous processes

(SP) and the transverse processes (TP).[62, 67, 69] To use the SP and TP as landmarks to measure the curve severity, the exact relation between the SP and TP and the vertebral endplates had to be clarified.

Using 3D reconstructed high-resolution CT scans and software developed for the purpose of the study, the relationship between the different landmarks was described in chapter 10. A moderate to very good correlation was seen between the SP angle and Cobb angle (thoracic R^2=0.80 and (thoraco)lumbar R^2=0.62) and even a better correlation between the TP angle and Cobb angle (thoracic R^2=0.84 and (thoraco)lumbar R^2=0.84). Therefore, the TPs and SPs are reliable to measure the curve severity. When comparing the reliability of the anatomical landmark angles to the Cobb angle, the results indicate that the TP angle qualifies slightly better for clinical use in ultrasound measurements.

Chapter 11. A Reliability and Validity Study for Different Coronal Angles using Ultrasound Imaging in Adolescent Idiopathic Scoliosis

Does the ultrasound image of AIS patients correspond with the curvatures on radiographs?
Several *in-vitro* and *in-vivo* studies compared the ultrasound spine deformity measurements to the traditional Cobb angle on radiographs in AIS.[62-67, 69, 70] In chapter 11, the reliability and validity of different ultrasound measurement techniques for coronal curve severity were described in 38 AIS patients (Figure 6). The coronal ultrasound angles were 15-37% lower as compared to the radiologic Cobb angles, as expected, since the ultrasound measurements are based on structures located more posteriorly than the vertebral body, on which the Cobb angle is based and this leads to a different projection of the complex 3D deformity.[11, 229, 233] Additionally, excellent linear correlations were
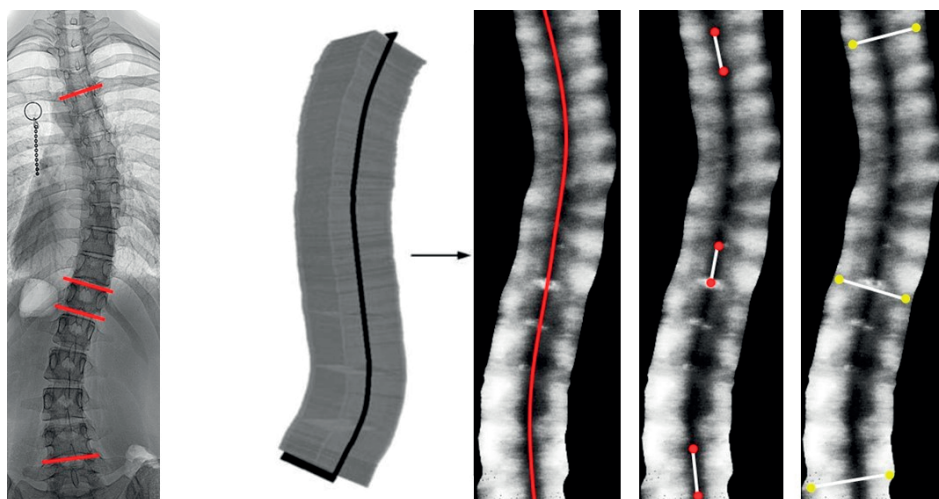

Figure 6. In chapter 11, the Cobb angles, as measured on the radiographs, were compared with the different ultrasound angles, as measured on the reconstructed coronal image.

observed between the ultrasound angles and Cobb angles (R^2 ≥0.970) and the mean absolute difference of the ultrasound measurements was below 5°, without significant difference between the different ultrasound measurements. Last, the intraclass correlation coefficients showed very reliable measurements and corresponded with the ICC of the traditional Cobb angle (range ICC 0.83–0.99), as described in a review by Langensiepen et al.[234] The data showed that the ultrasound angles are reliable and valid to measure the severity of the coronal curve and the relationship between the ultrasound angles and the Cobb angles can be expressed by the equations as given in chapter 11.

Therapeutic consequences for AIS

In the previous chapters the 3D aspects of AIS has been described. If the curves progress beyond a certain threshold, corrective scoliosis surgery may become necessary.[3, 76] An anterior or posterior approach to the spine can be used for this type of surgery.[102-108] The 3D surgical outcomes, as well as the patient-reported outcomes over time after anterior or posterior spinal fusion in AIS are described, that may contribute to a knowledge-based choice of surgical method for the individual patient with scoliosis.[253, 254]

Chapter 12. Surgical Outcomes of Anterior versus Posterior Fusion in Lenke Type 1 Adolescent Idiopathic Scoliosis

What are the differences in 2D, 3D and patient reported outcomes between the anterior and posterior fusion of AIS?

In total 53 Lenke curve type 1 AIS patients were analyzed (26 in the anterior cohort and 27 in the posterior cohort). The radiographs were available before surgery, after surgery and after two years follow-up, whereas the low-dose CT scans were only available before and after surgery, as part of the standard care in these centers. Using the anterior approach, fewer vertebrae were instrumented in a shorter surgery time and with less blood loss compared with the posterior approach. However, using the posterior approach, better coronal curve correction was achieved based on radiographs. In both cohorts, the (un-instrumented) secondary lumbar curves were also reduced, without any statistically significant difference between the cohorts, indicating that correction of the primary curve is sufficient to reduce the lumbar secondary curves as well in Lenke 1 deformities (Figure 7). Coronal correction remained unchanged during the follow-up time in the anterior cohort, whereas a small deterioration was seen in the posterior cohort, from 13±6° to 16±6° (p=0.004). The patients scored well on the SRS-22 and EQ-5D-3L questionnaires, without significant differences between the anterior and posterior cohorts postoperatively.

Previous authors reported that thoracic kyphosis is not restored very well using the posterior approach, in contrast to the anterior spinal fusion.[242, 250, 254] In chapter 12, however, is described that the anterior approach resulted in an increase in kyphosis of
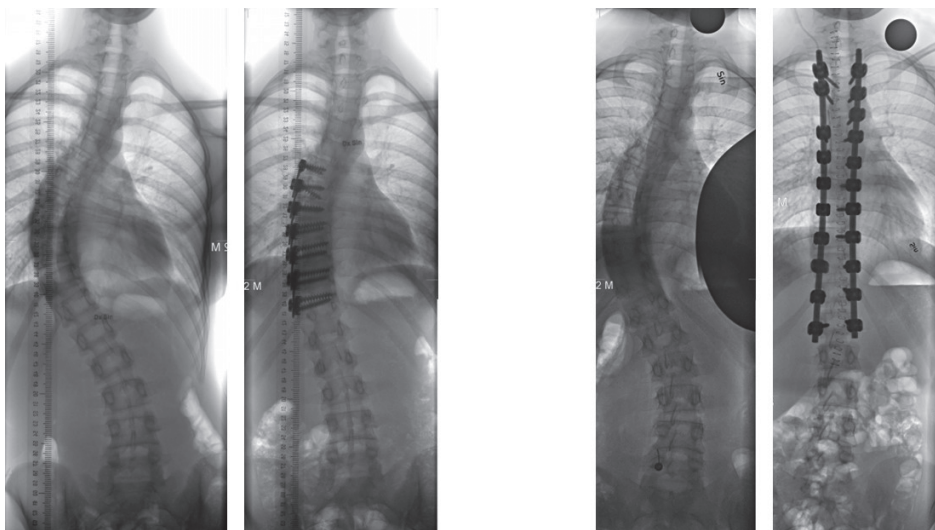
Figure 7. Pre- and postoperative radiographs of two Lenke curve type 1 patients, that were operated with an anterior or posterior approach.

8±9°, whereas this increase was only 2±9° in the posterior cohort, without significant difference, based on radiographs, and using 3D CT scans, no significant differences were seen either between the approaches regarding sagittal plane restoration and between the patient reported outcome measurements. As measured on the CT scans, both approaches resulted in a significant restoration, a kyphogenic effect. Each option, however, has specific advantages and challenges that the surgeon must acknowledge when treating each patient. The choice of surgical approach depends on these various factors, as well as the experience of the surgeon.

Chapter 13. A CT Based Guideline for Pedicle Screw Placement in Adolescent Idiopathic Scoliosis

What is the intra-operative 3D pedicle orientation for pedicle screw placement in AIS?

Regarding the anterior and posterior approach, the posterior approach is used in most cases, especially after the introduction of pedicle screw fixation.[245-248] The complication rate related to the pedicle screw placement such as nerve root or spinal cord compression, pseudarthrosis, and major vessel injury is relatively low (between 0 and 1%), however, the rate of screw misplacement in the thoracic region varies between 5.7 and 50%.[114, 247, 260-265] Previous authors provided already accurate descriptions of pedicle morphology in AIS as the angle between the convex and concave pedicle or as the angle between the pedicle and the vertebral body axis. [90, 145, 146, 148, 184, 185, 190, 196, 197, 266] However, pedicle orientation throughout the curve in AIS, as compared to the neutral

axis or operating table, remained undetermined so far in AIS, that is important to reduce the misplacement rate.

In chapter 13, the pedicle orientation and morphology was accurately described, in moderate to severe primary thoracic AIS curves, as compared to the neutral axis (perpendicular to the operating table), as well as the lamina, using high resolution CT scans. As compared to the neutral anterior-posterior axis, the mean apical transverse pedicle angle was 14.3º (95%CI: 12.0 – 16.6) on the convex side and 30.4º (95%CI: 28.1 – 32.8) on the concave side and decreased towards the junction zone, increased in curves with a higher Cobb angle and varies along the position of the vertebra within the curve. The sagittal pedicle angle as well as the angles between the pedicle and the lamina differs along the curve as well. The transverse and sagittal pedicle angles, as relative to the operating table and laminae, in different curve severities, as described in chapter 12, could serve as a gross guideline for orientation of the pedicle direction for pedicle screw placement in AIS.

GENERAL CONCLUSIONS AND FUTURE PERSPECTIVES

AIS is a complex 3D deformity, with severe consequences for the patient in terms of self-image, pain and treatment options.[1, 2] Understanding of the true morphology is important to better understand its etiopathogenesis, correctly interpret standard imaging, as well as adequately plan the correction of the curves. The consequences of the 3D pathoanatomy of AIS are described in this thesis.

The normal human posture and locomotion is unique and differs from other vertebrates, because of its unique sagittal spinopelvic alignment: a lordotic angulation between the ischial and iliac bones (pelvic lordosis), with a lordotic lumbar spine on top of that.[15-19] This unique biomechanical load on the human spine leads to a reduction of rotational stiffness of the posteriorly inclined spinal segments.[5, 7] The sagittal pelvic morphology, as expressed by the PI, and sagittal spinal alignment differ between non-scoliotic controls and AIS patients with different curve types, indicating that differences in spinal biomechanics as a result of different spinopelvic alignment could play a role in the onset and progression AIS.[136]

Once a scoliosis progresses, the apices rotate away from its original position around a longitudinal rotation axis that is localized far posterior to the spine and this axial rotation is accompanied by a smaller amount of intravertebral axial rotation and local mechanical torsion, increasing towards the apical region, as described in this thesis. The axial rotation of the curve leads to regional latero-flexion of the spinal column that is longer anteriorly than posteriorly at the apex.[47, 51] The anterior spinal column has for a long time been known to be longer than the posterior side.[2, 46-50] This anterior-posterior

length discrepancy of the primary and secondary scoliotic curves is caused by relative anterior lengthening as well as relative posterior shortening, with the facet joints acting as the fulcrum.[44, 50, 272] Our studies have shown that this phenomenon mainly occurs in the discs, and predominantly around the apex of the curve.[44, 50, 272, 273]

In more detail, the vertebral bodies and intervertebral discs at the apex become wedged in the sagittal and coronal plane and rotated in the transverse plane. Both, vertebral and disc morphology, contribute to this regional spinal deformation, but it was shown that the intervertebral discs contribute three to four times more than the vertebral bodies in severe AIS cases.[44, 50, 272, 273]

So, the 3D deformation of the spine in AIS is predominantly localized in the discs (as a secondary phenomenon to axial rotation) and hardly in the vertebral bodies (as a result of active growth). Additionally, non-idiopathic, neuromuscular scoliosis demonstrate the same pattern of 3D deformation with relative anterior spinal overgrowth and torsion on the different structures as idiopathic scoliosis.[273] It therefore does not seem to be part of the etiology of 'idiopathic' scoliosis, but rather its result. As consequence for the etio-pathogenesis, the extensive data on the 3D morphology of AIS as provided in this thesis suggests a more generalized passive mechanism that results in the 3D curvature, and that is not the consequence of a local process such as active bony anterior overgrowth or asymmetrical pedicle growth. The etiopathogenic consequence of the 3D deformity is that it probably is not an active but a passive phenomenon, that is not exclusive to 'idiopathic' scoliosis. Future research has to reveal the role of the rotational stability of the disc and sagittal spinal alignment during growth of AIS patients before the onset of the disease in the etiopathogenesis of AIS.

The RVAD, the differences in convex and concave rib vertebral angle (Metha's angle), has been presented as a predictor of curve progression, mostly in infantile curves but also in other types of scoliosis.[41] We showed that there is no actual asymmetry in the way the ribs are attached to the spine.[274] The observed asymmetry is the result of the projection on the coronal film of the 3D deformity, when reconstructed in the true coronal plane, no asymmetry persisted (Figure 5).[274] The more the apex of the curve is rotated and lordotic, the higher the RVAD becomes.[274] The RVAD therefore remains a valid prognostic measurement, because it provides information on the severity of the apical deformity.

In terms of diagnostic consequences, the ultrasound 3D imaging modality provides a favorable future perspective. Radiation exposure is a big issue for patients with AIS.[12, 60] 3D Ultrasound is a radiation-free modality, that could be used for imaging of patients with AIS.[62-67, 69, 70] Coronal ultrasound angles are based on different landmarks than the traditional Cobb angle measurement and cannot represent the same angle values. In this thesis, excellent correlations between the ultrasound and Cobb measurements were described for the TP as well as SP.[224] Therefore, the severity of the deformity in AIS

patients can be assessed by ultrasound imaging, avoiding hazardous ionizing radiation and also opens possibilities for screening. For clinical use, ultrasound imaging could be used during the follow-up, but since the ultrasound imaging is not able to visualize the vertebral bodies, at present, radiation is still necessary for diagnosis (e.g. congenital scoliosis) and preoperative planning, if desired. The potential possibilities of 3D ultrasound are dynamic imaging for assessment of curve flexibility in different dimensions, detection of intradural abnormalities (e.g. syringomyelia, Chiari malformation and spina bifida) and 'non-invasive' measurement of progression of the scoliotic curves, as well as screening of children at risk for development of AIS. These are part of ongoing studies. Especially the possibilities for population screening studies, to determine the normal spinal development in growing children, that could result in different spinal deformities creates new opportunities. Additionally, further research should investigate the possibilities of MRI to reproduce the contours of the osseous parts without using harmful radiation.

Treatment of scoliosis has to restore the coronal, sagittal and transverse alignment and the consequences for the patient.[3, 76] As described in this thesis, the anterior and posterior approaches restore the coronal curve, have a kyphogenic effect and correct the axial rotation. Therefore, the choice of surgical approach depends mostly on the experience of the surgeon. Additionally, the 3D morphology of the AIS curves results in a pedicle orientation that depends on several parameters, such as the curve severity and the level of the vertebra within the curve. In this thesis, the transverse and sagittal pedicle angles, as relative to the operating table and laminae, in different curve severities in, as described, could serve as a gross guideline for pedicle screw placement in AIS.

Further knowledge of the 3D morphology, will give more insight in the pathogenesis of AIS and possible risk factors for the onset and progression of AIS, leading to a primary treatment of AIS, instead of restoration of the curve, to decrease the severe consequences for the patient – in terms of self-image, pain and treatment options – as well as the economic burden for the society.

Nederlandse samenvatting

Scoliose is een driedimensionale (3D) rotatievervorming van de wervelkolom en romp met ernstige gevolgen voor de patiënt, zoals een verminderd zelfbeeld en pijn.[1, 2] Indien er sprake is van een ernstige scoliose is invasieve behandeling nodig.[1, 2] De *Scoliosis Research Society* definieert scoliose als een laterale kromming van de wervelkolom van ten minste 10 graden (Cobb hoek) in het coronale (voor- achterwaartse) vlak. Echter, bestaat scoliose uit complexe veranderingen in drie vlakken.[1, 29, 89] Er zijn verschillende aandoeningen bekend die scoliose veroorzaken, zoals congenitale afwijkingen, neuromusculaire aandoeningen en metabole stoornissen. In de meeste gevallen wordt er echter geen specifieke oorzaak gevonden en daarom wordt dit type 'idiopathisch' genoemd. Het meest voorkomende type, de adolescente idiopathische scoliose (AIS), ontwikkelt zich bij vooraf gezonde kinderen, meestal meisjes, tijdens de vroege puberteit en betreft 1-4% van de adolescenten.[3] De behandeling, indien nodig, is zeer invasief voor de patiënt en bestaat uit een brace die een groot aantal uren per dag moet worden gedragen, of een uitgebreide chirurgische procedure, met ernstige risico's voor de patiënt, zoals neurologische schade. Naast de enorme individuele impact, zowel fysiek als psychisch, heeft scoliose grote gevolgen voor de samenleving door de hoge kosten van de behandeling.[3, 4]

Ondanks uitgebreid onderzoek en recente studies waarin de rol van de menselijke sagittale balans op de rotatiestabiliteit van de wervelkolom is onderzocht, is de exacte etiologie van idiopathische scoliose nog steeds onduidelijk.[3, 5-8] Voor de opsporing van progressieve scoliose en voor klinische besluitvorming is follow-up vereist door middel van röntgenfoto's. Dit resulteert in een hoge blootstelling aan schadelijke straling tijdens de kritieke jaren van de groei en ontwikkeling die, mogelijk in combinatie met enige genetische aanleg, resulteert in een vijfmaal hogere kans op het ontwikkelen van kanker.[11, 12] Een betere kennis van de oorzaak en de 3D morfologie van AIS is belangrijk voor het begrijpen van de etiopathogenese, identificatie van prognostische factoren, vermindering van blootstelling aan straling en voor de ontwikkeling van eerdere en potentieel minder invasieve behandelingsopties.

OPZET VAN DIT PROEFSCHRIFT

In **hoofdstuk 1** zijn de unieke eigenschappen van de rechtopstaande wervelkolom van de mens en de verschillende morfologische kenmerken van AIS uiteengezet. Daarnaast zijn de onderzoeksdoelen per hoofdstuk beschreven. Het proefschrift is onderverdeeld in drie delen. In deel 1 worden de verschillende biomechanische aspecten in de ontstaanswijze en het verdere beloop van AIS besproken. In deel 2 wordt ingegaan op de beeldvorming van AIS en het reduceren van straling en in deel 3 worden de chirurgische behandelopties besproken.

Etiologie en 3D patho-anatomie van AIS

De wijze waarop mensen volledig rechtop lopen is uniek en speelt een belangrijke rol in het ontstaan en de progressie van idiopathische scoliose. De houding van de mens verschilt namelijk van andere dieren, voornamelijk doordat de mens drie goed ontwikkelde lordoses heeft: één tussen het os ilium en os ischii (de bekkenlordose), één in de lumbale regio van de wervelkolom en één in de cervicale regio.[15, 118] De lordosis, in combinatie met het vermogen om de heupen en knieën tegelijkertijd volledig te strekken, maakt de mens de enige diersoort waarbij het lichaamszwaartepunt zich recht boven het bekken bevindt, in plaats van voor het bekken, zoals bij andere diersoorten.[14, 15, 116, 117] Het is eerder aangetoond dat de unieke houding van de mens zorgt voor een veranderde biomechanische belasting op de wervelkolom en leidt tot een vermindering van de rotatiestabiliteit van de wervels die naar achter staan gekanteld.[5, 7, 8, 120] Dit kan uiteindelijk leiden tot scoliose.

In **hoofdstuk 2** worden antwoorden gegeven op de relevante vragen over de etiopathogenese van AIS. Schlösser et al. toonden aan dat de morfologie van de wervelkolom en het bekken veranderen tijdens de groei, en dat vóór en tijdens de piek van de groeispurt een groter aantal wervels achterwaarts gekanteld staat, in vergelijking met de periode na de groeispurt.[14, 23, 130, 131] Op het hoogtepunt van de groeispurt staat de wervelkolom van meisjes meer naar achter gekanteld dan bij jongens. Dit suggereert dat bij meisjes rond de piek van de groeispurt de wervelkolom onderhevig is aan grotere, posterieur gerichte schuifkrachten en dus rotatoir instabieler is. Dit verklaart mogelijk waarom AIS vaker voorkomt bij meisjes dan bij jongens. Daarnaast zijn de meeste thoracale wervels naar achter gekanteld in thoracale scoliose, terwijl in (thoraco)lumbale scoliose, de naar achter gekantelde wervels zich lager in de wervelkolom bevonden, wat een rol kan spelen in de ontwikkeling van de verschillende type bochten.

AIS presenteert zich meestal als een primaire rechts convexe thoracale bocht met twee links convexe compensatoire bochten; hoog-thoracaal en (thoraco)lumbaal.[40, 137] In eerdere studies is beschreven dat de anterieure zijde van de wervelkolom langer is dan de posterieure zijde.[47, 52-54] Schlösser et al. beschreven dat alle AIS bochten, structureel en niet-structureel, primair en compensatoir, thoracaal en (thoraco)lumbaal, een uniform patroon volgen gekenmerkt door meer deformiteit in de tussenwervelschrijven dan in de wervellichamen.[44, 50] Hierbij is voornamelijk de apex van de bocht aangedaan en komen de overgangszones tussen de bochten globaal overeen met de niet-aangedane wervelkolom.[44, 50] Dit is in tegenspraak met de theorie dat de anterieure overgroei het resultaat is van overmatige actieve botgroei.

Het bekken is, als basis van de wervelkolom, zeer belangrijk voor de stand van de wervelkolom. De stand en morfologie van het bekken ten opzichte van de wervelkolom, waaronder de bekkenlordose, variëren tussen individuen, leeftijden alsmede tussen verschillende pathologieën.[7, 47, 77] Veel van deze studies zijn gebaseerd op conventionele

röntgenfoto's.[77, 133] In 2012 beschreven Vrtovec et al. de verschillen in 3D bekkenincidentie (*pelvic incidence*) tussen AIS patiënten en kinderen zonder scoliose met behulp van CT scans. Hierin toonden zij aan dat deze 3D methode een stuk betrouwbaarder en accurater is dan traditionele metingen op twee-dimensionale (2D) röntgenfoto's.[82, 87] In **hoofdstuk 3** is, met behulp van deze 3D meetmethode, beschreven dat de bekkenincidentie verschilt tussen patiënten met (thoraco)lumbale scoliose en kinderen zonder scoliose, waarbij deze waarde niet verschilt tussen patiënten met een thoracale scoliose en kinderen zonder scoliose. Dit suggereert een relatie tussen de morfologie van het bekken en de wervelkolom en de ontwikkeling van verschillende type idiopathische scoliose.

In AIS roteren de apicale wervels weg van de middenlijn.[2, 46] De rotatie van de wervels maakt deel uit van het, onbekende, pathogenetische mechanisme dat leidt tot scoliose. Inzicht in het rotatiemechanisme van de verschillende wervels binnen scoliose en of de rotatie hoofdzakelijk lokaal is (gelegen binnen de wervel: intravertebrale rotatie en lokale mechanische torsie), of segmentaal is (vertebrale axiale rotatie), is belangrijk om de mogelijke mechanismen van de ontwikkeling van scoliose te begrijpen. In **hoofdstuk 4** is beschreven dat de longitudinale rotatie-as van de apicale wervels posterieur van de wervelkolom gelegen is. De afstand tussen de wervelkolom en de longitudinale rotatie-as, verschilt per niveau binnen de wervelkolom: als er veel rotatie is, zoals in de apicale wervel, ligt de rotatie-as dichter bij de wervel, indien er minder rotatie is ligt de rotatie-as verder van de wervel. Daarnaast was de axiale rotatie van de wervel groter dan de rotatie en torsie in de wervel.

In eerdere studies is de rotatie en asymmetrie in het transversale vlak van de wervels beschreven.[1, 2, 29, 30, 44, 46, 89, 90, 184-187] De rol van deze asymmetrie blijft onduidelijk, net zoals de vraag of dit een actief asymmetrisch groeipatroon betreft of een passief gevolg is van de asymmetrische biomechanische belasting zoals uitgelegd door de wet van Hueter-Volkmann en Wolff.[188, 189, 192, 193] Experimentele studies hebben aangetoond dat asymmetrische groei van de neurocentrale kraakbeenderen kan leiden tot asymmetrische groei van de wervel en rotatie kan induceren.[144, 194, 195] Echter, zijn de neurocentrale kraakbeenderen al gesloten voor de leeftijd van acht jaar.[142] Dit betekent dat als de asymmetrie een gevolg is van de asymmetrische groei door het neurocentrale kraakbeen, de asymmetrie al voor de adolescente leeftijd aanwezig moet zijn, wat het minder waarschijnlijk maakt dat de asymmetrie het gevolg is van actieve asymmetrische groei.[142, 144, 196]

De exacte transversale morfologie, zoals beschreven in **hoofdstuk 5** door middel van CT scans, is zowel belangrijk voor het begrijpen van de etiologie, als voor het plaatsen van de pedikelschroeven tijdens de chirurgische behandeling. De wervels en pedikels in AIS patiënten waren asymmetrischer dan in de niet-scoliotische wervelkolom. Echter, was de asymmetrie van de wervels en pedikels voornamelijk rond de apex gelokaliseerd, waarbij de overgangszone minder asymmetrisch was en overeenkwam met de normale

wervelkolom. Over het algemeen waren de concave pedikels dunner en langer dan de convexe pedikels, maar er werd geen correlatie aangetoond tussen de asymmetrie van de wervels en pedikels en de mate van scoliose. Deze bevindingen suggereren dat de asymmetrie niet het gevolg is van een actieve groeiafwijkingen, maar een passief gevolg zijn van het scoliosemechanisme.

In 1952 beschreef Somerville scoliose als een geroteerde lordose waarbij de voorkant langer is dan de achterkant, in plaats van een rechte kyphose.[46] Deze anterieure over-groei is in veel studies genoemd als een oorzaak van AIS.[47, 52-55] Daarnaast is beschreven dat de anterieure overgroei alleen rond de apex van de bocht aanwezig is en gelijk is in alle AIS bochten, in primaire en secundaire bochten en thoracale en (thoraco)lumbale scoliose.[44, 50] In de eerdere studies is de anterieure overgroei alleen onderzocht in AIS pa-tiënten. Indien dezelfde anterieure overgroei wordt gezien in scoliose met een bekende oorzaak, zoals neuromusculaire scoliose, is de anterieure overgroei meer waarschijnlijk een gevolg dan de oorzaak van de scoliose. In **hoofdstuk 6** is beschreven dat de ante-rieure overgroei niet specifiek is voor AIS, maar hetzelfde patroon wordt gezien bij neu-romusculaire scoliose, waarbij de deformiteit voornamelijk in de tussenwervelschijven werd gezien en niet in de wervellichamen zelf. Daarnaast neemt de anterieure overgroei lineair toe met de mate van scoliose. Dit toont aan dat anterieure overgroei secundair aan het scoliosemechanisme is, in plaats van de oorzaak van idiopathische scoliose.

De anterieure overgroei is beschreven als de lengtediscrepantie tussen de anterieure en posterieure zijde van de wervellichamen en tussenwervelschrijven. Hierin zijn de posterieure structuren, zoals de wervelboog, niet meegenomen, wat belangrijk is om onderscheid te maken tussen relatieve anterieure verlenging of relatieve posterieure verkorting. In **hoofdstuk 7** is de anterieure overgroei, inclusief de posterieure struc-turen, beschreven door middel van CT scans van AIS patiënten en kinderen zonder scoliose. Deze resultaten toonden aan dat de discrepantie tussen de anterieure en posterieure lengte een gevolg is van zowel anterieure verlenging, als posterieure ver-korting. Echter, werden de verschillen alleen waargenomen in de non-ossale structuren, waarbij de ossale structuren niet in lengte verschilden tussen de AIS wervelkolom en de niet-scoliotische wervelkolom.

Beeldvorming van AIS

Voor de diagnose, follow-up en klinische besluitvorming van AIS worden standaard staande röntgenfoto's gemaakt.[3, 11, 57] 2D röntgenfoto's zijn niet in staat om de 3D ei-genschappen van scoliose volledig in beeld te brengen. Om deze reden introduceerde Stagnara *le plan d'election*, een geroteerd beeld om het ware coronale profiel van de apicale segmenten van de bocht in beeld te brengen.[39] In 1972 introduceerde Mehta de RVAD (*rib vertebra angle difference*), als een voorspeller voor de progressie van de bocht.[41] De bocht heeft een hoog risico op progressie als de RVAD, het verschil tussen de

rib-wervelhoek aan de linker en rechter zijde, groter is dan 20°. Er zijn verschillende theorieën over de RVAD; er is beschreven dat de RVAD een resultaat is van asymmetrische krachten op de ribbenkast, of dat de RVAD het resultaat is van een 'hangende' rib, door verminderde stabiliteit van de wervelkolom en ribbenkast.[210, 211] [92, 93, 95, 97, 98, 210, 211] Echter, is de beschreven asymmetrie gebaseerd op 2D beeldvorming, waarbij geen rekening is gehouden met de complexe apicale 3D morfologie, waarbij rotatie en apicale lordose een belangrijke rol spelen.[91, 93, 94, 96-99, 101] Hierdoor is het de vraag of het ware asymmetrie betreft – en dus ook aanwezig in 3D – of dat de asymmetrie het resultaat is van een vereenvoudigde 2D weergave van een 3D vervorming.

In **hoofdstuk 8** is de RVAD gemeten op 2D beeldvorming (röntgenfoto en 2D reconstructie van een CT scan) en 3D beeldvorming (CT scan). De gemiddelde 2D RVAD was 25°, maar in 3D vervaagde dit verschil vrijwel volledig (3.1°). Dit geeft aan dat de 2D RVAD is gebaseerd op een vereenvoudigde 2D weergave van een 3D deformiteit en is niet gebaseerd op werkelijke asymmetrie. De 2D RVAD correleerde wel goed met de Cobb hoek, de rotatie en de mate van apicale lordose en is daardoor een goede 2D weerspiegeling van de 3D deformiteit en een bruikbare meting om de ernst van de 3D deformiteit te beoordelen.

Naast de voor-achterwaartse en zijwaartse röntgenfoto's, wordt vaak een liggende MRI of CT scan gemaakt om de ossale en non-ossale structuren beter in beeld te brengen.[3, 58] Door de beeldvorming worden de AIS patiënten blootgesteld aan ioniserende straling, wat leidt tot een negen tot tien keer verhoogde blootstelling dan de algemene bevolking en de AIS patiënten hebben een verhoogde kans op het ontwikkelen van kanker op latere leeftijd.[12, 60] MRI is niet-ioniserend, maar is kostbaar, tijdrovend, vaak in liggende positie vervaardigd en de ossale contouren zijn helaas nog niet goed in beeld te brengen. Om het aantal röntgenfoto's en scans te reduceren en daarmee de straling en de kosten te reduceren, is het belangrijk om te bepalen in hoeverre de morfologie overeenkomt tussen de verschillende houdingen en beeldvormingsmethoden. In **hoofdstuk 9** wordt de morfologie van de scoliose vergeleken tussen de staande röntgenfoto's, de CT scan in buikligging en de MRI in rugligging. Zowel de thoracale en (thoraco)lumbale Cobb hoeken, als de thoracale kyphose en lumbale lordose waren lager in liggende positie (CT en MRI) dan op de staande röntgenfoto's. Desondanks correleerden de hoeken wel goed onderling. Daarom is het mogelijk om de te verwachten hoeken te berekenen vanuit een andere positie, met de formules zoals beschreven in hoofdstuk 8, wat kan leiden tot een reductie van de beeldvorming.

Naast de traditionele beeldvormingsmethoden is er steeds meer aandacht voor stralingsvrije methoden, zoals echografie en oppervlaktetopografie.[61-71] In 1989 beschreven Suzuki et al. het gebruik van echografie al om de wervelboog af te beelden, waarna meerdere studies volgden om de wervelkolom af te beelden met echografie.[61-67, 69, 70] Met echografie is het, vooralsnog, niet mogelijk om de wervellichamen af te beelden,

maar alleen posterieure structuren, zoals de wervelboog. Deze structuren worden daarom gebruikt om de ernst van de scoliose te meten, in plaats gebruik te maken van de dek- en sluitplaten van de wervellichamen, zoals op een röntgenfoto.[62, 67, 69] Echter, is de exacte relatie tussen de posterieure structuren en de dek- en sluitplaten van de wervellichamen niet bekend. Met behulp van 3D reconstructies van hoge-resolutie CT scans en software speciaal ontwikkeld voor het doel van deze studie, is de relatie tussen de verschillende oriëntatiepunten beschreven in **hoofdstuk 10**. Ondanks een absoluut verschil in de gemeten hoeken langs de verschillende structuren, werden redelijke tot zeer goede correlaties aangetoond tussen de verschillende structuren. Daarom zijn de posterieure elementen geschikt om de ernst van scoliose te bepalen. Dit kan vervolgens worden gebruikt bij de echografische beeldvorming.

In **hoofdstuk 11** is de betrouwbaarheid en validiteit onderzocht om de ernst van de scoliose te meten met verschillende echografische meetmethoden bij 38 AIS patiënten. De echografische hoeken in het coronale vlak waren 15-37% lager dan de Cobb hoek gemeten op de voor-achterwaartse röntgenfoto. Dit is zoals verwacht, aangezien de radiografische Cobb hoek is gebaseerd op de dek- en sluitplaten van de wervellichamen en de echografische hoeken gebaseerd zijn op structuren die meer posterieur liggen ten opzichte van het wervellichaam en leidt tot een andere projectie van de complexe 3D deformiteit. De echografische hoeken correleerden echter wel goed met de radiografische Cobb hoek en de echografische metingen bleken zeer betrouwbaar bij herhaaldelijke metingen. Door de valide en betrouwbare metingen kan de ernst van de bocht in het coronale vlak worden bepaald door middel van echografie.

Therapeutische gevolgen van AIS

In de voorgaande hoofdstukken zijn de 3D kenmerken van AIS beschreven. Als de bochten progressief zijn kan een operatie noodzakelijk zijn.[3, 76] Dit kan zowel middels een anterieure als een posterieure benadering van de wervelkolom.[102-108] In **hoofdstuk 12** zijn de 2D en 3D uitkomsten evenals de patiënt gerapporteerde uitkomsten beschreven van beide benaderingen. In totaal werden 53 AIS patiënten met een thoracale scoliose (Lenke type 1) geïncludeerd. Hiervan waren 26 via de anterieure benadering geopereerd en 27 via de posterieure benadering. Röntgenfoto's en CT scans waren voor en na de operatie gemaakt om de 2D en 3D parameters te meten. Middels de anterieure bandering werden minder wervels geïnstrumenteerd in een kortere operatietijd met minder bloedverlies. Terwijl in de posterieure groep een betere correctie van de scoliose werd gezien. In beide cohorten reduceerde ook de secundaire, niet geïnstrumenteerde, lumbale bocht. Dit toont aan dat correctie van de primaire bocht voldoende is om de lumbale secundaire bocht eveneens te reduceren. De patiënten in beide groepen scoorden postoperatief goed op de SRS-22 en EQ-5D-3L-vragenlijsten, zonder significante verschillen tussen beide benaderingen. Daarnaast zorgden beide benaderingen voor

herstel van de kyphose. Beide benaderingen corrigeren dus de scoliose in 3D met elk hun eigen specifieke kenmerken en uitkomsten, zoals beschreven in hoofdstuk 12. De keuze van de chirurgische benadering hangt af van deze verschillende factoren, evenals de ervaring van de chirurg.

In de meeste gevallen wordt gekozen voor een posterieure benadering, vooral sinds de introductie van pedikelschroeven.[245-248] Bij het plaatsen van de schroeven treden relatief weinig complicaties op (tussen 0 en 1%), zoals schade van de zenuwwortel of compressie van het ruggenmerg, pseudarthrose en vasculaire schade, maar de kans dat de schroef wordt misplaatst varieert tussen 5.7 en 50%, veelal gebaseerd op postoperatieve CT scans.[114, 247, 260-265] In eerdere studies is de pedikelmorfologie in AIS al uitgebreid beschreven, als de hoek tussen de convexe en concave pedikel of als de hoek tussen de pedikel en de as van het wervellichaam.[90, 145, 146, 148, 184, 185, 190, 196, 197, 266] De oriëntatie van de pedikel, ten opzichte van een neutrale as of de operatietafel is echter nog onbekend, wat van belang is om de kans op misplaatsing te verminderen. In **hoofdstuk 13** is de pedikelas beschreven ten opzichte van de operatietafel en de wervelboog. De pedikelas van elke wervel in de scoliose is beschreven in het transversale en sagittale vlak. De hoeken variëren per niveau in de bocht, nemen toe naar mate de ernst van de bocht toeneemt en verschillen tussen convex en concaaf.

Eindconclusies en toekomstperspectieven

AIS is een complexe 3D deformiteit. Kennis van de morfologie is van essentieel belang voor het begrijpen van de etiopathogenese, correcte interpretatie van de beeldvorming en het adequaat plannen van de behandeling, zoals beschreven in dit proefschrift.

De houding van de mens, onder andere mogelijk gemaakt door de bekkenlordose en lumbale lordose, verschilt van alle andere gewervelde dieren. Door deze unieke houding verschilt de mechanische belasting op de wervelkolom van andere dieren, wat leidt tot een vermindering van de rotatiestabiliteit. Het bekken, als basis van de wervelkolom, verschilt tussen patiënten met AIS en kinderen zonder scoliose, maar ook tussen verschillende type bochten.

Rond de apex zijn de wervellichamen en tussenwervelschijven vervormd, waarbij de overgangszone tussen de bochten in de scoliotische wervelkolom vrijwel geen vervorming laat zien. De 3D vervorming van de wervelkolom in AIS is voornamelijk gelokaliseerd in de tussenwervelschijven en in mindere mate in de wervellichamen en lijkt daarom meer een resultaat van de scoliose (als een secundair gevolg van de axiale rotatie), dan de oorzaak. De wervels draaien weg vanuit de middenlijn rond een as die achter de wervelkolom ligt. De axiale rotatie is hoger dan de intravertebrale rotatie en torsie, toenemend richting de apex. De axiale rotatie leidt tot een regionale lateroflexie van de wervelkolom, waardoor de voorzijde langer is dan de achterzijde. Deze discrepantie tussen de anterieure en posterieure lengte wordt veroorzaakt door zowel ante-

rieure verlenging als posterieure verkorting, met de facetgewrichten als het draaipunt. Dit is een gegeneraliseerd fenomeen dat in alle primaire en secundaire bochten wordt gezien, evenals in scoliose met bekende oorzaak, zoals neuromusculaire scoliose. Het lijkt daarom geen deel uit te maken van de etiologie van scoliose als oorzaak, maar is eerder het gevolg van het scoliosemechanisme. Onze conclusie is dat de 3D misvorming, inclusief anterieure overgroei, geen actief maar een passief fenomeen is, dat niet exclusief is voor idiopathische scoliose.

Verschillende factoren zijn beschreven om de progressie van de bocht te voorspellen, waaronder de hoek van Mehta (*RVAD*), het verschil in ribwervelhoek tussen de convexe en concave zijde. Deze asymmetrie tussen convex en concaaf is echter niet gebaseerd op ware asymmetrie, maar komt voort uit een 2D projectie van een 3D deformiteit, aangezien de asymmetrie zo goed als verdwijnt in 3D. Desondanks, geeft de RVAD een goede weerspiegeling van de ware 3D deformiteit.

In dit proefschrift bleken de echografische metingen uitstekend te correleren met de radiografische Cobb hoek. Hierdoor is echografie een potentieel alternatief voor röntgenfoto's om zo de blootstelling aan schadelijke ioniserende straling te verminderen en kan het in de kliniek worden gebruikt om de ernst van de bocht te meten in het coronale vlak. De verdere mogelijkheden van 3D echografie om informatie te verschaffen over het sagittale en transversale vlak, om afwijkingen te detecteren (zoals syringomyelie, Chiari-misvorming en spina bifida) en om de progressie van scoliose te meten, maken deel uit van nog lopend onderzoek. Bovendien biedt de echografie mogelijkheden voor screening op spinale aandoeningen.

Het doel van de behandeling van scoliose is om de deformiteit te reduceren in het coronale, sagittale en transversale vlak. Zoals beschreven in dit proefschrift, kan dit chirurgisch via een anterieure en posterieure benadering, waarbij in beide gevallen reductie optreedt van de deformiteit. Daarom hangt de keuze van de chirurgische benadering grotendeels af van de ervaring van de chirurg.

Verdere kennis van de 3D morfologie zal meer inzicht geven in de pathogenese van AIS en mogelijke risicofactoren voor het ontstaan en de progressie van AIS, leidend tot een primaire behandeling van AIS, in plaats van herstel van de bocht.

References

1. Nicoladoni C. Anatomie und mechanismus der skoliose. *In: Kocher, König, von Mikulicz, eds. Bibliotheca medica. Stuttgart, Germany: Verlag von erwin nagele.* 1904.

2. Roaf R. The basic anatomy of scoliosis. *J Bone Joint Surg Br.* 1966;48:786-792.

3. Cheng JC, Castelein RM, Chu WC, et al. Adolescent idiopathic scoliosis. *Nature reviews disease primers.* 2015;1:15030.

4. Roach JW, Mehlman CT, Sanders JO. "Does the outcome of adolescent idiopathic scoliosis surgery justify the rising cost of the procedures?". *J Pediatr Orthop.* 2011;31:S77-80.

5. Kouwenhoven JW, Smit TH, van der Veen AJ, et al. Effects of dorsal versus ventral shear loads on the rotational stability of the thoracic spine: A biomechanical porcine and human cadaveric study. *Spine (Phila Pa 1976).* 2007;32:2545-2550.

6. Castelein RM. Pre-existent rotation of the normal spine at different ages and its consequences for the scoliotic mechanism. *Stud Health Technol Inform.* 2012;176:20-25.

7. Castelein RM, van Dieen JH, Smit TH. The role of dorsal shear forces in the pathogenesis of adolescent idiopathic scoliosis--a hypothesis. *Med Hypotheses.* 2005;65:501-508.

8. Janssen MM, Kouwenhoven JW, Castelein RM. The role of posteriorly directed shear loads acting on a pre-rotated growing spine: A hypothesis on the pathogenesis of idiopathic scoliosis. *Stud Health Technol Inform.* 2010;158:112-117.

9. Burwell RG, Clark EM, Dangerfield PH, et al. Adolescent idiopathic scoliosis (AIS): A multifactorial cascade concept for pathogenesis and embryonic origin. *Scoliosis Spinal Disord.* 2016;11:8-016-0063-1. eCollection 2016.

10. Kouwenhoven JW, Castelein RM. The pathogenesis of adolescent idiopathic scoliosis: Review of the literature. *Spine (Phila Pa 1976).* 2008;33:2898-2908.

11. Cobb J. Outline for the study of scoliosis. *The American Academy of Orthopaedic Surgeons (2nd edn), Instructional Course Lectures.* 1948;5:261.

12. Simony A, Christensen SB, Jensen KE, et al. Incidence of cancer and infertility, in patients treated for adolescent idiopathic scoliosis 25 years prior. *Eur Spine J.* 2015;24:S740.

13. Janssen MM, de Wilde RF, Kouwenhoven JW, et al. Experimental animal models in scoliosis research: A review of the literature. *Spine J.* 2011;11:347-358.

14. Schlösser TP, Janssen MM, Vrtovec T, et al. Evolution of the ischio-iliac lordosis during natural growth and its relation with the pelvic incidence. *Eur Spine J.* 2014;23:1433-1441.

15. Washburn SL. The analysis of primate evolution with particular reference to the origin of man. *Cold Spring Harb Symp Quant Biol.* 1950;15:67-78.

16. Whitcome KK, Shapiro LJ, Lieberman DE. Fetal load and the evolution of lumbar lordosis in bipedal hominins. *Nature.* 2007;450:1075-1078.

17. Tardieu C, Bonneau N, Hecquet J, et al. How is sagittal balance acquired during bipedal gait acquisition? comparison of neonatal and adult pelves in three dimensions. evolutionary implications. *J Hum Evol.* 2013;65:209-222.

18. Kummer B. Biomechanical problems of upright posture. *Ann Anat.* 1992;174:33-39.

19. Hogervorst T, Bouma HW, de Vos J. Evolution of the hip and pelvis. *Acta Orthop Suppl.* 2009;80:1-39.

20. During J, Goudfrooij H, Keessen W, et al. Toward standards for posture. postural characteristics of the lower back system in normal and pathologic conditions. *Spine (Phila Pa 1976).* 1985;10:83-87.

21. Duval-Beaupere G, Schmidt C, Cosson P. A barycentremetric study of the sagittal shape of spine and pelvis: The conditions required for an economic standing position. *Ann Biomed Eng.* 1992;20:451-462.

22. White AA, Panjabi MM. *Clinical Biomechanics of the Spine*. 1st ed. Philadephia, Toronto, United States of America: J.B. Lippincott Company, 1978.

23. Schlösser TP, Vincken KL, Rogers K, et al. Natural sagittal spino-pelvic alignment in boys and girls before, at and after the adolescent growth spurt. *Eur Spine J*. 2015;24:1158-1167.

24. Willner S, Johnson B. Thoracic kyphosis and lumbar lordosis during the growth period in children. *Acta Paediatr Scand*. 1983;72:873-878.

25. Poussa MS, Heliovaara MM, Seitsamo JT, et al. Development of spinal posture in a cohort of children from the age of 11 to 22 years. *Eur Spine J*. 2005;14:738-742.

26. Ueno M, Takaso M, Nakazawa T, et al. A 5-year epidemiological study on the prevalence rate of idiopathic scoliosis in tokyo: School screening of more than 250,000 children. *J Orthop Sci*. 2011;16:1-6.

27. Lonstein JE. Adolescent idiopathic scoliosis. *Lancet*. 1994;344:1407-1412.

28. SRS Terminology Committee and Working Group on Spinal Classification Revised Glossary of Terms. Revised Glossary of Terms. Available at: http://www.srs.org/professionals/online-education-and-resources/glossary/revised-glossary-of-terms.

29. Adams W. Lateral curvature of the spine, external characters and morbid anatomy (lecture 4). Lectures on the pathology and treatment of lateral and other forms of curvature of the spine. *London: Churchill*. 1882:69-93.

30. Albert E. Zur anatomie der skoliose. *Wiener klinische Rundschau*. 1895;33:513-515.

31. Perdriolle R, Becchetti S, Vidal J, et al. Mechanical process and growth cartilages. essential factors in the progression of scoliosis. *Spine (Phila Pa 1976)*. 1993;18:343-349.

32. Will RE, Stokes IA, Qiu X, et al. Cobb angle progression in adolescent scoliosis begins at the intervertebral disc. *Spine (Phila Pa 1976)*. 2009;34:2782-2786.

33. Parent S, Labelle H, Skalli W, et al. Vertebral wedging characteristic changes in scoliotic spines. *Spine (Phila Pa 1976)*. 2004;29:E455-62.

34. Xiong B, Sevastik JA, Hedlund R, et al. Radiographic changes at the coronal plane in early scoliosis. *Spine (Phila Pa 1976)*. 1994;19:159-164.

35. Stokes IA, Aronsson DD. Disc and vertebral wedging in patients with progressive scoliosis. *J Spinal Disord*. 2001;14:317-322.

36. Stokes IA, Windisch L. Vertebral height growth predominates over intervertebral disc height growth in adolescents with scoliosis. *Spine (Phila Pa 1976)*. 2006;31:1600-1604.

37. Modi HN, Suh SW, Song HR, et al. Differential wedging of vertebral body and intervertebral disc in thoracic and lumbar spine in adolescent idiopathic scoliosis - A cross sectional study in 150 patients. *Scoliosis*. 2008;3:11-7161-3-11.

38. Xu HG, Qiu GX, Wang YP, et al. Imaging study of wedge changes in the vertebral bodies and intervertebral discs in adolescent idiopathic scoliosis. *Orthop Surg*. 2009;1:300-304.

39. Stagnara P, De Mauroy JC, Dran G, et al. Reciprocal angulation of vertebral bodies in a sagittal plane: Approach to references for the evaluation of kyphosis and lordosis. *Spine (Phila Pa 1976)*. 1982;7:335-342.

40. Lenke LG, Betz RR, Harms J, et al. Adolescent idiopathic scoliosis: A new classification to determine extent of spinal arthrodesis. *J Bone Joint Surg Am*. 2001;83-A:1169-1181.

41. Mehta MH. The rib-vertebra angle in the early diagnosis between resolving and progressive infantile scoliosis. *J Bone Joint Surg Br*. 1972;54:230-243.

42. Nash CL,Jr, Moe JH. A study of vertebral rotation. *J Bone Joint Surg Am*. 1969;51:223-229.

43. Glaser DA, Doan J, Newton PO. Comparison of 3Dimensional spinal reconstruction accuracy: Biplanar radiographs with EOS versus computed tomography. *Spine (Phila Pa 1976).* 2012;37:1391-1397.

44. Schlösser TP, van Stralen M, Brink RC, et al. Three-dimensional characterization of torsion and asymmetry of the intervertebral discs versus vertebral bodies in adolescent idiopathic scoliosis. *Spine (Phila Pa 1976).* 2014 Sep 1;39(19):E1159-66.

45. Grivas TB, Vasiliadis E, Malakasis M, et al. Intervertebral disc biomechanics in the pathogenesis of idiopathic scoliosis. *Stud Health Technol Inform.* 2006;123:80-83.

46. Somerville EW. Rotational lordosis; the development of single curve. *J Bone Joint Surg Br.* 1952;34-B:421-427.

47. Dickson RA, Lawton JO, Archer IA, et al. The pathogenesis of idiopathic scoliosis. biplanar spinal asymmetry. *J Bone Joint Surg Br.* 1984;66:8-15.

48. Willner S. A study of height, weight and menarche in girls with idiopathic structural scoliosis. *Acta Orthop Scand.* 1975;46:71-83.

49. Brink RC, Schlösser TP, Colo D, et al. Anterior spinal overgrowth is the result of the scoliotic mechanism and is located in the disc. *Spine (Phila Pa 1976).* 2017 Jun 1;42(11):818-822.

50. Schlösser TP, van Stralen M, Chu WC, et al. Anterior overgrowth in primary curves, compensatory curves and junctional segments in adolescent idiopathic scoliosis. *PLoS One.* 2016;11:e0160267.

51. Deacon P, Dickson RA. Vertebral shape in the median sagittal plane in idiopathic thoracic scoliosis. A study of true lateral radiographs in 150 patients. *Orthopedics.* 1987;10:893-895.

52. Guo X, Chau WW, Chan YL, et al. Relative anterior spinal overgrowth in adolescent idiopathic scoliosis. results of disproportionate endochondral-membranous bone growth. *J Bone Joint Surg Br.* 2003;85:1026-1031.

53. Chu WC, Lam WW, Chan YL, et al. Relative shortening and functional tethering of spinal cord in adolescent idiopathic scoliosis?: Study with multiplanar reformat magnetic resonance imaging and somatosensory evoked potential. *Spine (Phila Pa 1976).* 2006;31:E19-25.

54. Newell N, Grant CA, Keenan BE, et al. Quantifying progressive anterior overgrowth in the thoracic vertebrae of adolescent idiopathic scoliosis patients: A sequential magnetic resonance imaging study. *Spine (Phila Pa 1976).* 2016 Apr;41(7):E382-7.

55. Porter RW. Can a short spinal cord produce scoliosis? *Eur Spine J.* 2001;10:2-9.

56. Schlösser TP, Shah SA, Reichard SJ, et al. Differences in early sagittal plane alignment between thoracic and lumbar adolescent idiopathic scoliosis. *Spine J.* 2014;14:282-290.

57. Brooks HL, Azen SP, Gerberg E, et al. Scoliosis: A prospective epidemiological study. *J Bone Joint Surg Am.* 1975;57:968-972.

58. Brink R, Colo C, Schlösser T, et al. Upright, prone and supine spinal morphology and alignment in adolescent idiopathic scoliosis. *Scoliosis and Spinal Disorders.* 2017 Feb 22;12:6.

59. Newton PO, Khandwala Y, Bartley CE, et al. New EOS imaging protocol allows a substantial reduction in radiation exposure for scoliosis patients. *Spine Deform.* 2016;4:138-144.

60. Presciutti SM, Karukanda T, Lee M. Management decisions for adolescent idiopathic scoliosis significantly affect patient radiation exposure. *Spine J.* 2014;14:1984-1990.

61. Suzuki S, Yamamuro T, Shikata J, et al. Ultrasound measurement of vertebral rotation in idiopathic scoliosis. *J Bone Joint Surg.* 1989;2:71-B.

62. Li M, Cheng J, Ying M, et al. Could clinical ultrasound improve the fitting of spinal orthosis for the patients with AIS? *Eur Spine J.* 2012;21:1926-1935.

63. Chen W, Le L, Lou E. Ultrasound imaging of spinal vertebrae to study scoliosis. *Open Journal of Acoustics.* 2012;2:95-103.

64. Chen W, Lou EH, Zhang PQ, et al. Reliability of assessing the coronal curvature of children with scoliosis by using ultrasound images. *J Child Orthop.* 2013;7:521-529.

65. Nguyen DV, Vo QN, Le LH, et al. Validation of 3D surface reconstruction of vertebrae and spinal column using 3D ultrasound data--a pilot study. *Med Eng Phys.* 2015;37:239-244.

66. Young M, Hill DL, Zheng R, et al. Reliability and accuracy of ultrasound measurements with and without the aid of previous radiographs in adolescent idiopathic scoliosis (AIS). *Eur Spine J.* 2015.

67. Wang Q, Li M, Lou EH, et al. Reliability and validity study of clinical ultrasound imaging on lateral curvature of adolescent idiopathic scoliosis. *PLoS One.* 2015;10:e0135264.

68. Komeili A, Westover L, Parent EC, et al. Correlation between a novel surface topography asymmetry analysis and radiographic data in scoliosis. *Spine Deform.* 2015;3:303-311.

69. Zheng YP, Lee TT, Lai KK, et al. A reliability and validity study for scolioscan: A radiation-free scoliosis assessment system using 3D ultrasound imaging. *Scoliosis Spinal Disord.* 2016;11:13-016-0074-y. eCollection 2016.

70. Zheng R, Young M, Hill D, et al. Improvement on the accuracy and reliability of ultrasound coronal curvature measurement on adolescent idiopathic scoliosis with the aid of previous radiographs. *Spine (Phila Pa 1976).* 2016;41:404-411.

71. Knott P, Sturm P, Lonner B, et al. Multicenter comparison of 3D spinal measurements using surface topography with those from conventional radiography. *Spine Deform.* 2016;4:98-103.

72. Richards BS, Bernstein RM, D'Amato CR, et al. Standardization of criteria for adolescent idiopathic scoliosis brace studies: SRS committee on bracing and nonoperative management. *Spine (Phila Pa 1976).* 2005;30:2068-75.

73. Canavese F, Kaelin A. Adolescent idiopathic scoliosis: Indications and efficacy of nonoperative treatment. *Indian J Orthop.* 2011;45:7-14.

74. Weinstein SL, Dolan LA, Wright JG, et al. Effects of bracing in adolescents with idiopathic scoliosis. *N Engl J Med.* 2013;369:1512-1521.

75. Weinstein SL, Ponseti IV. Curve progression in idiopathic scoliosis. *J Bone Joint Surg Am.* 1983;65:447-455.

76. Weinstein SL, Dolan LA, Cheng JC, et al. Adolescent idiopathic scoliosis. *Lancet.* 2008;371:1527-1537.

77. Mac-Thiong JM, Labelle H, Charlebois M, et al. Sagittal plane analysis of the spine and pelvis in adolescent idiopathic scoliosis according to the coronal curve type. *Spine (Phila Pa 1976).* 2003;28:1404-1409.

78. Roussouly P, Pinheiro-Franco JL. Biomechanical analysis of the spino-pelvic organization and adaptation in pathology. *Eur Spine J.* 2011;20 Suppl 5:609-618.

79. Le Huec JC, Aunoble S, Philippe L, et al. Pelvic parameters: Origin and significance. *Eur Spine J.* 2011;20 Suppl 5:564-571.

80. Farshad M, Catanzaro S, Schmid SL. The spinopelvic geometry in different lenke curve types of adolescent idiopathic scoliosis. *Spine Deform.* 2016;4:425-431.

81. Legaye J, Duval-Beaupere G, Hecquet J, et al. Pelvic incidence: A fundamental pelvic parameter for three-dimensional regulation of spinal sagittal curves. *Eur Spine J.* 1998;7:99-103.

82. Pasha S, Aubin CE, Sangole AP, et al. Three-dimensional spinopelvic relative alignment in adolescent idiopathic scoliosis. *Spine (Phila Pa 1976).* 2014;39:564-570.

83. Borges PA, Ocampos GP, Mancuso Filho JA, et al. The sagital balance in idiopatic and neuromuscular scoliosis. *Acta Ortop Bras.* 2014;22:179-182.

84. Clement JL, Geoffray A, Yagoubi F, et al. Relationship between thoracic hypokyphosis, lumbar lordosis and sagittal pelvic parameters in adolescent idiopathic scoliosis. *Eur Spine J.* 2013;22:2414-2420.

85. La Maida GA, Zottarelli L, Mineo GV, et al. Sagittal balance in adolescent idiopathic scoliosis: Radiographic study of spino-pelvic compensation after surgery. *Eur Spine J.* 2013;22 Suppl 6:S859-67.

86. Yong Q, Zhen L, Zezhang Z, et al. Comparison of sagittal spinopelvic alignment in chinese adolescents with and without idiopathic thoracic scoliosis. *Spine (Phila Pa 1976).* 2012;37:E714-20.

87. Vrtovec T, Janssen MM, Pernus F, et al. Analysis of pelvic incidence from 3Dimensional images of a normal population. *Spine (Phila Pa 1976).* 2012;37:E479-85.

88. Ghostine B, Sauret C, Assi A, et al. Influence of patient axial malpositioning on the trueness and precision of pelvic parameters obtained from 3D reconstructions based on biplanar radiographs. *Eur Radiol.* 2017;27:1295-1302.

89. Von Meyer H. Die mechanik der skoliose. ein beitrag zur lehre von den missgestaltungen des knochengerüstes. *Virchows Arch.* 1866:225-253.

90. Liljenqvist UR, Link TM, Halm HF. Morphometric analysis of thoracic and lumbar vertebrae in idiopathic scoliosis. *Spine (Phila Pa 1976).* 2000;25:1247-1253.

91. Kristmundsdottir F, Burwell RG, James JI. The rib-vertebra angles on the convexity and concavity of the spinal curve in infantile idiopathic scoliosis. *Clin Orthop Relat Res.* 1985;(201):205-209.

92. Oda I, Abumi K, Lu D, et al. Biomechanical role of the posterior elements, costovertebral joints, and rib cage in the stability of the thoracic spine. *Spine (Phila Pa 1976).* 1996;21:1423-1429.

93. Sevastik B, Xiong B, Sevastik J, et al. Rib-vertebral angle asymmetry in idiopathic, neuromuscular and experimentally induced scoliosis. *Eur Spine J.* 1997;6:84-88.

94. McAlindon RJ, Kruse RW. Measurement of rib vertebral angle difference. intraobserver error and interobserver variation. *Spine (Phila Pa 1976).* 1997;22:198-199.

95. Watkins R,4th, Watkins R,3rd, Williams L, et al. Stability provided by the sternum and rib cage in the thoracic spine. *Spine (Phila Pa 1976).* 2005;30:1283-1286.

96. Kuklo TR, Potter BK, Lenke LG. Vertebral rotation and thoracic torsion in adolescent idiopathic scoliosis: What is the best radiographic correlate? *J Spinal Disord Tech.* 2005;18:139-147.

97. Modi HN, Suh SW, Song HR, et al. Drooping of apical convex rib-vertebral angle in adolescent idiopathic scoliosis of more than 40 degrees: A prognostic factor for progression. *J Spinal Disord Tech.* 2009;22:367-371.

98. Canavese F, Turcot K, Holveck J, et al. Changes of concave and convex rib-vertebral angle, angle difference and angle ratio in patients with right thoracic adolescent idiopathic scoliosis. *Eur Spine J.* 2011;20:129-134.

99. Corona J, Sanders JO, Luhmann SJ, et al. Reliability of radiographic measures for infantile idiopathic scoliosis. *J Bone Joint Surg Am.* 2012;94:e86.

100. Foley G, Aubin C, Parent S, et al. Physical significance of the rib vertebra angle difference and its 3Dimensional counterpart in early-onset scoliosis. *Spine Deformity.* 2013;1:259-265.

101. Pizones J, Zuniga L, Sanchez-Mariscal F, et al. Relationship between the different torsion-related thoracic deformity parameters of adolescent idiopathic scoliosis. *Eur J Orthop Surg Traumatol.* 2016;26:763-769.

102. Harrington PR. Treatment of scoliosis. correction and internal fixation by spine instrumentation. *J Bone Joint Surg Am.* 1962;44-A:591-610.

103. Cotrel Y, Dubousset J. A new technic for segmental spinal osteosynthesis using the posterior approach. *Rev Chir Orthop Reparatrice Appar Mot.* 1984;70:489-494.

104. Cotrel Y, Dubousset J, Guillaumat M. New universal instrumentation in spinal surgery. *Clin Orthop Relat Res.* 1988;227:10-23.

105. Webb JK, Burwell RG, Cole AA, et al. Posterior instrumentation in scoliosis. *Eur Spine J.* 1995;4:2-5.

106. Hamill CL, Lenke LG, Bridwell KH, et al. The use of pedicle screw fixation to improve correction in the lumbar spine of patients with idiopathic scoliosis. is it warranted? *Spine (Phila Pa 1976).* 1996;21:1241-1249.

107. Newton PO, Wenger DR, Mubarak SJ, et al. Anterior release and fusion in pediatric spinal deformity. A comparison of early outcome and cost of thoracoscopic and open thoracotomy approaches. *Spine (Phila Pa 1976).* 1997;22:1398-1406.

108. Sudo H, Ito M, Kaneda K, et al. Long-term outcomes of anterior dual-rod instrumentation for thoracolumbar and lumbar curves in adolescent idiopathic scoliosis: A twelve to twenty-three-year follow-up study. *J Bone Joint Surg Am.* 2013;95:e49.

109. Barr SJ, Schuette AM, Emans JB. Lumbar pedicle screws versus hooks. results in double major curves in adolescent idiopathic scoliosis. *Spine (Phila Pa 1976).* 1997;22:1369-1379.

110. Suk SI, Lee CK, Kim WJ, et al. Segmental pedicle screw fixation in the treatment of thoracic idiopathic scoliosis. *Spine (Phila Pa 1976).* 1995;20:1399-1405.

111. Suk SI, Lee SM, Chung ER, et al. Selective thoracic fusion with segmental pedicle screw fixation in the treatment of thoracic idiopathic scoliosis: More than 5-year follow-up. *Spine (Phila Pa 1976).* 2005;30:1602-1609.

112. Boos N, Webb JK. Pedicle screw fixation in spinal disorders: A european view. *Eur Spine J.* 1997;6:2-18.

113. Halm H, Niemeyer T, Link T, et al. Segmental pedicle screw instrumentation in idiopathic thoracolumbar and lumbar scoliosis. *Eur Spine J.* 2000;9:191-197.

114. Liljenqvist UR, Halm HF, Link TM. Pedicle screw instrumentation of the thoracic spine in idiopathic scoliosis. *Spine (Phila Pa 1976).* 1997;22:2239-2245.

115. Schlösser TP, van der Heijden GJ, Versteeg AL, et al. How 'idiopathic' is adolescent idiopathic scoliosis? A systematic review on associated abnormalities. *PLoS One.* 2014;9:e97461.

116. Schlösser TP, Janssen MM, Hogervorst T, et al. The odyssey of sagittal pelvic morphology during human evolution: A perspective on different hominoidae. *Spine J.* 2017 Aug;17(8):1202-1206.

117. Foster AD, Raichlen DA, Pontzer H. Muscle force production during bent-knee, bent-hip walking in humans. *J Hum Evol.* 2013;65:294-302.

118. Lovejoy CO. The natural history of human gait and posture. part 1. spine and pelvis. *Gait Posture.* 2005;21:95-112.

119. Rak Y. Lucy's pelvic anatomy: Its role in bipedal gait. *Journal of Human Evolution.* 1991;20:283-290.

120. Janssen MM, Drevelle X, Humbert L, et al. Differences in male and female spino-pelvic alignment in asymptomatic young adults: A three-dimensional analysis using upright low-dose digital biplanar X-rays. *Spine (Phila Pa 1976).* 2009;34:E826-32.

121. Vercauteren M. Dorso-lumbale curvendistributie en etiopathogenie van de scoliosis adolescentium. 1980. Available from: http://lib.ugent.be/catalog/rug01:000167513.

122. Janssen MM, Vincken KL, van Raak SM, et al. Sagittal spinal profile and spinopelvic balance in parents of scoliotic children. *Spine J.* 2013;13:1789-1800.

123. Vialle R, Ilharreborde B, Dauzac C, et al. Is there a sagittal imbalance of the spine in isthmic spondylolisthesis? A correlation study. *Eur Spine J.* 2007;16:1641-1649.

124. Vialle R, Levassor N, Rillardon L, et al. Radiographic analysis of the sagittal alignment and balance of the spine in asymptomatic subjects. *J Bone Joint Surg Am.* 2005;87:260-267.

125. Roussouly P, Gollogly S, Berthonnaud E, et al. Sagittal alignment of the spine and pelvis in the presence of L5-s1 isthmic lysis and low-grade spondylolisthesis. *Spine (Phila Pa 1976).* 2006;31:2484-2490.

126. Scheuermann HW. The classic: Kyphosis dorsalis juvenilis. *Clin Orthop Relat Res.* 1977;(128):5-7.

127. Wynne-Davies R. Familial (idiopathic) scoliosis. A family survey. *J Bone Joint Surg Br.* 1968;50:24-30.

128. Dickson RA. The aetiology of spinal deformities. *Lancet.* 1988;1:1151-1155.

129. Altaf F, Gibson A, Dannawi Z, et al. Adolescent idiopathic scoliosis. *BMJ.* 2013;346:f2508.

130. Dimeglio A. Growth in pediatric orthopaedics. *J Pediatr Orthop.* 2001;21:549-555.

131. Risser JC. The iliac apophysis; an invaluable sign in the management of scoliosis. *Clin Orthop.* 1958;11:111-119.

132. Grivas TB, Dangas S, Samelis P, et al. Lateral spinal profile in school-screening referrals with and without late onset idiopathic scoliosis 10 degrees-20 degrees. *Stud Health Technol Inform.* 2002;91:25-31.

133. Upasani VV, Tis J, Bastrom T, et al. Analysis of sagittal alignment in thoracic and thoracolumbar curves in adolescent idiopathic scoliosis: How do these two curve types differ? *Spine (Phila Pa 1976).* 2007;32:1355-1359.

134. Vahid Tari SH, Ameri Mahabadi E, Ghandehari H, et al. Spinopelvic sagittal alignment in patients with adolescent idiopathic scoliosis. *Shafa Orthopedic Journal.* 2015;2:e739.

135. Vrtovec T, Pernus F, Likar B. A review of methods for quantitative evaluation of axial vertebral rotation. *Eur Spine J.* 2009;18:1079-1090.

136. Brink RC, Vavruch L, Schlösser TPC, et al. Three-dimensional pelvic incidence is much higher in (thoraco)lumbar scoliosis than in controls. *Eur Spine J.* 2018; aug 20.

137. Wynne-Davies R. Infantile idiopathic scoliosis. causative factors, particularly in the first six months of life. *J Bone Joint Surg Br.* 1975;57:138-141.

138. Kouwenhoven JW, Bartels LW, Vincken KL, et al. The relation between organ anatomy and pre-existent vertebral rotation in the normal spine: Magnetic resonance imaging study in humans with situs inversus totalis. *Spine (Phila Pa 1976).* 2007;32:1123-1128.

139. Kouwenhoven JW, Vincken KL, Bartels LW, et al. Analysis of preexistent vertebral rotation in the normal quadruped spine. *Spine (Phila Pa 1976).* 2006;31:E754-8.

140. Janssen MM, Vincken KL, Kemp B, et al. Pre-existent vertebral rotation in the human spine is influenced by body position. *Eur Spine J.* 2010;19:1728-1734.

141. Janssen MM, Kouwenhoven JW, Schlösser TP, et al. Analysis of preexistent vertebral rotation in the normal infantile, juvenile, and adolescent spine. *Spine (Phila Pa 1976).* 2011;36:E486-91.

142. Schlösser TP, Vincken KL, Attrach H, et al. Quantitative analysis of the closure pattern of the neurocentral junction as related to preexistent rotation in the normal immature spine. *Spine J.* 2013;13:756-763.

143. Schlösser TPC, Semple T, Carr SB, et al. Scoliosis convexity and organ anatomy are related. *Eur Spine J.* 2017;26:1595-1599.

144. Taylor JR. Scoliosis and growth. patterns of asymmetry in normal vertebral growth. *Acta Orthop Scand.* 1983;54:596-602.

145. Brink RC, Schlösser TP, Colo D, et al. Asymmetry of the vertebral body and pedicles in the true transverse plane in adolescent idiopathic scoliosis: A CT-based study. *Spine Deform.* 2017;5:37-45.

146. Takeshita K, Maruyama T, Chikuda H, et al. Diameter, length, and direction of pedicle screws for scoliotic spine: Analysis by multiplanar reconstruction of computed tomography. *Spine (Phila Pa 1976).* 2009;34:798-803.

147. Abul-Kasim K, Ohlin A. Patients with adolescent idiopathic scoliosis of lenke type-1 curve exhibit specific pedicle width pattern. *Eur Spine J*. 2012;21:57-63.

148. Liljenqvist UR, Allkemper T, Hackenberg L, et al. Analysis of vertebral morphology in idiopathic scoliosis with use of magnetic resonance imaging and multiplanar reconstruction. *J Bone Joint Surg Am*. 2002;84-A:359-368.

149. Archer IA, Dickson RA. Stature and idiopathic scoliosis. A prospective study. *J Bone Joint Surg Br*. 1985;67:185-188.

150. Chu WC, Man GC, Lam WW, et al. Morphological and functional electrophysiological evidence of relative spinal cord tethering in adolescent idiopathic scoliosis. *Spine (Phila Pa 1976)*. 2008;33:673-680.

151. Guo X, Chau WW, Chan YL, et al. Relative anterior spinal overgrowth in adolescent idiopathic scoliosis--result of disproportionate endochondral-membranous bone growth? summary of an electronic focus group debate of the IBSE. *Eur Spine J*. 2005;14:862-873.

152. Porter RW. Idiopathic scoliosis: The relation between the vertebral canal and the vertebral bodies. *Spine (Phila Pa 1976)*. 2000;25:1360-1366.

153. Marty C, Boisaubert B, Descamps H, et al. The sagittal anatomy of the sacrum among young adults, infants, and spondylolisthesis patients. *Eur Spine J*. 2002;11:119-125.

154. Roussouly P, Nnadi C. Sagittal plane deformity: An overview of interpretation and management. *Eur Spine J*. 2010;19:1824-1836.

155. Kalra MK, Quick P, Singh S, et al. Whole spine CT for evaluation of scoliosis in children: Feasibility of sub-milliSievert scanning protocol. *Acta Radiol*. 2013;54:226-230.

156. Abul-Kasim K, Overgaard A, Maly P, et al. Low-dose helical computed tomography (CT) in the perioperative workup of adolescent idiopathic scoliosis. *Eur Radiol*. 2009;19:610-618.

157. Lenke LG, Edwards CC,2nd, Bridwell KH. The Lenke classification of adolescent idiopathic scoliosis: How it organizes curve patterns as a template to perform selective fusions of the spine. *Spine (Phila Pa 1976)*. 2003;28:S199-207.

158. Roussouly P, Labelle H, Rouissi J, et al. Pre- and post-operative sagittal balance in idiopathic scoliosis: A comparison over the ages of two cohorts of 132 adolescents and 52 adults. *Eur Spine J*. 2013;22 Suppl 2:S203-15.

159. Vrtovec T, Janssen MM, Likar B, et al. Evaluation of pelvic morphology in the sagittal plane. *Spine J*. 2013;13:1500-1509.

160. Vaz G, Roussouly P, Berthonnaud E, et al. Sagittal morphology and equilibrium of pelvis and spine. *Eur Spine J*. 2002;11:80-87.

161. Philippot R, Wegrzyn J, Farizon F, et al. Pelvic balance in sagittal and lewinnek reference planes in the standing, supine and sitting positions. *Orthop Traumatol Surg Res*. 2009;95:70-76.

162. Labelle H, Aubin CE, Jackson R, et al. Seeing the spine in 3D: How will it change what we do? *J Pediatr Orthop*. 2011;31:S37-45.

163. Illes T, Somoskeoy S. Comparison of scoliosis measurements based on three-dimensional vertebra vectors and conventional two-dimensional measurements: Advantages in evaluation of prognosis and surgical results. *Eur Spine J*. 2013;22:1255-1263.

164. Parent S, Labelle H, Skalli W, et al. Morphometric analysis of anatomic scoliotic specimens. *Spine (Phila Pa 1976)*. 2002;27:2305-2311.

165. Molnar S, Mano S, Kiss L, et al. Ex vivo and in vitro determination of the axial rotational axis of the human thoracic spine. *Spine (Phila Pa 1976)*. 2006;31:E984-91.

166. Smith RM, Pool RD, Butt WP, et al. The transverse plane deformity of structural scoliosis. *Spine (Phila Pa 1976)*. 1991;16:1126-1129.

167.	Louis R. *Surgery of the Spine. Surgical Anatomy and Operative Approaches.* 1st ed. New York: Springer-Verlag, 1983.

168.	Gregersen GG, Lucas DB. An in vivo study of the axial rotation of the human thoracolumbar spine. *J Bone Joint Surg Am.* 1967;49:247-262.

169.	Lindahl O. Resection of vertebral transverse processes in idiopathic scoliosis. *Acta Orthop Scand.* 1966;37:342-347.

170.	Bouillet R, Vincent A. Idiopathic scoliosis. *Acta Orthop Belg.* 1967;33:93-388.

171.	Kotwicki T, Napiontek M. Intravertebral deformation in idiopathic scoliosis: A transverse plane computer tomographic study. *J Pediatr Orthop.* 2008;28:225-229.

172.	Vavruch L, Forsberg D, Dahlstrom N, et al. Vertebral axial asymmetry in adolescent idiopathic scoliosis. *Spine Deform.* 2018;6:112-120.e1.

173.	Stokes IA. Three-dimensional terminology of spinal deformity. A report presented to the scoliosis research society by the scoliosis research society working group on 3D terminology of spinal deformity. *Spine (Phila Pa 1976).* 1994;19:236-248.

174.	Fujimori T, Bastrom TP, Bartley CE, et al.. Comparison of typical thoracic curves and atypical thoracic curves within the Lenke 1 classification. *Spine Deform.* 2014;2:308-315.

175.	Kouwenhoven JW, Vincken KL, Bartels LW, et al. Analysis of preexistent vertebral rotation in the normal spine. *Spine (Phila Pa 1976).* 2006;31:1467-1472.

176.	Kashimoto T, Yamamuro T, Hatakeyama K. Anatomical and biomechanical factors in the curve pattern formation of idiopathic scoliosis. *Acta Orthop Scand.* 1982;53:361-368.

177.	Lindahl O, Raeder E. Mechanical analysis of forces involved in idiopathic scoliosis. *Acta Orthop Scand.* 1962;32:27-38.

178.	Aaro S, Dahlborn M. Estimation of vertebral rotation and the spinal and rib cage deformity in scoliosis by computer tomography. *Spine (Phila Pa 1976).* 1981;6:460-467.

179.	Aaro S, Dahlborn M. The longitudinal axis rotation of the apical vertebra, the vertebral, spinal, and rib cage deformity in idiopathic scoliosis studied by computer tomography. *Spine (Phila Pa 1976).* 1981;6:567-572.

180.	Raso VJ, Russell GG, Hill DL, et al. Thoracic lordosis in idiopathic scoliosis. *J Pediatr Orthop.* 1991;11:599-602.

181.	Wessberg P, Danielson BI, Willen J. Comparison of cobb angles in idiopathic scoliosis on standing radiographs and supine axially loaded MRI. *Spine (Phila Pa 1976).* 2006;31:3039-3044.

182.	Lee MC, Solomito M, Patel A. Supine magnetic resonance imaging cobb measurements for idiopathic scoliosis are linearly related to measurements from standing plain radiographs. *Spine (Phila Pa 1976).* 2013;38:E656-61.

183.	Shi B, Mao S, Wang Z, et al. How does the supine MRI correlate with standing x-ray of different curve severity in adolescent idiopathic scoliosis? *Spine (Phila Pa 1976).* 2015 Aug 1;40(15):1206-12.

184.	Parent S, Labelle H, Skalli W, et al. Thoracic pedicle morphometry in vertebrae from scoliotic spines. *Spine (Phila Pa 1976).* 2004;29:239-248.

185.	Chu WC, Yeung HY, Chau WW, et al. Changes in vertebral neural arch morphometry and functional tethering of spinal cord in adolescent idiopathic scoliosis--study with multi-planar reformat magnetic resonance imaging. *Stud Health Technol Inform.* 2006;123:27-33.

186.	Rajwani T, Bagnall KM, Lambert R, et al. Using magnetic resonance imaging to characterize pedicle asymmetry in both normal patients and patients with adolescent idiopathic scoliosis. *Spine (Phila Pa 1976).* 2004;29:E145-52.

187. Sarwahi V, Sugarman EP, Wollowick AL, et al. Prevalence, distribution, and surgical relevance of abnormal pedicles in spines with adolescent idiopathic scoliosis vs. no deformity: A CT-based study. *J Bone Joint Surg Am*. 2014;96:e92.

188. Beguiristain JL, De Salis J, Oriaifo A, et al. Experimental scoliosis by epiphysiodesis in pigs. *Int Orthop*. 1980;3:317-321.

189. Canadell J, Beguiristain JL, Gonzalez Iturri J, et al. Some aspects of experimental scoliosis. *Arch Orthop Trauma Surg*. 1978;93:75-85.

190. Cui G, Watanabe K, Hosogane N, et al. Morphologic evaluation of the thoracic vertebrae for safe free-hand pedicle screw placement in adolescent idiopathic scoliosis: A CT-based anatomical study. *Surg Radiol Anat*. 2012;34:209-216.

191. Watanabe K, Lenke LG, Matsumoto M, et al. A novel pedicle channel classification describing osseous anatomy: How many thoracic scoliotic pedicles have cancellous channels? *Spine (Phila Pa 1976)*. 2010;35:1836-1842.

192. Volkmann R. Beiträge zur anatomie und chirurgie der geschwülste. *Langenbecks Arch Chir*. 1873;15:556-561.

193. Hueter C. Anatomische studien an den extremitätengelenken neugeborener und erwachsener. *Virchow Arch*. 1862;26:484-519.

194. Roaf R. Vertebral growth and its mechanical control. *J Bone Joint Surg Br*. 1960;42-B:40-59.

195. Knutsson F. A contribution to the discussion of the biological cause of idiopathic scoliosis. *Acta Orthop Scand*. 1963;33:98-104.

196. Rajwani T, Bhargava R, Moreau M, et al. MRI characteristics of the neurocentral synchondrosis. *Pediatr Radiol*. 2002;32:811-816.

197. Upendra B, Meena D, Kandwal P, et al. Pedicle morphometry in patients with adolescent idiopathic scoliosis. *Indian J Orthop*. 2010;44:169-176.

198. Kuraishi S, Takahashi J, Hirabayashi H, et al. Pedicle morphology using computed tomography-based navigation system in adolescent idiopathic scoliosis. *J Spinal Disord Tech*. 2013;26:22-28.

199. Glassman SD, Bridwell K, Dimar JR, et al. The impact of positive sagittal balance in adult spinal deformity. *Spine (Phila Pa 1976)*. 2005;30:2024-2029.

200. Hayashi K, Upasani VV, Pawelek JB, et al. Three-dimensional analysis of thoracic apical sagittal alignment in adolescent idiopathic scoliosis. *Spine (Phila Pa 1976)*. 2009;34:792-797.

201. Newton PO, Fujimori T, Doan J, et al. Defining the "three-dimensional sagittal plane" in thoracic adolescent idiopathic scoliosis. *J Bone Joint Surg Am*. 2015;97:1694-1701.

202. Dede O, Buyukdogan K, Demirkiran HG, et al. The development of thoracic vertebral sagittal morphology during childhood. *Spine Deformity*. 2016;4:391-394.

203. Roth M. Idiopathic scoliosis and scheuermann's disease: Essentially identical manifestations of neuro-vertebral growth disproportion. *Radiol Diagn (Berl)*. 1981;22:380-391.

204. Porter RW. The pathogenesis of idiopathic scoliosis: Uncoupled neuro-osseous growth? *Eur Spine J*. 2001;10:473-481.

205. Deng M, Hui SC, Yu FW, et al. MRI-based morphological evidence of spinal cord tethering predicts curve progression in adolescent idiopathic scoliosis. *Spine J*. 2015;15:1391-1401.

206. Chu WC, Rasalkar DD, Cheng JC. Asynchronous neuro-osseous growth in adolescent idiopathic scoliosis--MRI-based research. *Pediatr Radiol*. 2011;41:1100-1111.

207. Dubousset J, Herring JA, Shufflebarger H. The crankshaft phenomenon. *J Pediatr Orthop*. 1989;9:541-550.

208. Ursu TR, Porter RW, Navaratnam V. Development of the lumbar and sacral vertebral canal in utero. *Spine (Phila Pa 1976)*. 1996;21:2705-2708.

209. Foley G, Aubin CE, Labelle H, et al. The rib vertebra angle difference and its measurement in 3D for the evaluation of early onset scoliosis. *Stud Health Technol Inform.* 2012;176:238-241.

210. Grivas TB, Samelis P, Chadziargiropoulos T, et al. Study of the rib cage deformity in children with 10 degrees-20 degrees of cobb angle late onset idiopathic scoliosis, using rib-vertebra angles--aetiologic implications. *Stud Health Technol Inform.* 2002;91:20-24.

211. Burwell RG, Cole AA, Cook TA, et al. Pathogenesis of idiopathic scoliosis. the nottingham concept. *Acta Orthop Belg.* 1992;58 Suppl 1:33-58.

212. Bernstein P, Hentschel S, Platzek I, et al. The assessment of the postoperative spinal alignment: MRI adds up on accuracy. *Eur Spine J.* 2012;21:733-738.

213. Perdriolle R, Vidal J. Thoracic idiopathic scoliosis curve evolution and prognosis. *Spine (Phila Pa 1976).* 1985;10:785-791.

214. Keenan BE, Izatt MT, Askin GN, et al. Supine to standing cobb angle change in idiopathic scoliosis: The effect of endplate pre-selection. *Scoliosis.* 2014;9:16-7161-9-16. eCollection 2014.

215. Altman DG, Bland JM. Measurement in medicine: The analysis of method comparison studies. *Journal of the Royal Statistical Society Series D (The Statistician).* 1983;32:307-317.

216. Al-Aubaidi Z, Lebel D, Oudjhane K, et al. Three-dimensional imaging of the spine using the EOS system: Is it reliable? A comparative study using computed tomography imaging. *J Pediatr Orthop B.* 2013;22:409-412.

217. Yazici M, Acaroglu ER, Alanay A, et al. Measurement of vertebral rotation in standing versus supine position in adolescent idiopathic scoliosis. *J Pediatr Orthop.* 2001;21:252-256.

218. Harmouche R, Cheriet F, Labelle H, et al. 3D registration of MR and X-ray spine images using an articulated model. *Comput Med Imaging Graph.* 2012;36:410-418.

219. Schmitz A, Jaeger UE, Koenig R, et al. A new MRI technique for imaging scoliosis in the sagittal plane. *Eur Spine J.* 2001;10:114-117.

220. Deviren V, Berven S, Kleinstueck F, et al. Predictors of flexibility and pain patterns in thoracolumbar and lumbar idiopathic scoliosis. *Spine (Phila Pa 1976).* 2002;27:2346-2349.

221. Schlösser T, Stralen M, Chu W, et al. The true three-dimensional deformity of the spine in adolescent idiopathic scoliosis. *Spine (Phila Pa 1976).* 2014 Sep 1;39(19):E1159-66.

222. Lou EH, Chan AC, Donauer A, et al. Ultrasound-assisted brace casting for adolescent idiopathic scoliosis, IRSSD best research paper 2014. *Scoliosis.* 2015;10:13-015-0037-8. eCollection 2015.

223. Cheung C, Zhou G, Law S, et al. Ultrasound volume projection imaging for assessment of scoliosis. *Medical Imaging, IEEE Transactions on.* 2015;PP:1-1.

224. Brink RC, Wijdicks SPJ, Tromp IN, et al. A reliability and validity study for different coronal angles using ultrasound imaging in adolescent idiopathic scoliosis. *Spine J.* 2018 Jun;18(6):979-985.

225. Ungi T, King F, Kempston M, et al. Spinal curvature measurement by tracked ultrasound snapshots. *Ultrasound Med Biol.* 2014;40:447-454.

226. Li M, Cheng J, Ying M, et al. A preliminary study of estimation of cobb's angle from the spinous process angle using a clinical ultrasound method. *Spine Deform.* 2015;3:476-482.

227. Zheng R, Chan AC, Chen W, et al. Intra- and inter-rater reliability of coronal curvature measurement for adolescent idiopathic scoliosis using ultrasonic imaging method-A pilot study. *Spine Deform.* 2015;3:151-158.

228. Chen H, Schlösser TPC, Brink RC, et al. The height-width-depth ratios of the intervertebral discs and vertebral bodies in adolescent idiopathic scoliosis vs controls in a chinese population. *Sci Rep.* 2017;7:46448.

229. Herzenberg JE, Waanders NA, Closkey RF, et al. Cobb angle versus spinous process angle in adolescent idiopathic scoliosis. the relationship of the anterior and posterior deformities. *Spine (Phila Pa 1976)*. 1990;15:874-879.

230. Cheung C, Zheng Y. Development of 3D ultrasound system for assessment of adolescent idiopathic scoliosis (AIS). In: Lim CT, Goh JCH, eds. *6th World Congress of Biomechanics (WCB 2010). August 1-6, 2010 Singapore*. Vol 31. Springer Berlin Heidelberg, 2010:584-587.

231. Cheung CW, Law SY, Zheng YP. Development of 3D ultrasound system for assessment of adolescent idiopathic scoliosis (AIS): And system validation. *Conf Proc IEEE Eng Med Biol Soc.* 2013;2013:6474-6477.

232. Zhou GQ, Jiang W, Lai KL, et al. Automatic measurement of spine curvature on 3D ultrasound volume projection image with phase features. *IEEE Trans Med Imaging.* 2017.

233. Vrtovec T, Pernus F, Likar B. A review of methods for quantitative evaluation of spinal curvature. *Eur Spine J.* 2009;18:593-607.

234. Langensiepen S, Semler O, Sobottke R, et al. Measuring procedures to determine the cobb angle in idiopathic scoliosis: A systematic review. *Eur Spine J.* 2013;22:2360-2371.

235. Yoon WW, Chang AC, Tyler P, et al. The use of ultrasound in comparison to radiography in magnetically controlled growth rod lengthening measurement: A prospective study. *Eur Spine J.* 2015;24:1422-1426.

236. Ohrt-Nissen S, Hallager DW, Henriksen JL, et al. Curve magnitude in patients referred for evaluation of adolescent idiopathic scoliosis: Five years' experience from a system without school screening. *Spine Deform.* 2016;4:120-124.

237. Hong A, Jaswal N, Westover L, et al. Surface topography classification trees for assessing severity and monitoring progression in adolescent idiopathic scoliosis (AIS). *Spine (Phila Pa 1976)*. 2017 Jul 1;42(13):E781-E787.

238. Mohokum M, Schulein S, Skwara A. The validity of rastersterography: A systematic review. *Orthop Rev (Pavia)*. 2015;7:5899.

239. Pino-Almero L, Minguez-Rey MF, Rodriguez-Martinez D, et al. Clinical application of back surface topography by means of structured light in the screening of idiopathic scoliosis. *J Pediatr Orthop B.* 2017;26:64-72.

240. Dohin B, Dubousset JF. Prevention of the crankshaft phenomenon with anterior spinal epiphysiodesis in surgical treatment of severe scoliosis of the younger patient. *Eur Spine J.* 1994;3:165-168.

241. Betz RR, Harms J, Clements DH,3rd, et al. Comparison of anterior and posterior instrumentation for correction of adolescent thoracic idiopathic scoliosis. *Spine (Phila Pa 1976)*. 1999;24:225-239.

242. Rhee JM, Bridwell KH, Won DS, et al. Sagittal plane analysis of adolescent idiopathic scoliosis: The effect of anterior versus posterior instrumentation. *Spine (Phila Pa 1976)*. 2002;27:2350-2356.

243. Schmidt C, Liljenqvist U, Lerner T, et al. Sagittal balance of thoracic lordoscoliosis: Anterior dual rod instrumentation versus posterior pedicle screw fixation. *Eur Spine J.* 2011;20:1118-1126.

244. Nohara A, Kawakami N, Saito T, et al. Comparison of surgical outcomes between anterior fusion and posterior fusion in patients with AIS lenke type 1 or 2 that underwent selective thoracic fusion -long-term follow-up study longer than 10 postoperative years. *Spine (Phila Pa 1976)*. 2015;40:1681-1689.

245. Imrie M, Yaszay B, Bastrom TP, et al. Adolescent idiopathic scoliosis: Should 100% correction be the goal? *J Pediatr Orthop.* 2011;31:S9-13.

246. Helenius I, Remes V, Yrjonen T, et al. Harrington and cotrel-dubousset instrumentation in adolescent idiopathic scoliosis. long-term functional and radiographic outcomes. *J Bone Joint Surg Am.* 2003;85-A:2303-2309.

247.   Kim YJ, Lenke LG, Cho SK, et al. Comparative analysis of pedicle screw versus hook instrumentation in posterior spinal fusion of adolescent idiopathic scoliosis. *Spine (Phila Pa 1976)*. 2004;29:2040-2048.

248.   Dickson RA, Archer IA. Surgical treatment of late-onset idiopathic thoracic scoliosis. the leeds procedure. *J Bone Joint Surg Br*. 1987;69:709-714.

249.   Potter BK, Kuklo TR, Lenke LG. Radiographic outcomes of anterior spinal fusion versus posterior spinal fusion with thoracic pedicle screws for treatment of lenke type I adolescent idiopathic scoliosis curves. *Spine (Phila Pa 1976)*. 2005;30:1859-1866.

250.   Sucato DJ, Agrawal S, O'Brien MF, et al. Restoration of thoracic kyphosis after operative treatment of adolescent idiopathic scoliosis: A multicenter comparison of three surgical approaches. *Spine (Phila Pa 1976)*. 2008;33:2630-2636.

251.   Nota SP, Braun Y, Ring D, et al. Incidence of surgical site infection after spine surgery: What is the impact of the definition of infection? *Clin Orthop Relat Res*. 2015;473:1612-1619.

252.   Fang A, Hu SS, Endres N, et al. Risk factors for infection after spinal surgery. *Spine (Phila Pa 1976)*. 2005;30:1460-1465.

253.   de Kleuver M, Lewis SJ, Germscheid NM, et al. Optimal surgical care for adolescent idiopathic scoliosis: An international consensus. *Eur Spine J*. 2014;23:2603-2618.

254.   Newton PO, Marks MC, Bastrom TP, et al. Surgical treatment of lenke 1 main thoracic idiopathic scoliosis: Results of a prospective, multicenter study. *Spine (Phila Pa 1976)*. 2013;38:328-338.

255.   Devlin NJ, Brooks R. EQ-5D and the EuroQol group: Past, present and future. *Appl Health Econ Health Policy*. 2017;15:127-137.

256.   Asher MA, Lai SM, Glattes RC, et al. Refinement of the SRS-22 health-related quality of life questionnaire function domain. *Spine (Phila Pa 1976)*. 2006;31:593-597.

257.   Lonner BS, Kondrachov D, Siddiqi F, et al. Thoracoscopic spinal fusion compared with posterior spinal fusion for the treatment of thoracic adolescent idiopathic scoliosis. *J Bone Joint Surg Am*. 2006;88:1022-1034.

258.   Kim YJ, Lenke LG, Bridwell KH, et al. Prospective pulmonary function comparison of anterior spinal fusion in adolescent idiopathic scoliosis: Thoracotomy versus thoracoabdominal approach. *Spine (Phila Pa 1976)*. 2008;33:1055-1060.

259.   Newton PO, Perry A, Bastrom TP, et al. Predictors of change in postoperative pulmonary function in adolescent idiopathic scoliosis: A prospective study of 254 patients. *Spine (Phila Pa 1976)*. 2007;32:1875-1882.

260.   Abul-Kasim K, Ohlin A, Strombeck A, et al. Radiological and clinical outcome of screw placement in adolescent idiopathic scoliosis: Evaluation with low-dose computed tomography. *Eur Spine J*. 2010;19:96-104.

261.   Di Silvestre M, Parisini P, Lolli F, et al. Complications of thoracic pedicle screws in scoliosis treatment. *Spine (Phila Pa 1976)*. 2007;32:1655-1661.

262.   Upendra BN, Meena D, Chowdhury B, et al. Outcome-based classification for assessment of thoracic pedicular screw placement. *Spine (Phila Pa 1976)*. 2008;33:384-390.

263.   Suk SI, Kim WJ, Lee SM, et al. Thoracic pedicle screw fixation in spinal deformities: Are they really safe? *Spine (Phila Pa 1976)*. 2001;26:2049-2057.

264.   Belmont PJ,Jr, Klemme WR, Dhawan A, et al. In vivo accuracy of thoracic pedicle screws. *Spine (Phila Pa 1976)*. 2001;26:2340-2346.

265.   Sarlak AY, Tosun B, Atmaca H, et al. Evaluation of thoracic pedicle screw placement in adolescent idiopathic scoliosis. *Eur Spine J*. 2009;18:1892-1897.

266. Hong JY, Suh SW, Easwar TR, et al. Clinical anatomy of vertebrae in scoliosis: Global analysis in four different diseases by multiplanar reconstructive computed tomography. *Spine J.* 2013;13:1510-1520.

267. Suk SI. Pedicle screw instrumentation for adolescent idiopathic scoliosis: The insertion technique, the fusion levels and direct vertebral rotation. *Clin Orthop Surg.* 2011;3:89-100.

268. Kim YJ, Lenke LG, Cheh G, et al. Evaluation of pedicle screw placement in the deformed spine using intraoperative plain radiographs: A comparison with computerized tomography. *Spine (Phila Pa 1976).* 2005;30:2084-2088.

269. Chung KJ, Suh SW, Desai S, et al. Ideal entry point for the thoracic pedicle screw during the free hand technique. *Int Orthop.* 2008;32:657-662.

270. Zindrick MR, Wiltse LL, Doornik A, et al. Analysis of the morphometric characteristics of the thoracic and lumbar pedicles. *Spine (Phila Pa 1976).* 1987;12:160-166.

271. Davis CM, Grant CA, Pearcy MJ, et al. Is there asymmetry between the concave and convex pedicles in adolescent idiopathic scoliosis? A CT investigation. *Clin Orthop Relat Res.* 2017;475:884-893.

272. Brink RC, Schlösser TP, Vincken KL, et al. Anterior-posterior length discrepancy in adolescent idiopathic scoliosis is the result of anterior disc expansion and compression of the interspinous space. *Spine J.* 2018 May 4. pii: S1529-9430(18)30204-3.

273. Brink RC, Schlösser TPC, Colo D, et al. Anterior spinal overgrowth is the result of the scoliotic mechanism and is located in the disc. *Spine (Phila Pa 1976).* 2017;42:818-822.

274. Brink RC, Schlösser TPC, van Stralen M, et al. What is the actual 3D representation of the rib vertebra angle difference (mehta's angle)? *Spine (Phila Pa 1976). 2018 Jan 15;43(2):E92-E97*.

List of Abbreviations and Definitions

2D	Two-dimensional
3D	Three-dimensional
95%CI	95% confidence interval
A-C%	Anterior spine-spinal canal length ratio
A-L%	Anterior spine-lamina length ratio
A-S%	Anterior spine-spinous process length ratio
A-P%	Anterior-posterior length ratio
AIS	Adolescent idiopathic scoliosis
ANOVA	Analysis of variance
Apex	The most laterally deviated vertebra or disc in a scoliotic curve in the coronal plane
Axial rotation	Rotation in the transverse plane around the anterior-posterior axis of the body
Cobb	Angle between lines drawn on endplates of the end vertebrae
COL	Center of lamina
COM	Center of mass
CT	Computed tomography
Cobb end vertebrae	The cranial and caudal vertebrae that bound a scoliotic curve in the coronal plane
Concave	Curving in (or hollowed inward)
Convex	Curving out (extending outward)
DRR	Digitally reconstructed radiograph
EQ-5D-3L	3-level questionnaire version of EuroQol group
FU	Follow-up
ICC	Intraclass correlation coefficient
Idiopathic	A disease that is not linked to any physical impairment or previous medical history
Intravertebral axial rotation	Rotation between the vertebral body and posterior elements
IV	Instrumented vertebra
IVD	Intervertebral disc
Kyphosis	Forward curvature of a part of the spine in the sagittal plane
LIV	Lower instrumented vertebra
Local mechanical torsion	Vertebral deformation due to the relative axial rotation of the endplates; rotation difference between the upper and lower endplate
LL	Lumbar lordosis

Longitudinal rotation axis	The axis from which the vertebral bodies rotates away from the midline
Lordosis	Backward curvature of a part of the spine in the sagittal plane
MAD	Mean absolute difference
MAE	mean absolute error
Mehta's angle	Rib Vertebra Angle Difference (RVAD)
mm	Millimeter
MRI	Magnetic resonance imaging
NCJ	Neurocentral junction
NM	Neuromuscular
P	Statistical significance
PA	Postero-anterior radiography
Pelvic lordosis	The angulation of the ilium relative to the ischium
PI	Pelvic incidence
r	Pearson's correlation coefficient
RASO	Relative anterior spinal overgrowth
R^2	Coefficient of determination
RVAD	Rib Vertebra Angle Difference
Scoliosis	A curvature of the spine of at least ten degrees in the coronal plane
sd or SD	Standard deviation
SP	Spinous process
SRS	Scoliosis Research Society
SRS-22	Scoliosis Research Society 22-item patient questionnaire
TK	Thoracic kyphosis
TP	Transverse process
UIV	Upper instrumented vertebra
Vertebral axial rotation	The vertebral transverse plane angulation.

Acknowledgement and Curriculum Vitae

ACKNOWLEDGEMENT

opportunity to visit their University Centers multiple times. Especially, prof. J.C.Y. Cheng, prof. W.C.W. Chu, prof. H. Tropp, Ludvig Vavruch and Tomaz Vrtovec, thank you very much for the support in our collaborative projects and during my visits at your centers.

Dr. M.C. Kruyt binnen de scolioselijn heb jij altijd een scherpe en kritische blik op de onderzoeksideeën en uitvoering daarvan. Dit heeft gezorgd voor een hogere weten-schappelijke kwaliteit van de studies. Dank hiervoor.

De Alexandre Suerman commissie, dank voor het vertrouwen en het mogelijk maken van dit promotietraject. Lisan van Os, dank voor de begeleiding en het organiseren van de masterclasses.

Beste Jelle, tijdens onze studententijd waren we huisgenoten aan de Goedestraat, tijdens het onderzoek zijn we zelfs kamergenoten geworden in het UMC. Dank voor de adviezen en steun als collega, maar bovenal als goede vriend.

Beste Sebas, als kamergenoot en arts-onderzoeker in dezelfde onderzoekslijn heb ik veel gehad aan je adviezen over de onderzoeken.

Collega's van de orthopedie en voornamelijk alle onderzoekers van Q, dank voor de bijdrage aan dit proefschrift, maar voornamelijk aan de plezierige tijd inclusief alle bor-rels, feesten, Kubb NK's, en orthoski's.

Simone Sienema dank voor alle hulp bij het plannen van afspraken en het helpen bij een hoop praktische zaken.

Studiedeelnemers, dank voor uw deelname aan het onderzoek.

Collega's uit het OLVG: tijdens dit promotietraject heb ik ook een periode bij jullie als ANIOS mogen werken. Dit was een erg leerzame en plezierige tijd, een erg mooie combinatie tussen de kliniek en de wetenschap en heeft ervoor gezorgd dat ik klaar ben om in 2019 als AIOS te starten.

Naast de inhoudelijke bijdrage wil ik mijn familie, schoonfamilie en vrienden bedan-ken voor alle steun tijdens dit traject. In het bijzonder mijn ouders, Bart & Simone (en Boaz), Tom en Wouter (helaas ben jij er niet meer). Dank voor de onvoorwaardelijke steun en de nodige gezellige afleiding tijdens het onderzoek.

Lieve Yvonne, jij bent er altijd voor mij. Naast mijn vrouw ben je mijn paranymf en zijn wij de trotse ouders van Tijn. Dank voor je geduld tijdens dit traject en wellicht kan ik nu ook wel eens een avond naast je op de bank zitten zonder laptop.

CURRICULUM VITAE

Rob Brink was born in Kampen, The Netherlands on July 24, 1990. In 2008, he graduated from high school (VWO, RSG Slingerbos, Harderwijk) and started medical school at the Utrecht University in The Netherlands. In 2013 he started his research career on adolescent idiopathic scoliosis at the department of Orthopaedic Surgery, University Medical Center Utrecht, The Netherlands, under supervision of prof. dr. René M. Castelein and dr. Tom P.C. Schlösser. During his medical study he performed a research internship at the department of Orthopedics and traumatology, The Chinese University of Hong Kong (supervisors prof. dr. Jack C.Y. Cheng and prof. dr. Winnie C.W. Chu). In December 2015 he completed his medical degree and received a grant from the Alexandre Suerman MD-PhD Talent Programme (a personal grant to facilitate his PhD project for three years). In January 2016 he started his doctoral program as a full-time medical doctor and PhD-candidate on the 3D morphology of idiopathic scoliosis at the University Medical Center Utrecht. He performed his research in close collaboration with image processing experts and he was supervised by prof. dr. René M. Castelein, prof. dr. Max A. Viergever, dr. Tom P.C. Schlösser and dr. Marijn van Stralen. As part of existing collaborations, he took part in the International Asia Studies Programme at the department of Orthopaedics and Traumatology, Chinese University of Hong Kong and visited this University two more times as PhD-candidate. Furthermore, collaborative projects were started with the University of Linköping, Sweden and the University of Ljubljana, Slovenia. The present work has resulted in numerous presentations at international conferences, peer-reviewed publications and this thesis. In 2019 he will start his training in orthopaedic surgery.